NATIONAL ACADEMY OF SCIENCES OF ARMENIA
INSTITUTE OF MECHANICS

Areg A. Hunanyan

Amplitude-Frequency Interaction and Localization of Electroelastic Shear Wave in Piezoelectric Waveguide with Near-Surface Weak Inhomogeneities

(01.02.04 – Deformable Body Mechanics)

DISSERTATION

Submitted for the Degree of Candidate of Phys.-Math. Sciences

Supervisor: Corr. Member of NAS RA
Dr. Prof. Ara S. Avetisyan

Yerevan – 2017

Contents

INTRODUCTION

Parallel to development of new directions of modern technologies, applications of ***elastic wave phenomena*** are becoming increasingly important in the fields of electronics, measuring devices and telecommunications (processing, amplification and of delay signal), in medicine (x-ray diagnosis, ultrasonic measurement), in metallurgy (non-destructive control of structural elements made of different materials) and in other areas. Currently, for mobile phones, computers and other precise measuring devices of radio-electronics, every month are produced millions of wave filters, resonators and periodic topographic lattices.

Typically, these technical elements are simple (single-layer) or composite (multilayer) waveguides composed of layers of different materials: dielectrics, conductors, piezoelectrics, magnetics, and newly created inhomogeneous materials [20],[30],[39],[47],[61],[62],[67],[96]. In each case of selected material there exist different physico-mechanical material relations describing the electro-magneto-elastic connections between wave characteristics in given layer and the nature of transmission of wave energy in the adjacent layer (including vacuum). The use of inhomogeneous materials in waveguides often comes out from technical need, for instance, to achieve the desired characteristics of the wave field. In the theory of coupled physico-mechanical fields as piecewise-homogeneous structures, such as layered inhomogeneity, i.e., when the physico-mechanical characteristics of the material of the waveguide are piecewise-constant functions $\gamma_s(x_\alpha) \in \left\{ c_{ijmn}^{(s)};\ e_{mij}^{(s)};\ \varepsilon_{rp}^{(s)};\ d_{mij}^{(s)};\ \mu_{rp}^{(s)};\ \rho^{(s)} \right\}$ in each layer $\left\{ x_\alpha \right\} \in \Omega_s$,
as well as continuous material inhomogeneity of any waveguide layer, i.e., when the same waveguide material physico-mechanical characteristics are described by continuous functions

$$\gamma(x_\alpha) \in \left\{ c_{ijmn}(x_\alpha); e_{mij}(x_\alpha); \varepsilon_{rp}(x_\alpha); d_{mij}(x_\alpha); \mu_{rp}(x_\alpha); \rho(x_\alpha) \right\} \text{ in } \left\{ x_\alpha \right\} \in \Omega_0$$

are investigated. In the theory of coupled physico-mechanical fields, the investigation problem of high frequency wave propagation in waveguides is particularly important for studies of dynamic processes in layered waveguides, with joints between layers of non-smooth (rough, wavy) surfaces.

Surface non-smoothness is the system of surface irregularities with relatively small steps on the base length. The linear dimensions of the roughness and waviness are measured in micrometers (μm) or nanometers (nm). They refer to the microgeometry of the solid body and define its most important exploitation properties. Quantitatively, the surface roughness is set independently of the method of its processing. For a wide class of surfaces, the horizontal step of the irregularities is in the range from 1 to 1000 μm and the height 0.01 to 10 μm.

Roughness and waviness, as residual deformations of layers near the processing surface of the deformable element are consequences of the material surface processing. These technological factors in general, lead to geometric inhomogeneity of the structural element surface or to physical inhomogeneity of the material in the near-surface zones of given element.

Due to the nature of the residual geometric surface roughness and physico-mechanical characteristics of the material, the surface of the structural element will react differently to the boundary electromechanical or thermomechanical loads, which in turn leads to additional surface loads compared with the case of the model of perfectly smooth surfaces of homogeneous material [16].

In many studies of wave processes in layered structures (see, for instance [22], [35],[38],[39],[51],[62],[71,72],[74],[78],[96],[97],[105],[108]), the presence of residual surface geometric and near-surface physical inconsistencies during the layer processing are often neglected, considering it as a structure element. But it is clear that perfectly smooth surface is an idealized model. It is clear that based on this approximate model it is impossible to identify all existing near-surface dynamic phenomena of the wave process, or, at least, to quantitatively identify the characteristics of the wave field in the near-surface zones of the waveguide.

A complete description of wave phenomena can be found in the different books of different decades [1], [5], [27], [29, 30], [43], [69], [76], [83,84], [93], [110], where you can also find overview of earlier works. Wave phenomena are diverse. In particular, the detection of dispersion for the normal wave signal propagation in homogeneous finite

elastic medium. In primary sources it is shown, that the dispersion is possible for perfectly smooth body surface:

- localization of wave energy of plane deformation in the near-surface zone of mechanically free surface of half-space [92] (Rayleigh wave, 1885),
- localization of wave energy of plane deformation in the near-surface zone of contact between two thick layers [99] (Stoneley wave, 1924),
- localization of wave energy of plane deformation in the near-surface zone of contact between two thick layers [68] (Lamb wave, 1917),
- localization of wave energy of elastic anti-plane deformation in near-surface joint zone of elastic half-space with more soft elastic layer [73] (Love wave, 1911),
- localization of wave energy of electroelastic shear deformation near free surface of piezoelectric crystal [28], [50], (Bleustein-Gulyaev wave, 1968-1969).

However, it is known that the wave signal propagation in waveguides with material inhomogeneity, as well with geometric inhomogeneity of the surface layers of the composite waveguide, leads to dissipation of wave signal energy (see, for instance, [4],[7,8,13÷16],[32],[34],[36],[37], [40÷46],[70],[100,101]). Arising nonlinear amplitude-phase interaction leads to change of wave dispersion, thereby changing the conditions of possible localization of wave energy near the separating surfaces [8],[14,15],[27],[51,54],[85÷88],[98],[103], [111].

It is obvious that from the point of view of reliability of obtained results, we need more accurate reasonable model for boundary inhomogeneities in layered waveguides. This is particularly important in the propagation of high-frequency (shortwave) wave signal of length commensurable with linear dimensions of the actual roughness on the waveguide surfaces.

Accounting non-smoothness on the element surface or the near-surface inhomogeneity of the material, significantly complicates the modeling in general, as well as the mathematical solution of the boundary value problem. But it provides an opportunity to identify near-surface wave phenomena and more accurately evaluate the quantitative characteristics of the wave field in the near-surface zones of the joints of different mediums.

Mathematical modeling is the basis of the study of most modern physical problems and development of many modern innovative technologies. Important objects of study, requiring application of mathematical modeling, are different possible types of contacts of rough surfaces in layered structures. The modeling problem gets more complicated in the theory of coupled physico-mechanical fields, when dynamic processes are studied in composite waveguides with joints of rough surface heterogeneous layers. In layered waveguides we often meet adjacent to each other piezoelectrics with magnetic or dielectric with a perfect conductor. However, we should pay attention to the fact that the layer-waveguide of electroelastic or magneto-elastic materials in vacuum is already multi-layered (composite).

In mechanics of materials with coupled physico-mechanical fields the common problem of electro-magneto-elasticity, is solved in quasistatic statement. Contact conditions of bordering mediums are presented by full continuity of the corresponding parameters of all physico-mechanical fields [3],[15],[65],[69],[76],[79] etc. Naturally, the number of possible combinations of mixed boundary conditions on the surfaces of waveguide layers is increased, which can affect to the propagation mode of coupled waves in it. In piezo-crystals the problem of existence of surface waves is more complicated, because acoustoelectric wave propagates already in two mediums. This implies theorems of existence of acoustoelectric waves only for a special type of boundary conditions [15], [69], [76], [79]. Possible combinations of mixed boundary conditions in problems of linear electroelastic piezoelectrics are given in [15].

The basis of mathematical modeling is always physical and/or structural modeling (physically and/or structurally more accurate representations of the problem), when, based on the nature of the problems, physical or geometric visual hypothetical representations for some specific components of physico-mechanical fields are proposed. Non-reasonable mathematical modeling may simplify the mathematical study in many ways. However, as a rule the results of the adopted simplifications are losses in physical characteristics. An important subject of study requiring application of mathematical modeling methods are optical layered structures.

As in mechanics of deformable solid medium, considering the nature of quantities describing the stress-strain state in thin-walled structural elements, for modeling of a new two-dimensional mathematical boundary value problem, based on the element thinness and boundary conditions on the surfaces and at the ends, different hypotheses about distributions of characteristic quantities were introduced [2], [63], [91], [102].

Similar hypothetical approach is successfully used also in mechanics of continuous medium, taking into account the associated physical and mechanical fields. In that way the theory of magneto-elasticity of thin plates and shells was constructed [3], representing elastic displacement and potentials of magnetic and electric fields in thin-walled elements in form of linear distributions over the element thickness. To this end, an asymptotic approach was also developed in [21, 86].

Different modeling of the effects related to the influence of surface roughness and surface inhomogeneity of the waveguide material on the amplitude and phase coefficients of normal wave signal on reflection and transmission division borders of layers with different optical parameters, on appearance of internal resonance or forbidden frequency zones, were considered in a huge number of works (see, for instance, [26, 31, 33, 48, 49, 55-58, 75,77, 89, 90, 94, 95]). Most theoretical studies of acoustic problems of rough surface were carried out eihter by the method of integral transformation, by calculating the Green's function, or by theory of perturbation.

a) two homogeneous half-spaces connected with homogeneous thin layer of binding material (glue), with geometrically inhomogeneous surfaces of contact – adhesion of bodies,

b) two homogeneous half-spaces connected with virtually selected, physically inhomogeneous layer with smooth surfaces of contact – ultrasonic welding.

By the input of magneto (electro, thermo) elastic layered systems hypothesis (MELS hypothesis) on distributions of characteristic values of physico-mechanical fields over the thickness of the newly formed inner layer, mathematical boundary value problem of electro-magneto-elasticity of three-layer composite is brought [16], [9÷11]. Distribution of characteristic values of physical-mechanical fields is set by surface-exponential functions, providing surface roughness effect in the equations and boundary conditions of electro-magneto-elasticity.

In this thesis the results of theoretical studies and numerical analysis of the wave field characteristics in piezoelectric waveguides for propagation of the normal electro-active elastic shear wave in it are given. Researches [12], [16], [17], [25], [53,54], [59] are carried out taking into account the ***weak inhomogeneity of the material layers of the waveguide and weak geometric inhomogeneity of the surfaces of these layers***.

In the introduction of this thesis the actuality of the research topic is outlined providing a brief overview of existing results to the problem of wave propagation in weakly inhomogeneous media and in waveguides taking into account weakly inhomogeneous non-smoothness of its surfaces.

The first chapter provides basic relations of linear electroelasticity for inhomogeneous piezoelectric layer-waveguide and modeling of propagation of pure shear (SH) high-frequency wave signal in electroelastic waveguides. General issues concerning amplitude-phase nonlinear interaction for the propagation of linear wave signal in geometrically and physically weakly inhomogeneous piezoelectric layer-waveguide are discussed in [6], [8], [9], [10], [12], [13], [15], [17]. Some issues of modeling of high frequency electroelastic wave signal propagation in piezoelectric waveguides are also discussed. Brief description of the hypotheses (MELS) input method in studies of near-surface wave phenomena is given in [9], [10], [12].

In the second chapter the effect of weak inhomogeneities of the material and the surface of the elastic layer-waveguide on the propagation of high-frequency, pure elastic shear (SH) wave signal. Propagation of high frequency pure shear (SH) wave signal in elastic layer-waveguide of weakly inhomogeneous material with mechanical free or rigidly clamped perfectly smooth surfaces is investigated. Analysis of amplitude-frequency behaviors of propagating normal waves in weakly inhomogeneous elastic waveguide are given in [25], [54].

The impact of the weak inhomogeneity of mechanically free or rigidly clamped surfaces of homogeneous elastic layer-waveguide on propagation of pure shear *(SH)* high frequency signal is investigated. The comparative analysis of the effects of weak inhomogeneity of the

material and surfaces on the propagation of high-frequency (SH) shear wave signals in the elastic layer-waveguide is given in [12], [13], [53].

In the third chapter the influence of surface weak inhomogeneities on the propagation of high-frequency (SH) electroelastic wave signal in the piezoelectric layer-waveguide is investigated.

Propagation of high-frequency electroelastic (SH) wave signal in homogeneous piezoelectric layer-waveguide with mechanically free, as well as with rigidly clamped, by perfect conductor (or dielectric), weakly inhomogeneous surfaces is observed in [16],[17], [59]. Comparative analysis of the effects of different surface conditions on distributions of characteristics of the normal waves is given.

In the last section 3.3 we consider the propagation of high-frequency electroelastic (SH) wave signal in homogeneous piezoelectric layer-waveguide with surface weak inhomogeneities filled with perfect conductor (or dielectric) [17].

In conclusion the main results obtained in the thesis are given.

The reference list includes 112 references used by the author while writing the thesis.

CHAPTER 1

BASIC RELATIONS AND MODELING ISSUES IN PROBLEM OF PROPAGATION OF MODELING OF HIGH FREQUENCY ELECTROELASTIC SHEAR (SH) WAVE SIGNAL IN ELECTROELASTIC WAVEGUIDES

1.1 Main equations, material relations and boundary conditions of linear electroelasticity for piezoelectric layer waveguide with material and surface inhomogeneities

Mechanical, electrical, thermal and now on magnetic properties in newly created materials, in real piezoelectric crystals are coupled, and their study should be done together. The investigation of these properties and their coupling can be done using thermodynamic methods and thermodynamic potentials, which are available in different well-known references [6, 76, 79].

For internal energy U of magneto-electro-thermo-elastic medium, by selecting the elastic deformation u_{ij}^{*}, where $i, j = 1,2,3$, electric and magnetic fields strains E_i and H_k, and temperature T as independent variables, we will obtain

$$dU = \sigma_{ij} du_{ij} + D_m dE_m + B_k dH_k + SdT, \tag{1.1.1}$$

where $u_{ij} = (1/2) \cdot \left(\partial u_i / \partial x_j + \partial u_j / \partial x_i \right)$ is the tensor of elastic deformation, σ_{ij} is the mechanical stress, S is the entropy density, T is the temperature, E_i and H_k are the strains of the electric and magnetic fields, respectively, D_n and B_i are the induction vectors of electric and magnetic fields, respectively. By introducing the designations $\sigma_{ij} = \left(\partial U / \partial u_{ij} \right)_{D,B,S}$ for mechanical stresses; $D_m = \left(\partial U / \partial E_m \right)_{u,H,T}$ for electric field induction; $B_k = \left(\partial U / \partial H_k \right)_{E,u,T}$ for magnetic field induction; $S = \left(\partial U / \partial T \right)_{E,H,u}$ for entropy density, the full differentials get the forms

$$d\sigma_{ij} = \left(\frac{\partial \sigma_{ij}}{\partial u_{nk}} \right)_{E,H,T} du_{nk} + \left(\frac{\partial \sigma_{ij}}{\partial E_m} \right)_{u,H,T} dE_m + \left(\frac{\partial \sigma_{ij}}{\partial H_k} \right)_{E,u,T} dH_k + \left(\frac{\partial \sigma_{ij}}{\partial T} \right)_{E,H,u} dT, \tag{1.1.2}$$

$$dD_m = \left(\frac{\partial D_m}{\partial u_{nk}}\right)_{E,H,T} du_{nk} + \left(\frac{\partial D_m}{\partial E_k}\right)_{u,H,T} dE_k + \left(\frac{\partial D_m}{\partial H_k}\right)_{E,u,T} dH_k + \left(\frac{\partial D_m}{\partial T}\right)_{E,H,u} dT\,, \qquad (1.1.3)$$

$$dB_m = \left(\frac{\partial B_m}{\partial u_{nk}}\right)_{E,H,T} du_{nk} + \left(\frac{\partial B_m}{\partial E_k}\right)_{u,H,T} dE_k + \left(\frac{\partial B_m}{\partial H_k}\right)_{E,u,T} dH_k + \left(\frac{\partial B_m}{\partial T}\right)_{E,H,u} dT\,, \qquad (1.1.4)$$

$$dS = \left(\frac{\partial S}{\partial u_{nk}}\right)_{E,H,T} du_{nk} + \left(\frac{\partial S}{\partial E_m}\right)_{u,H,T} dE_m + \left(\frac{\partial S}{\partial H_k}\right)_{E,u,T} dH_k + \left(\frac{\partial S}{\partial T}\right)_{E,H,u} dT\,. \qquad (1.1.5)$$

Material equations of state in the linear theory of electro-magneto-thermo-elasticity are obtained by integrating these equalities, assuming in them all sixteen partial derivatives to be constants [76, 79]

$\left(\partial\sigma_{ij}/\partial u_{nk}\right)_{E,H,T} \equiv c_{ijnk}$ are the modules of elasticity of anisotropic medium, which form a tensor of rank four(4),

$\left(\partial\sigma_{ij}/\partial E_m\right)_{u,H,T} = -\left(\partial D_m/\partial u_{ij}\right)_{E,H,T} \equiv e_{ijm}$ - piezoelectric constants which form a tensor of the third rank,

$\left(\partial\sigma_{ij}/\partial H_k\right)_{E,u,T} = -\left(\partial B_m/\partial u_{nk}\right)_{E,H,T} \equiv g_{ijk}$ are the piezomagnetic constants, which form a tensor of rank 3,

$\left(\partial\sigma_{ij}/\partial T\right)_{E,H,u} = -\left(\partial S/\partial u_{nk}\right)_{E,H,T} \equiv \lambda_{ij}$ are the coefficients of temperature stresses, which form a tensor of rank 2,

$\left(\partial D_m/\partial E_k\right)_{u,H,T} \equiv \varepsilon_{mk}$ are the components of dielectric permittivity of anisotropic medium, which form a tensor of rank 2,

$\left(\partial B_m/\partial H_k\right)_{E,u,T} \equiv \mu_{mk}$ are the components of magnetic permeability of anisotropic medium, which form a tensor of rank 2,

$\left(\partial D_m/\partial H_k\right)_{E,u,T} = \left(\partial B_m/\partial E_k\right)_{u,H,T} \equiv h_{mk}$ is the tensor of coefficients of electromagnetic contacts, of rank 2,

$\left(\partial D_m/\partial T\right)_{E,H,u} = \left(\partial S/\partial E_m\right)_{u,H,T} \equiv p_m$ are the pyroelectric coefficients,

$\left(\partial B_m/\partial T\right)_{E,H,u} = \left(\partial S/\partial H_k\right)_{E,u,T} \equiv q_m$ are the pyro-magnetic coefficients,

$\left(\partial S/\partial T\right)_{E,H,u} \square \left(\rho/T_0\right)\cdot c$, where c is the medium thermal capacity, ρ is the material density, T_0 is the initial temperature.

As a result, integrating the differential relations (1.1.2)÷(1.1.5), we obtain the following linear material equations of the medium for mechanical stresses $\sigma_{ij}(u_{nm},E_k,\theta)$, electric field displacements (electric induction) $D_j(u_{nm},E_k,\theta)$, magnetic field induction $B_j(u_{nm},E_k,\theta)$ and entropy increment $\Delta S(u_{nm},E_k,\theta)$, depending on elastic deformations u_{ij}, electric field stress E_n and temperature changes $\theta = T - T_0$:

$$\sigma_{ij} = c_{ijnk}u_{nk} - e_{ijm}E_m - g_{ijk}H_k - \lambda_{ij}\theta, \tag{1.1.6}$$

$$D_m = e_{mnk}u_{nk} + \varepsilon_{mk}E_k + h_{mn}H_n + p_m\theta, \tag{1.1.7}$$

$$B_m = g_{mnk}u_{nk} + h_{mk}E_k + \mu_{mn}H_n + q_m\theta, \tag{1.1.8}$$

$$S = \lambda_{nk}u_{nk} + p_mE_m + q_kH_k + \frac{\rho c}{T_0}\cdot\theta. \tag{1.1.9}$$

The obtained material equations of state describe the interaction of the elastic, electromagnetic and temperature fields in the medium, explicitly expressed by heat-elastic, piezoelectric and piezomagnetic material properties simultaneously. At some natural materials, some properties are absent or results to negligible effects in computations. In such cases these effects are not considered in the material relations.

The setting of material relations (1.1.6)÷(1.1.9) in the equations of motion of the medium, Maxwell's equations and thermal conductivity equation leads to a coupled system of governing equations of electro-magneto-thermo-elasticity. Mass forces of electromagnetic nature resulting from the interaction of induced currents with electromagnetic field, besides given terms in the material relations, are usually not considered in formulation of motion equations of the medium for these materials (materials with linear interactions of physico-mechanical fields):

$$\sigma_{ij,j} = \rho\ddot{u}_i. \tag{1.1.10}$$

In the absence of free electric charges and conduction current the electromagnetic field in the medium is described by the static Maxwell equations:

$$\in_{ijk} E_{j,k} + \dot{B}_i = 0; \qquad \in_{ijk} H_{j,k} - \dot{D}_i = 0; \tag{1.1.11}$$

$$B_{j,j} = 0; \qquad D_{n,n} = 0. \tag{1.1.12}$$

Combined solution of the motion equation (1.1.10) and the Maxwell equations (1.1.11), (1.1.12), describes elastic waves and associated electromagnetic field, as well as electromagnetic waves, accompanied by medium deformation. It follows from the above equations, that if the speed of the elastic wave is $V = V(\omega)$, the corresponding speed of electromagnetic wave is $\mathrm{v}(\omega) \sim 10^5 \cdot V(\omega)$. Therefore, the magnetic field can be neglected in the study of elastic wave propagation, which is due to electric field, propagating together with elastic wave with speed $V(\omega)$ the electric field, which is due to magnetic field propagating with the same speed $V(\omega)$ can be neglected as well. They are as small as $V(\omega)/\mathrm{v}(\omega) \sim 10^{-5}$. Based on this, it is permissible to use the quasi-static approximation of the electromagnetic field in most of problems associated with propagation of electro-magneto-acoustic wave

$$\in_{ijk} E_{j,k} = -\dot{B}_i \cong 0; \qquad D_{n,n} = 0; \tag{1.1.13}$$

for electric oscillations accompanying acoustic wave and

$$\in_{ijk} H_{j,k} = \dot{D}_i \cong 0; \qquad B_{j,j} = 0; \tag{1.1.14}$$

for magnetic oscillations accompanying acoustic wave. In these approximations, the electric and magnetic fields will be potential and will be expressed via scalar potentials, respectively,

$$E_n = -\varphi_{,n}; \tag{1.1.15}$$

$$H_j = -\psi_{,j}. \tag{1.1.16}$$

Thus, in the full system of equations for the linear homogeneous electro-magneto-thermo-elastic medium from Maxwell's equations (1.1.11) and (1.1.12), there remain the equations of statics together with potentials of electric and magnetic fields (1.1.15) and (1.1.16), respectively.

Taking into account the similarity of interrelation of physico-mechanical fields in the material equations (1.1.6)÷(1.1.9), we can assume, that phenomena arising due to interaction of acoustic waves with given physical fields will also be identical. Based on aforesaid, without losing the generality of argumentation, as well as avoiding bulky formulas, we shall consider only the electroacoustic interaction in piezo-electric media, where the complete system will be

$$\sigma_{ij,j} = \rho\ddot{u}_i; \qquad D_{n,n} = 0; \qquad \text{with respect} \qquad E_n = -\varphi_{,n}. \tag{1.1.17}$$

Material relations (1.1.6)÷(1.1.9) can be reduced also for mechanical stresses and induction of electric field (electric displacement) to the known form

$$\sigma_{ij} = c_{ijnk}u_{n,k} + e_{mij}\varphi_{,m}; \tag{1.1.18}$$

$$D_m = e_{mnk}u_{n,k} - \varepsilon_{mk}\varphi_{,k}. \tag{1.1.19}$$

Material equations are true in the case of homogeneous medium and for medium with ordered inhomogeneity (see below), in which physico-mechanical characteristics of the material, $\gamma \in \left\{c_{ijnk}, \rho, e_{mij}, \varepsilon_{ik}\right\}$, form the tensors describing the specific anisotropy of the piezo-dielectric material and determine the structural composition of the associated wave field parameters.

$$\begin{pmatrix} \begin{pmatrix} * & * & * & * & * & * \\ * & * & * & * & * & * \\ * & * & \hat{c}_{ijnk} & * & * & * \\ * & * & * & * & * & * \\ * & * & * & * & * & * \\ * & * & * & * & * & * \end{pmatrix}_{6\times 6} & \begin{pmatrix} * & * & * \\ * & * & * \\ * & e_{ijm} & * \\ * & * & * \\ * & * & * \\ * & * & * \end{pmatrix}_{3\times 6} \\ \begin{pmatrix} * & * & * & * & * & * \\ * & * & e_{mij} & * & * & * \\ * & * & * & * & * & * \end{pmatrix}_{6\times 3} & \begin{pmatrix} * & * & * \\ * & \varepsilon_{nk} & * \\ * & * & * \end{pmatrix}_{3\times 3} \end{pmatrix}_{9\times 9}, \tag{1.1.20}$$

In general case of anisotropy and inhomogeneity of piezoelectric material, the quasi-static equations of electroelasticity are obtained from (1.1.17) taking into account the material relations (1.1.18) and (1.1.19) for inhomogeneous medium:

$$\sigma_{ij}(x_p) = c_{ijnk}(x_p)\cdot u_{n,k}(x_p) + e_{mij}\cdot\varphi_{,m}(x_p), \tag{1.1.21}$$

$$D_m(x_p) = e_{mnk}(x_p)\cdot u_{n,k}(x_p) - \varepsilon_{mk}(x_p)\cdot\varphi_{,k}(x_p), \tag{1.1.22}$$

which can be written in the form of system of partial differential equations with variable coefficients:

$$\begin{aligned} &c_{ijnk}(x_p)\cdot u_{n,jk}(x_p;t) + e_{mij}(x_p)\cdot\varphi_{,mj}(x_p;t) + c_{ijnk,j}(x_p)\cdot u_{n,k}(x_p;t) + \\ &+e_{mij,j}(x_p)\cdot\varphi_{,m}(x_p;t) = \rho(x_p)\cdot\ddot{u}_i(x_p;t), \end{aligned} \tag{1.1.23}$$

$$\varepsilon_{mj}(x_p)\cdot\varphi_{,mj}(x_p;t)+\varepsilon_{mj,j}(x_p)\cdot\varphi_{,m}(x_p;t)=$$
$$=e_{mij}(x_p)\cdot u_{i,jm}(x_p;t)+e_{mij,j}(x_p)\cdot u_{i,m}(x_p;t). \qquad (1.1.24)$$

For investigation of electroelastic wave signal propagation in two-layer waveguide consisting of two piezoelectric inhomogeneous layers contacted with rough surface $x_\gamma = h_*(x_\alpha, x_\beta)$, the system of equations (1.1.23) and (1.1.24) are solving in each mono layer, together with corresponding continuity conditions of electromechanical fields at contact surface of mediums.

For completeness of the basic relations of mathematical boundary value problem, generated in the waveguides, it is necessary to attach boundary conditions on the surface of each component of the composite waveguide to equations (1.1.23) and (1.1.24). In general, boundary conditions must be adequately formulated in the internal problem and provide compactness of the mathematical boundary value problem.

Formally, continuity conditions of mechanical fields in boundary mediums for electro-(magneto-thermo)-elastic medium are the usual relations of the elasticity theory. These are the continuity condition for mechanical stresses $\sigma_{ij}^{(m)}$ at the interfaces of the mediums $\Sigma_m(x_i)$:

$$\left(\sigma_{ij}^{(1)}-\sigma_{ij}^{(2)}\right)\cdot n_j\Big|_{\Sigma_m(x_i)}=0; \qquad (1.1.25)$$

as well as the continuity conditions for elastic displacements $u_k^{(m)}$ at the interfaces of the mediums $\Sigma_m(x_i)$:

$$u_k^{(1)}\Big|_{\Sigma_m(x_i)}=u_k^{(2)}\Big|_{\Sigma_m(x_i)}. \qquad (1.1.26)$$

In layered waveguides between two boundary material layers can exist as the conditions of full contact (1.1.25) and (1.1.26), as well as the mixed surface conditions of incomplete contact. Since in problems of electro-(magneto-) elasticity, the vacuum is considered to be interacting “medium” too, conditions of mechanically open borders on the outer surfaces of the waveguide must be imposed:

$$\sigma_{ij}^{(1)}\cdot n_j\Big|_{\Sigma_0(x_i)}=0. \qquad (1.1.27)$$

In the case of a rigidly fixed outer surface of the waveguide we will have conditions of consolidation:

$$u_k^{(1)}\Big|_{\Sigma_0(x_i)} = 0. \qquad (1.1.28)$$

In the electroelastic medium, conjugacy conditions on the medium interfaces are represented in the form of continuity of the tangential components of electric field strength and normal components of electric displacements in boundary mediums. Taking into account (1.1.13), these conditions can be written on the medium interfaces, as follows:

$$\varphi^{(1)}\Big|_{\Sigma_m(x_i)} = \varphi^{(2)}\Big|_{\Sigma_m(x_i)}; \qquad (1.1.29)$$

$$\left(D_j^{(1)} - D_j^{(2)}\right)\cdot n_j\Big|_{\Sigma_m(x_i)} = 0. \qquad (1.1.30)$$

It also follows from (1.1.13), that in these problems the normal components of strengths and tangential components of induction of magnetic field of order $V(\omega)/\mathrm{v}(\omega) \square 10^{-5}$ in the boundary mediums will be continuous, which are determined from

$$\frac{\partial B_i}{\partial t} = \in_{ijk} \frac{\partial \varphi}{\partial x_k \partial x_j}. \qquad (1.1.31)$$

As in the case of surface mechanical conditions, electrical conditions on the surface of the medium, may be specified differently. In the case of metalized (shielded) surface of the dielectric material, instead of conditions (1.1.29) and (1.1.30), “electrically closed” boundary condition is specified,

$$\varphi^{(1)}\Big|_{\Sigma_0(x_i)} = 0. \qquad (1.1.32)$$

When adjacent dielectric (not piezoelectric) layer has very small dielectric permittivity, then $\varepsilon_{ik}^{(1)} \square \varepsilon_{\alpha\gamma}^{(2)}$, implying $\varepsilon_{\alpha\gamma}^{(2)} \big/ \varepsilon_{ik}^{(1)} \to 0$ and instead of surface conditions (1.1.29) and (1.1.30) we merely have condition of "electrically open" boundaries (the electric field is seeping to the outer medium):

$$D_j^{(1)} \cdot n_j\Big|_{\Sigma_0(x_i)} = 0. \qquad (1.1.33)$$

The diversity of mechanical and electrical surface conditions allows us to technologically form physically different surfaces by selection of different combinations of comparable boundary conditions, which in turn determine the dispersion of propagation and localization ability of high frequency wave signals near that surface. Here, as in the case of the equations of linear electroelasticity (1.1.17), without losing the generality, we present the continuity conditions of physico-mechanical fields on the surfaces of piezoelectric layer

$\{|x_1|<\infty;\ h_-(x_1,x_3)\le x_2\le h_+(x_1,x_3);\ |x_1|<\infty\}$ (see Fig. 1.1.1), with material ratios (1.1.18), (1.1.19), and geometrically heterogeneous surfaces $x_1=h_-(x_1,x_3)$, $x_2=h_+(x_1,x_3)$, where $\{h_-(x_1,x_3);\ h_+(x_1,x_3)\}\in L_1\{\square\}$. Moreover, the surface $x_1=h_-(x_1,x_3)$ of the piezoelectric layer is bordered with vacuum, and the other surface $x_2=h_+(x_1,x_3)$ is bordered by another piezoelectric layer.

In the case of non-smooth surface $x_2=h_+(x_1,x_3)$ of the division to two media, the boundary conditions of the linear electroelasticity will be the continuity conditions of the mechanical and electrical fields

$$\begin{bmatrix}\sigma_{ij}^{(1)}(x_1,h_+(x_1,x_3),x_3,t)-\\ -\sigma_{ij}^{(2)}(x_1,h_+(x_1,x_3),x_3,t)\end{bmatrix}\cdot n_j^{(+)}\left(x_1,h_+(x_1,x_3),x_3\right)=0, \tag{1.1.34}$$

$$\begin{bmatrix}D_j^{(1)}(x_1,h_+(x_1,x_3),x_3,t)-\\ -D_j^{(2)}(x_1,h_+(x_1,x_3),x_3,t)\end{bmatrix}\cdot n_j^{(+)}\left(x_1,h_+(x_1,x_3),x_3\right)=0, \tag{1.1.35}$$

$$u_i^{(1)}(x_1,h_+(x_1,x_3),x_3,t)=u_i^{(2)}(x_1,h_+(x_1,x_3),x_3,t), \tag{1.1.36}$$

$$\varphi^{(1)}(x_1,h_+(x_1,x_3),x_3,t)=\varphi^{(2)}(x_1,h_+(x_1,x_3),x_3,t). \tag{1.1.37}$$

On the mechanically free surface $x_2=h_-(x_1,x_3)$, where the piezoelectric layer is bordered with vacuum, the continuity conditions of the electric and elastic fields are written as

$$\left[\sigma_{ij}^{(1)}(x_1,h_-(x_1,x_3),x_3,t)\right]\cdot n_j^{(-)}\left(x_1,h_-(x_1,x_3),x_3\right)=0, \tag{1.1.38}$$

$$\begin{bmatrix}D_j^{(1)}(x_1,h_-(x_1,x_3),x_3,t)-\\ -D_j^{(e)}(x_1,h_-(x_1,x_3),x_3,t)\end{bmatrix}\cdot n_j^{(-)}\left(x_1,h_-(x_1,x_3),x_3\right)=0, \tag{1.1.39}$$

$$\varphi^{(1)}(x_1,h_-(x_1,x_3),x_3,t)=\varphi^{(e)}(x_1,h_-(x_1,x_3),x_3,t). \tag{1.1.40}$$

If the mechanically free surface $x_2=h_-(x_1,x_3)$ is covered with grounded thin, good well-conductive layer, then the conditions (1.1.39), (1.1.40) will be replaced by the condition of electrically closed boundary

$$\varphi^{(1)}(x_1,h_-(x_1,x_3),x_3,t)=0. \tag{1.1.41}$$

If the dielectric permittivity of the piezoelectric is large enough, i.e. $\varepsilon_{ik}^{(1)}\ \square\ \varepsilon_0$, then the conditions (1.1.39), (1.1.40) will replace the condition of electrically open boundary

$$\left[D_j^{(1)}(x_1, h_-(x_1, x_3), x_3, t) \right] \cdot n_j^{(-)}\left(x_1, h_-(x_1, x_3), x_3\right) = 0. \quad (1.1.42)$$

It is obvious that, the full continuity conditions of elastic field (1.1.34) and (1.1.36) were replaced by the condition (1.1.38) in the case of the mechanically free surface. However, if the surface is rigidly fixed, then the full continuity conditions of the elastic field (1.1.34) and (1.1.36) are replaced by the condition of clamping

$$u_i^{(1)}(x_1, h_+(x_1, x_3), x_3, t) = 0. \quad (1.1.43)$$

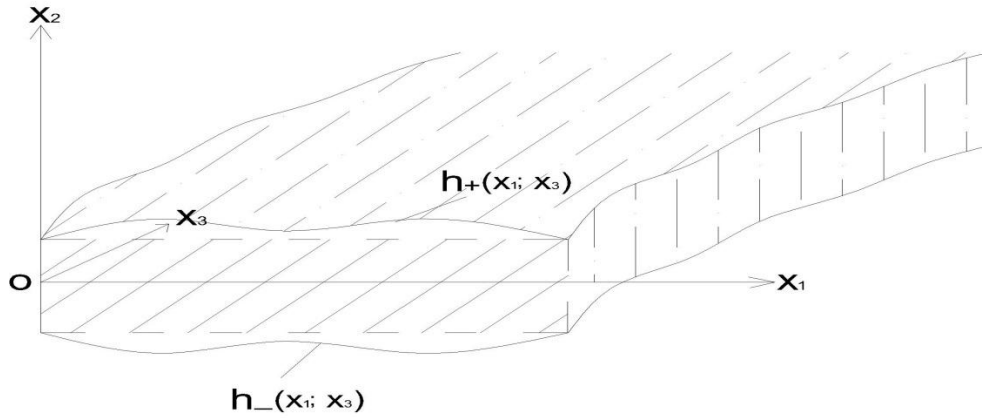

Fig. 1.1.1 Homogeneous piezoelectric waveguide with weakly inhomogeneous surfaces

Taking into account, that the conditions of mechanically free boundary (1.1.38) and clamping (1.1.43) are limiting conditions imposed on the mechanical field, and the conditions of electrically "open" (1.1.42) and electrically "closed" (1.1.41) boundaries similarly are limiting on electric fields, except natural combinations of (1.1.34)÷(1.1.37) and (1.1.38)÷(1.1.40), introduce frequently met some combinations of surface conditions compact from a mathematical point of view:

a) Surface $x_2 = h_*(x_1, x_3)$ of piezoelectric layer is rigidly fixed with well conductor or electrically conductive adhesive. Then the electro-mechanical conditions on the surface take rather simple forms:

$$u_i^{(1)}(x_1, h_*(x_1, x_3), x_3, t) = 0, \quad (1.1.44)$$

$$\varphi^{(1)}(x_1, h_*(x_1, x_3), x_3, t) = 0. \quad (1.1.45)$$

b) Mechanically free surface $x_2 = h_*(x_1, x_3)$ of piezoelectric layer is with large dielectric permittivity. Then the electro-mechanical conditions on the surface also acquire simple forms:

$$\left[\sigma_{ij}^{(1)}(x_1, h_*(x_1, x_3), x_3, t)\right] \cdot n_j^{(*)}\left(x_1, h_*(x_1, x_3), x_3\right) = 0, \tag{1.1.46}$$

$$\left[D_j^{(1)}(x_1, h_*(x_1, x_3), x_3, t)\right] \cdot n_j^{(*)}\left(x_1, h_*(x_1, x_3), x_3\right) = 0. \tag{1.1.47}$$

c) Mechanically free surface $x_2 = h_*(x_1, x_3)$ of piezoelectric layer is covered by electrically conductive nanocoating. Then the electro-mechanical conditions on the surface again acquire simple forms:

$$\left[\sigma_{ij}^{(1)}(x_1, h_*(x_1, x_3), x_3, t)\right] \cdot n_j^{(*)}\left(x_1, h_*(x_1, x_3), x_3\right) = 0, \tag{1.1.48}$$

$$\varphi^{(1)}(x_1, h_*(x_1, x_3), x_3, t) = 0. \tag{1.1.49}$$

d) Surface $x_2 = h_*(x_1, x_3)$ of piezoelectric layer is rigidly fixed with "soft" dielectric, which has very small dielectric permittivity compared with the piezoelectric, i.e $\varepsilon_{ik}^{(1)} \square \varepsilon_{\alpha\gamma}^{(2)}$. Then the electro-mechanical conditions on the surface admits simple forms:

$$u_i^{(1)}(x_1, h_*(x_1, x_3), x_3, t) = 0, \tag{1.1.50}$$

$$\left[D_j^{(1)}(x_1, h_*(x_1, x_3), x_3, t)\right] \cdot n_j^{(*)}\left(x_1, h_*(x_1, x_3), x_3\right) = 0. \tag{1.1.51}$$

The appearance of the unit normal with variable components $n_j^{(*)}\left(x_\alpha, h_*(x_\alpha, x_\gamma), x_\gamma\right)$, due to the non-smoothness of the surface $x_\gamma = h_*(x_\alpha, x_\beta)$ in the boundary conditions naturally complicates the boundary value problem.

As physical anisotropy and inhomogeneity of the medium an important role in the problems of electro-magneto-elasticity will play the geometrical heterogeneity of the surface, beginning with the question of the possible separation of plane and antiplane deformations of electro-active fields.

The investigation of possible formulation of two-dimensional problems in a body with non-smooth surfaces shows that for arbitrary $x_\gamma = h_*(x_\alpha, x_\beta)$ the problem of plane deformation $\left\{u_\alpha\left(x_\alpha, x_\beta, t\right);\ u_\beta\left(x_\alpha, x_\beta, t\right);\ 0;\ \varphi\left(x_\alpha, x_\beta, t\right)\right\}$ or antiplane deformation $\left\{0;\ 0;\ u_\gamma\left(x_\alpha, x_\beta, t\right);\ \varphi\left(x_\alpha, x_\beta, t\right)\right\}$ could not be separated.

It is clear from geometric considerations, that the separation of these electro-active deformation fields is possible if the surface irregularities are parallel to the axis ox_γ. Then

the tangent plane at any point of the body surface is perpendicular to the coordinate plane $\{x_\alpha, 0, x_\beta\}$ or to any line $x_\gamma = const$. The equation of a surface line on these lines can be written in the form $x_\alpha = H(x_\beta)$ or $x_\beta = L(x_\alpha)$. The unit normal with variable components $n_j^{(*)}\left(x_\alpha, h_*(x_\alpha, x_\gamma), x_\gamma\right)$ will not change the direction on the axis ox_γ, and therefore in two-dimensional problems [9, 10] we can take

$$n_j^{(*)}\left(x_\alpha, L(x_\alpha)\right) = \left\{ \frac{\partial L(x_\alpha)/\partial x_\alpha}{\sqrt{1+\left[\partial L(x_\alpha)/\partial x_\alpha\right]^2}};\ \frac{1}{\sqrt{1+\left[\partial L(x_\alpha)/\partial x_\alpha\right]^2}};\ 0 \right\} \tag{1.1.52}$$

or

$$n_j^{(*)}\left(H(x_\beta), x_\beta\right) = \left\{ \frac{1}{\sqrt{1+\left[\partial H(x_\beta)/\partial x_\beta\right]^2}};\ \frac{\partial H(x_\beta)/\partial x_\beta}{\sqrt{1+\left[\partial H(x_\beta)/\partial x_\beta\right]^2}};\ 0 \right\} \tag{1.1.53}$$

Taking into account the changes of the surface normal (1.1.52), the full continuity conditions (1.1.34)÷(1.1.37) of the electromechanical fields on the surface $x_\beta = L(x_\alpha)$ in the problem of electro-active plane deformation $\left\{u_\alpha\left(x_\alpha, x_\beta, t\right);\ u_\beta\left(x_\alpha, x_\beta, t\right);\ 0;\ \varphi\left(x_\alpha, x_\beta, t\right)\right\}$ can be written in these forms

$$\begin{aligned}
&\left[\sigma_{\alpha\alpha}^{(1)}(x_\alpha, L(x_\alpha), t) - \sigma_{\alpha\alpha}^{(2)}(x_1, L(x_\alpha), t)\right]\cdot L_{,\alpha}(x_\alpha) + \\
&+\left[\sigma_{\beta\alpha}^{(1)}(x_\alpha, L(x_\alpha), t) - \sigma_{\beta\alpha}^{(2)}(x_\alpha, L(x_\alpha), t)\right] = 0, \\
&\left[\sigma_{\beta\alpha}^{(1)}(x_\alpha, L(x_\alpha), t) - \sigma_{\beta\alpha}^{(2)}(x_\alpha, L(x_\alpha), t)\right]\cdot L_{,\alpha}(x_\alpha) + \\
&+\left[\sigma_{\beta\beta}^{(1)}(x_\alpha, L(x_\alpha), t) - \sigma_{\beta\beta}^{(2)}(x_\alpha, L(x_\alpha), t)\right] = 0,
\end{aligned} \tag{1.1.54}$$

$$\begin{aligned}
&\left[D_\alpha^{(1)}(x_\alpha, L(x_\alpha), t) - D_\alpha^{(2)}(x_\alpha, L(x_\alpha), t)\right]\cdot L_{,\alpha}(x_\alpha) + \\
&+\left[D_\beta^{(1)}(x_\alpha, L(x_\alpha), t) - D_\beta^{(2)}(x_\alpha, L(x_\alpha), t)\right] = 0,
\end{aligned} \tag{1.1.55}$$

$$\begin{aligned}
&u_\alpha^{(1)}(x_\alpha, L(x_\alpha), t) = u_\alpha^{(2)}(x_\alpha, L(x_\alpha), t), \\
&u_\beta^{(1)}(x_\alpha, L(x_\alpha), t) = u_\beta^{(2)}(x_\alpha, L(x_\alpha), t),
\end{aligned} \tag{1.1.56}$$

$$\varphi^{(1)}(x_\alpha, L(x_\alpha), t) = \varphi^{(2)}(x_\alpha, L(x_\alpha), t), \tag{1.1.57}$$

which include material ratios of non-zero characteristics of electromechanical fields for plane deformation, i.e.

$$\begin{aligned}
\sigma_{\alpha\alpha}(x_\alpha,x_\beta) &= c_{\alpha\alpha nk}(x_\alpha,x_\beta)\cdot u_{n,k}(x_\alpha,x_\beta)+\\
&+e_{\alpha ij}(x_\alpha,x_\beta)\cdot\varphi_{,\alpha}(x_\alpha,x_\beta)+e_{\beta ij}(x_\alpha,x_\beta)\cdot\varphi_{,\beta}(x_\alpha,x_\beta),\\
\sigma_{\alpha\beta}(x_\alpha,x_\beta) &= c_{\alpha\beta nk}(x_\alpha,x_\beta)\cdot u_{n,k}(x_\alpha,x_\beta)+\\
&+e_{\alpha ij}(x_\alpha,x_\beta)\cdot\varphi_{,\alpha}(x_\alpha,x_\beta)+e_{\beta ij}(x_\alpha,x_\beta)\cdot\varphi_{,\beta}(x_\alpha,x_\beta),\\
\sigma_{\beta\beta}(x_\alpha,x_\beta) &= c_{\beta\beta nk}(x_\alpha,x_\beta)\cdot u_{n,k}(x_\alpha,x_\beta)+\\
&+e_{\alpha ij}(x_\alpha,x_\beta)\cdot\varphi_{,\alpha}(x_\alpha,x_\beta)+e_{\beta ij}(x_\alpha,x_\beta)\cdot\varphi_{,\beta}(x_\alpha,x_\beta),
\end{aligned} \tag{1.1.58}$$

$$\begin{aligned}
D_\alpha(x_\alpha,x_\beta) &= e_{\alpha nk}(x_\alpha,x_\beta)\cdot u_{n,k}(x_\alpha,x_\beta)-\varepsilon_{\alpha k}(x_\alpha,x_\beta)\cdot\varphi_{,k}(x_\alpha,x_\beta),\\
D_\beta(x_\alpha,x_\beta) &= e_{\beta nk}(x_\alpha,x_\beta)\cdot u_{n,k}(x_\alpha,x_\beta)-\varepsilon_{\beta k}(x_\alpha,x_\beta)\cdot\varphi_{,k}(x_\alpha,x_\beta).
\end{aligned} \tag{1.1.59}$$

Here the summation goes over $n;k\in\{\alpha;\beta\}$.

Change of surface normal (1.1.52) converts the boundary conditions of electromechanical fields of mechanically free surface (1.1.38)÷(1.1.40) on the line $x_\beta = L(x_\alpha)$ of the medium separation from vacuum into

$$\begin{aligned}
&\sigma_{\alpha\alpha}(x_\alpha,L(x_\alpha),t)\cdot L_{,\alpha}(x_\alpha)+\sigma_{\alpha\beta}(x_\alpha,L(x_\alpha),t)=0,\\
&\sigma_{\beta\alpha}(x_\alpha,L(x_\alpha),t)\cdot L_{,\alpha}(x_\alpha)+\sigma_{\beta\beta}(x_\alpha,L(x_\alpha),t)=0,
\end{aligned} \tag{1.1.60}$$

$$\begin{aligned}
&\left[D_\alpha^{(1)}(x_\alpha,L(x_\alpha),t)+\varepsilon_0\varphi_{,\alpha}^{(e)}(x_\alpha,L(x_\alpha),t)\right]\cdot L_{,\alpha}(x_\alpha)+\\
&+\left[D_\beta^{(1)}(x_\alpha,L(x_\alpha),t)+\varepsilon_0\varphi_{,\beta}^{(e)}(x_\alpha,L(x_\alpha),t)\right]=0,
\end{aligned} \tag{1.1.61}$$

$$\varphi(x_\alpha,L(x_\alpha),t)=\varphi^{(e)}(x_\alpha,L(x_\alpha),t). \tag{1.1.62}$$

Taking into account the changes of the surface normal (1.1.52), the full continuity conditions (1.1.34)÷(1.1.37) of the electromechanical fields on the surface of mediums separation $x_\beta = L(x_\alpha)$, in the problem of electro-active antiplane deformation $\left\{0;\ 0;\ u_\gamma\left(x_\alpha,x_\beta,t\right);\ \varphi\left(x_\alpha,x_\beta,t\right)\right\}$ are also simplified:

$$\begin{aligned}
&\left[\sigma_{\gamma\alpha}^{(1)}(x_\alpha,L(x_\alpha),t)-\sigma_{\gamma\alpha}^{(2)}(x_\alpha,L(x_\alpha),t)\right]\cdot L_{,\alpha}(x_\alpha)+\\
&+\left[\sigma_{\gamma\beta}^{(1)}(x_\alpha,L(x_\alpha),t)-\sigma_{\gamma\beta}^{(2)}(x_\alpha,L(x_\alpha),t)\right]=0,
\end{aligned} \tag{1.1.63}$$

$$\begin{aligned}
&\left[D_\alpha^{(1)}(x_\alpha,L(x_\alpha),t)-D_\alpha^{(2)}(x_\alpha,L(x_\alpha),t)\right]\cdot L_{,\alpha}(x_\alpha)+\\
&+\left[D_\beta^{(1)}(x_\alpha,L(x_\alpha),t)-D_\beta^{(2)}(x_\alpha,L(x_\alpha),t)\right]=0,
\end{aligned} \tag{1.1.64}$$

$$u_\gamma^{(1)}(x_\alpha,L(x_\alpha),t)=u_\gamma^{(2)}(x_\alpha,L(x_\alpha),t), \tag{1.1.65}$$

$$\varphi^{(1)}(x_\alpha, L(x_\alpha), t) = \varphi^{(2)}(x_\alpha, L(x_\alpha), t), \tag{1.1.66}$$

The material ratios of non-zero characteristics of electromechanical field of anti-plane deformation are included in the surface conditions (1.1.63)-(1.1.66)

$$\begin{aligned}\sigma_{\gamma\alpha}(x_\alpha, x_\beta) &= c_{\alpha\gamma\gamma k}(x_\alpha, x_\beta)\cdot u_{\gamma,k}(x_\alpha, x_\beta) + \\ &+ e_{\alpha ij}(x_\alpha, x_\beta)\cdot \varphi_{,\alpha}(x_\alpha, x_\beta) + e_{\beta ij}(x_\alpha, x_\beta)\cdot \varphi_{,\beta}(x_\alpha, x_\beta),\end{aligned} \tag{1.1.67}$$

$$\begin{aligned}\sigma_{\gamma\beta}(x_\alpha, x_\beta) &= c_{\gamma\beta\gamma k}(x_\alpha, x_\beta)\cdot u_{\gamma,k}(x_\alpha, x_\beta) + \\ &+ e_{\alpha ij}(x_\alpha, x_\beta)\cdot \varphi_{,\alpha}(x_\alpha, x_\beta) + e_{\beta ij}(x_\alpha, x_\beta)\cdot \varphi_{,\beta}(x_\alpha, x_\beta),\end{aligned} \tag{1.1.68}$$

$$D_\alpha(x_\alpha, x_\beta) = e_{\alpha\gamma k}(x_\alpha, x_\beta)\cdot u_{\gamma,k}(x_\alpha, x_\beta) - \varepsilon_{\alpha k}(x_\alpha, x_\beta)\cdot \varphi_{,k}(x_\alpha, x_\beta), \tag{1.1.69}$$

$$D_\beta(x_\alpha, x_\beta) = e_{\beta\gamma k}(x_\alpha, x_\beta)\cdot u_{\gamma,k}(x_\alpha, x_\beta) - \varepsilon_{\beta k}(x_\alpha, x_\beta)\cdot \varphi_{,k}(x_\alpha, x_\beta). \tag{1.1.70}$$

Here the summation goes over $k \in \{\alpha; \beta\}$.

1.2 Amplitude-phase nonlinear interaction in propagation of linear signal in geometrically and physically weak inhomogeneous piezoelectric layer-waveguide

There is huge body of references devoted to study of dynamic problems, in particular, to propagation of wave signals in inhomogeneous waveguides (see, for instance [18, 19, 23, 25, 27], etc.). However, it worths to concern to a very important phenomenon, which occurs due to physical or geometrical inhomogeneity of media surface in propagation of normal wave signal. This is a nonlinear interaction between amplitude and phase of wave signal during its propagation in inhomogeneous medium (infinite or bounded by non-smooth surfaces).

In general case of anisotropy and inhomogeneity of the piezoelectric material, the quasi-static equations of electroelasticity are obtained from (1.1.17) taking into account the material ratios (1.1.18) and (1.1.19) for the inhomogeneous medium:

$$\sigma_{ij}(x_p) = c_{ijnk}(x_p)\cdot u_{n,k}(x_p) + e_{mij}\cdot\varphi_{,m}(x_p), \tag{1.2.1}$$

$$D_m(x_p) = e_{mnk}(x_p)\cdot u_{n,k}(x_p) - \varepsilon_{mk}(x_p)\cdot\varphi_{,k}(x_p), \tag{1.2.2}$$

and is written in the form of the following system of partial differential equations with variable coefficients:

$$\begin{aligned} &c_{ijnk}(x_p)\cdot u_{n,jk}(x_p;t) + e_{mij}(x_p)\cdot\varphi_{,mj}(x_p;t) + c_{ijnk,j}(x_p)\cdot u_{n,k}(x_p;t) + \\ &+e_{mij,j}(x_p)\cdot\varphi_{,m}(x_p;t) = \rho(x_p)\cdot\ddot{u}_i(x_p;t), \end{aligned} \tag{1.2.3}$$

$$\begin{aligned} &\varepsilon_{mj}(x_p)\cdot\varphi_{,mj}(x_p;t) + \varepsilon_{mj,j}(x_p)\cdot\varphi_{,m}(x_p;t) = \\ &= e_{mij}(x_p)\cdot u_{i,jm}(x_p;t) + e_{mij,j}(x_p)\cdot u_{i,m}(x_p;t). \end{aligned} \tag{1.2.4}$$

For investigation of electroelastic signal propagation in two-layer waveguide consisting of two piezoelectric inhomogeneous layers contacting by the rough surfaces $x_\gamma = h_*(x_\alpha, x_\beta)$, the system of equations (1.2.3) and (1.2.4) are solved in each mono layer separately, together with continuity conditions of the electromechanical fields (1.1.34)÷(1.1.37) which take the forms:

$$\left[\begin{matrix} \sigma_{ij}^{(1)}(x_\alpha, x_\beta, h_*(x_\alpha, x_\beta), t) - \\ -\sigma_{ij}^{(2)}(x_\alpha, x_\beta, h_*(x_\alpha, x_\beta), t) \end{matrix}\right] \cdot n_j^{(*)}(x_\alpha, x_\beta, h_*(x_\alpha, x_\beta), t) = 0, \tag{1.2.5}$$

$$\left[\begin{matrix} D_j^{(1)}(x_\alpha, x_\beta, h_*(x_\alpha, x_\beta), t) - \\ -D_j^{(2)}(x_\alpha, x_\beta, h_*(x_\alpha, x_\beta), t) \end{matrix}\right] \cdot n_j^{(*)}(x_\alpha, x_\beta, h_*(x_\alpha, x_\beta), t) = 0, \tag{1.2.6}$$

$$u_i^{(1)}(x_\alpha, x_\beta, h_*(x_\alpha, x_\beta, t)) = u_i^{(2)}(x_\alpha, x_\beta, h_*(x_\alpha, x_\beta, t)), \tag{1.2.7}$$

$$\varphi^{(1)}(x_\alpha, x_\beta, h_*(x_\alpha, x_\beta, t)) = \varphi^{(2)}(x_\alpha, x_\beta, h_*(x_\alpha, x_\beta, t)). \tag{1.2.8}$$

If the piezoelectric layer with non-smooth surface $x_\gamma = h_*(x_\alpha, x_\beta)$ is bordered with vacuum, then together with equations (1.2.3) and (1.2.4), electrostatics equations in vacuum must be solved

$$\nabla^2 \varphi^{(e)}(x_\alpha, x_\beta, h_*(x_\alpha, x_\beta), t) = 0, \tag{1.2.9}$$

Subjected to boundary conditions of continuity of electromechanical fields on the mechanically free surface (1.1.38)÷(1.1.40):

$$\left[\sigma_{ij}^{(1)}(x_\alpha, x_\beta, h_*(x_\alpha, x_\beta), t)\right] \cdot n_j^{(*)}(x_\alpha, x_\beta, h_*(x_\alpha, x_\beta), t) = 0, \tag{1.2.10}$$

$$\left[\begin{matrix} D_j^{(1)}(x_\alpha, x_\beta, h_*(x_\alpha, x_\beta), t) - \\ -D_j^{(e)}(x_\alpha, x_\beta, h_*(x_\alpha, x_\beta), t) \end{matrix}\right] \cdot n_j^{(*)}(x_\alpha, x_\beta, h_*(x_\alpha, x_\beta), t) = 0, \tag{1.2.11}$$

$$\varphi^{(1)}(x_\alpha, x_\beta, h_*(x_\alpha, x_\beta, t)) = \varphi^{(e)}(x_\alpha, x_\beta, h_*(x_\alpha, x_\beta, t)). \tag{1.2.12}$$

The formulated mathematical boundary value problem is complicated by the fact that the variable coefficients characterizing the physical inhomogeneity of the material and geometrical inhomogeneity of the contact surfaces occur as in the electroelasticity equations, as well as in boundary conditions.

Without loss of generality, consider the propagation of monochromatic electroelastic pure shear (*SH*) wave signal $A_0(y) \cdot \exp i(kx - \omega t)$ in the inhomogeneous layer-waveguide $\left\{|x| < \infty;\ h_-(x,z) \le y \le h_+(x,z);\ |z| < \infty\right\}$ which is of piezoelectric material of hexagonal symmetry of 6mm class, with rough surfaces $y = h_\pm(x,z)$. On the line $z = const$, where the oz axis is selected parallel to the axis of crystal symmetry, i.e. $oz \parallel \vec{p}$, the anti-plane electro-active deformation $\left\{0;\ 0;\ w(x,y,t);\ \varphi(x,y,t)\right\}$ is separated from the plane, non-electro-active deformation $\left\{u(x,y,t);\ v(x,y,t);\ 0;\ 0\right\}$, and the equations for electroelastic shear deformation with respect to the elastic shear $w(x,y,t)$ and electric potential $\varphi(x,y,t)$ take quite simple forms

$$\begin{aligned}&\left\{c_{44}(x,y)w_{,x}(x,y)+e_{15}(x,y)\varphi_{,x}(x,y)\right\}_{,x}+\\&+\left\{c_{44}(x,y)w_{,y}(x,y)+e_{15}(x,y)\varphi_{,y}(x,y)\right\}_{,y}=\rho(x,y)\ddot{w}(x,y),\end{aligned}\tag{1.2.13}$$

$$\begin{aligned}&\left\{e_{15}(x,y)w_{,x}(x,y)-\varepsilon_{11}(x,y)\varphi_{,x}(x,y)\right\}_{,x}+\\&+\left\{e_{15}(x,y)w_{,y}(x,y)-\varepsilon_{11}(x,y)\varphi_{,y}(x,y)\right\}_{,y}=0.\end{aligned}\tag{1.2.14}$$

The boundary conditions (1.1.63)÷(1.1.66) for mechanically free surfaces of the waveguide are simplified too

$$\sigma_{zx}^{(1)}(x,h_{\pm}(x),t)\cdot h_{\pm,x}(x)+\sigma_{yz}^{(1)}(x,h_{\pm}(x),t)=0\,,\tag{1.2.15}$$

$$\begin{aligned}&\left[D_x^{(1)}(x,h_{\pm}(x),t)-D_x^{(e)}(x,h_{\pm}(x),t)\right]\cdot h_{\pm,x}(x)+\\&+\left[D_y^{(1)}(x,h_{\pm}(x),t)-D_y^{(e)}(x,h_{\pm}(x),t)\right]=0,\end{aligned}\tag{1.2.16}$$

$$\varphi^{(1)}(x,h_{\pm}(x),t)=\varphi_{\pm}^{(e)}(x,h_{\pm}(x),t)\,,\tag{1.2.17}$$

where the shear stress and the displacement components of the electric field for a given slice of piezo-crystal are determined from the material ratio (1.1.67)÷(1.1.70):

$$\begin{aligned}&\sigma_{zx}^{(1)}(x,y)=c_{44}(x,y)\cdot u_{z,x}(x,y)+e_{15}(x,y)\cdot\varphi_{,x}(x,y),\\&\sigma_{yz}^{(1)}(x,y)=c_{44}(x,y)\cdot u_{z,y}(x,y)+e_{15}(x,y)\cdot\varphi_{,y}(x,y),\\&D_x^{(1)}(x,y)=e_{15}(x,y)\cdot u_{z,x}(x,y)-\varepsilon_{11}(x,y)\cdot\varphi_{,x}(x,y),\\&D_y^{(1)}(x,y)=e_{15}(x,y)\cdot u_{z,y}(x,y)-\varepsilon_{11}(x,y)\cdot\varphi_{,y}(x,y).\end{aligned}\tag{1.2.18}$$

For vacuum areas will have

$$\begin{aligned}&D_x^{\pm(e)}(x,y)=-\varepsilon_0(x,y)\cdot\varphi_{\pm,x}(x,y),\\&D_y^{\pm(e)}(x,y)=-\varepsilon_0(x,y)\cdot\varphi_{\pm,y}(x,y).\end{aligned}\tag{1.2.19}$$

In both vacuum half-spaces $y\le h_{-}(x,z)$ and $y\ge h_{+}(x,z)$ the electrostatics equations for the electric potential are solved

$$\varphi_{\pm,xx}^{(e)}(x,y,t)+\varphi_{\pm,yy}^{(e)}(x,y,t)=0\,.\tag{1.2.20}$$

During propagation of the monochromatic electroelastic wave signal $A_0(y)\cdot\exp i(\vec{k}\cdot\vec{x}-\omega t)$ in inhomogeneous piezoelectric medium, the signal faces with the physical inhomogeneity of the material, and in the presence of a rough surface of the medium separation, the signal faces with the surface inhomogeneities. Resulting dissipation

causes the amplitude-phase interaction [8, 14] and hence the unknown wave field admits the following general representation

$$w(x,y,t)=\exp\left\{U_w(x,y)+i\left[\theta_w(x,y)-\omega t\right]\right\},$$
$$\varphi(x,y,t)=\exp\left\{U_\varphi(x,y)+i\left[\theta_\varphi(x,y)-\omega t\right]\right\},\qquad(1.2.21)$$
$$\varphi_\pm^{(e)}(x,y,t)=\exp\left\{U_\pm(x,y)+i\left[\theta_\pm(x,y)-\omega t\right]\right\}.$$

The introduced functions $\left\{U_w(x,y);\ U_\varphi(x,y);\ U_\pm(x,y)\right\}$ are the logarithms of the amplitudes of the corresponding components of the wave field, i.e.

$U_w(x,y)\ \square\ \ln W_0(x,y),\qquad U_\varphi(x,y)\ \square\ \ln\varphi_0(x,y)\ ,\qquad U_\pm(x,y)\ \square\ \ln\varphi_\pm^{(0)}(x,y).$

Phase functions $\left\{\theta_w(x,y);\ \theta_\varphi(x,y);\ \theta_\pm(x,y)\right\}$ also correspond by indices to the corresponding components of the forming wave field.

By substituting (1.2.21) in the equations of electroelasticity (1.2.13), (1.2.14) and (1.2.20), as well as by separating real and imaginary parts, we obtain the system of eight nonlinear differential equations in partial derivatives with following variable coefficients with respect to the amplitude and phase functions:

$$\begin{aligned}
&c_{44}(x,y)\cdot\left\{\begin{matrix}W_{0,xx}(x,y)+W_{0,yy}(x,y)+C_t^{-2}(x,y)\cdot\omega^2\cdot W_0(x,y)-\\-W_0(x,y)\cdot\theta^2{}_{w,x}(x,y)-W_0(x,y)\cdot\theta^2{}_{w,y}(x,y)\end{matrix}\right\}\cdot\sin\left[\theta_w(x,y)\right]+\\
&+c_{44}(x,y)\cdot\left\{\begin{matrix}2\cdot\left[W_{0,x}(x,y)\cdot\theta_{w,x}(x,y)+W_{0,y}(x,y)\cdot\theta_{w,y}(x,y)\right]+\\+W_0(x,y)\cdot\left[\theta_{w,xx}(x,y)+\theta_{w,yy}(x,y)\right]\end{matrix}\right\}\cdot\cos\left[\theta_w(x,y)\right]+\\
&+\left\{c_{44,x}(x,y)\cdot W_{0,x}(x,y)+c_{44,y}(x,y)\cdot W_{0,y}(x,y)\right\}\cdot\sin\left[\theta_w(x,y)\right]+\\
&+W_0(x,y)\cdot\left\{c_{44,x}(x,y)\cdot\theta_{w,x}(x,y)+c_{44,y}(x,y)\cdot\theta_{w,y}(x,y)\right\}\cdot\cos\left[\theta_w(x,y)\right]+\\
&+e_{15}(x,y)\cdot\left\{\begin{matrix}\varphi_{0,xx}(x,y)+\varphi_{0,yy}(x,y)-\\-\varphi_0(x,y)\cdot\left[\theta^2{}_{\varphi,x}(x,y)+\theta^2{}_{\varphi,y}(x,y)\right]\end{matrix}\right\}\cdot\sin\left[\theta_\varphi(x,y)\right]+\\
&+e_{15}(x,y)\cdot\left\{\begin{matrix}2\cdot\left[\varphi_{0,x}(x,y)\cdot\theta_{\varphi,x}(x,y)+\varphi_{0,y}(x,y)\cdot\theta_{\varphi,y}(x,y)\right]+\\+\varphi_0(x,y)\cdot\left[\theta_{\varphi,xx}(x,y)+\theta_{\varphi,yy}(x,y)\right]\end{matrix}\right\}\cdot\cos\left[\theta_\varphi(x,y)\right]+\\
&+\left\{e_{15,x}(x,y)\cdot\varphi_{0,x}(x,y)+e_{15,y}(x,y)\cdot\varphi_{0,y}(x,y)\right\}\cdot\sin\left[\theta_\varphi(x,y)\right]+\\
&+\varphi_0(x,y)\cdot\left\{e_{15,x}(x,y)\cdot\theta_{\varphi,x}(x,y)+e_{15,y}(x,y)\cdot\theta_{\varphi,y}(x,y)\right\}\cdot\cos\left[\theta_\varphi(x,y)\right]=0,
\end{aligned}\qquad(1.2.22)$$

$$
\begin{aligned}
&c_{44}(x,y)\cdot\left\{\begin{matrix}W_{0,xx}(x,y)+W_{0,yy}(x,y)+C_t^{-2}(x,y)\cdot\omega^2\cdot W_0(x,y)-\\ -W_0(x,y)\cdot\left[{\theta^2}_{w,x}(x,y)+{\theta^2}_{w,y}(x,y)\right]\end{matrix}\right\}\cdot\sin\left[\theta_w(x,y)\right]+\\
&+c_{44}(x,y)\cdot\left\{\begin{matrix}2\cdot\left[W_{0,x}(x,y)\cdot\theta_{w,x}(x,y)+W_{0,y}(x,y)\cdot\theta_{w,y}(x,y)\right]+\\ +W_0(x,y)\cdot\left[\theta_{w,xx}(x,y)+\theta_{w,yy}(x,y)\right]\end{matrix}\right\}\cdot\cos\left[\theta_w(x,y)\right]+\\
&+\left\{c_{44,x}(x,y)\cdot W_{0,x}(x,y)+c_{44,y}(x,y)\cdot W_{0,y}(x,y)\right\}\cdot\sin\left[\theta_w(x,y)\right]+\\
&+W_0(x,y)\cdot\left\{c_{44,x}(x,y)\cdot\theta_{w,x}(x,y)+c_{44,y}(x,y)\cdot\theta_{w,y}(x,y)\right\}\cdot\cos\left[\theta_w(x,y)\right]+\\
&+e_{15}(x,y)\cdot\left\{\begin{matrix}\varphi_{0,xx}(x,y)+\varphi_{0,yy}(x,y)-\\ -\varphi_0(x,y)\cdot\left[{\theta^2}_{\varphi,x}(x,y)+{\theta^2}_{\varphi,y}(x,y)\right]\end{matrix}\right\}\cdot\sin\left[\theta_\varphi(x,y)\right]+\\
&+e_{15}(x,y)\cdot\left\{\begin{matrix}2\cdot\left[\varphi_{0,x}(x,y)\cdot\theta_{\varphi,x}(x,y)+\varphi_{0,y}(x,y)\cdot\theta_{\varphi,y}(x,y)\right]+\\ +\varphi_0(x,y)\cdot\left[\theta_{\varphi,xx}(x,y)+\theta_{\varphi,yy}(x,y)\right]\end{matrix}\right\}\cdot\cos\left[\theta_\varphi(x,y)\right]+\\
&+\left\{e_{15,x}(x,y)\cdot\varphi_{0,x}(x,y)+e_{15,y}(x,y)\cdot\varphi_{0,y}(x,y)\right\}\cdot\sin\left[\theta_\varphi(x,y)\right]+\\
&+\varphi_0(x,y)\cdot\left\{e_{15,x}(x,y)\cdot\theta_{\varphi,x}(x,y)+e_{15,y}(x,y)\cdot\theta_{\varphi,y}(x,y)\right\}\cdot\cos\left[\theta_\varphi(x,y)\right]=0,
\end{aligned}
\tag{1.2.23}
$$

$$
\begin{aligned}
&e_{15}(x,y)\cdot\left\{\begin{matrix}W_{0,xx}(x,y)+W_{0,yy}(x,y)-\\ -W_0(x,y)\cdot\left[{\theta^2}_{w,x}(x,y)+{\theta^2}_{w,y}(x,y)\right]\end{matrix}\right\}\cdot\cos\left[\theta_w(x,y)\right]-\\
&-e_{15}(x,y)\cdot\left\{\begin{matrix}2\cdot\left[W_{0,x}(x,y)\cdot\theta_{w,x}(x,y)+W_{0,y}(x,y)\cdot\theta_{w,y}(x,y)\right]+\\ +W_0(x,y)\cdot\left[\theta_{w,xx}(x,y)+\theta_{w,yy}(x,y)\right]\end{matrix}\right\}\cdot\sin\left[\theta_w(x,y)\right]+\\
&+\left\{e_{15,x}(x,y)\cdot W_{0,x}(x,y)+e_{15,y}(x,y)\cdot W_{0,y}(x,y)\right\}\cdot\cos\left[\theta_w(x,y)\right]-\\
&-W_0(x,y)\cdot\left\{e_{15,x}(x,y)\cdot\theta_{w,x}(x,y)+e_{15,y}(x,y)\cdot\theta_{w,y}(x,y)\right\}\cdot\sin\left[\theta_w(x,y)\right]-\\
&-\varepsilon_{11}(x,y)\cdot\left\{\begin{matrix}\varphi_{0,xx}(x,y)+\varphi_{0,yy}(x,y)-\\ -\varphi_0(x,y)\cdot\left[{\theta^2}_{\varphi,x}(x,y)+{\theta^2}_{\varphi,y}(x,y)\right]\end{matrix}\right\}\cdot\cos\left[\theta_\varphi(x,y)\right]+\\
&+\varepsilon_{11}(x,y)\cdot\left\{\begin{matrix}2\cdot\left[\varphi_{0,x}(x,y)\cdot\theta_{\varphi,x}(x,y)+\varphi_{0,y}(x,y)\cdot\theta_{\varphi,y}(x,y)\right]+\\ +\varphi_0(x,y)\cdot\left[\theta_{\varphi,xx}(x,y)+\theta_{\varphi,yy}(x,y)\right]\end{matrix}\right\}\cdot\sin\left[\theta_\varphi(x,y)\right]-\\
&-\left\{\varepsilon_{11,x}(x,y)\cdot\varphi_{0,x}(x,y)+\varepsilon_{11,y}(x,y)\cdot\varphi_{0,y}(x,y)\right\}\cdot\cos\left[\theta_\varphi(x,y)\right]+\\
&+\varphi_0(x,y)\cdot\left\{\varepsilon_{11,x}(x,y)\cdot\theta_{\varphi,x}(x,y)+\varepsilon_{11,y}(x,y)\cdot\theta_{\varphi,y}(x,y)\right\}\cdot\sin\left[\theta_\varphi(x,y)\right]=0,
\end{aligned}
\tag{1.2.24}
$$

$$e_{15}(x,y)\cdot\left\{\begin{matrix}W_{0,xx}(x,y)+W_{0,yy}(x,y)-\\-W_0(x,y)\cdot\left[\theta^2{}_{w,x}(x,y)+\theta^2{}_{w,y}(x,y)\right]\end{matrix}\right\}\cdot\sin\left[\theta_w(x,y)\right]+$$

$$+e_{15}(x,y)\cdot\left\{\begin{matrix}2\cdot\left[W_{0,x}(x,y)\cdot\theta_{w,x}(x,y)+W_{0,y}(x,y)\cdot\theta_{w,y}(x,y)\right]+\\+W_0(x,y)\cdot\left[\theta_{w,xx}(x,y)+\theta_{w,yy}(x,y)\right]\end{matrix}\right\}\cdot\cos\left[\theta_w(x,y)\right]+$$

$$+\left\{e_{15,x}(x,y)\cdot W_{0,x}(x,y)+e_{15,y}(x,y)\cdot W_{0,y}(x,y)\right\}\cdot\sin\left[\theta_w(x,y)\right]+$$

$$+W_0(x,y)\cdot\left\{e_{15,x}(x,y)\cdot\theta_{w,x}(x,y)+e_{15,y}(x,y)\cdot\theta_{w,y}(x,y)\right\}\cdot\cos\left[\theta_w(x,y)\right]-$$

$$-\varepsilon_{11}(x,y)\cdot\left\{\begin{matrix}\varphi_{0,xx}(x,y)+\varphi_{0,yy}(x,y)-\\-\varphi_0(x,y)\cdot\left[\theta^2{}_{\varphi,x}(x,y)+\theta^2{}_{\varphi,y}(x,y)\right]\end{matrix}\right\}\cdot\sin\left[\theta_\varphi(x,y)\right]-$$

$$-\varepsilon_{11}(x,y)\cdot\left\{\begin{matrix}2\cdot\left[\varphi_{0,x}(x,y)\cdot\theta_{\varphi,x}(x,y)+\varphi_{0,y}(x,y)\cdot\theta_{\varphi,y}(x,y)\right]+\\+\varphi_0(x,y)\cdot\left[\theta_{\varphi,xx}(x,y)+\theta_{\varphi,yy}(x,y)\right]\end{matrix}\right\}\cdot\cos\left[\theta_\varphi(x,y)\right]-$$

$$-\left\{\varepsilon_{11,x}(x,y)\cdot\varphi_{0,x}(x,y)+\varepsilon_{11,y}(x,y)\cdot\varphi_{0,y}(x,y)\right\}\cdot\sin\left[\theta_\varphi(x,y)\right]- \qquad (1.2.25)$$

$$-\varphi_0(x,y)\cdot\left\{\varepsilon_{11,x}(x,y)\cdot\theta_{\varphi,x}(x,y)+\varepsilon_{11,y}(x,y)\cdot\theta_{\varphi,y}(x,y)\right\}\cdot\cos\left[\theta_\varphi(x,y)\right]=0,$$

$$\varphi_{0+,xx}(x,y)+\varphi_{0+,yy}(x,y)-\varphi_{0+}(x,y)\cdot\left[\theta^2{}_{\varphi+,x}(x,y)+\theta^2{}_{\varphi+,y}(x,y)\right]=0, \qquad (1.2.26)$$

$$\begin{aligned}&2\cdot\left[\varphi_{0+,x}(x,y)\cdot\theta_{\varphi+,x}(x,y)+\varphi_{0+,y}(x,y)\cdot\theta_{\varphi+,y}(x,y)\right]+\\&+\varphi_{0+}(x,y)\cdot\left[\theta_{\varphi+,xx}(x,y)+\theta_{\varphi+,yy}(x,y)\right]=0,\end{aligned} \qquad (1.2.27)$$

$$\varphi_{0-,xx}(x,y)+\varphi_{0-,yy}(x,y)-\varphi_{0-}(x,y)\cdot\left[\theta^2{}_{\varphi-,x}(x,y)+\theta^2{}_{\varphi-,y}(x,y)\right]=0, \qquad (1.2.28)$$

$$\begin{aligned}&2\cdot\left[\varphi_{0-,x}(x,y)\cdot\theta_{\varphi-,x}(x,y)+\varphi_{0-,y}(x,y)\cdot\theta_{\varphi-,y}(x,y)\right]+\\&+\varphi_{0-}(x,y)\cdot\left[\theta_{\varphi-,xx}(x,y)+\theta_{\varphi-,yy}(x,y)\right]=0.\end{aligned} \qquad (1.2.29)$$

Subjected to the boundary conditions on non-smooth surfaces $y=h_{\pm}(x,z)$:

conditions of mechanically free surfaces

$$\begin{aligned}&c_{44}(x,h_{\pm}(x))\left\{\begin{matrix}\left[h'_{\pm}(x)W_{0,x}(x,h_{\pm}(x))+W_{0,y}(x,h_{\pm}(x))\right]\cdot\cos\left[\theta_w(x,h_{\pm}(x))\right]-\\-W_0(x,h_{\pm}(x))\cdot\left[\begin{matrix}h'_{\pm}(x)\theta_{w,x}(x,h_{\pm}(x))+\\+\theta_{w,y}(x,h_{\pm}(x))\end{matrix}\right]\cdot\sin\left[\theta_w(x,h_{+}(x))\right]\end{matrix}\right\}+\\&+e_{15}(x,h_{\pm}(x))\left\{\begin{matrix}\left[h'_{\pm}(x)\varphi_{0,x}(x,h_{\pm}(x))+\varphi_{0,y}(x,h_{\pm}(x))\right]\cdot\cos\left[\theta_\varphi(x,h_{\pm}(x))\right]-\\-\varphi_0(x,h_{\pm}(x))\cdot\left[\begin{matrix}h'_{\pm}(x)\theta_{\varphi,x}(x,h_{\pm}(x))+\\+\theta_{\varphi,y}(x,h_{\pm}(x))\end{matrix}\right]\cdot\sin\left[\theta_\varphi(x,h_{\pm}(x))\right]\end{matrix}\right\}=0,\end{aligned} \qquad (1.2.30)$$

$$
\begin{aligned}
&c_{44}(x,h_{\pm}(x))\left\{\begin{array}{l}\left[h'_{\pm}(x)W_{0,x}(x,h_{\pm}(x))+W_{0,y}(x,h_{\pm}(x))\right]\cdot\sin\left[\theta_w(x,h_{\pm}(x))\right]+\\ +W_0(x,h_{\pm}(x))\cdot\left[\begin{array}{l}h'_{\pm}(x)\theta_{w,x}(x,h_{\pm}(x))+\\ +\theta_{w,y}(x,h_{\pm}(x))\end{array}\right]\cdot\cos\left[\theta_w(x,h_{\pm}(x))\right]\end{array}\right\}+\\
&+e_{15}(x,h_{\pm}(x))\left\{\begin{array}{l}\left[h'_{\pm}(x)\varphi_{0,x}(x,h_{\pm}(x))+\varphi_{0,y}(x,h_{\pm}(x))\right]\cdot\sin\left[\theta_{\varphi}(x,h_{\pm}(x))\right]+\\ +\varphi_0(x,h_{\pm}(x))\cdot\left[\begin{array}{l}h'_{\pm}(x)\theta_{\varphi,x}(x,h_{\pm}(x))+\\ +\theta_{\varphi,y}(x,h_{\pm}(x))\end{array}\right]\cdot\cos\left[\theta_{\varphi}(x,h_{\pm}(x))\right]\end{array}\right\}=0,
\end{aligned}
\tag{1.2.31}
$$

continuity conditions of the normal component of electric field displacements

$$
\begin{aligned}
&e_{15}(x,h_{\pm}(x))\cdot\left\{\begin{array}{l}\left[h'_{\pm}(x)W_{0,x}(x,h_{\pm}(x))+W_{0,y}(x,h_{\pm}(x))\right]\cdot\cos\left[\theta_w(x,h_{\pm}(x))\right]-\\ -W_0(x,h_{\pm}(x))\left[\begin{array}{l}h'_{\pm}(x)\cdot\theta_{w,x}(x,h_{\pm}(x))+\\ +\theta_{w,y}(x,h_{\pm}(x))\end{array}\right]\cdot\sin\left[\theta_w(x,h_{\pm}(x))\right]\end{array}\right\}-\\
&-\varepsilon_{11}(x,h_{\pm}(x))\cdot\left\{\begin{array}{l}\left[h'_{\pm}(x)\varphi_{0,x}(x,h_{\pm}(x))+\varphi_{0,y}(x,h_{\pm}(x))\right]\cdot\cos\left[\theta_{\varphi}(x,h_{\pm}(x))\right]-\\ -\left[\begin{array}{l}h'_{\pm}(x)\cdot\theta_{\varphi,x}(x,h_{\pm}(x))+\\ +\theta_{\varphi,y}(x,h_{\pm}(x))\end{array}\right]\cdot\varphi_0(x,h_{\pm}(x))\cdot\sin\left[\theta_{\varphi}(x,h_{\pm}(x))\right]\end{array}\right\}+\\
&+\varepsilon_0\cdot\left\{\begin{array}{l}\left[h'_{\pm}(x)\varphi_{0+,x}(x,h_{\pm}(x))+\varphi_{0\pm,y}(x,h_{\pm}(x))\right]\cdot\cos\left[\theta_{\varphi\pm}(x,h_{\pm}(x))\right]-\\ -\varepsilon_0\cdot\left[h'_{\pm}(x)\theta_{\varphi\pm,x}(x,h_{\pm}(x))+\theta_{\varphi\pm,y}(x,h_{\pm}(x))\right]\cdot\varphi_{0\pm}(x,h_{\pm}(x))\end{array}\right\}=0,
\end{aligned}
\tag{1.2.32}
$$

$$
\begin{aligned}
&e_{15}(x,h_{\pm}(x))\cdot\left\{\begin{array}{l}\left[h'_{\pm}(x)W_{0,x}(x,h_{\pm}(x))+W_{0,y}(x,h_{\pm}(x))\right]\cdot\sin\left[\theta_w(x,h_{\pm}(x))\right]+\\ +W_0(x,h_{\pm}(x))\cdot\left[\begin{array}{l}h'_{\pm}(x)\cdot\theta_{w,x}(x,h_{\pm}(x))+\\ +\theta_{w,y}(x,h_{\pm}(x))\end{array}\right]\cdot\cos\left[\theta_w(x,h_{\pm}(x))\right]\end{array}\right\}-\\
&-\varepsilon_{11}(x,h_{\pm}(x))\cdot\left\{\begin{array}{l}\left[h'_{\pm}(x)\varphi_{0,x}(x,h_{\pm}(x))+\varphi_{0,y}(x,h_{\pm}(x))\right]\cdot\sin\left[\theta_{\varphi}(x,h_{\pm}(x))\right]+\\ +\varphi_0(x,h_{\pm}(x))\cdot\left[\begin{array}{l}h'_{\pm}(x)\cdot\theta_{\varphi,x}(x,h_{\pm}(x))+\\ +\theta_{\varphi,y}(x,h_{\pm}(x))\end{array}\right]\cdot\cos\left[\theta_{\varphi}(x,h_{\pm}(x))\right]\end{array}\right\}+\\
&+\varepsilon_0\cdot\left\{\begin{array}{l}\left[h'_{\pm}(x)\varphi_{0\pm,x}(x,h_{\pm}(x))+\varphi_{0\pm,y}(x,h_{\pm}(x))\right]\cdot\sin\left[\theta_{\varphi\pm}(x,h_{\pm}(x))\right]+\\ +\varphi_{0\pm}(x,h_{\pm}(x))\left[\begin{array}{l}h'_{\pm}(x)\cdot\theta_{\varphi\pm,x}(x,h_{\pm}(x))+\\ +\theta_{\varphi\pm,y}(x,h_{\pm}(x))\end{array}\right]\cdot\cos\left[\theta_{\varphi\pm}(x,h_{\pm}(x))\right]\end{array}\right\}=0,
\end{aligned}
\tag{1.2.33}
$$

continuity conditions of the electric field potential

$$
\varphi_0(x,h_{\pm}(x))\cdot\cos\left[\theta_{\varphi}(x,h_{\pm}(x))\right]=\varphi_{0\pm}(x,h_{\pm}(x))\cdot\cos\left[\theta_{\varphi\pm}(x,h_{\pm}(x))\right],
\tag{1.2.34}
$$

$$
\varphi_0(x,h_{\pm}(x))\cdot\sin\left[\theta_{\varphi}(x,h_{\pm}(x))\right]=\varphi_{0\pm}(x,h_{\pm}(x))\cdot\sin\left[\theta_{\varphi\pm}(x,h_{\pm}(x))\right],
\tag{1.2.35}
$$

attenuation conditions of the electric field at infinity

$$\lim_{y\to+\infty}\varphi_{0+}(x,y)\cdot\cos\left[\theta_{\varphi+}(x,y)\right]=\lim_{y\to-\infty}\varphi_{0-}(x,y)\cdot\cos\left[\theta_{\varphi-}(x,y)\right]=0, \tag{1.2.36}$$

$$\lim_{y\to+\infty}\varphi_{0+}(x,y)\cdot\sin\left[\theta_{\varphi+}(x,y)\right]=\lim_{y\to-\infty}\varphi_{0-}(x,y)\cdot\sin\left[\theta_{\varphi-}(x,y)\right]=0. \tag{1.2.37}$$

Even enough the mathematical boundary value problem obtained above, is selected for a simple anisotropy of piezo-crystals, obviously gives a complicated amplitude-phase interaction. This problem can be solved only numerically, and it is necessary to have powerful mathematical and software backgrounds. Nevertheless, the numerical solutions do not always reveal the full picture of physical phenomena for such problems.

1.3 Some issues of modeling on problems of propagation of high frequency electroelastic wave signal in piezoelectric waveguides. Method of hypotheses (MELS) in studies of surface wave phenomena

An approach of modeling of mathematical boundary value problem of electroelasticity is suggested in this section by introducing virtual cross-sections in the near-surface zones of bordering mediums. By selection of surface exponential functions (***SEF***), taking into account the nature of the process dynamics, new hypotheses on distributions are formulated in each selected layer, corresponding to the desired physical-mechanical values [***hypotheses Magneto (Electro; Thermo) Elastic Layered Systems-MELS***] depending on the method of joining the rough boundaries of media with different associated physical-mechanical fields.

Different methods of layers joint naturally lead to formation of different three-layer packs in the near-surface zone of the joints (Figs. 1.3.2 and 1.3.3). The main role in the formed connecting thin layers plays roughness defined by random functions $y = h_m(x)$, which is described by the main parameters of the roughness (Fig. 1.3.1).

The profilogram gives an idea about the relief profile of non-smooth surface: quantity, form and size of the ledges and non-smoothness depressions. For relative roughness functions we can assume that $h_m(x) \in L_1\{\square\}$, considering that, in practice, the height of the ledges and depressions of the surface micro non-smoothness is in the range from 10 nm to 500 μm or more, and the relation of the roughness average step in the maximum profile is $S_{im} \square 100 \cdot R_{\max}$.

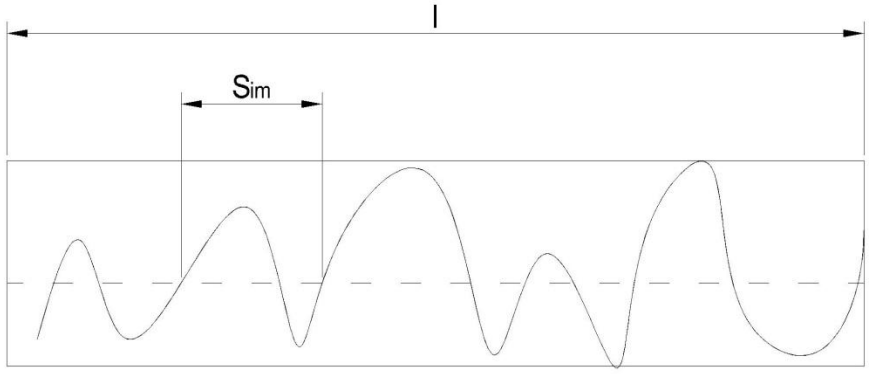

Fig. 1.3.1 Profilogram and roughness main parameters: l - base line, S_{im} - average step profile roughness

In general, the materials of bordering mediums may have different physico-mechanical properties and are described by different thermodynamical material relations.

First we consider the case of glued half-spaces [9, 10], from which, by setting the material constants of the adhesive mediums to zero, we get the contact problem of rough surfaces with vacuum gap of variable thickness.

Model 1. Two elastic deformable half-spaces of material characterized by related physical fields (electroelasticity, magneto-elasticity, thermo-elasticity, etc.) are connected by adhesive with appropriate physical-mechanical characteristics. Corresponding quasi-static equations of electroelasticity in the n-th layer are solved in each half-space $\Omega_1 = \{|x| < \infty, -\infty < y \le h_1(x), |z| < \infty\}$ and $\Omega_2 = \{|x| < \infty, h_2(x) \le y < \infty, |z| < \infty\}$, as well as in internal gluing gap $\Omega_3 = \{|x| < \infty, h_1(x) \le y \le h_2(x), |z| < \infty\}$ of variable width $\xi(x) = |h_2(x) - h_1(x)|$:

$$c_{ijkm} u^{(n)}_{k,im} + e_{ijm} \varphi_{n,im} = \rho_n \ddot{u}^{(n)}_j, \qquad e_{ijm} u^{(n)}_{j,im} - \varepsilon_{im} \varphi_{n,im} = 0. \tag{1.3.1}$$

The number of equations $n \in \{1; 2; ...\}$ and the unknowns naturally depends on the associated physico-mechanical fields.

The full continuity conditions of physico-mechanical fields must be satisfied on the surfaces of mediums separation $\Sigma_m = \{y = h_m(x)\}; \quad m = 1; 2.$

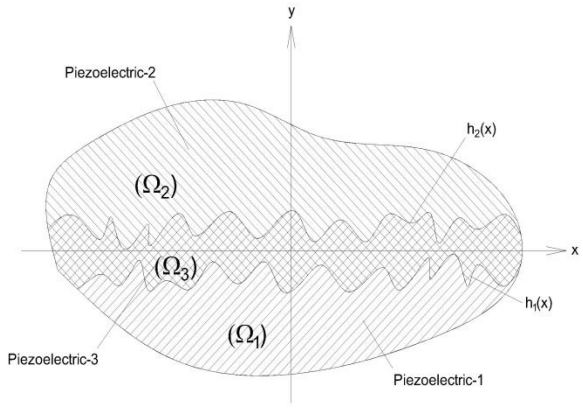

Fig. 1.3.2 Rough surface contact in piezoelectric composite waveguide by method of glue

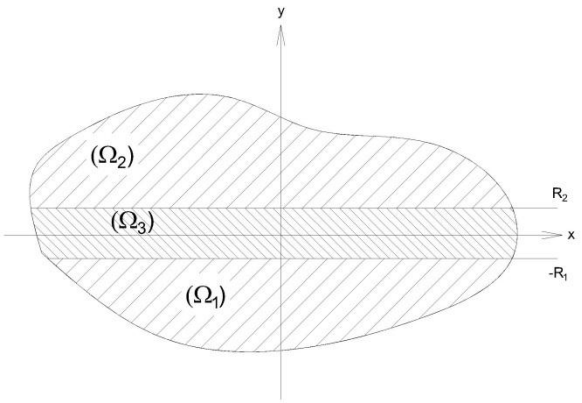

Fig. 1.3.3 Rough surface contact in piezoelectric composite waveguide by method of ultrasonic welding

The above three groups of equations (1.3.1), and the following boundary conditions on each surface $y = h_m(x)$:

$$\left(\sigma^{(m)}_{ij}(x, h_m(x), t) - \sigma^{(3)}_{ij}(x, h_m(x), t)\right) \cdot n^{(m)}_j \left(x, h_m(x)\right) = 0, \tag{1.3.2}$$

$$\left(D^{(m)}_j(x, h_m(x), t) - D^{(3)}_j(x, h_m(x), t)\right) \cdot n^{(m)}_j \left(x, h_m(x)\right) = 0, \tag{1.3.3}$$

$$w_i^{(m)}(x,h_m(x),t)=w_i^{(3)}(x,h_m(x),t)\,, \tag{1.3.4}$$

$$\varphi_m(x,h_m(x),t)=\varphi_3(x,h_m(x),t)\,, \tag{1.3.5}$$

with variable normal $\vec{n}^{(m)}\left(x\right)=\left\{n_j^{(m)}\left(x,h_m(x)\right)\right\}$ for $m=1;2$,

$$n_j^{(m)}\left(x,h_m(x)\right)=\left\{\frac{h_m'(x)}{\sqrt{1+\left[h_m'(x)\right]^2}};\frac{1}{\sqrt{1+\left[h_m'(x)\right]^2}};0\right\}, \tag{1.3.6}$$

together with vanishing conditions of the corresponding physico-mechanical fields at infinity, for indices $i;j\in\{1;2;3\}$ and $m\in\{1,2\}$

$$\lim_{y\to(-1)^m\infty} w_m\left(x,y,t\right)\to 0\,,\qquad \lim_{y\to(-1)^m\infty} \varphi_m\left(x,y,t\right)\to 0\,, \tag{1.3.7}$$

form a mathematical boundary problem in three-layer composite waveguide with rough surfaces in contacts.

It is known, that in any plane ox_1x_2 (axis $oz\|\bar{p}$ and slice $x_3=const$), it is possible to separate the quasistatic equations of electroelasticity (1.3.1) of the electro-active plane deformable state $\left\{u_1\left(x_1,x_2,t\right);u_2\left(x_1,x_2,t\right);0;0\right\}$ from the electro-active anti-plane deformable state $\left\{0;0;u_3\left(x_1,x_2,t\right);\varphi\left(x_1,x_2,t\right)\right\}$ [6]. This gives an opportunity to separately investigate the influence of surface roughness on propagation of plane deformation wave signal and on propagation of electro-active anti-plane deformation wave-signal.

In this case, two homogeneous piezoelectric half-spaces are associated with homogeneous thin layer of glue (material of appropriate characteristics), with geometrically inhomogeneous surfaces of contact.

The inhomogeneity in the formed composite has geometrical nature and they are caused by the functions of surface irregularities $\Sigma_m=\left\{y=h_m(x)\right\};\quad m=1;2$, appearing in the boundary conditions (1.3.2) and (1.3.5). Residual physical inhomogeneity of the material after processing the layer surfaces may remain in the thin near-surface zones of the homogeneous half-spaces. Then, for the study of wave process in the waveguide, the quasistatic equations of electroelasticity of inhomogeneous medium (1.1.23) and (1.1.24) are solved in these virtually selected zones.

Model 2. Two elastic deformable half-spaces of material characterized by related physical fields (electroelasticity, magneto-elasticity, thermo-elasticity, etc.) are interrelated

by method of thermal pressure, so that depression of one roughness was flooded with projections of the other. Then, at the connection junction of the half-spaces a thin, transversely-inhomogeneous layer of the following thickness

$$2H_0 = R_2 + R_1 + \frac{1}{L}\int_0^L \left\{ R_2 + R_1 - \left[h_2(x) + h_1(x) \right] \right\} dx \tag{1.3.8}$$

is formed, where $R_m = \left| \max h_m(x) - \min h_m(x) \right|$ is the depression (height) maximum values of surface roughness $h_m(x)$, respectively, L is the total period of surface roughness change $h_m(x)$.

In the virtually selected layers for the physico-mechanical characteristic functions $\gamma^{(3)}(y) \square \left\{ c_{ijkn}^{(3)}(y); \rho^{(3)}(y); e_{mij}^{(3)}(y); \varepsilon_{nk}^{(3)}(y) \right\}$ of the material, natural requirements are the conditions of equality of physico-mechanical constants on the perfectly smooth planes $y = \pm H_0$, respectively, i.e.

$$\gamma\left(-H_0\right) = \gamma^{(1)} \square \left\{ c_{ijkn}^{(1)}; \rho^{(1)}; e_{mij}^{(1)}; \varepsilon_{nk}^{(1)} \right\}, \quad \gamma\left(+H_0\right) = \gamma^{(2)} \square \left\{ c_{ijkn}^{(2)}; \rho^{(2)}; e_{mij}^{(2)}; \varepsilon_{nk}^{(2)} \right\}$$

Thus, it is possible to represent the material inhomogeneity by any integrable function of type $\gamma^{(3)} = f(y, R_m, \gamma^{(m)}); \quad m = 1;2$, with conditions on the virtual layer surfaces. As a result of diffusion, it is natural to impose a new phenomenological condition $f\left(\left(h_1(x) + h_2(x)\right)/2\right) = \left(\gamma_1 + \gamma_2\right)/2$ on the deformed mid-surface of the formed inhomogeneous layer $y = \left(h_1(x) + h_2(x)\right)/2$. This additional condition does not simplify and does not complicate the solution of the dynamic problem.

The physical modeling chosen leads to the fact that in studies of dynamic process in piezoelectric two-layer waveguides with welded layers need to virtually cut the internal inhomogeneous layer $\Omega_3 = \left\{ |x| < \infty; \quad -H_0 < y \le H_0; \quad |z| < \infty \right\}$, in which the quasi-static equations of electroelasticity with coefficients varying over the thickness of the virtual layer are solved [14, 15]

$$\begin{aligned} & c_{ijnk}(x_p) \cdot u_{n,jk}(x_p;t) + e_{mij}(x_p) \cdot \varphi_{,mj}(x_p;t) + c_{ijnk,j}(x_p) \cdot u_{n,k}(x_p;t) + \\ & + e_{mij,j}(x_p) \cdot \varphi_{,m}(x_p;t) = \rho(x_p) \cdot \ddot{u}_i(x_p;t), \end{aligned} \tag{1.3.9}$$

$$\varepsilon_{mj}(x_p)\cdot\varphi_{,mj}(x_p;t)+\varepsilon_{mj,j}(x_p)\cdot\varphi_{,m}(x_p;t)=$$
$$=e_{mij}(x_p)\cdot u_{i,jm}(x_p;t)+e_{mij,j}(x_p)\cdot u_{i,m}(x_p;t). \qquad (1.3.10)$$

The quasistatic equations of electroelastic homogeneous piezoelectric materials (1.3.1) will be solved in the homogeneous piezoelectric half-spaces $\Omega_1=\{|x|<\infty;\ -\infty<y\le -H_0;\ |z|<\infty\}$ and $\Omega_2=\{|x|<\infty;\ R_1\le y<\infty;\ |z|<\infty\}$.

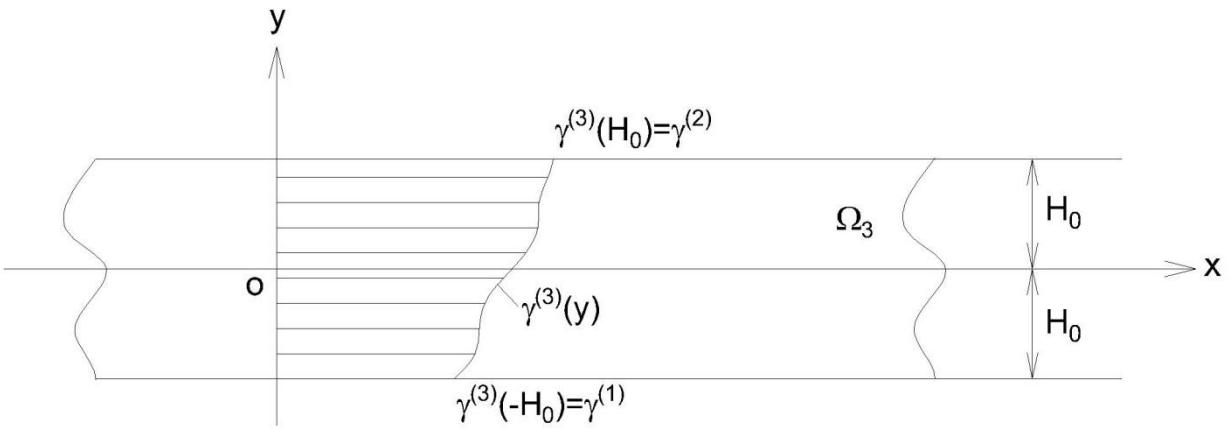

Fig. 1.3.4 Virtually selected inhomogeneous layer in the contact area of rough surfaces in piezoelectric composite waveguide by ultrasonic welding

Obviously, considering the residual technological and structural inhomogeneities of a layered structures the study of wave distribution problem becomes much more complicated in layered waveguides. The variable coefficients in the equations and boundary conditions lead to the nonlinear interaction between the amplitude and phase functions of the propagating wave signal in the internal inhomogeneous layers [8, 14].

In this case of modeling, electro-mechanical boundary conditions (1.3.2) and (1.3.5) are rather simplified by replacing the surface normals $\vec{n}^{(m)}(x)=\{n_j^{(m)}(x,h_m(x))\}$ by unit normal $n_j^{(\pm)}=\{0;\ \pm 1;\ 0\}$:

$$\sigma_{i2}^{(m)}(x;\ (-1)^m\cdot H_0;\ t)-\sigma_{i2}^{(3)}(x;\ (-1)^m\cdot H_0;\ t)=0, \qquad (1.3.11)$$

$$D_2^{(m)}(x;\ (-1)^m\cdot H_0;\ t)-D_2^{(3)}(x;\ (-1)^m\cdot H_0;\ t)=0, \qquad (1.3.12)$$

$$w_i^{(m)}(x;\ (-1)^m\cdot H_0;\ t)=w_i^{(3)}(x;\ (-1)^m\cdot H_0;\ t), \qquad (1.3.13)$$

$$\varphi_m(x;\ (-1)^m\cdot H_0;\ t)=\varphi_3(x;\ (-1)^m\cdot H_0;\ t). \qquad (1.3.14)$$

For analytical analysis of wave processes in composite waveguides, the author in studies [9] and [10] proposes hypotheses on the distribution of characteristic values of physico-mechanical fields or thermodynamic material characteristics of the formed inhomogeneous material. Those hypotheses come from physical-mathematical considerations of obtained schemes. They also observe the compactness of the mathematical boundary value problem.

Mathematical modeling of boundary value problems by the introduction of MELS hypotheses (hypotheses of Magneto Elastic Layered System). The maximal ledges and maximal depressions in the surface roughness are much small compared to the effective thickness of bordering layers

$$R_{\max}^{(m)} = \left| \max_{x\in\{X\}} h_m(x) - \min_{x\in\{X\}} h_m(x) \right| \square \ \min\{H_1; H_2\}. \tag{1.3.15}$$

Consequently, in both formulations given above, the obtained layers will be very thin compared to the base thickness of bordering layers. Thus, the thickness of the adhesive layer will be

$$H_3(x) \square \left| h_2(x) - h_1(x) \right| \sim R_{\max}^{(m)} = \left| \max_{x\in\{X\}} h_m(x) - \min_{x\in\{X\}} h_m(x) \right|. \tag{1.3.16}$$

Naturally, it will be of the order of the sum of two maximal ledges of the bordering layer surface roughness.

The thickness of the formed laterally inhomogeneous thin layer in the zone of the welded joints of the half-spaces

$$2H_0 = R_2 + R_1 + \frac{1}{L}\int_0^L \left\{ R_2 + R_1 - \left[h_2(x) + h_1(x) \right] \right\} dx$$

will be of the order of the sum of two maximal ledges of bordering layer surface roughness. Taking into account the thinness of the formed surface layers, they can be considered as weak surface inhomogeneity.

Then, for studies on the propagation of wave signals with length $\lambda = 2\pi/k \square \{H_0; H_3\}$ comparable to the thickness of the formed layer, we can use the model of a thin layer. The thin layers obtained in both models are inhomogeneous. Equations and/or boundary conditions contain variable coefficients, which lead to nonlinear interaction between the amplitude and phase of the propagating wave signal [8, 14]. Avoiding the difficulties of

constructing exact solutions, in [9, 10, 12, 13] hypothetically constructed solutions in the formed inhomogeneous layers is proposed to use.

In the first model the unknowns are the elastic shear displacement $\mathrm{w}_3^*(x,y,t)$ and the electric field potential $\varphi_3^*(x,y,t)$ for which functional distributions have the following forms

$$\mathrm{w}_3^*(x,y,t) = f(h_m(x),y)\cdot\left[\mathrm{w}_2(x,h_2(x),t) - \mathrm{w}_1(x,h_1(x),t)\right] + \mathrm{w}_1(x,h_1(x),t), \tag{1.3.17}$$

$$\varphi_3^*(x,y,t) = f(h_m(x),y)\left[\varphi_2(x,h_2(x),t) - \varphi_1(x,h_1(x),t)\right] + \varphi_1(x,h_1(x),t). \tag{1.3.18}$$

Here $\mathrm{w}_n(x,h_n(x),t)$ and $\varphi_n(x,h_n(x),t)$, $n=1;2$, are the boundary values of the elastic shear and the electric potential on the corresponding non-smooth surfaces. Distribution function $f(h_m(x),y)$ of the wave field in the hypotheses of (1.3.17) and (1.3.18) is selected in such a way that it is quite simple and completely (without loss of physical phenomena) describes the nature of the unknowns on the surfaces and along the thickness of the adhesive layer $h_1(x) \le y \le h_2(x)$. The choice of this function must provide the physico-mechanical field continuity on the surfaces of medium slices $y = h_m(x) \quad m=1;2$:

$$\mathrm{w}_3^*(x,h_m(x),t) = \mathrm{w}_m(x,h_m(x),t), \tag{1.3.19}$$

$$\varphi_3^*(x,h_m(x),t) = \varphi_m(x,h_m(x),t) \tag{1.3.20}$$

This requires that on surfaces $y = h_m(x)$ the following conditions must be satisfied:

$$f(h_m(x),y)\big|_{y=h_1(x)} = 0 \qquad \text{and} \qquad f(h_m(x),y)\big|_{y=h_2(x)} = 1. \tag{1.3.21}$$

For complete description of the nature of the physico-mechanical fields in thin layer of piezoelectric material (glue), it is necessary that the representations (1.3.17) and (1.3.18) satisfy the equations of the electroelastic anti-plane deformations (1.3.1) for $n=3$

$$\tilde{G}_3\mathrm{w}_{3,yy}^* = \rho_3\ddot{\mathrm{w}}_3^* - \tilde{G}_3\mathrm{w}_{3,xx}^*, \qquad \varphi_{3,xx}^* + \varphi_{3,yy}^* = \left(e_3/\varepsilon_3\right)\left(\mathrm{w}_{3,xx}^* + \mathrm{w}_{3,yy}^*\right). \tag{1.3.22}$$

Taking into account the form of the normal shear electroelastic wave signal on the non-smooth surfaces $y = h_m(x)$, the distribution function of the boundary value problem obtain the following form:

$$d^2 f(y)/dy^2 - k^2\alpha_3^2 f(y) = 0, \text{ for } f(y=h_1(x)) = 0, \quad f(y=h_2(x)) = 1, \tag{1.3.23}$$

from where it follows a new representation for distribution functions:

$$f(h_m(x),y)=\frac{e^{\alpha_3 k(y-h_1(x))}-e^{-\alpha_3 k(y-h_1(x))}}{e^{\alpha_3 k(h_2(x)-h_1(x))}-e^{-\alpha_3 k(h_2(x)-h_1(x))}}=\frac{sh[\alpha_3 k(y-h_1(x))]}{sh[\alpha_3 k(h_2(x)-h_1(x))]}, \quad (1.3.24)$$

which, in contrast to the results in [9, 10], also includes the wave nature of inner adhesive layer $\alpha_3 k=\sqrt{k^2-\left(G_3\left(1+\chi_3^2\right)\omega^2\right)/\rho_3}$. The obtained surface of the exponential function is sufficiently good. In the intervals $h_1(x)\le y\le h_2(x)$, $f(h_m(x),y)\in[0;1]$ is monotone increasing, i.e. $df/dy>0$, and is normalized by the multiplier of characterizing the width of the adhesive layer, $\xi(x)=h_2(x)-h_1(x)$.

When a very short wave signal, i.e. $\lambda \ll H_3 \ll \max\limits_{x\in\{X\}}\left|h_2(x)-h_1(x)\right|$, or a fast wave signal, $V_\phi^2>G_3\left(1+\chi_3^2\right)/\rho_3$, is propagating, the distribution function naturally becomes sinusoidal

$$f(h_m(x),y)=\frac{sh[\alpha_3 k(y-h_1(x))]}{sh[\alpha_3 k(h_2(x)-h_1(x))]}=\frac{sh[\beta_{3n} k(y-h_1(x))]}{sh[\beta_{3n} k(h_2(x)-h_1(x))]}, \quad (1.3.25)$$

where

$$\beta_{3n}=n\cdot\sqrt{\left(G_3\left(1+\chi_3^2\right)\omega_n^2\right)/\left(k_n^2\rho_3\right)-1}. \quad (1.3.26)$$

Introducing hypotheses ***MELS*** (1.3.17) and (1.3.18), the relevant thermodynamic material relations for the adhesive layer material take the form

$$\left.\begin{aligned}\sigma_{31}^{(3*)}&=G_n\left(\partial w_3^*/\partial x\right)+e_n\left(\partial\varphi_3^*/\partial x\right)\\ \sigma_{23}^{(3*)}&=G_n\left(\partial w_3^*/\partial y\right)+e_n\left(\partial\varphi_3^*/\partial y\right)\end{aligned}\right\}$$ define the shear electromechanical stress,

$$\left.\begin{aligned}D_1^{(3*)}&=e_n\left(\partial w_3^*/\partial x\right)-\varepsilon_n\left(\partial\varphi_3^*/\partial x\right)\\ D_2^{(3*)}&=e_n\left(\partial w_3^*/\partial y\right)-\varepsilon_n\left(\partial\varphi_3^*/\partial y\right)\end{aligned}\right\}$$ define the components of the electric field

displacement. MELS hypotheses also allow to divide the boundary conditions (1.3.2)-(1.3.5) into two groups:

a) The first is the group of continuity conditions (1.3.2) and (1.3.3) of the mechanical stress and electric induction on the contact surfaces $y=h_m(x)$ taking into account ***MELS*** hypotheses (1.3.17) and (1.3.18):

$$h_1'(x)\left(\sigma_{31}^{(1)}(x,h_1(x),t)-\sigma_{31}^{(3^*)}(x,h_1(x),t)\right)+\left(\sigma_{32}^{(1)}(x,h_1(x),t)-\sigma_{32}^{(3^*)}(x,h_1(x),t)\right)=0,$$
$$h_2'(x)\left(\sigma_{31}^{(2)}(x,h_2(x),t)-\sigma_{31}^{(3^*)}(x,h_2(x),t)\right)+\left(\sigma_{32}^{(2)}(x,h_2(x),t)-\sigma_{32}^{(3^*)}(x,h_2(x),t)\right)=0, \quad (1.3.27)$$

$$h_1'(x)\left(D_1^{(1)}(x,h_1(x),t)-D_1^{(3^*)}(x,h_1(x),t)\right)+\left(D_2^{(1)}(x,h_1(x),t)-D_2^{(3^*)}(x,h_1(x),t)\right)=0,$$
$$h_2'(x)\left(D_1^{(2)}(x,h_2(x),t)-D_1^{(3^*)}(x,h_2(x),t)\right)+\left(D_2^{(2)}(x,h_2(x),t)-D_2^{(3^*)}(x,h_2(x),t)\right)=0. \quad (1.3.28)$$

In comparison with the case of smooth contact surfaces $y=const$, from the boundary conditions (1.3.27) it is clear that on the respective surfaces of the joints appear the difference of dynamic mechanical efforts

$$\Delta\sigma_{32}^{(m3)}(x,h_m(x),t)=h_m'(x)\left(\sigma_{31}^{(m)}(x,h_m(x),t)-\sigma_{31}^{(3^*)}(x,h_m(x),t)\right), \quad (1.3.29)$$

which do not exist in the absence of roughness.

Similarly, it is obvious from the boundary conditions (1.3.28), that for non-smooth surfaces of the medium contact, in comparison with the case of smooth contact surfaces $y=const$, also appear the difference of dynamic displacements of electric field

$$\Delta D_2^{(m3)}(x,h_m(x),t)=h_m'(x)\left(D_1^{(m)}(x,h_m(x),t)-D_1^{(3^*)}(x,h_m(x),t)\right), \quad (1.3.30)$$

which do not exist in the absence of roughness.

The conditions (1.3.17) and (1.3.18) in the case of normal wave signals

$$\mathrm{w}_n(x,y,t)=W_{0n}\exp((-1)^n\alpha_n ky)\cdot e^{i(kx-\omega t)},$$
$$\varphi_n(x,y,t)=\left\{\Phi_{0n}\exp((-1)^n ky+\left(e_n/\varepsilon_n\right)W_{0n}\exp((-1)^n\alpha_n ky)\right\}\cdot e^{i(kx-\omega t)} \quad (1.3.31)$$

are written as four algebraic equations with respect to the four independent wave amplitude constants in corresponding half-spaces $\{W_{01};W_{02};\Phi_{01};\Phi_{02}\}$.

From the condition of existence of nontrivial wave solutions, we obtain a dispersion transcendental equation

$$\det\left\|\hat{B}_{ij}\left[\{\gamma_3\},h_m(x),n_j^{(m)}(x),\alpha_n(\omega/k)\right]\right\|_{4\times4}=0 \quad (1.3.32)$$

determining the process frequency nature.

b) The other group of boundary conditions, the continuity of elastic displacements and electric field potentials on rough joints, based on (1.3.4), (1.3.5), (1.3.17), (1.3.18) and (1.3.31) gives a new system of four inhomogeneous algebraic equations with respect to the

four amplitude constants

$$\left\{A_{31};A_{32};B_{31};B_{32}\right\}:\hat{B}_{ij}^{*}\left[\left\{\gamma_n\right\},h_m(x),h'_m(x),\alpha_n(\omega/k),\right]\times A_j^{*}=b_i\left[A_r,h_m(x),h'_m(x),\alpha_n(\omega/k)\right].(1.3.3$$

The frequency-amplitude descriptions for the phenomenon identification is obtained from (1.3.33), due to the surface roughness, near-border new phenomena at the joints between the composite waveguide layers. The actual system of equations (1.3.33) determines the wave field in the joining layer, loaded by dynamic mechanical efforts and electric displacements $\Delta D_2^{(\mathrm{m}3)}(x,h_m(x),t)$ on the rough surfaces $y=h_m(x)$. Naturally, for determination of wave amplitudes $\left\{A_{31};A_{32};B_{31};B_{32}\right\}$ in the layer, we can obtain the conditions of internal resonance occurrence as follows:

$$\det\left\|\hat{B}_{ij}^{*}\left[\left\{\gamma_n\right\},h_m(x),h'_m(x),\alpha_n(\omega/k)\right]\right\|_{4\times4}=0 \qquad (1.3.34)$$

It is easy to see, that the presence of roughness of the layer surfaces coefficients and terms in the system of algebraic equations are now complex numbers. Therefore, to identify the effect of the roughness on dispersion, or the probability of the appearance of internal resonance, the wave field must be represented by complex wave number and complex amplitude as follows:

$$F_n(x,y,t)\square\left\{A_n(x,y)+iA_n^{*}(x,y)\right\}\cdot\exp i\left\{\left(k_1+ik_2\right)x-\omega t\right\}. \qquad (1.3.35)$$

Then, the real $\mathrm{Re}\left[F_n(x,y,t)\right]=A_n(x,y)\cdot\cos(kx-\omega t)-A_n^{*}(x,y)\cdot\sin(kx-\omega t)$ and the imaginary $\mathrm{Im}\left[F_n(x,y,t)\right]=A_n(x,y)\sin(kx-\omega t)+A_n^{*}(x,y)\cos(kx-\omega t)$ parts of the wave solutions determined from the systems of the characteristic equations will characterize the effect of roughness on the dispersion, dissipation and internal resonance for propagation of wave signal in a three-layer composite.

CHAPTER 2

INFLUENCE OF MATERIAL AND SURFACE WEAK INHOMOGENEITIES OF THE ELASTIC LAYER-WAVEGUIDE ON THE PROPAGATION OF HIGH-FREQUENCY, PURE ELASTIC SHEAR (SH) WAVE SIGNAL

2.1 The propagation of high frequency pure shear (SH) wave signal in elastic layer-waveguide of weakly inhomogeneous material with mechanically free or rigidly clamped perfectly smooth surfaces

Two model problems on distributions of pure shear, horizontally polarized, elastic normal waves $\vec{U}(x,y,t)=\{0;\ 0;\ \mathrm{w}(x,y,t)\}$ in an isotropic weakly inhomogeneous layer-waveguide are considered [25, 54].

The shear component of the displacement vector has the following form

$$\mathrm{w}(x,y,t)=A_0\cdot\exp\left[i(k_0x-\omega_0t)\right], \tag{2.1.1}$$

where A_0 is the constant amplitude, k_0 is the wave number, and ω_0 is the frequency of the normal wave. Our aim is to identify the loss of stability of the normal wave (2.1.1) for different types of boundary conditions on perfectly smooth surfaces of the waveguide.

Assume, that the normal wave (2.1.1) is distributed in the isotropic, elastic, longitudinally weakly inhomogeneous layer $\{|x|<\infty;\ |y|\le h_0;\ |z|<\infty\}$ with rigidly clumped surfaces $y=\pm h_0$ (see Fig. 2.1.1.a). Then the equation of medium motion has the following form:

$$\frac{\partial\sigma_{zx}}{\partial x}+\frac{\partial\sigma_{zy}}{\partial y}=\rho(x)\frac{\partial^2\mathrm{w}}{\partial t^2}, \tag{2.1.2}$$

where the mechanical stresses according to Hooke's law can be written in the following form:

$$\sigma_{zx}(x,y,t)=G(x)\frac{\partial\mathrm{w}(x,y)}{\partial x};\qquad \sigma_{zy}(x,y,t)=G(x)\frac{\partial\mathrm{w}(x,y)}{\partial y}. \tag{2.1.3}$$

Here $G(x)$ is the shear modulus of the material, which, as the density of the material, i.e. $\rho(x)$, for longitudinally weakly inhomogeneous medium are presented in the following forms:

$$G(x) = G_0\left[1+\varepsilon_1\sin(k_1x)+\delta_1\cos(k_1x)\right];$$
$$\rho(x) = \rho_0\left[1+\varepsilon_2\sin(k_1x)+\delta_2\cos(k_1x)\right]. \qquad (2.1.4)$$

Here $k_1 = \pi/a$ is the number of inhomogeneity waviness of the material layer, a is the half step of inhomogeneity waviness of the material layer, $\varepsilon_1;\ \varepsilon_2;\ \delta_1;\ \delta_2$ are the small amplitudes of inhomogeneity, which, for weak inhomogeneity of the material satisfy the restriction $\varepsilon_n^2+\delta_n^2 \ll 1$, G_0 is the shear modulus and ρ_0 is the density of the corresponding homogeneous material.

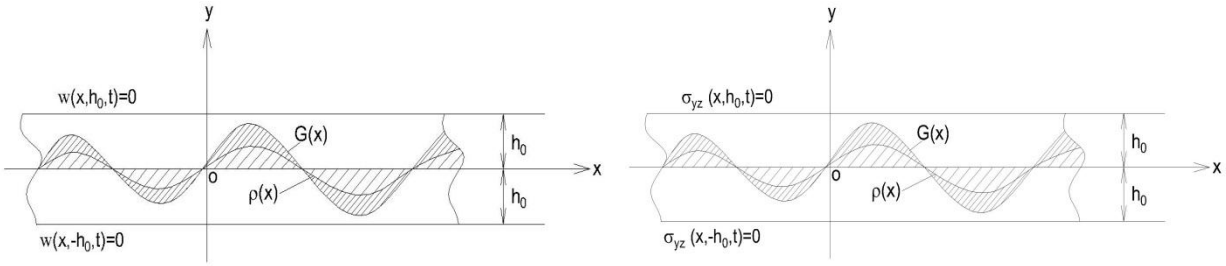

a) b)

Fig. 2.1.1 Inhomogeneous elastic waveguide with smooth surfaces

We obtain the equation of motion with variable periodic coefficients considering (2.1.3) and (2.1.4)

$$\left[1+\varepsilon_1\sin(k_1x)+\delta_1\cos(k_1x)\right]\Delta \mathrm{w} + k_1\left[\varepsilon_1\cos(k_1x)-\delta_1\sin(k_1x)\right]\frac{\partial \mathrm{w}}{\partial x} =$$
$$= c_t^{-2}\left[1+\varepsilon_2\sin(k_1x)+\delta_2\cos(k_1x)\right]\frac{\partial^2 \mathrm{w}}{\partial t^2}, \qquad (2.1.5)$$

where $\Delta \equiv \partial^2/\partial x^2+\partial^2/\partial y^2$ is the Laplace operator, and $c_{0t}^2 \equiv G_0/\rho_0$ is the speed of shear normal wave.

On clamped planes $y=\pm h_0$ the boundary conditions have the form

$$\mathrm{w}(x,-h_0,t) = \mathrm{w}(x,+h_0,t) = 0. \qquad (2.1.6)$$

Then, the wave solution of the equation of motion (2.1.5) satisfying the clamped boundary conditions (2.1.6) can be expanded into the form of Fourier series

$$\mathrm{w}(x,y,t) = \sum_{n=1}^{\infty}\mathrm{w}_n(x)\cdot\sin(\mu_n y)\cdot e^{i\omega_n t}, \qquad (2.1.7)$$

where $\mu_n = \pi n / h_0$ is the wave number of the waveguide. It is obvious, that under these boundary conditions the zero form does not exist, i.e. $\mathrm{w}_0(x) \equiv 0$.

The representation of the solution in the form of (2.1.7), leads the equation of motion (2.1.5) to the infinite system of ordinary differential equations with periodic coefficients with respect to the amplitude functions of each succession of the n-th wave form

$$\begin{aligned}
&\left[\mathrm{w}_n''(x) + \mu_n^2\left(\eta_n^2 - 1\right)\mathrm{w}_n(x)\right] + \\
&+\varepsilon_1 \sin(k_1 x)\left[\mathrm{w}_n''(x) - (k_1\delta_1/\varepsilon_1)\mathrm{w}_n'(x) + \mu_n^2\left(\varepsilon_{21}\eta_n^2 - 1\right)\mathrm{w}_n(x)\right] + \\
&+\delta_1 \cos(k_1 x)\left[\mathrm{w}_n''(x) + (k_1\varepsilon_1/\delta_1)\mathrm{w}_n'(x) + \mu_n^2(\delta_{21}\eta_n^2 - 1)\mathrm{w}_n(x)\right] = 0.
\end{aligned} \tag{2.1.8}$$

where $\eta_n^2 \equiv \omega_n^2/(c_{0t}^2\mu_n^2)$ is the given phase speed of the n-th wave form.

It is obvious, that due to the inhomogeneity of the material, the process is represented by the interaction of three coupled normal wave modes characterized by equations (2.1.8), given in the square brackets. Since the interaction is due to the inhomogeneity functions $\varepsilon_1 \sin(k_1 x)$ and $\delta_1 \cos(k_1 x)$ from (2.1.4), the solution of (2.1.8) with variable periodic coefficients is natural to seek in terms of expansion by given functions of the inhomogeneity

$$\mathrm{w}_n(x) = a_{0n} + \sum_{m=1}^{\infty} \gamma^m \cdot \left(a_{mn}\cos(k_m x) + b_{mn}\sin(k_m x)\right); \qquad n; m \in \mathbb{N}, \tag{2.1.9}$$

where $k_m \equiv mk_1 = (m\pi/a)$ is the wave number in the direction of wave propagation corresponding to the m-th harmonic of the wave, and $\gamma \equiv \max\left\{\sqrt{\varepsilon_i^2 + \delta_i^2}\right\}$, $i = 1;2$ is a small parameter which characterizes the weak inhomogeneity of the material.

Substituting (2.1.9) into (2.1.8) we obtain a recurrent infinite system of homogeneous algebraic equations for the constant amplitudes $\{a_{mn};\ b_{mn}\}$ generated by the interaction of the propagating normal wave modes (wave signal) and the longitudinal weak inhomogeneity of the material

$$\begin{aligned}
&\mu_n^2\left(\eta_n^2 - 1\right)a_{0n} + \\
&+\mu_n^2\gamma\left[\left(\eta_n^2 - \varepsilon_{12}\right)(\varepsilon_2/\gamma)\sin(k_1 x) + \left(\eta_n^2 - \delta_{12}\right)(\delta_2/\gamma)\cos(k_1 x)\right]a_{0n} + \\
&+\sum_{m=1}^{\infty}\gamma^m\left[\mu_n^2\left(\eta_n^2 - 1\right) - k_m^2\right]\cdot\left[\sin(k_m x)b_{mn} + \cos(k_m x)a_{mn}\right] +
\end{aligned}$$

$$+\sum_{m=1}^{\infty}\gamma^m\cdot\left[\left(\mu_n^2\left(\varepsilon_{21}\eta_n^2-1\right)-k_m^2\right)\sin(k_m x)-(k_1\delta_1/\varepsilon_1)k_m\cos(k_m x)\right]\varepsilon_1\sin(k_1 x)b_{mn}+$$

$$+\sum_{m=1}^{\infty}\gamma^m\cdot\left[\left(\mu_n^2(\delta_{21}\eta_n^2-1)-k_m^2\right)\sin(k_m x)+(k_1\varepsilon_1/\delta_1)k_m\cos(k_m x)\right]\delta_1\cos(k_1 x)b_{mn}+$$

$$+\sum_{m=1}^{\infty}\gamma^m\cdot\left[\left(\mu_n^2\left(\varepsilon_{21}\eta_n^2-1\right)-k_m^2\right)\cos(k_m x)+(k_1\delta_1/\varepsilon_1)k_m\sin(k_m x)\right]\varepsilon_1\sin(k_1 x)a_{mn}+ \quad (2.1.10)$$

$$+\sum_{m=1}^{\infty}\gamma^m\cdot\left[\left(\mu_n^2(\delta_{21}\eta_n^2-1)-k_m^2\right)\cos(k_m x)-(k_1\varepsilon_1/\delta_1)k_m\sin(k_m x)\right]\delta_1\cos(k_1 x)a_{mn}=0.$$

In the resulting relations there appear the coefficients ν_j; α_j; β_j characterizing the interaction between independent normal harmonics and the distributions of wave signal in the layer with the weak longitudinal inhomogeneity (2.1.4)

$$\nu_m=\mu_n^2\left(\eta_n^2-1\right)-k_m^2; \quad (2.1.11)$$

$$\alpha_m=\mu_n^2\left(\varepsilon_2\eta_n^2-\varepsilon_1\right)-\varepsilon_1 k_m^2; \quad (2.1.12)$$

$$\beta_m=\mu_n^2\left(\delta_2\eta_n^2-\delta_1\right)-\delta_1 k_m^2. \quad (2.1.13)$$

Considering the fact that in the zeroth approximation $\gamma^0=1$ and $k_0=0$ correspond to the normal form on axis $0x$ in the case of homogeneous medium, the solution in the first approximation will have the following form

$$\mathrm{w}_{0n}(x,y,t)=\sum_{n=1}^{\infty}a_{0n}\sin(\mu_{0n}y)\cdot e^{i\omega_{0n}t}. \quad (2.1.14)$$

From (2.1.14) it follows that in the zeroth approximation the weakly inhomogeneous layer allows only one group of discrete frequencies $\omega_{0n}=c_{0t}\left(\pi n/h_0\right)$ for propagating shear wave with appropriate numbers of formations $\mu_n=\pi n/h_0$.

In the first approximation, $m=1$, from (2.1.9) we will obtain

$$\mathrm{w}_1(x,y,t)=\sum_{n=1}^{\infty}\left[a_{0n}+\gamma a_{1n}\cos(k_1 x)+\gamma b_{1n}\sin(k_1 x)\right]\sin(\mu_{1n}y)\cdot e^{i\omega_0 t}. \quad (2.1.15)$$

For derivation of the wave number μ_{1n} and amplitudes of the first approximation we derive from three coupled infinite system of equations:

$$\mu_n^2\left[\left(\eta_n^2-1\right)+\varepsilon_2\left(\eta_n^2-\varepsilon_{12}\right)\sin(k_1 x)+\delta_2\left(\eta_n^2-\delta_{12}\right)\cos(k_1 x)\right]a_{0n}=0; \quad (2.1.16)$$

$$\left[\mu_n^2\left(\eta_n^2-1\right)-k_1^2\right]\cdot b_{1n}\cdot\sin(k_1 x)=0; \quad (2.1.17)$$

$$\left[\mu_n^2\left(\eta_n^2-1\right)-k_1^2\right]\cdot a_{1n}\cdot\cos(k_1x)=0. \qquad (2.1.18)$$

From the condition of existence of non-trivial solutions of the system (2.1.16)÷(2.1.18) we compute the wave number of formation of the first approximation obtain

$$\mu_{1n}(k_1x)=\left(\pi n/h_0\right)\sqrt{\frac{1+\varepsilon_2\sin(k_1x)+\delta_2\cos(k_1x)}{1+\varepsilon_1\sin(k_1x)+\delta_1\cos(k_1x)}}. \qquad (2.1.19)$$

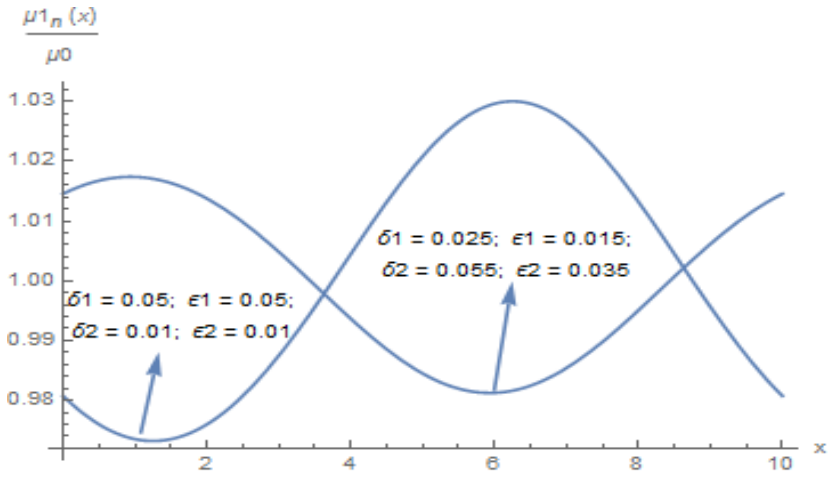

Fig. 2.1.2 The forms of change of formation coefficient (or frequency) on propagation of normal wave signal

It is obvious that the quantities under the square root are positively defined especially (in the case of weak inhomogeneity of the material, when $\varepsilon_n^2+\delta_n^2 \square 1$).Therefore, forbidden frequency zones in the first approximation do not arise. From (2.1.19) we see that the coefficient of formation (or phase function) $\mu_{1n}=\mu_{0n}\cdot f(x)$ is already variable because of the inhomogeneity of the material (Fig. 2.1.2). Fig. 2.1.2 also shows that at relatively large compared to the density stiffness coefficients, when $\varepsilon_1>\varepsilon_2$ and $\delta_1>\delta_2$, and at relatively large compared to the stiffness, density coefficients, when $\varepsilon_1<\varepsilon_2$ and $\delta_1<\delta_2$, the changes of the vibration frequencies are different, while remaining periodic.

From coincidence of harmonics, amplitudes $\{a_{1n}\}$ and $\{b_{1n}\}$ of the first approximation expressed in terms of the amplitudes of the wave signal $\{a_{0n}\}$, can be computed as follows

$$b_{1n}=\frac{\mu_{1n}^2\left(\varepsilon_2\left(\pi n/h_0\right)^2-\varepsilon_1\right)}{\left(\left(\pi n/h_0\right)^2-\left(\pi/a\right)^2\right)-\mu_{1n}^2}a_{0n};\ a_{1n}=\frac{\mu_{1n}^2\left(\delta_2\left(\pi n/h_0\right)^2-\delta_1\right)}{\left(\left(\pi n/h_0\right)^2-\left(\pi/a\right)^2\right)-\mu_{1n}^2}a_{0n}. \qquad (2.1.20)$$

From (2.1.20) it is clear, that the amplitude distortion compared with the distortion of the phase function, is quadratic. The numbers of resonant harmonics, when $a_{1n}\to\infty$ and/or

$b_{1n} \to \infty$, for which there occurs internal resonance, which can be found from here as well (Fig.1.3)

$$n = (h_0/a)\sqrt{\frac{1+\gamma_1 \sin(k_1 x+\varphi_1)}{\gamma_□ \sin(k_1 x+\varphi_□)}}. \qquad (2.1.21)$$

Here

$$\gamma_1 □ \sqrt{\varepsilon_1^{\,2}+\delta_1^{\,2}}\,;\ \varphi_□ □ \arccos\frac{(\varepsilon_1-\varepsilon_2)}{\sqrt{(\varepsilon_1-\varepsilon_2)^2+(\delta_1-\delta_2)^2}} = \arcsin\frac{(\delta_1-\delta_2)}{\sqrt{(\varepsilon_1-\varepsilon_2)^2+(\delta_1-\delta_2)^2}};$$

$$\gamma_□ □ \sqrt{(\varepsilon_1-\varepsilon_2)^2+(\delta_1-\delta_2)^2}\,; \qquad \varphi_1 □ \arccos\frac{\varepsilon_1}{\sqrt{\varepsilon_1^{\,2}+\delta_1^{\,2}}} = \arcsin\frac{\delta_1}{\sqrt{\varepsilon_1^{\,2}+\delta_1^{\,2}}}.$$

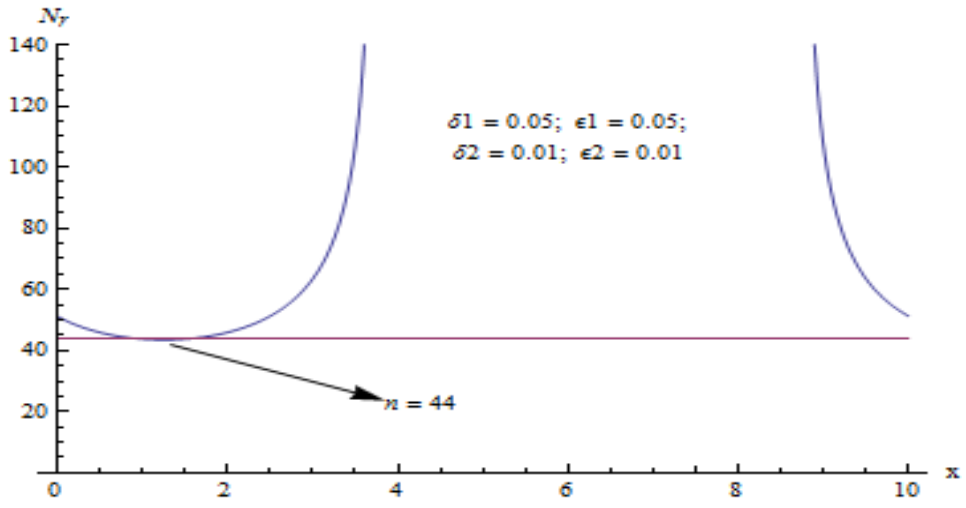

Fig. 2.1.3 The line of resonance by harmonic x_r □ N_r and by cuts

It is easy to get the instability zones of harmonics from (2.1.21) (when the quantities under the square root are positive. (Fig. 2.1.3))

$$a(2m-1-\varphi_□/\pi) \le x \le a(2m-\varphi_□/\pi); \qquad m = 0;1;2;... \qquad (2.1.22)$$

Whence it follows that in some cases of medium inhomogeneity, the quantities under the square root can be negative and then the corresponding harmonics lose stability and will be represented by exponential functions $\exp\left[\pm\mu_{1n}(\varepsilon_i;\delta_i;a/h_0)\cdot y\right]$.

From Fig. 2.1.3, in each section we can find the numbers of resonant forms. It is seen that starting from a certain number of harmonics, resonant forms periodically exist at certain intervals, for particular values of the characteristics of inhomogeneity of the material, Fig. 2.1.4 (see formulas (2.1.23) and (2.1.24)).

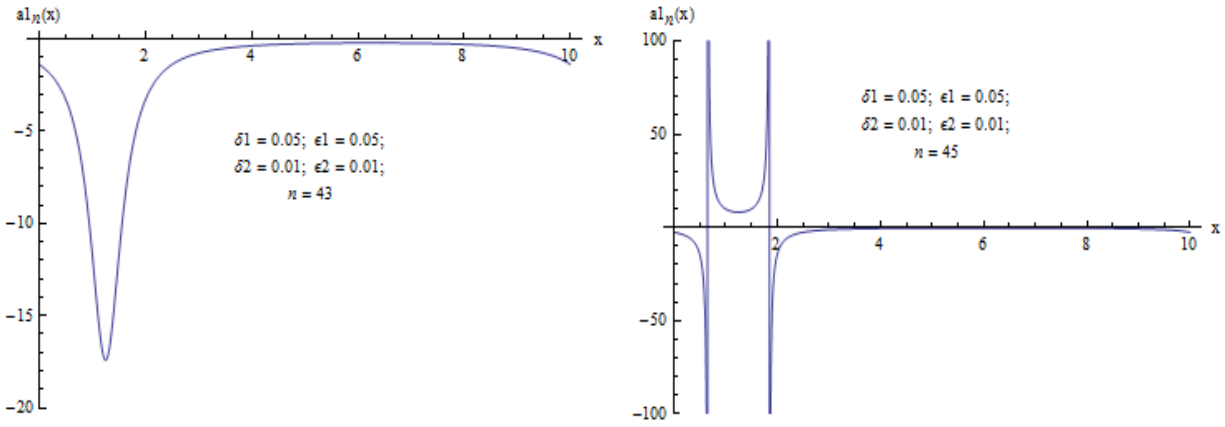

a) b)

Fig. 2.1.4 The character of changes of amplitudes for certain material inhomogeneity characteristics, before and after occurrence of the resonance

The number of resonant harmonics will be

$$N_r = \left(h_0/a\right)\sqrt{\frac{1+\gamma_1 \sin(k_1 x_r + \varphi_1)}{\gamma_{\square} \sin(k_1 x_r + \varphi_{\square})}}, \tag{2.1.23}$$

and the respective values x_r of the intervals of definition will be

$$a\left(2m+1-\varphi_{\square}/\pi\right) > x_r > a\left(2m-\varphi_{\square}/\pi\right); \qquad m = 0;1;2;... \tag{2.1.24}$$

In the second approximation, $m = 2$, the solution will have the following form

$$\mathrm{w}_2(x,y,t) = \mathrm{w}_1(x) + \gamma^2 \sum_{n=1}^{\infty}\left[a_{2n}\cos(k_2 x) + b_{2n}\sin(k_2 x)\right]\sin(\mu_{2n} y)\cdot e^{i\omega_0 t}.$$ Considering (2.1.15), (2.1.19) and (2.1.20), from (2.1.10) with respect to a_{0n}, a_{2n} and b_{2n} we have three infinite systems of homogeneous algebraic equations. From the condition of existence of non-trivial solution, the formation number in the second approximation will be computed as follows

$$\mu_n = \left(n\pi/h_0\right)\sqrt{\mathrm{N}\left(\varepsilon_i;\delta_i;k_1 x\right)/\mathrm{M}\left(\varepsilon_i;\delta_i;k_1 x\right)}, \tag{2.1.25}$$

where

$$\mathrm{N}(\varepsilon_i;\delta_i;k_1x)\ \begin{bmatrix} 1+\dfrac{\varepsilon_2 n^2a^2+\left(n^2a^2-h_0{}^2\right)\beta_{1n}}{n^2a^2}\sin(k_1x)+ \\ \dfrac{1}{2}\left(\varepsilon_2\beta_{1n}+\delta_2\alpha_{1n}\right)+\dfrac{\delta_2 n^2a^2+\left(n^2a^2-h_0{}^2\right)\alpha_{1n}}{n^2a^2}\cos(k_1x)+ \\ +\dfrac{n^2a^2\left(\delta_2\beta_{1n}+\varepsilon_2\alpha_{1n}\right)-2h_0^2\left(\delta_1\beta_{1n}+\varepsilon_1\alpha_{1n}\right)}{2n^2a^2}\sin(2k_1x)+ \\ +\dfrac{2h_0^2(\varepsilon_1\beta_{1n}-\delta_1\alpha_{1n})-n^2a^2\left(\varepsilon_2\beta_{1n}-\delta_2\alpha_{1n}\right)}{2n^2a^2}\cos(2k_1x) \end{bmatrix};$$

$$\mathrm{M}(\varepsilon_i;\delta_i;k_1x)\ \frac{1}{2}\begin{bmatrix} \left(\varepsilon_1\beta_{1n}+\delta_1\alpha_{1n}\right)+ \\ +2\left(1+\left(\varepsilon_1-\beta_{1n}\right)\sin(k_1x)+\left(\delta_1-\alpha_{1n}\right)\cos(k_1x)\right)+ \\ +\left(\delta_1\alpha_{1n}-\varepsilon_1\beta_{1n}\right)\cos(2k_1x)-\left(\delta_1\beta_{1n}+\varepsilon_1\alpha_{1n}\right)\sin(2k_1x) \end{bmatrix}. \qquad (2.1.26)$$

The amplitudes a_{2n} and b_{2n} will be found from coincidence of harmonics as follows

$$a_{2n}=A_{21}+A_{22},$$

$$b_{2n}=\frac{\left(\mu_n^2\left(\varepsilon_2\eta_n^2-\varepsilon_1\right)-\varepsilon_1k_1^2\right)b_{1n}+k_1\delta_1a_{1n}}{2\gamma\left(\mu_n^2\left(\eta_n^2-1\right)-k_2^2\right)},$$

$$A_{21}=\frac{\left(\mu_n^2\left(\delta_2\eta_n^2-\delta_1\right)-2\delta_1k_1^2\right)a_{1n}-\left(\mu_n^2\left(\varepsilon_2\eta_n^2-\varepsilon_1\right)-2\varepsilon_1k_1^2\right)b_{1n}}{2\gamma\left(\mu_n^2\left(\eta_n^2-1\right)-k_2^2\right)},$$

$$A_{22}=-\frac{\gamma\left(\mu_n^2\left(\varepsilon_2\eta_n^2-\varepsilon_1\right)-\varepsilon_1k_1^2\right)b_{1n}+\gamma k_1^2\delta_1a_{1n}+\mu_n^2\left(\eta_n^2-1\right)a_{0n}}{\gamma^2\left(\mu_n^2\left(\eta_n^2-1\right)-k_2^2\right)}.$$

The wave solution in the second approximation will have the following form:

$$\mathrm{w}_2(x,y,t)=\mathrm{w}_1(x,y,t)+\gamma^2\sum_{n=1}^{\infty}a_{0n}\begin{bmatrix}1+\beta_2\left(\varepsilon_i;\delta_i;\left(na/h_0\right)\right)\sin(k_2x)\\ +\alpha_2\left(\varepsilon_i;\delta_i;\left(na/h_0\right)\right)\cos(k_2x)\end{bmatrix}\sin(\mu_{2n}y)e^{i\omega_0t}. \qquad (2.1.27)$$

From the obtained relations find the forbidden frequency zones (the number of harmonics, for which the following inequality holds)

$$\left|-b_n\pm\sqrt{b_n^2-c_n}\right|>1, \qquad (2.1.28)$$

where

$$b_n \approx \frac{\left[\left(na/4h_0\right)^2-1\right]\left(\left(na/4h_0\right)^2(\delta_2-\delta_1)-\delta_1\right)}{\gamma_1^2/4+\left[\left(\left(na/4h_0\right)^2(\delta_2-\delta_1)-\delta_1\right)\right]^2+\left[\left(\left(na/4h_0\right)^2\left(\varepsilon_2-\varepsilon_1\right)-\varepsilon_1\right)\right]^2};$$

$$c_n \approx \frac{\left[\left(na/4h_0\right)^2-1\right]^2-\left[\left(\left(na/4h_0\right)^2\left(\varepsilon_2-\varepsilon_1\right)-\varepsilon_1\right)\right]^2-\delta_1^2/4}{\gamma_1^2/4+\left[\left(\left(na/4h_0\right)^2(\delta_2-\delta_1)-\delta_1\right)\right]^2+\left[\left(\left(na/4h_0\right)^2\left(\varepsilon_2-\varepsilon_1\right)-\varepsilon_1\right)\right]^2}. \quad (2.1.29)$$

From the relations (2.1.25) and (2.1.26) the zones of instability of the harmonics are easily obtained (when the quantities under the square root is negative), whence it follows that in some cases of medium inhomogeneity, the quantities under the square root can be negative and then the corresponding harmonics lose stability and will be represented by the exponential functions $\exp\left[\pm\mu_{2n}(\varepsilon_i;\delta_i;a/h_0)\cdot y\right]$.

Numerical analysis of the obtained amplitude-phase distortion will be given along with the case of mechanically free boundary conditions of the waveguide. The zones of the forbidden frequencies for different values of parameters characterizing inhomogeneity of the material are given in Fig 1.4**.** In one case the forbidden frequency occurs for a limited number of harmonics n_i, $i\in\left\{m_1,m_1+1,...k\right\}$, but in the other case there is an unlimited number of harmonics $i\geq m_2$.

Assume, that the normal wave is propagating in isotropic, elastic, longitudinally weak inhomogeneous layer with mechanically free surfaces $y=\pm h_0$ (see Fig. 2.1.1.b):

$$\left.\frac{\partial \mathrm{w}(x,y,t)}{\partial y}\right|_{y=-h_0}=\left.\frac{\partial \mathrm{w}(x,y,t)}{\partial y}\right|_{y=+h_0}=0. \quad (2.1.30)$$

The weak inhomogeneity has the form set in (2.1.4). Proceeding like the case of clamped surfaces, the wave solution of the equations of motion satisfying (2.1.30) can be represented in the form

$$\mathrm{w}(x,y,t)=\sum_{n=0}^{\infty}\mathrm{w}_n(x)\cdot\cos(\mu_n y)\cdot e^{i\omega_n t}, \quad (2.1.31)$$

where $\mathrm{w}_n(x)$ is shown in the (2.1.9). The character of amplitude-phase distortion on the propagation of wave signal will be the same as in the case of clamped surfaces of the layer.

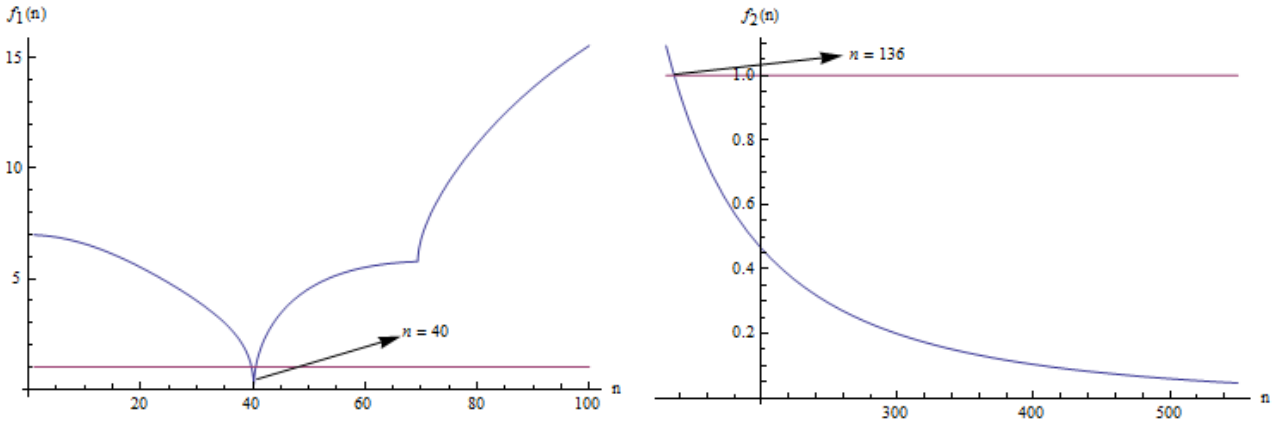

a) $\left|b_n-\sqrt{b_n^2-c_n}\right|>1$ b) $\left|-b_n-\sqrt{b_n^2-c_n}\right|>1$

Fig. 2.1.5 The zones of forbidden frequencies for particular values of material inhomogeneity characteristics

Unlike the case of the waveguide with clamped surfaces, in this case the solution of the zeroth approximation is obtained in the form

$$\mathrm{w}_0(x,y,t)=a_{00}+\sum_{n=1}^{\infty}a_{0n}\cos(\mu_{0n}y)\cdot e^{i\omega_{0n}t}, \tag{2.1.32}$$

where $a_{00}=\mathrm{w}_0(x,\pm h_0,t)$ are the values of the shear strain on surfaces.

Considering the fact, that the nature of the change in the direction of the propagation of the wave signal is characterized by the equation (2.1.8), the wave field in the waveguide in the case of the mechanically free surfaces in the following approximations are obtained:

a) in the first approximation, the solution is obtained in the form accounting the material inhomogeneity

$$\mathrm{w}_1(x,y,t)=a_{00}+\gamma\sum_{n=1}^{\infty}\left[a_{1n}\cos(k_1x)+b_{1n}\sin(k_1x)\right]\cos(\mu_{1n}y)\cdot e^{i\omega_0t}, \tag{2.1.33}$$

where the wave characteristics are as follows: μ_{1n} is the wave formation number, a_{1n} and b_{1n} are the amplitudes of harmonics described in relations (2.1.19) and (2.1.20) accordingly.

b) in the second approximation, the wave field has the following form:

$$\mathrm{w}_2(x,y,t)=\mathrm{w}_1(x)+\gamma^2\sum_{n=1}^{\infty}a_{0n}\begin{bmatrix}\alpha_2\left(\varepsilon_i;\delta_i;\left(na/h_0\right)\right)\cos(k_2x)+\\+\beta_2\left(\varepsilon_i;\delta_i;\left(na/h_0\right)\right)\sin(k_2x)\end{bmatrix}\cos(\mu_{2n}y)e^{i\omega_0t}, \tag{2.1.34}$$

where the wave characteristics are the followings: μ_{2n} is the wave formation number, a_{2n} and b_{2n} are the amplitudes of harmonics described in relations (2.1.25), (2.1.26) and

(2.1.28), (2.1.29) respectively.

As shown above, the frequency characteristics for different boundary conditions on the smooth surfaces of the waveguide of weakly inhomogeneous material are identical and because of the inhomogeneity are changed identically. The weak inhomogeneity leads to distortion of the formation coefficients (Fig. 2.1.2) as in nature, as well as in value. Formation coefficients $\mu_{1n}(k_1 x)$ are already changing periodically from the value $\mu_{0n} = (\pi n / h_0)$. At the clamped surfaces of the layer the first harmonic with constant amplitude does not exist, as in the case of a homogeneous medium. Depending on the characteristics of the inhomogeneity of the material, at certain frequencies $n = N_r$ of the wave signal in certain sections $x = x_r$ internal resonance occurs (Fig. 2.1.4). The weak inhomogeneity of the material of the waveguide may lead to filtration of specific frequencies of the normal wave (Fig. 2.1.5).

In Figures 2.1.6 a) and b) the levels of wave surfaces for different boundary conditions are given. It is obvious that the wave surface generally preserves the leveled character, existing in the case of homogeneous medium: preserves the symmetry (or asymmetry) over the thickness of the waveguide, but are distorted in the direction of wave propagation. On the lines of level changes jagged deviations are clearly appeared, characterized by the inhomogeneity of the material of the waveguide. At specific frequencies of the wave signal, the interaction of the signal and inhomogeneity leads to parametric resonance.

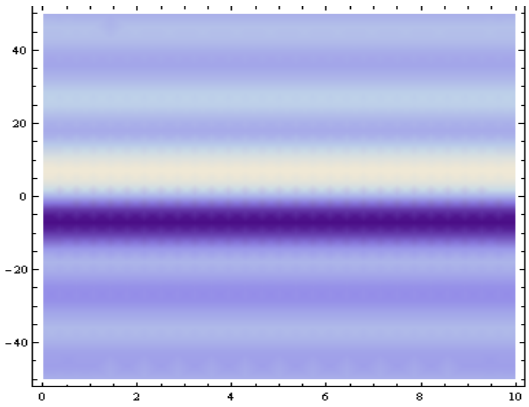

Fig. 2.1.6 a) The levels of the wave surface when the surfaces of the waveguide are clamped

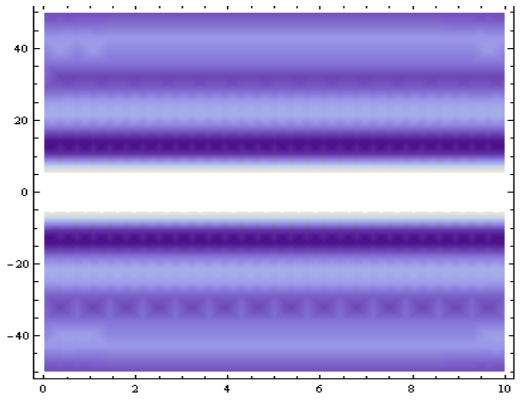

Fig. 2.1.6 b) The levels of the wave surface when the surfaces of the waveguide are mechanically free

2.2 The propagation of high frequency pure shear (SH) wave signal in elastic homogeneous layer-waveguide with mechanically free or rigidly clamped weakly inhomogeneous surfaces

Let us assume that the pure shear normal wave signal

$$w(x,y,t) = W_0(y) \times \exp\left[i(k_0 x - \omega_0 t)\right], \tag{2.2.1}$$

$$u(x,y,t) \equiv 0, \qquad v(x,y,t) \equiv 0, \tag{2.2.2}$$

is propagating in the elastic, isotropic waveguide $\Omega = \left\{|x| < \infty;\ h_-(x) \le y \le h_+(x);\ |z| < \infty\right\}$ with rough surfaces $y = h_-(x)$ and $y = h_+(x)$ (see Fig. 2.2.1). Here $k_0 \equiv \left(2\pi/\lambda_0\right)$ is the wave number and λ_0 is the length of wave signal. Then, the equation of motion of the medium has the following form:

$$\frac{\partial^2 w(x,y,t)}{\partial x^2} + \frac{\partial^2 w(x,y,t)}{\partial y^2} = c_0^{-2} \frac{\partial^2 w(x,y,t)}{\partial t^2}. \tag{2.2.3}$$

where $c_0^2 = G_0/\rho_0$ is the speed of the shear normal wave in the waveguide.

It is assumed, that the roughness of the waveguide surfaces $y = h_\pm(x)$ are represented by the following harmonic functions:

$$\begin{cases} h_+(x) = h_0\left[1 + \varepsilon_+ \cdot \sin(k_+ \cdot x) + \delta_+ \cdot \cos(k_+ \cdot x)\right], \\ h_-(x) = -h_0\left[1 + \varepsilon_- \cdot \sin(k_- \cdot x) + \delta_- \cdot \cos(k_- \cdot x)\right], \end{cases} \tag{2.2.4}$$

where h_0 is the half-thickness of basic layer of the waveguide, $\varepsilon_\pm$ and $\delta_\pm$ are the relative amplitude coefficients of the heights of roughness profiles with $\left\{\varepsilon_\pm;\ \delta_\pm\right\} \ll 1$, because the heights of the protrusions of roughness $h_0 \cdot \varepsilon_\pm$ and $h_0 \cdot \delta_\pm$ are always much less than the basic layer thickness: $\left\{h_0 \cdot \varepsilon_\pm;\ h_0 \cdot \delta_\pm\right\} \ll h_0$, $k_\pm \equiv 2\pi/\lambda_\pm$ is the number of the waviness of roughness profile and $\lambda_\pm$ is the step (wavelength) of the roughness profiles.

The boundary conditions on mechanically free non-smooth surfaces of the waveguide $\sigma_{ij}(x,y) \cdot n_j^\pm(x) = 0$ are written respectively in this form:

$$h'_\pm(x) \cdot \left.\frac{\partial w(x,y)}{\partial x}\right|_{y=h_\pm(x)} + \left.\frac{\partial w(x,y)}{\partial y}\right|_{y=h_\pm(x)} = 0. \tag{2.2.5}$$

It is evident from (2.2.3)-(2.2.5), that its solution must explicitly depend on the roughness of the surfaces. Since the roughness is weak $\{h_0 \cdot \varepsilon_{\pm};\ h_0 \cdot \delta_{\pm}\} \ll h_0$, the interaction of roughness will mainly be available in case of high-frequency (shortwave) wave signals, for which $\lambda_0 \ll \lambda_{\pm} \ll h_0$, or equivalently $k_0 h_0 \gg k_{\pm} h_0 \gg 1$. Then, one might be interested in investigation of the influence of surfaces roughness of the waveguide on the propagation of normal high-frequency shear waves.

There are two methods to solve the problem [13]: the method of successive approximations and the method of introduced hypotheses. Later in this article we will compare wave characteristics of the received wave fields.

When high-frequency, normal shear signal (2.2.1) is propagated in elastic waveguide, interaction of the wave signal with the roughness of the surfaces in the near-surface areas occurs, which consequently leads to amplitude and phase distortion of the primary signal. New harmonics appear and a new amplitude-phase interaction is formed.

We use Fourier method of variables separation, and the solution of the boundary value problem (2.2.3)-(2.2.5) is represented in the following form:

$$w(x,y,t) = \sum_{n=1}^{\infty} W_n(y) \cdot X_n(x) \cdot \exp(-i\omega_{0n} t)\,. \tag{2.2.6}$$

Then the conditions of mechanically free surfaces of the waveguide, on rough surfaces $y = h_{\pm}(x)$ respectively, for each harmonic of propagating wave will have the following form

$$W_n'(h_{\pm}(x)) = \mp h_0 k_{\pm} \cdot \left[\varepsilon_{\pm} \cdot \cos(k_{\pm} \cdot x) - \delta_{\pm} \cdot \sin(k_{\pm} \cdot x)\right] \cdot \frac{X_n'(x)}{X_n(x)} \cdot W_n(h_{\pm}(x)) \cdot W_n'(h_{\pm}(x)) \tag{2.2.7}$$

It is suggested, that the equations for determining the desired functions $X_n(x)$ and $W_n(y)$ are shown in the form

$$\begin{cases} W_n''(y) + k_n^2 \left[\eta_n^2 - 1\right] W_n(y) = 0, \\ X_n''(x) + k_n^2 X_n(x) = 0, \end{cases} \tag{2.2.8}$$

where the following assignment for appropriate harmonics $\eta_n^2 \ll \omega_n^2 k_n^{-2} c_0^{-2}$ has been taken into account, k_n is the wave number (formation coefficient through the thickness of the waveguide), corresponding to the generated n-th harmonic.

From surface conditions (2.2.7) it follows that the undamped solutions of (2.2.8) in the directions of the propagation $\pm Ox$ (for $\mathrm{Im}\left[k_n\right]\equiv 0$) are shown in the following form

$$\begin{cases} W_n(y) = C_{1n}\exp\left(ik_n\alpha_n y\right) + C_{2n}\exp\left(-ik_n\alpha_n y\right), \\ X_n(x) = C_{\pm}\exp\left(\pm ik_n x\right), \end{cases} \tag{2.2.9}$$

which, for slow waves, i.e. when $\alpha_n^2 \equiv \eta_n^2 - 1 < 0$, corresponds to the damped harmonics from the surface up to the depth of the waveguide, and for fast waves, i.e. when $\alpha_n^2 = \eta_n^2 - 1 \geq 0$, corresponds to harmonic forms over the thickness of the waveguide.

From (2.2.8) it also follows that fast damped waves occur in the directions of wave propagation $\pm Ox$ in the case of $\mathrm{Re}\left[k_n\right]\equiv 0$:

$$\begin{cases} W_n''(y) - k_n^2\left[\eta_n^2 - 1\right]W_n(y) = 0, \\ X_n''(x) - k_n^2 X_n(x) = 0. \end{cases}$$

For slow wave, i.e. when $\alpha_n^2 < 0$, the solution corresponds to harmonic forms over the thickness of the waveguide, and for fast wave, i.e. when $\alpha_n^2 \geq 0$, it corresponds to damped harmonics from the surface up to the depth of the waveguide.

Taking into account that the roughness of the surface of the waveguide is weak and its impact on the propagating wave is described by boundary conditions (2.2.7), the solution of system (2.2.8) is represented in this form

$$X_n(x) = \sum_{m=0}^{\infty} \gamma^m \cdot A_{mn}\exp\left(ik_{*m}x\right). \tag{2.2.10}$$

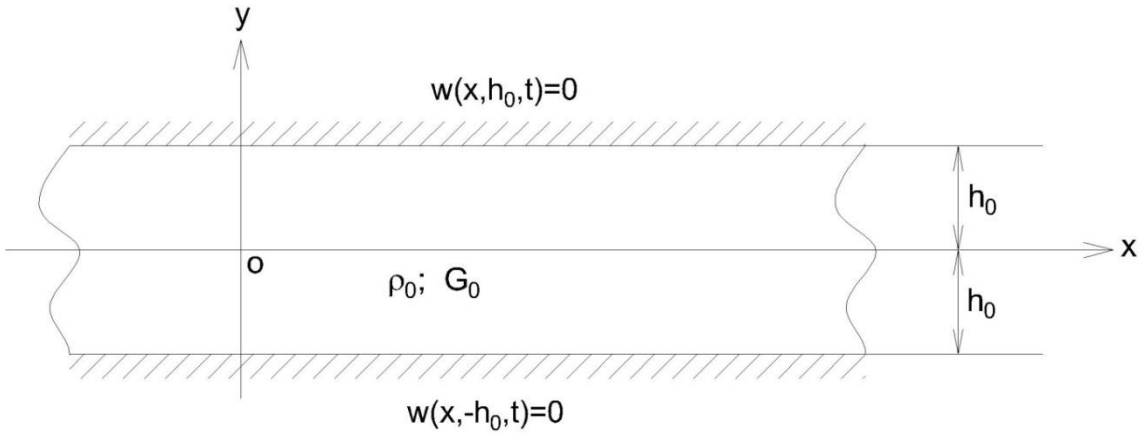

Fig. 2.2.1 The model of elastic waveguide as a multilayer waveguide

Moreover, the value $m=0$ corresponds to the case of homogeneous waveguide. Here, the introduced wave number k_{*m} should be formed by the impact of normal wave signal and roughness of the surfaces of the waveguide.

The roughness of the surfaces, in its turn, is characterized by the greatest common divisor of wave numbers $k_* \equiv \min\{k_+/p;\ k_-/q\} = 2\pi/\lambda_*$ is the smallest common wave number of roughness on the surfaces corresponding to the generated m-th harmonic waves, and $\gamma \equiv \max\left\{\sqrt{\varepsilon_\pm^2+\delta_\pm^2}\right\} \ll 1$ is a small parameter characterizing the weak roughness of the surfaces of the waveguide.

$$
\begin{aligned}
&k_n\alpha_n\left[C_{n1}\exp\left(ik_n\alpha_n h_\pm(x)\right)-C_{n2}\exp\left(-ik_n\alpha_n h_\pm(x)\right)\right]\cdot\sum_{m=0}^{\infty}\gamma^m\cdot A_{mn}\exp\left(ik_{*m}x\right)= \\
&=\mp h_0 k_\pm\cdot\left[\varepsilon_\pm\cdot\cos(k_\pm x)-\delta_\pm\cdot\sin(k_\pm x)\right]\times \\
&\times\left[C_{n1}\exp\left(ik_n\alpha_n h_\pm(x)\right)+C_{n2}\exp\left(-ik_n\alpha_n h_\pm(x)\right)\right]\cdot\sum_{m=0}^{\infty}k_{*m}\gamma^m\cdot A_{mn}\exp\left(ik_{*m}x\right).
\end{aligned}
\tag{2.2.11}
$$

Considering that the right hand sides of boundary conditions (2.2.11) are in small $m+1$ order in the $n=0$ approximation, for non-trivial solutions of (2.2.11) we obtain the dispersion equation with the following solution

$$
\omega_{0n}=k_{0n}c_0=\frac{2\pi c_0}{\lambda_{0n}}=\frac{\pi n c_0}{h_0}. \tag{2.2.12}
$$

Consequently, interaction of the normal wave (2.2.1) with surface roughness $h_\pm(x)$ is not occur in the $n=0$ approximation, and the propagating wave is still normal as in $n=0$ approximation of longitudinally weakly rough waveguide with mechanically free surfaces [54]

$$
w_0(x,y,t)=\sum_{n=1}^{\infty}A_{0n}\cdot\exp\left[i\left(\frac{\pi n x}{h_0}-\omega_{0n}t\right)\right]. \tag{2.2.13}
$$

From the conditions of synchronization of the surface distortions at the mid-plane of the waveguide $y=0$, we get

$$
\exp\left[i\left(k_{+m}-k_{-m}\right)x\right]=-\frac{k_+\cdot\left[\varepsilon_+\cdot\cos(k_+\cdot x)-\delta_+\cdot\sin(k_+\cdot x)\right]}{k_-\cdot\left[\varepsilon_-\cdot\cos(k_-\cdot x)-\delta_-\cdot\sin(k_-\cdot x)\right]}. \tag{2.2.14}
$$

Considering that the wave number is formed as $k_{1n}(x) = k_{+n} - k_{-n}$ and $k_* = \min\{k_+/p;\ k_-/q\} = 2\pi/\lambda_*$, it is easy to get the allowed wavelengths from (2.2.14) for the first approximation:

$$\lambda_*(x) = \lambda_0 \cdot 2\pi \arccos^{-1}\left\{-\frac{k_+ \cdot [\varepsilon_+ \cdot \cos(k_+ \cdot x) - \delta_+ \cdot \sin(k_+ \cdot x)]}{k_- \cdot [\varepsilon_- \cdot \cos(k_- \cdot x) - \delta_- \cdot \sin(k_- \cdot x)]}\right\}. \tag{2.2.15}$$

Then from the boundary equations (2.2.11) for the first approximation we will have

$$\exp\left(ik_{0n}\alpha_n\left(h_+(x) - h_-(x)\right)\right) - \exp\left(-ik_{0n}\alpha_n\left(h_+(x) - h_-(x)\right)\right) = 0,$$

therefore formation coefficient of generated distortions of waves is obtained as

$$k_{0n}\alpha_{1n} = \frac{\pi n}{h_+(x) - h_-(x)}. \tag{2.2.16}$$

The wave number of the first generated harmonic depends on the surfaces of the non-smooth waveguide

$$k_{1n}(x) = \left(\frac{\pi n}{h_0}\right)\left(h_+(x) - h_-(x)\right)\left[h_0^2 + \left(h_+(x) - h_-(x)\right)^2\right]^{-1/2}. \tag{2.2.17}$$

In the first approximation, the interaction of the normal wave with surface non-smoothness affects to the propagating wave:

$$w_1(x, y, t) = \sum_{n=1}^{\infty} W_{1n}(y) \cdot X_{1n}(x) \cdot \exp(-i\omega_{0n}t), \tag{2.2.18}$$

where

$$\begin{cases} W_{1n}(y) = C_{1n}\exp\left(i\dfrac{h_0 \cdot k_{1n}(x)y}{h_+(x) - h_-(x)}\right) + C_{2n}\exp\left(-i\dfrac{h_0 \cdot k_{1n}(x)y}{h_+(x) - h_-(x)}\right), \\ X_{1n}(x) = \gamma A_{0n}\exp\left(ik_{1n}(x) \cdot x\right). \end{cases} \tag{2.2.19}$$

Note that if the rough surfaces are “symmetric” with respect to the mid-plane of the waveguide, i.e.

$$-h_-(x) = h_+(x) = h(x) = h_0\left[1 + \varepsilon \cdot \sin(k \cdot x) + \delta \cdot \cos(k \cdot x)\right], \tag{2.2.20}$$

then from relations (2.2.16) and (2.2.17) for the wave number over the thickness of the waveguide and the coefficient of formation, respectively, are obtained as follows

$$k_{1n}^s(x) = \frac{\pi n}{h_0} \cdot \left[\frac{h_0^2}{4h^2(x)} + 1\right]^{-1/2}; \tag{2.2.21}$$

$$k_{1n}^{s}(x)\cdot\alpha_{1n}^{s}(x)=\frac{\pi n}{h(x)}\cdot\left[\frac{h_0^2}{h^2(x)}+4\right]^{-1/2}. \tag{2.2.22}$$

The solution (2.2.19) will be correspondingly transformed into

$$\begin{cases} W_{1n}^{s}(y)=C_{1n}^{s}\exp\left(i\left(\dfrac{h_0\cdot k_{1n}^{s}(x)}{h(x)}\right)y\right)+C_{2n}^{s}\exp\left(-i\left(\dfrac{h_0\cdot k_{1n}^{s}(x)}{h(x)}\right)y\right), \\ X_{1n}^{s}(x)=\gamma A_{0n}\exp\left(ik_{1n}^{s}(x)\cdot x\right). \end{cases} \tag{2.2.23}$$

In the case of "synchronous" (parallel to each other) roughness on the surfaces of the waveguide, will have the following representations:

$$\begin{cases} h_{+}(x)=h_0\left[1+\varepsilon\cdot\sin(k\cdot x)+\delta\cdot\cos(k\cdot x)\right], \\ h_{-}(x)=-h_0\left[1-\varepsilon\cdot\sin(k\cdot x)-\delta\cdot\cos(k\cdot x)\right]. \end{cases} \tag{2.2.24}$$

Then from relations (2.2.16) and (2.2.17) for the wave number over the thickness of the waveguide and the coefficient of formation, respectively, are obtained as follows:

$$k_{1n}^{*}(x)=\frac{\sqrt{5}}{10}\cdot\frac{\pi n}{h_0}; \qquad k_{1n}^{*}(x)\cdot\alpha_{1n}^{*}(x)=\frac{\sqrt{5}}{20}\cdot\frac{\pi n}{h_0}. \tag{2.2.25}$$

The solution (2.2.19) changes accordingly

$$\begin{cases} W_{1n}^{*}(y)=C_{1n}^{*}\exp\left(i\dfrac{\sqrt{5}}{20}\cdot\dfrac{\pi n}{h_0}y\right)+C_{2n}^{*}\exp\left(-i\dfrac{\sqrt{5}}{20}\cdot\dfrac{\pi n}{h_0}y\right), \\ X_{1n}(x)=\gamma A_{0n}\exp\left(i\dfrac{\sqrt{5}}{20}\cdot\dfrac{\pi n}{h_0}x\right). \end{cases} \tag{2.2.26}$$

The Second Approach: To analyze the propagation of the normal, pure shear wave signal (2.2.1) and (2.2.2), taking into account that in the isotropic waveguide $\Omega:=\left\{|x|<\infty;\ h_{-}(x)\le y\le h_{+}(x);\ |z|<\infty\right\}$ roughness of surfaces $y=h_{-}(x)$ and $y=h_{+}(x)$ are described by the functions (2.2.4), the near-surface thin layers with variable thickness (the waveguide is presented as three-layer, see Fig. 2.2.1) are virtually selected $\Omega=\Omega_{-}\cup\Omega_0\cup\Omega_{+}$, where

$$\begin{cases} \Omega_{-}\ \square\ \left\{|x|<\infty;\ h_{-}(x)\le y\le -h_0+\gamma_{-};\ |z|<\infty\right\}, \\ \Omega_0\ \square\ \left\{|x|<\infty;\ -h_0+\gamma_{-}\le y\le h_0-\gamma_{+};\ |z|<\infty\right\}, \\ \Omega_{+}\ \square\ \left\{|x|<\infty;\ h_0-\gamma_{+}\le y\le h_{+}(x);\ |z|<\infty\right\}. \end{cases} \tag{2.2.27}$$

We intend to solve the equation of medium motion (2.2.3) for all three layers separately with boundary conditions (2.2.5) on mechanically free, non-smooth surfaces $y = h_-(x)$ and $y = h_+(x)$ for elastic displacements $w_\pm(x,y,t)$ (respectively for layers $\Omega_\pm$), and the conditions of continuity on virtual cross-sections $y = -h_0 + \gamma_-$ and $y = h_0 - \gamma_+$

$$\begin{aligned} &w_0(x,y,t)\big|_{y=-h_0+\gamma_-} = w_-(x,y,t)\big|_{y=-h_0+\gamma_-}, \\ &w_0(x,y,t)\big|_{y=h_0-\gamma_+} = w_+(x,y,t)\big|_{y=h_0-\gamma_+}, \end{aligned} \tag{2.2.28}$$

$$\begin{aligned} &\left.\frac{\partial w_0(x,y,t)}{\partial y}\right|_{y=-h_0+\gamma_-} = \left.\frac{\partial w_-(x,y,t)}{\partial y}\right|_{y=-h_0+\gamma_-}, \\ &\left.\frac{\partial w_0(x,y,t)}{\partial y}\right|_{y=h_0-\gamma_+} = \left.\frac{\partial w_+(x,y,t)}{\partial y}\right|_{y=h_0-\gamma_+}. \end{aligned} \tag{2.2.29}$$

Considering the thinness of the surface layers $\Omega_\pm$, the solution in them are represented with the hypotheses of MELS [12] taking into account the nature of the changes arising from surface roughness $y = h_-(x)$ and $y = h_+(x)$

$$w_+(x,y) = \frac{sh\left(\mu_+\left[y - h_0 + \gamma_+\right]\right)}{sh\left(\mu_+\left[h_+(x) - h_0 + \gamma_+\right]\right)} \cdot \left[w_+\left(x, h_+(x)\right) - w_0\left(x, h_0 - \gamma_+\right)\right] + w_0\left(x, h_0 - \gamma_+\right), \tag{2.2.30}$$

$$w_-(x,y) = \frac{sh\left(\mu_-\left[y + h_0 - \gamma_-\right]\right)}{sh\left(\mu_-\left[h_-(x) + h_0 - \gamma_-\right]\right)} \cdot \left[w_-\left(x, h_-(x)\right) - w_0\left(x, -h_0 + \gamma_-\right)\right] + w_0\left(x, -h_0 + \gamma_-\right), \tag{2.2.31}$$

where the values $w_+\left(x, h_+(x)\right)$ and $w_-\left(x, h_-(x)\right)$ are determined from the conditions on mechanically free surface (2.2.5) as follows:

$$w_+\left(x, h_+(x)\right) = \frac{\mu_+ \cdot cth\left(\mu_+\left[h_+(x) - h_0 + \gamma_+\right]\right) \cdot \left[1 - \left\{h_+'(x)\right\}^2\right]}{\mu_+ \cdot cth\left(\mu_+\left[h_+(x) - h_0 + \gamma_+\right]\right) \cdot \left[1 - \left\{h_+'(x)\right\}^2\right] + h_+'(x)} \cdot w_0\left(x, h_0 - \gamma_+\right); \tag{2.2.32}$$

$$w_-\left(x, h_-(x)\right) = \frac{\mu_- \cdot cth\left(\mu_-\left[h_-(x) + h_0 - \gamma_-\right]\right) \cdot \left[1 - \left(h_-'(x)\right)^2\right]}{\mu_- \cdot cth\left(\mu_-\left[h_-(x) + h_0 - \gamma_-\right]\right) \cdot \left[1 - \left(h_-'(x)\right)^2\right] + h_-'(x)} \cdot w_0\left(x, -h_0 + \gamma_-\right). \tag{2.2.33}$$

Substituting (2.2.32) and (2.2.33) into (2.2.30) and (2.2.31), we reach the solution in the near-surface thin layers of the waveguide formed by the propagation of the normal wave $w_0(x,y,t)=W_0(y)\cdot\exp\left[i(k_0x-\omega_0t)\right]$ in the basic layer Ω_0:

$$w_+(x,y)=\left\{\begin{array}{l}1-\dfrac{sh\left(\mu_+\left[y-h_0+\gamma_+\right]\right)}{sh\left(\mu_+\left[h_+(x)-h_0+\gamma_+\right]\right)}\times\\ \times\dfrac{h_+'(x)}{\mu_+\cdot cth\left(\mu_+\left[h_+(x)-h_0+\gamma_+\right]\right)\cdot\left[1-\left\{h_+'(x)\right\}^2\right]+h_+'(x)}\end{array}\right\}\cdot w_0\left(x,h_0-\gamma_+\right);\qquad(2.2.34)$$

$$w_-(x,y)=\left\{\begin{array}{l}1-\dfrac{sh\left(\mu_-\left[y+h_0-\gamma_-\right]\right)}{sh\left(\mu_-\left[h_-(x)+h_0-\gamma_-\right]\right)}\times\\ \times\dfrac{h_-'(x)}{\mu_-\cdot cth\left(\mu_-\left[h_-(x)+h_0-\gamma_-\right]\right)\cdot\left[1-(h_-'(x))^2\right]+h_-'(x)}\end{array}\right\}\cdot w_0\left(x,-h_0+\gamma_-\right).\qquad(2.2.35)$$

Let us represent the normal wave in the basic layer Ω_0 in a common form

$$w_0(x,y,t)=\left[A\cos(\mu_*y)+B\sin(\mu_*y)\right]\cdot\exp\left[i(k_*x-\omega_0t)\right],\qquad(2.2.36)$$

here $k_*=\min\left\{pk_+;qk_-\right\}=2\pi/\lambda_*$ is the smallest common wave number of the roughness on the surfaces corresponding to the generated harmonic of the wave.

From the conditions of continuity of mechanical stresses (2.2.29), we obtain a dispersion equation to determine the formation coefficient μ_*:

$$\begin{array}{l}\mu_*^2-\mu_*\cdot ctg\left(\mu_*(2h_0-(\gamma_++\gamma_-)\right)\cdot\left(f_+\left(\mu_+;h_+(x)\right)-f_-\left(\mu_-;h_-(x)\right)\right)=\\ =-f_+\left(\mu_+;h_+(x)\right)\cdot f_-\left(\mu_-;h_-(x)\right),\end{array}\qquad(2.2.37)$$

in which

$$f_+\left(\mu_+;h_+(x)\right)=\left[\begin{array}{l}\dfrac{1}{sh\left(\mu_+\left[h_+(x)-h_0+\gamma_+\right]\right)}\times\\ \times\dfrac{1}{\mu_+\cdot cth\left(\mu_+\left[h_+(x)-h_0+\gamma_+\right]\right)\cdot\left[1-\left\{h_+'(x)\right\}^2\right]+h_+'(x)}\cdot\mu_+h_+'(x)\end{array}\right];\qquad(2.2.38)$$

$$f_{-}\left(\mu_{-};h_{-}(x)\right)\equiv\left[\frac{1}{sh\left(\mu_{-}\left[h_{-}(x)+h_{0}-\gamma_{-}\right]\right)}\times\right.$$
$$\left.\times\frac{1}{\mu_{-}\cdot cth\left(\mu_{-}\left[h_{-}(x)+h_{0}-\gamma_{-}\right]\right)\cdot\left[1-\left\{h'_{-}(x)\right\}^{2}\right]+h_{-}'(x)}\cdot\mu_{-}h_{-}'(x)\right]. \qquad (2.2.39)$$

They characterize the influence of the rough surfaces on the formation coefficient. It is obvious, that the solution of the dispersion equation (2.2.37) significantly depends on the surface roughness $h_{\pm}(x)$.

Numerical Analysis of Obtained Results: Considering the surface roughness, in the first approach, the solutions for formation coefficient $k_{0n}\alpha_{1n}$ and wave number $k_{n1}(x)$ are obtained in the forms (2.2.16) and (2.2.17) respectively. As expected, the variable thickness through the waveguide plays the main role in these expressions $\zeta(x)\equiv h_{+}(x)-h_{-}(x)$, by means of which the wave process can be controlled.

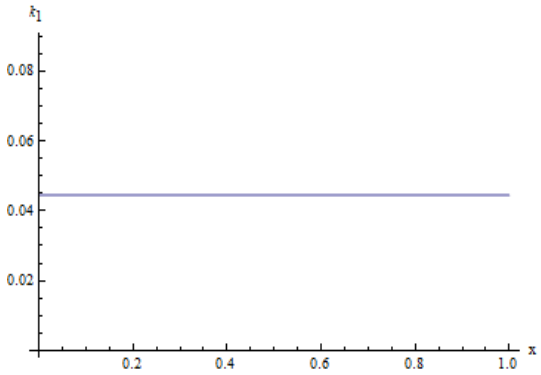

Fig. 2.2.2 a) The wave number for "synchronous" surface roughness of the waveguide (the first approach)

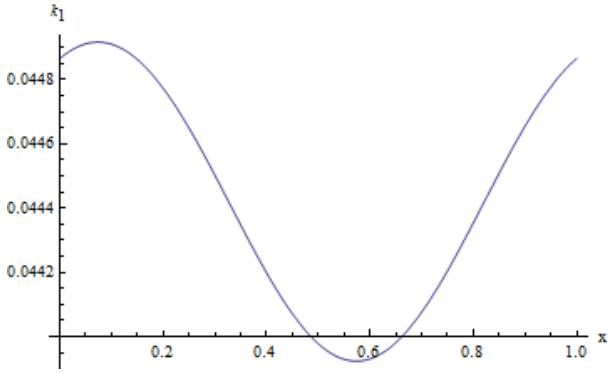

Fig. 2.2.2 b) The wave number for "symmetric" surface roughness of the waveguide (the first approach)

Graphics of the formation coefficient and the wave number for different particular characteristic surfaces of roughness are given in Figs. 2.2.2 and 2.2.3 using the relations (2.2.20)-(2.2.26), respectively. From the figures of the wave number and formation coefficient it follows that for "symmetric" surface roughness of the waveguide (2.2.20) the changes of these values are characteristically different from the case of "synchronous" surface roughness (2.2.24).

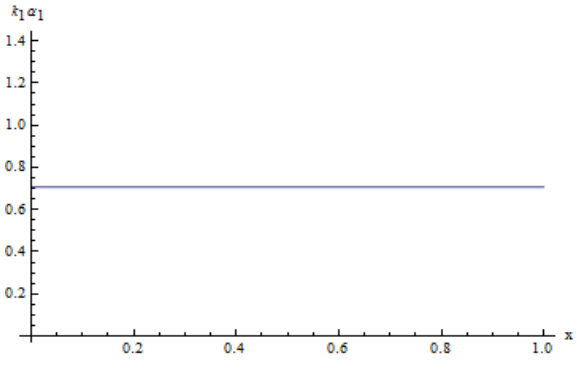

Fig. 2.2.3 a) The formation coefficient for "synchronous" surface roughness of the waveguide (the first approach)

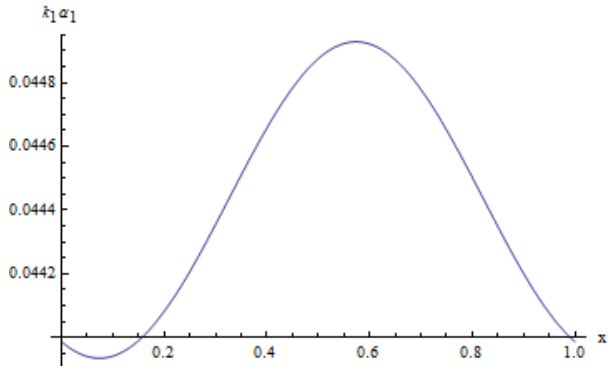

Fig. 2.2.3 b) The formation coefficient for "symmetric" surface roughness of the waveguide (the first approach)

From Figs. 2.2.2 b) and 2.2.3 b) it is obvious that in the case of "symmetric" surface roughness of the waveguide (2.2.20), the wave number and the formation coefficient are periodically changed with respect to the half-thickness of the waveguide in the interval $x \in [0, \lambda_*]$.

In the case of "synchronous" surface roughness of the waveguide (2.2.24) the wave number and the formation coefficient are only changed by a constant value for each n-th harmonic. In the general case of arbitrary surface roughness $y = h_-(x)$ and $y = h_+(x)$ from (2.2.14)-(2.2.19) it follows that due to the difference of surface roughness in the near-surface areas there occur qualitatively identical, but quantitatively different harmonics, a synchronization which occurs at the mid-plane $y = 0$. From (2.2.16) and (2.2.17) it is obvious that the wave number $k_{1n}(x)$ and the formation coefficient $k_{0n}\alpha_{1n}(x)$ for the propagation of the waves is always positive, since $h_+(x) - h_-(x) > 0$. From relations (2.2.23) and (2.2.26) we can easily get the nature of the changes of elastic shear through the thickness of the waveguide, according to the variable thickness of the waveguide (see Fig. 2.2.4). The picture of elastic shear $W_{1n}^s(y)$ over the thickness of the waveguide for the "symmetric" surface roughness is defined by relation (2.2.23) and is shown in Fig. 2.2.4 a). Fig. 2.2.4 shows that over the thickness of the waveguide for the "symmetric" surface roughness (2.2.20), the normal waveform is periodically distorted depending on the law of variation of its thickness $\zeta(x)$. Accordingly, the phase velocity of the generated harmonic

is also changed. The elastic shear $W_{1n}^{*}(y)$ over the thickness of the waveguide for "synchronous" surface roughness is defined by relation (2.2.26) and is shown in Fig. 2.2.4 b). From (2.2.25) it follows that in this case only short waves with lengths $\lambda_{*} = \sqrt{5} \cdot h_0 / n$ propagate for large numbers of harmonics n, such that $n\lambda_{*} \square \sqrt{5} \cdot h_0$.

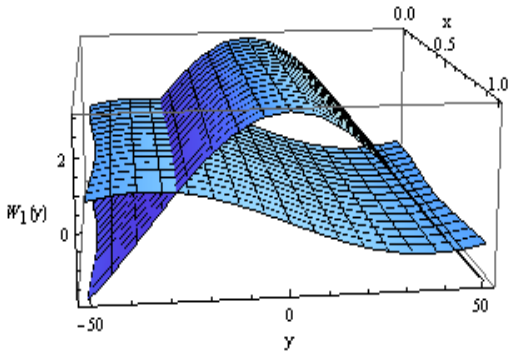

Fig. 2.2.4 a) The elastic shear through the thickness of the waveguide for "symmetric" surface roughness (the first approach)

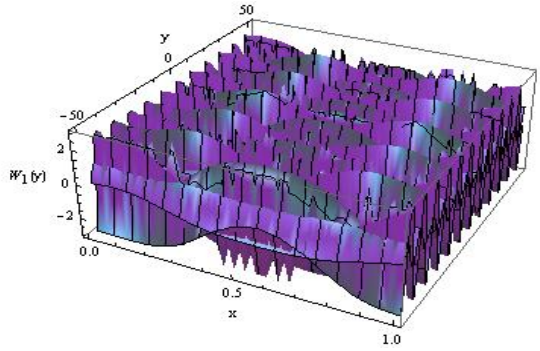

Fig. 2.2.4 b) The elastic shear through the thickness of the waveguide for "synchronous" surface roughness (the first approach)

Solving the problem with the method of hypotheses MELS, through the thickness of the waveguide we obtain the expression of elastic shear in the basic layer Ω_0 in the form of (2.2.36), which is analytically continued in both near-surface zones Ω_{-} and Ω_{+}, accordingly (2.2.35) and (2.2.34). The image over the thickness of the waveguide is constructed after determining the formation coefficient μ_{*} from the dispersion equation (2.2.37). From relations (2.2.34)-(2.2.39) it is obvious that the solutions, received in the near-surface zones Ω_{-} and Ω_{+}, are characteristically the same, but numerically different at different surface roughness $h_{+}(x)$ and $h_{-}(x)$.

The dispersion equation (2.2.37) is much simplified in the cases of "symmetric" (2.2.20) and "synchronous" (2.2.24) surface roughness, considering the expressions of the coefficients of the dispersion equation $f_{+}\left(\mu_{+}; h_{+}(x)\right)$ and $f_{-}\left(\mu_{-}; h_{-}(x)\right)$, in relations (2.2.38) and (2.2.39) respectively. Fig. 2.2.5 shows the graphical dependence of the formation coefficient μ_{*} on x. To each formation coefficient μ_{*n} naturally corresponds a wave number $k_{*n} = 2\pi / \lambda_{*} = \sqrt{\omega_{0n}^2 c_0^{-2} - \mu_{*n}^2}$.

From the dispersion equation (2.2.37) and the relations (2.2.38) and (2.2.39) it is evident that in the absence of roughness on the surfaces of the waveguide, i.e. when $h'_+(x) = h'_-(x) \equiv 0$, both introduced multipliers (2.2.38) and (2.2.39) become zero and from the dispersion equation we obtain the case of homogeneous waveguide $\mu_{*n} = \mu_{0n} = \frac{\pi n}{h_0}$.

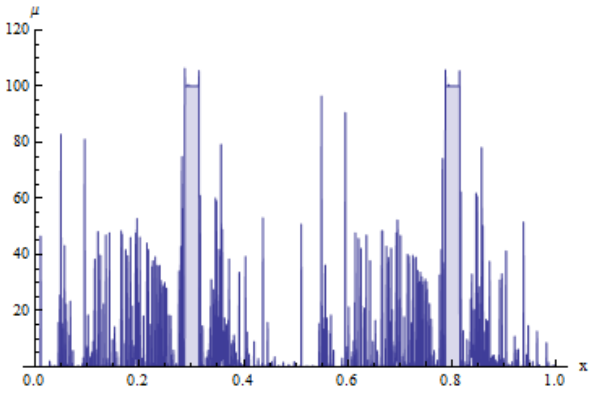

Fig. 2.2.5 a) The formation coefficient for "synchronous" surface roughness of the waveguide (the second approach)

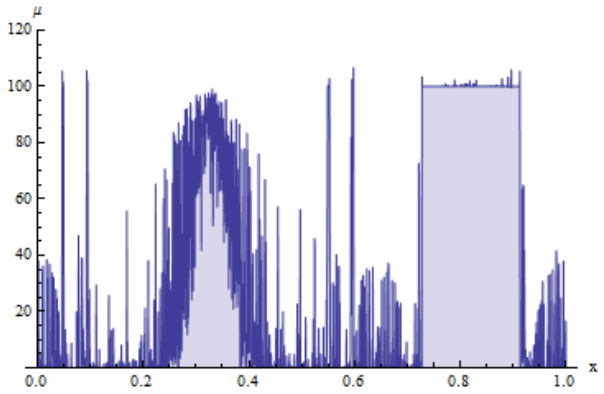

Fig. 2.2.5 b) The formation coefficient for "symmetric" surface roughness of the waveguide (the second approach)

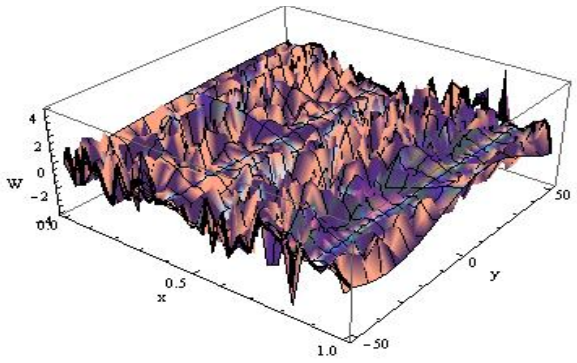

Fig. 2.2.6 a) The elastic shear through the thickness of the waveguide for "symmetric" surface roughness (the second approach)

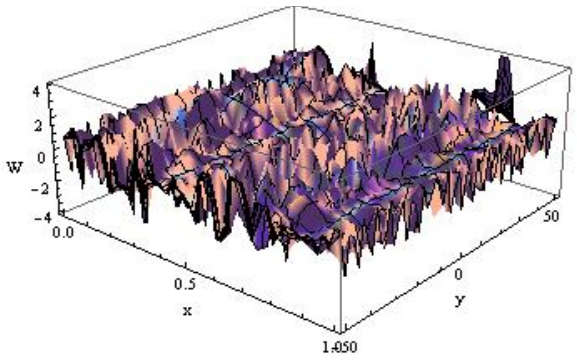

Fig. 2.2.6 b) The elastic shear through the thickness of the waveguide for "synchronous" surface roughness (the second approach)

From the obtained graphs it is also seen how the presence of "symmetric" (2.2.20) or "synchronous" (2.2.24) surface roughness of relatively homogeneous waveguide leads to distortion of forms (formation coefficient μ_{*n} and wave number k_{*n}).

From relations (2.2.37)-(2.2.39) and the received graphs it is also clear that weak surface roughness do not lead to appearance of damped propagating harmonics through the

depth of the waveguide. Partial localization of the wave energy occurs only in the thin surface rough layers, which can be seen in the given figures of elastic shear over the thickness of the waveguide. The images of elastic shear throughout the thickness of the waveguide in particular “symmetric” (2.2.20) and “synchronous” (2.2.24) surface roughness cases are shown in Fig. 2.2.6.

2.3 Comparative analysis of the influence of weak inhomogeneity effect of elastic layer-waveguide surface in propagation of high-frequency (SH) shear wave signals

The propagation of high-frequency monochromatic horizontally polarized shear wave signal in isotropic elastic half-space occupying in Cartesian coordinate plane the domain $\{|x|<\infty;\ -\infty<y\le h(x);\ |z|<\infty\}$ with non-smooth, load free surface $y=h(x)$ is investigated [12]. The coordinate axis $y=0$ is directed along maximal tangential ledge of the non-smooth surface (Fig. 2.3.1). Another characteristic line of the surface heterogeneity (non-smooth) will be the tangent line of maximal cavity $y=-\max\left|h_{\max}(x)-h_{\min}(x)\right|=-R$ of irregularities of the half-space surface.

The problem of horizontally polarized displacement in the half-space is separated from that for plain deformation, and the displacement $w(x,y,t)$ of the shear wave (SH) satisfies the equation

$$\frac{\partial^2 w(x,y,t)}{\partial x^2}+\frac{\partial^2 w(x,y,t)}{\partial y^2}=c_t^{-2}\frac{\partial^2 w(x,y,t)}{\partial t^2}, \tag{2.3.1}$$

where $c_t^2=G/\rho$ is the speed of shear body wave in the medium.

The normal to the geometrically inhomogeneous surface $y=h(x)$ which is free from mechanical loads reads as follows:

$$\vec{n}\left(h(x)\right)=\left\{h'(x)\Big/\sqrt{1+\left[h'(x)\right]^2};\ 1\Big/\sqrt{1+\left[h'(x)\right]^2};0\right\}, \tag{2.3.2}$$

the boundary condition $\sigma_{zx}(x,y,t)\cdot n_x\left(h(x)\right)+\sigma_{xy}(x,y,t)\cdot n_y\left(h(x)\right)=0$ takes the form

$$h'(x)\cdot\left.\frac{\partial w(x,y,t)}{\partial x}\right|_{y=h(x)}+\left.\frac{\partial w(x,y,t)}{\partial y}\right|_{y=h(x)}=0. \tag{2.3.3}$$

Naturally, it is merely a model problem about propagation of high-frequency horizontally polarized monochromatic shear wave signal in the isotropic elastic layer-waveguide $\{|x|<\infty;\ y\le|h(x)|;\ |z|<\infty\}$, the surfaces $y=\pm h(x)$ of which are non-smooth and free from mechanical loads, considered in short-wave approximation $\lambda_0 \square H_0$, where H_0 is the basic depth of the elastic waveguide.

In the case of short-wave approximation along with condition (2.3.3), we have to indicate also a condition on the wave field at infinity, i.e. when $y \to -\infty$. For instance, if the attenuation condition is satisfied at infinity, i.e.

$$w(x,y,t)\big|_{y\to-\infty} \to 0, \tag{2.3.4}$$

then there exists a localized wave on the surface $y = h(x)$ of the half-space due to presence of surface geometric heterogeneities. If the wave field is not attenuated at infinity, then the presence of the surface geometric heterogeneity does not lead to localization of the wave signal.

The equation (2.3.1) with the boundary condition (2.3.3) and the condition of attenuation at infinity (2.3.4) form a mathematical boundary value problem. To reveal the effects of heterogeneity of the half-space surface on the amplitude-frequency characteristic of the propagating plane wave signal $w(x,y,t) = W_0 A(y) \times \exp\{i(k_0 x - \omega_0 t)\}$, and then assess the accuracy of the method of sections and the virtual hypotheses MELS [9, 10], the solution of the formulated boundary value problem will be implemented in two ways. The first way is the direct solution.

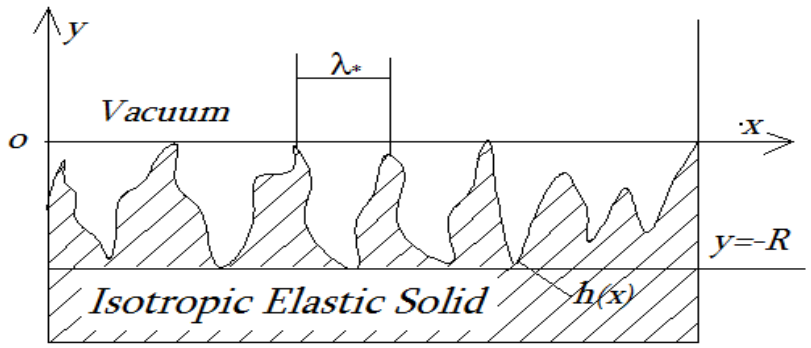

Fig. 2.3.1 Virtual selection of near-surface rough zones as inhomogeneous layer of variable thickness

Physical heterogeneity of the environment or geometrical heterogeneity of the waveguide surface naturally lead to interaction of amplitude-phase of the plane monochromatic wave signal $w(x,y,t) = W_0 A(y) \times \exp\{i(kx - \omega t)\}$. Due to geometric heterogeneity of the waveguide surface the propagating wave is presented as follows:

$$w(x,y,t) = W_0 \exp U(x,y) \times \exp\{i[\theta(x,y) - \omega t]\}, \tag{2.3.5}$$

where $U(x,y)=\ln\left[A_w(x,y)\right]$ is the logarithm of the amplitude function, $A_w(x,y)$ is the amplitude function, and $\{\theta(x,y)-\omega t\}$ is the phase function of the propagating wave. Then from the linear boundary value problem (2.3.1), (2.3.3) and (2.3.4) we come to the nonlinear interaction of the logarithm of the amplitude function $U(x,y)$ and phase function $\{\theta(x,y)-\omega t\}$ [8, 19].

Since the presence of the half-space non-smoothness (see (2.3.3)) leads to amplitude-phase interaction, the solutions of the obtained boundary value problem are presented with complex characteristics, namely wave attenuation coefficient $\alpha \square \sqrt{1-\eta^2/k^2}=\alpha_1+i\alpha_2$ and wave number $k \square k_1+ik_2$. Here $\eta \square \omega/\left(\left(k_1+ik_2\right)c_t\right)=\eta_1+i\eta_2$ is the complex relative phase velocity. Satisfying the complex representation of the wave

$$w(x,y,t)=W_0\exp\left(\alpha_1k_1-\alpha_2k_2\right)y\times\exp\left(-k_2x\right)\times \\ \times\exp\left\{i\left[k_1x+\left(\alpha_1k_2+\alpha_2k_1\right)y-\omega t\right]\right\}, \tag{2.3.6}$$

from conditions (2.3.3) and (2.3.4) we obtain complex dispersion equation

$$ik_1h'(x)+i\left(\alpha_1k_2+\alpha_2k_1\right)+\left(\alpha_1k_1-\alpha_2k_2\right)-k_2h'(x)=0, \tag{2.3.7}$$

from which we obtain conditions for existence of non-trivial solution

$$\alpha_1\equiv 0; \qquad \alpha_2=-h'(x); \quad \Rightarrow \quad \alpha=\alpha_1+i\alpha_2=0-ih'(x);$$

$$k_2\equiv 0; \quad \Rightarrow \eta_2\equiv 0; \quad \Rightarrow \quad k_1=k(x)=\left(\omega_0/c_t\right)\left\{1+\left[h'(x)\right]^2\right\}^{-1/2}. \tag{2.3.8}$$

Thus, for propagation of plane shear wave signal $w_0(x,y,t)=W_0\times\exp\left\{i\left(k_0x-\omega_0t\right)\right\}$ in elastic half-space with non-smooth surface $y=h(x)$, from the propagating plane body waves are formed not attenuated wave fields as along the depth of the elastic half-space, as well as along the direction of the propagation

$$w(x,y,t)=w_+(x,y,t)+w_-(x,y,t), \tag{2.3.9}$$

or in expanded form

$$\mathrm{w}_{\pm}(x,y,t)=W_0\times\exp\left\{\mp ik_0h'(x)\left[1+\left[h'(x)\right]^2\right]^{-1/2}\cdot y\right\}\times \\ \times\exp\left\{i\left[\pm k_0\left[1+\left[h'(x)\right]^2\right]^{-1/2}\cdot x-\omega_0t\right]\right\}. \tag{2.3.10}$$

Unlike half-space with smooth boundary, the propagation of plane shear wave signal in half-space with non-smooth surface brings to distortion of permanent amplitude on plane fronts of propagating and reflecting waves, i.e. $k_0 x \pm \omega_0 t = 0$. Thus,

$$w_{\pm}(x,y,t) = W_0 \times \exp\left\{ik_0\left[\pm x - h'(x)\cdot y\right]\cdot\left[1+\left[h'(x)\right]^2\right]^{-1/2}\right\}\times \exp\left\{-i\omega_0 t\right\}.$$

The distorted wave field in the half-space $\left\{|x|<\infty;\ -\infty < y \le h(x);\ |z|<\infty\right\}$ will take the following form

$$\mathrm{w}(x,y,t) = W_0 \times \left\{\begin{array}{l}\exp\left\{ik_0\left[x - h'(x)\cdot y\right]\cdot\left[1+\left[h'(x)\right]^2\right]^{-1/2}\right\}+\\ +\exp\left\{-ik_0\left[x + h'(x)\cdot y\right]\cdot\left[1+\left[h'(x)\right]^2\right]^{-1/2}\right\}\end{array}\right\}\times \exp\left\{-i\omega_0 t\right\}. \qquad (2.3.11)$$

From relations (2.3.9)-(2.3.11) it becomes obvious, that the distortion of propagating and reflecting waves occurs along the unit tangent vector of the non-smooth surface: $\vec{\tau}\left(h(x)\right) = \left\{1\Big/\sqrt{1+\left[h'(x)\right]^2};\ \mp h'(x)\Big/\sqrt{1+\left[h'(x)\right]^2};\ 0\right\}$. (2.3.12)

Moreover, the presence of the non-smoothness $h'(x) \neq 0$ on the half-space surface generates vibrations in the direction of "$-y$" of the form

$$\cos\left[k_0 h'(x)\left[1+\left[h'(x)\right]^2\right]^{-1/2} y\right] - i\cdot\sin\left[k_0 h'(x)\left[1+\left[h'(x)\right]^2\right]^{-1/2} y\right], \qquad (2.3.13)$$

and the presence of the non-smooth surface $h'(x) \neq 0$ leads to the distortion of the flat front of propagation in the direction "$\pm x$", i.e. $k_0 x \mp \omega_0 t = 0$ of the form

$$\cos\left[k_0 x\cdot\left[1+\left[h'(x)\right]^2\right]^{-1/2}\right]. \qquad (2.3.14)$$

Let $\omega_0 = const$ is the eigen-frequency of the wave signal source for the established dynamics, and the speed of bulk shear wave $c_t = \sqrt{G_0/\rho_0} = const$ in the half-space material. Then, dispersion will occur either in wavelength or wave number

$$\begin{array}{l}\lambda(x) = \lambda_0\cdot\sqrt{1+\left[h'(x)\right]^2},\\ k(x) = k_0\left[1+\left[h'(x)\right]^2\right]^{-1/2}.\end{array} \qquad (2.3.15)$$

It follows from (2.3.15) that $\lambda(x) \geq \lambda_0$, i.e. the surface heterogeneity increases the wavelength with respect to the length of the wave signal. Then the corresponding frequency of oscillation will be $\omega(x) = \omega_0 \left[1 + \left[h'(x) \right]^2 \right]^{-1/2} \leq \omega_0$.

The nature of the change in the wavelength, or self-induced oscillation frequency (dispersion) for the propagation of the wave signal is definitely determined by the nature of the surface heterogeneity and depends on the relative linear characteristics of non-smoothness: λ_* is the average pitch and R is the maximal height of the ledge of surface roughness.

The analytical solution and discussion of the results were convincingly possible due to maximal simplicity of the selected model boundary value problem. In the case of complicated mathematical boundary value problem corresponding to geometric heterogeneity (docking of two rough surfaces with or without adhesive) or when it is necessary to take into account arising physical inhomogeneity of the material of the waveguide, the method of direct solutions will not always be of help.

For a more complete detection of surface wave phenomena near the non-smooth surface of the half-space let us resolve the problem by the method of virtual sections and introducing the hypotheses MELS [9, 10]. Since surface non-smoothness as a geometric heterogeneity is localized in the near-surface area of the half-space, along the line $y = -R$, where $-R$ is the maximal valley of non-smoothness, let us virtually cut the homogeneous near-surface layer of variable thickness $\left\{ |x| < \infty;\ -R \leq y \leq h(x);\ |z| < \infty \right\}$. Then we also will have the homogeneous half-space $\left\{ |x| < \infty;\ -\infty < y \leq -R;\ |z| < \infty \right\}$, which is in full contact with the virtually cut layer (Fig. 2.3.1).

It is obvious that in the resulting layered waveguide along with equation (2.3.1) in two separated areas, boundary condition (2.3.3) on the mechanically free, non-smooth surface $y = h(x)$ and conditions of the wave amplitude attenuation at infinity, on the plane of the virtual section $y = -R$, the conditions of conjugation of the elastic field

$$w_1(x,y,t)\big|_{y=-R} = w_2(x,y,t)\big|_{y=-R};$$
$$\frac{\partial w_1(x,y,t)}{\partial y}\bigg|_{y=-R} = \frac{\partial w_2(x,y,t)}{\partial y}\bigg|_{y=-R}, \qquad (2.3.16)$$

must be satisfied.

The solution in half-space attenuating at infinity has the known form $w_1(x,y,t) = W_{01}\exp(\alpha k y)\cdot e^{i(kx-\omega t)}$. Taking into account the thinness of introduced layer of variable thickness, let us represent the solution in it by means of shear displacements on the surfaces of introduced layer:

$$w_2(x,y,t) - w_1(x,-R,t) = g_w(x,y)\cdot\left[w_2(x,h(x),t) - w_1(x,-R,t)\right]. \quad (2.3.17)$$

Here, the shear wave field distribution function along the variable thickness of the layer is taken to be

$$g_w(x,y) \; sh\left[\alpha k\left(y+R\right)\right]/sh\left[\alpha k\left(h(x)+R\right)\right], \quad (2.3.18)$$

in order to satisfy conditions of conjugation (2.3.16) on the plane of virtual sections. For this it is necessary that on the surface of the layer $g_w\left(x,h(x)\right)=1$ and $g_w\left(x,-R\right)=0$. Moreover, taking into account that in homogeneous half-space have the known form $w_1(x,y,t) = W_{01}\exp(\alpha k y)\cdot e^{i(kx-\omega t)}$, in homogeneous layer $\left\{|x|<\infty;\ -R\le y\le h(x);\ |z|<\infty\right\}$ it must be expressed by wave harmonics $\exp(\pm\alpha k y)$. Then, the elastic shear in the layer will take the form

$$w_2(x,y,t) = W_{01}\left\{1+sh\left[\alpha k\left(y+R\right)\right]\right\}\cdot\exp(-\alpha kR)\cdot\exp\left\{i\left(kx-\omega t\right)\right\}, \quad (2.3.19)$$

when $y\in\left[-R,h\left(x\right)\right]$

For investigation of existence of nontrivial solutions, from the boundary conditions (2.3.3) we obtain the dispersion equation

$$ikh'(x)\left\{1+sh\left[\alpha k\left(h(x)+R\right)\right]\right\}+\alpha k\cdot ch\left[\alpha k\left(h(x)+R\right)\right]=0. \quad (2.3.20)$$

Obviously, in the case of waveguide smooth surface, i.e. when $h'(x)\equiv 0$, equations (2.3.20) and (2.3.7) has only the trivial solution $\alpha k = 0$ corresponding to non dispersion and non attenuation along the depth of the shear waves. Simplifying (2.3.20) we will arrive at

$$\alpha k = -ikh'(x)\frac{1+sh\left[\alpha k\left(h(x)+R\right)\right]}{ch\left[\alpha k\left(h(x)+R\right)\right]}. \quad (2.3.21)$$

For ultrasonic wavelengths, i.e. when $\lambda_0 \; 2\pi R_{\max}\alpha\left(1+h(x)/R_{\max}\right)$, from (2.3.21) it follows that the wave interaction argument $\alpha k\left(h(x)+R\right)\to 0$. For wave signals ”longer”

than the height of maximal ledge $R_{\max}$, i.e. when $\lambda \ll 2\pi R\alpha\left(1+h(x)/R\right)$, from (2.3.21) it follows that the wave interaction argument $\alpha k\left(h(x)+R\right) \ll 1$. It is easy to see that in both cases the factor on the right hand side of (2.3.21) tends to unity without changing the sign and the equation itself acquires the form (2.3.7), naturally with bounded solutions (2.3.8):

$$\alpha = \alpha_1 + i\alpha_2 = 0 - ih'(x); \qquad k_0(x) = k_0\left\{1+\left[h'(x)\right]^2\right\}^{-1/2};$$

$$\omega_0(x) = \omega_0\left[1+\left[h'(x)\right]^2\right]^{-1/2} \le \omega_0; \qquad \lambda_0(x) = \lambda_0 \cdot \sqrt{1+\left[h'(x)\right]^2}\,. \tag{2.3.22}$$

Therefore, introducing unknown function $\alpha = -i\gamma(x)$ the solution of (2.3.21) will take the form

$$\alpha = \mp ih'(x); \quad k_{n^*}(x) = \pm n\pi\left[\left(h(x)+R\right)\right]^{-1}\cdot\left[h'(x)\right]^{-2}; \quad n \in \mathbb{N} \tag{2.3.23}$$

In fact, the heterogeneity of the half-space surface when signal (2.3.19) with parameters (2.3.22) is propagating generates similarity oscillations due to the ratio of the wave signal length and variable thickness of the virtually selected layer

$$w_{n^*}(x,y,t) = W_{0n}\left\{1 - sh\left[i\frac{n\pi\left(1+y/R\right)}{\left[1+h(x)/R\right]\cdot h'(x)}\right]\right\}\cdot\exp\left(i\frac{n\pi}{\left[1+h(x)/R\right]\cdot h'(x)}\right)\times$$
$$\times\exp\left\{\pm i\frac{n\left(\lambda_0/R\right)}{2\left[1+h(x)/R\right]\cdot\left[h'(x)\right]^2}\left(k_0x-\omega_0t\right)\right\}. \tag{2.3.24}$$

The length and frequency of the generated oscillations are represent by relations

$$\lambda_{n^*}(x) = \left[2\left(h(x)+R\right)/n\right]\cdot\left[h'(x)\right]^2;\ \omega_{n^*}(x) = \pm n\pi c_t\cdot\left[\left(h(x)+R\right)\right]^{-1}\cdot\left[h'(x)\right]^{-2}, \tag{2.3.25}$$

respectively. It becomes obvious from (2.3.25) that these in-layered oscillations do not exist if $h'(x) \equiv 0$, or simply vanish when $h(x) \to -R$ or in the case of large numbers of forms $n \gg 1$.

Thus, considering the characteristics of the dispersions (2.3.23) in the near-surface selected layer of thickness $y \in \left[-R;\ h(x)\right]$, for elastic shear we obtain

$$w_*(x,y,t) = \sum_{n=1}^{\infty}\left[w_{n^*}(x,y,t) + \overline{w}_{n^*}(x,y,t)\right]. \tag{2.3.26}$$

Thus, using the method of virtual sections and introducing hypothesis MELS, from (2.3.17) and (2.3.18) new, commensurable with linear dimensions of the non-smoothness

oscillations of length $\lambda \sim \left|\alpha k\left(h(x)+R\right)\right|$ are revealed. At that naturally all possible modes of length $\lambda_{n^*}(x)$ from (2.3.24) occur. Note that in the weakly inhomogeneous surface of the half-space when the variable thickness of near-surface layer is much smaller than the wavelength of the signal, i.e. $\left(h(x)+R\right) \ll \lambda_0$, and in the case of strictly inhomogeneous surface of the half-space when the variable thickness of near-surface layer is much bigger than the wavelength of the signal, i.e. $\left(h(x)+R\right) \gg \lambda_0$, we get the same wave fields with characteristics (2.3.22).

Equivalent Dynamic Bearing Load On The Surface. The presence of inhomogeneous surface leads to interaction of plain wave with non-smoothness. Introducing the equation of motion (2.3.1) in the virtually cut layer $-R \le y \le h(x)$ in the form

$$G\frac{\partial^2 w}{\partial x^2}+\frac{\partial \sigma_{yz}}{\partial y}=\rho\frac{\partial^2 w}{\partial t^2}, \tag{2.3.27}$$

and integrating it over the variable thickness of layer we derive the difference between mechanical tension on the virtual surface $y=-R$ which is equivalent to presence of the cut layer of variable thickness in the near-surface layer

$$\sigma_{yz}\Big|_{-R}^{h(x)}=\int_{-R}^{h(x)}\left\{-G\frac{\partial^2 w_*}{\partial x^2}+\rho\frac{\partial^2 w_*}{\partial t^2}\right\}\cdot dy=G\int_{-R}^{h(x)}\frac{\partial^2 w_*}{\partial y^2}dy. \tag{2.3.28}$$

Taking into account the surface conditions (2.3.3) and (2.3.16) and the expression (2.3.26), (2.3.24) for shear in the cut layer $-R \le y \le h(x)$ and (2.3.9), as well as (2.3.11) for shear in the homogeneous half-space $-\infty < y \le -R$, for equivalent load we will obtain

$$\Delta\sigma=\sigma_{yz}\Big|_{-R}^{h(x)}=-G\left\{h'(x)\cdot\frac{\partial w_*}{\partial x}\Big|_{y=h(x)}+\frac{\partial w}{\partial y}\Big|_{y=-R}\right\}. \tag{2.3.29}$$

Consequently, the problem of propagation of shear wave signal in a half-space with non-smooth surface is equivalent to the problem of propagation of monochromatic shear signal in a half-space loaded with dynamic force $\left|\Delta\sigma\right|=\sigma_{yz}\Big|_{-R}^{h(x)}+\overline{\sigma}_{yz}\Big|_{-R}^{h(x)}$ and smooth surface $y=-R$.

Internal resonance. It was shown above, that when shear wave signal is propagating in a waveguide with non-smooth surface, stationary oscillations with characteristics (2.3.8) and

(2.3.15) occur. On the other hand, due to the presence of non-smoothness commensurable with the wavelength of the propagating signal, oscillations in the near-surface area $-R \le y \le h(x)$ are generated characterized by relations (2.3.23) and (2.3.25). Since in the first version of solution (2.3.11), the induced frequency has the form $\omega(x) = \omega_0 \left[1 + \left[h'(x)\right]^2\right]^{-1/2} \le \omega_0$, then it will be resonant at

$$\omega_r(x) = \omega_0 \left[1 + \left[h'(x)\right]^2\right]^{-1/2} \approx \omega_0, \tag{2.3.30}$$

or at the critical points, where $h'(x) \approx 0$.

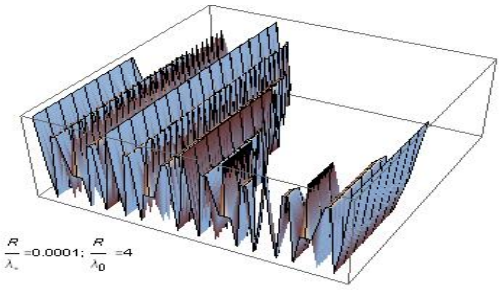

Fig. 2.3.2.a. Shortwave signal with $\lambda_0 = 0.25 \cdot R$ for macro inhomogeneous surface with $\lambda_* = 10^4 \cdot R$.

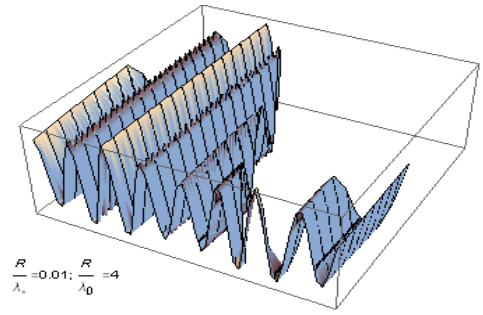

Fig. 2.3.2.b. Shortwave signal with $\lambda_0 = 0.25 \cdot R$ for waviness surface with $\lambda_* = 10^2 \cdot R$.

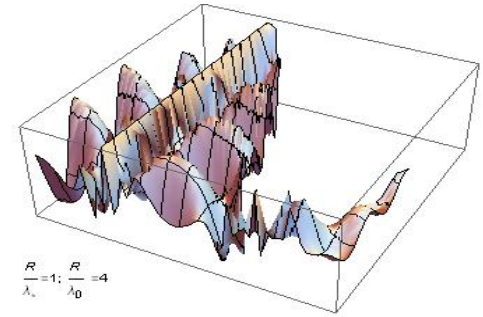

Fig. 2.3.2.c. Shortwave signal with $\lambda_0 = 0.25 \cdot R$ for rough (sawtooth) surface with $\lambda_* = R$.

In the case of corrugated (sinusoidal) surface of the half-space when $h(x) = (R/2) \cdot \left[\sin(2\pi x/\lambda_*) - 1\right]$ we obtain $h'(x) = (\pi R/\lambda_*) \cdot \cos(2\pi x/\lambda_*)$, therefore the induced frequency will be resonant when $h'(x) = (\pi R/\lambda_*) \cdot \cos(2\pi x/\lambda_*) \approx 0$. This implies, that in the case of macro non-smoothness of the half-space surface when the average pitch

of the irregularities is smaller or equal than the maximal height of the ledges, i.e. $\lambda_*/R_{\max} \geq 10^4$, we have $\max\left|\left[h'(x)\right]^2\right| \ll 10^{-7}$ for all wavelengths of the signal.

Thus, in this case the surface of the half space behaves as an ideally smooth, and internal resonance occurs in the excitations of eigen-frequencies $\omega_r(x) \approx \omega_0$.

From the other hand side, for this heterogeneity and in cases when the linear parameters of the corrugated (sinusoidal) surface correspond to other classifications of non-smooth surface, for instance, surface waviness with $\lambda_*/R_{\max} \gg 50 \div 100$ or surface roughness with $\lambda_*/R_{\max} \leq 10$, then the internal resonance can occur in separate segments of the configurations of the surface.

Local internal resonances may occur in surrounding areas of the critical points of the surface roughness, near the tops of the ledges or near pits troughs where the derivative of then non-smoothness tends to zero, i.e. $\left|h'(x)\right| \to 0$. In the case of corrugated surface of the half-space these zones are $\Delta x_m \approx (1+m)\cdot\lambda_*/4 \pm \varepsilon(o)$, $m \in \mathbb{Z}$. For virtually cut near-surface layer $-R \leq y \leq h(x)$ in the case, when the non-smoothness is commensurable with the wavelength of the propagating signal, oscillations generated in the near-surface area, characterized by multiple frequencies $\omega_{n*}(x) = \pm n\pi c_t \cdot \left[\left(h(x)+R\right)\right]^{-1} \cdot \left[h'(x)\right]^{-2}$ are revealed. Equating the value of $\omega_{n*}(x)$ to the value of the frequency of stationary waves $\omega(x) = \omega_0\left[1+\left[h'(x)\right]^2\right]^{-1/2} \leq \omega_0$, we will obtain a condition of internal resonance with respect to the ratio of the wavelength and geometric characteristics of the non-smoothness:

$$\lambda_0 \approx \frac{2}{n}\cdot\frac{\left(h(x)+R\right)\cdot\left[h'(x)\right]^2}{\sqrt{1+\left[h'(x)\right]^2}}. \qquad (2.3.31)$$

In the case of corrugated (sinusoidal) surface when $h(x) = (R/2)\cdot\left[\sin\left(2\pi x/\lambda_*\right)-1\right]$ the internal resonance will occur at

$$n \approx \frac{R}{\lambda_0}\frac{\left[\sin\left(\xi(x)\right)+1\right]\cdot\left[\left(\pi R/\lambda_*\right)\cdot\cos\left(\xi(x)\right)\right]^2}{\sqrt{1+\left[\left(\pi R/\lambda_*\right)\cdot\cos\left(\xi(x)\right)\right]^2}} \ll F\left[\left(R/\lambda_*\right);\left(R/\lambda_0\right);\left(\xi(x)\right)\right], \qquad (2.3.32)$$

where $\xi(x) \ll 2\pi x/\lambda_* \in [0;2\pi]$ is the scaling argument along the surface.

From solution of (2.3.11) it follows that in the near-surface layer $-R \le y \le h(x)$, as well as throughout the depth of the half-space, a single dispersive, not attenuated form of oscillations is propagating. If the presence of the surface heterogeneity generates oscillations along the variable thickness of the layer of the form $\cos\left[k_0 h'(x)\left[1+\left[h'(x)\right]^2\right]^{-1/2} y \right] - i \cdot \sin\left[k_0 h'(x)\left[1+\left[h'(x)\right]^2\right]^{-1/2} y \right]$ then these heterogeneities distort the plane fronts of the wave signal $\pm ik_0 x \to \pm ik_0\left[1-\sqrt{1+\left[h'(x)\right]^2}\right]\cdot x$ along directions of propagation and reflection.

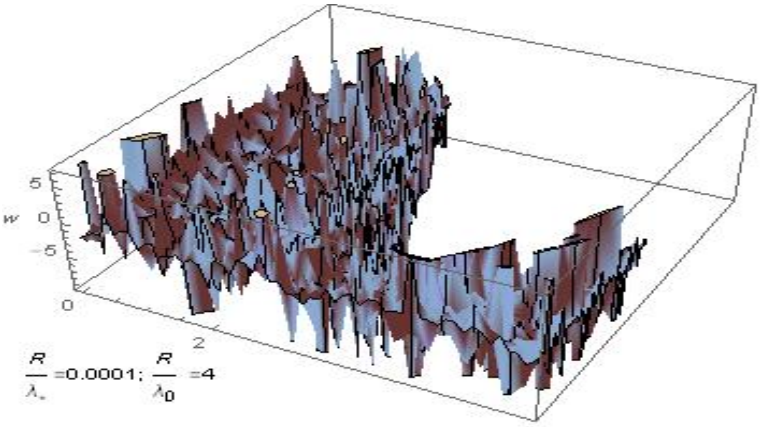

Fig. 2.3.3.a. Shortwave signal with $\lambda_0 = 0.25 \cdot R$ for macro inhomogeneous surface with $\lambda_* = 10^4 \cdot R$.

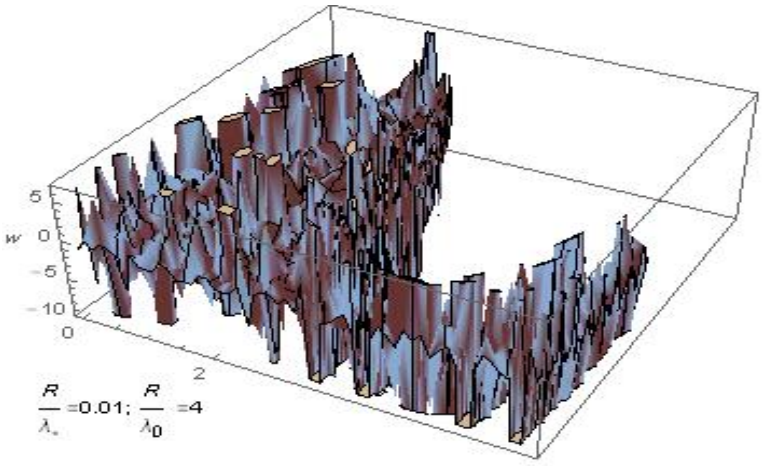

Fig. 2.3.3.b. Shortwave signal with $\lambda_0 = 0.25 \cdot R$ for waviness surface with $\lambda_* = 10^2 \cdot R$.

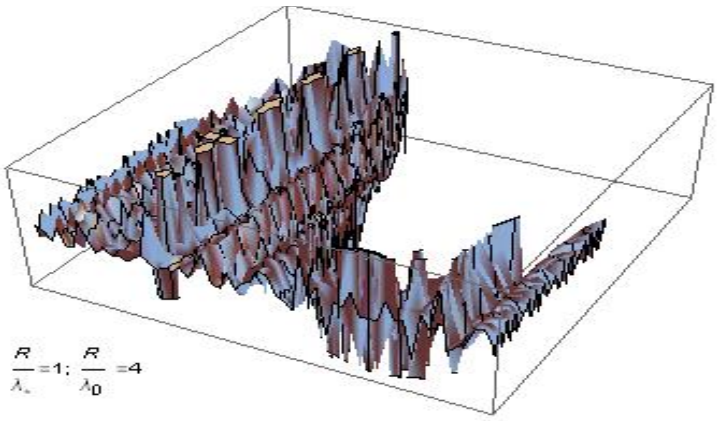

Fig. 2.3.3.c. Shortwave signal with $\lambda_0 = 0.25 \cdot R$ for rough (sawtooth) with surface $\lambda_* = R$.

For different characteristic of inhomogeneities of the surface of the half-space; macro inhomogeneity with $\lambda_*/R_{\max} \square 10^4$, waviness with $\lambda_*/R_{\max} \square 10^2$, roughness with $\lambda_*/R_{\max} \square 10$ or sawtoothness with $\lambda_*/R_{\max} \square 1.0$, the forms of the wave surface corresponding to the solution of (2.3.11) are shown in Fig. 2.3.2.a; b; c. For similar parameters, the forms of the wave surfaces corresponding to the solution of (2.3.26) taking into account (2.3.24) are shown in Fig. 2.3.3.a; b; c.

From Fig. 2.3.2 and Fig. 2.3.3 it is avident that in the case of the surface sawtooth inhomogeneity, the wave surface is distorted more quickly and dramatically compared with weakly inhomogeneous surface.

From solution (2.3.26) with (2.3.24) it is obvious that the new approach reveals the effect of surface inhomogeneities analytically, and the wave field is represented as a package of waveforms. It can be seen as well that in the case of weakly inhomogeneous surfaces when the wavelength of the signal is much larger than the height of the surface roughness $\lambda \square 2\pi R\alpha\left(1+h(x)/R\right)$, solutions of the distortion of phase function in directions of propagation and reflection of the wave are the same $\pm ik_1 x \to \pm ik_1\left[1-\sqrt{1+\left[h'(x)\right]^2}\right]\cdot x$ in both approaches, while the distortions of the amplitude along the thickness of the virtually cut thin layer in the near-surface area are different: the difference is $\Delta W = \left\{\cos\left[k_1 h'(x)\left(y+R\right)\right]-1\right\}\times\exp\left\{ik_1 h'(x)R\right\}$.

In the particular case of corrugated (sinusoidal) surface of the half-space $h(x) = \left(R/2\right)\cdot\left[\sin\left(2\pi x/\lambda_0\right)-1\right]$ where λ_* is the average pitch, and R is the maximal height of the ledge (or the maximal depth) of the non-smooth surface, distortions of the

amplitude functions from non-smooth surface along the depth of the half-space for different types of weakly inhomogeneous surfaces with $\lambda \square \max\{\lambda_0; R\}$ are plotted in Fig. 2.3.2.

Note, that for macro roughness with $\lambda_* / R \geq 1000$ or surface waviness with $\lambda_* / R \square 50 \div 1000$, the weak inhomogeneity of the surface is governed by the ratio of the wavelength of the signal and the average pitch of irregularities is $p \square \lambda_0 / \lambda_*$, while in cases of roughness with $\lambda_* / R \leq 50$ (or even greater) and sawtoothness with $\lambda_* / R \leq 1$, the weak heterogeneity is governed by the ratio of the signal wavelength and the maximal height of the non-smoothness is $q \square \lambda_0 / R$. It turns out that in cases of weakly inhomogeneous macro roughness or waviness of the surface (thick waveguide) in the near-surface zone, the elastic shear does not differ qualitatively, and the quantitative relative difference is of order $10^{-12} \div 10^{-8}$ (Fig. 2.3.2.a).

In the case of rough irregularity of the surface (Fig. 2.3.2.b), the elastic shear is strongly distorted along the depth of the half-space when $\lambda_0 / R \square 0{,}5 \div 2$, and especially in the near-surface area $-R \leq y \leq h(x)$ significant quantitative differences between solutions (2.3.11) and (2.3.26) arise. Distortions of the phase functions from the non-smooth surface along the signal wavelength $\lambda_0 = 0{,}5 \cdot \lambda_*$ is plotted in Fig. 2.3.4 for different types of surface inhomogeneities.

In the case of macro inhomogeneous surface, the phase distortion can be neglected and is established along the propagation of the wave signal quite slowly (Fig. 2.3.4.a). From comparison of the distortion graphs (Fig. 2.3.4.a, 2.3.4.b, 2.3.4.c) it is clear that the waviness and the roughness are more sensitive for high frequency wave signals. It is also evident that the distortion of the phase functions starts immediately after the signal passage of the first ledge of the non-smooth surface.

The analysis of possible internal resonance is also carried out numerically in particular case of corrugated (sinusoidal) surface of the half-space $h(x) = (R/2) \cdot \left[\sin(2\pi x / \lambda_0) - 1\right]$. From the condition of coincidence of minimal frequency of multiple induced harmonics $\omega_{n*}(x) = \pm n\pi c_t \cdot \left[\left(h(x) + R\right)\right]^{-1} \cdot \left[h'(x)\right]^{-2}$ with the main frequency distortion of the amplitude $\omega(x) = \omega_0 \left[1 + \left[h'(x)\right]^2\right]^{-1/2} \leq \omega_0$, we get the resonant wavelength of the signal.

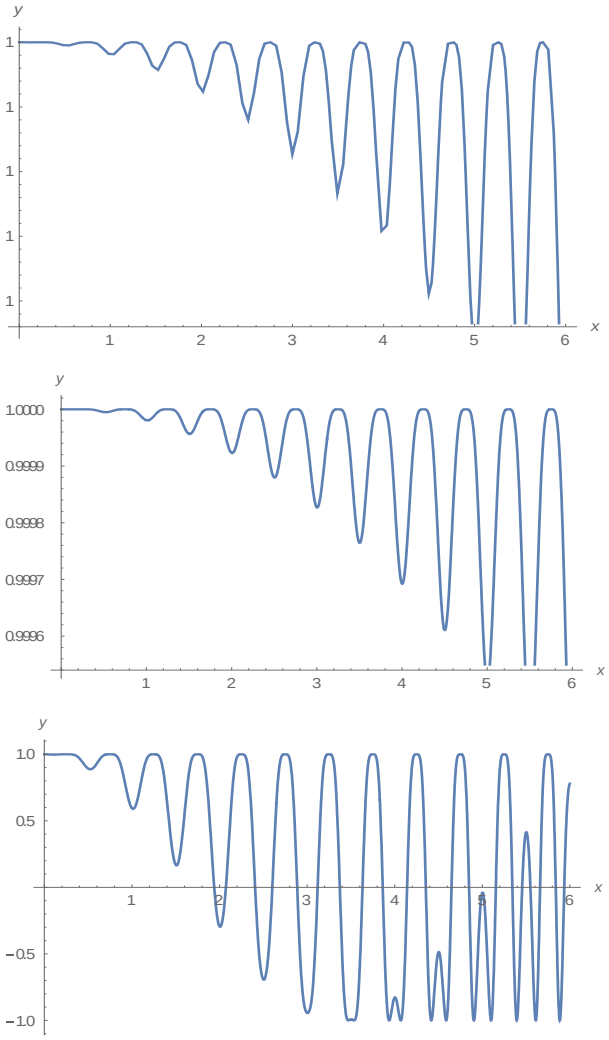

a. Shortwave, comparable in length with signal $\lambda_0 = 0.5 \cdot \lambda_*$ for macro inhomogeneous surface $\lambda_* = 10^4 \cdot R$

b. Shortwave, comparable in length with signal $\lambda_0 = 0.5 \cdot \lambda_*$ for waviness surface

c. Shortwave, comparable in length with signal $\lambda_0 = 0.5 \cdot \lambda_*$ for strong rough surface $\lambda_* = 0.8 \cdot R$

Fig. 2.3.4: The distortion of phase function at the propagation of wave signal in the case of different types of irregularities of the surface

For macro inhomogeneity when $\lambda_* / R_{\max} \gg 10^4$ and for waviness when $\lambda_* / R_{\max} \gg 10^2$, internal resonance can occur in the half-space, when ultrashort wave signals propagate correspondingly for $\lambda_0 \ll 10^{-11} \lambda_*$ and $\lambda_0 \ll 10^{-5} \lambda_*$. If the surface is rough, $\lambda_* / R_{\max} \gg 10$, or sawtooth, $\lambda_* / R_{\max} \gg 1.0$, then the internal resonance occurs for wavelengths $\lambda_0 \ll 10^{-2} \lambda_*$ and $\lambda_0 \ll 3.6 \cdot \lambda_*$ (Fig. 2.3.5.1–2.3.5.4), correspondingly, commensurable with the sizes of the non-smoothness.

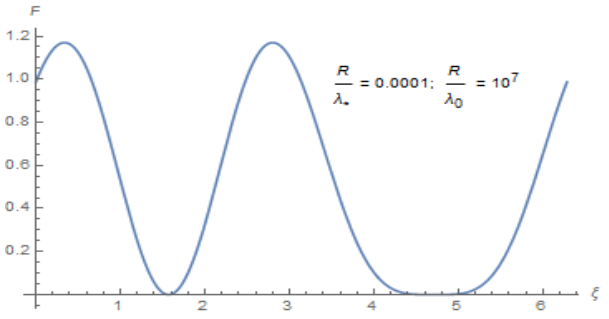

Fig. 2.3.5.1. Resonant length $\lambda_0 = 10^{-11} \cdot \lambda_*$

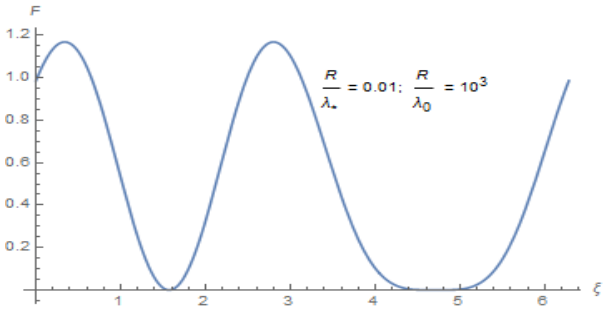

Fig. 2.3.5.2. Resonant length $\lambda_0 = 10^{-5} \cdot \lambda_*$

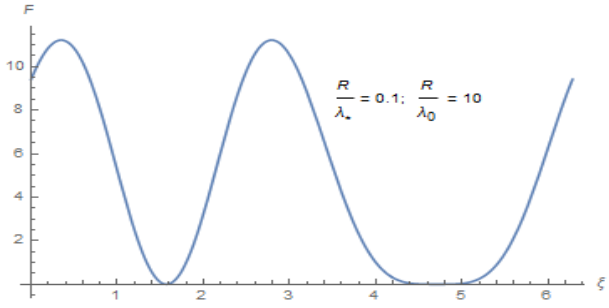

Fig. 2.3.5.3. Resonant length $\lambda_0 = 10^{-2} \cdot \lambda_*$

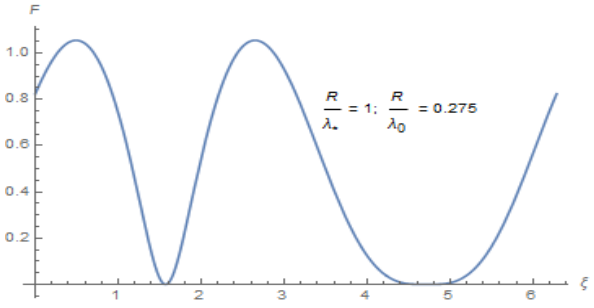

Fig. 2.3.5.4. Resonant length $\lambda_0 = 3.6 \cdot \lambda_*$

2.4 The propagation of plane wave signal in piezoelectric waveguide with surface geometrical and physical inhomogeneities

The case of propagation of horizontally polarized (*SH*) electroelastic monochromatic wave signal $F(x,y,t)=F_{j0}(y)\cdot\exp i(kx-\omega t)$ in piezoelectric layer-waveguide is considered [16]. The piezoelectric material belongs to one of these classes of symmetry: 2mm – rhombic, 4mm – tetragonal, 6mm – hexagonal, in which the material anisotropy allows the separation of plane non-electroactive and antiplane electroactive deformations [6]. Using the method of virtual cuts [10], the piezoelectric homogeneous waveguide with near-surface inhomogeneities, is modeled as three-layer composite in vacuum (Fig. 2.4.1), with two vacuum half-spaces $\Omega_0^+=\{|x|<\infty, h_0-R\le y<+\infty, |z|<\infty\}$ and $\Omega_0=\{|x|<\infty, -h_0+R\le y\le h_0-R, |z|<\infty\}$, $\Omega_0^-=\{|x|<\infty, -\infty<y\le -h_0+R, |z|<\infty\}$.

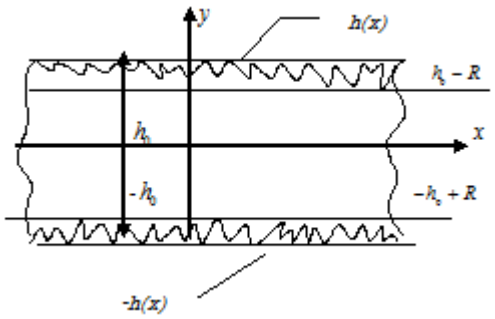

Fig. 2.4.1. Layer with near-surface inhomogeneities (surface roughness and burning of material)

The main piezoelectric layer is homogeneous, near-surface inhomogeneous piezoelectric layer $\Omega_1=\{|x|<\infty, h_0-R\le y\le h(x), |z|<\infty\}$ from above and near-surface inhomogeneous piezoelectric layer from the bottom $\Omega_2=\{|x|<\infty, -h(x)\le y\le -h_0+R, |z|<\infty\}$, where $2h_0$ is the base thickness of layer-waveguide, R is the maximal height of profile irregularities, $y=\pm h(x)$ are the rough surfaces of layer, $R=\max\left(h_{\max}(x)-h_{\min}(x)\right)\ll h_0$.

For the study of propagation of horizontally polarized electroelastic monochromatic signal $\{\vec{u},\varphi\}=\{0;0;w(x,y,t);\varphi(x,y,t)\}$, the quasi-static equations of electroelasticity can be represented in a unified vector form in the selected layers:

$$\operatorname{div}\vec{\sigma}_n = \rho_n(x,y)\ddot{w}_n; \quad \operatorname{div}\vec{D}_n = 0; \qquad \vec{E}_k = -\operatorname{grad}\varphi_n, \qquad n;k = 0;1;2. \tag{2.4.1}$$

The mechanical stresses $\sigma_{zx}^{(n)}$, $\sigma_{yz}^{(n)}$ and the components of the electric displacement vector $D_x^{(n)}$, $D_y^{(n)}$, for piezoelectric of mentioned symmetries can be written in the following forms:

$$\begin{aligned}
\sigma_{zx}^{(n)} &= G_n(x,y)w_{n,x} + e_n(x,y)\varphi_{n,x},\\
\sigma_{yz}^{(n)} &= G_n(x,y)w_{n,y} + e_n(x,y)\varphi_{n,y},\\
D_x^{(n)} &= e_n(x,y)w_{n,x} - \varepsilon_n(x,y)\varphi_{n,x},\\
D_y^{(n)} &= e_n(x,y)w_{n,y} - \varepsilon_n(x,y)\varphi_{n,y},
\end{aligned} \tag{2.4.2}$$

where the material physico-mechanical characteristics $G_n(x,y)$, $e_n(x,y)$, $\varepsilon_n(x,y)$, $\rho_n(x,y)$ are piecewise continuous, weakly varying functions in layers Ω_n, respectively:

$$\gamma_n(x,y) \Box \begin{cases} \gamma_1(y) = \gamma_0\left[1+\delta_0\sin\left(\alpha_m^+(x)y - \beta_m^+(x)\right)\right], & y \in \left[h_0 - R; h(x)\right] \\ \gamma_0, & y \in \left[-h_0 + R; h_0 - R\right] \\ \gamma_2(y) = \gamma_0\left[1+\delta_0\sin\left(\alpha_m^-(x)y - \beta_m^-(x)\right)\right], & y \in \left[-h(x); -h_0 + R\right] \end{cases} \tag{2.4.3}$$

Here $\alpha_m^{\pm}(x)y - \beta_m^{\pm}(x) = \pi(4m+1)\left(y \mp (h_0 - R)\right)/2\left[\pm h(x) \mp (h_0 - R)\right]$.

The representation (2.4.3) describes the continuity of physical-mechanical characteristics of the material on the virtual cuts $y = \pm(h_0 - R)$, as well as slightly tightened material characteristics $\gamma_0(1+\delta_0)$ on free rough surfaces $y = \pm h(x)$ of the layer. The parameter $m \in \{\mathrm{N}\}$ formally can be taken as the number of cycles of surface processing, and $\delta_0 \Box (R/2h_0) \Box 1$ is a small geometrical parameter that describes the surface roughness.

On the mechanically free surface $y = \pm h(x)$ the boundary conditions

$$\begin{aligned}
&h'(x)\cdot\sigma_{zx}^{(1)}(x,h(x),t) + \sigma_{yz}^{(1)}(x,h(x),t) = 0, \quad \varphi_1(x,h(x),t) = \varphi_{0+}\exp(-kh(x))\cdot e^{i(kx-\omega t)},\\
&h'(x)\cdot D_x^{(1)}(x,h(x),t) + D_y^{(1)}(x,h(x),t) = -k\varepsilon_0^+\left[i\cdot h'(x) - 1\right]\cdot\varphi_{0+}\exp(-kh(x))\cdot e^{i(kx-\omega t)},
\end{aligned} \tag{2.4.4}$$

$$\begin{aligned}
&-h'(x)\cdot\sigma_{zx}^{(2)}(x,-h(x),t) + \sigma_{yz}^{(2)}(x,-h(x),t) = 0, \quad \varphi_2(x,-h(x),t) = \varphi_{0-}\exp(kh(x))\cdot e^{i(kx-\omega t)},\\
&-h'(x)\cdot D_x^{(2)}(x,-h(x),t) + D_y^{(2)}(x,-h(x),t) = k\varepsilon_0^-\left[i\cdot h'(x) - 1\right]\cdot\varphi_{0-}\exp(kh(x))\cdot e^{i(kx-\omega t)}
\end{aligned} \tag{2.4.5}$$

are satisfied.

On the virtual cuts $y=\pm\left(h_0-R\right)$ full continuity conditions of electromechanical fields are satisfied.

For the study of the phenomena of the propagation of horizontally polarized (SH) elastic and electric monochromatic signal $F(x,y,t)=F_{j0}(y)\cdot\exp i(kx-\omega t)$ in the virtually selected layers $n=1,2$ taking into account (2.4.3), the equations of electroelasticity can be represented as follows:

$$\begin{aligned}&G_0\left(1+\delta_0 f_n(y,h(x))\right)\cdot w_{n,xx}+e_0\left(1+\delta_0 f_n(y,h(x))\right)\cdot\varphi_{n,xx}\\&+G_0\delta_0 f_{n,x}(y,h(x))\cdot w_{n,x}+e_0\delta_0 f_{n,x}(y,h(x))\cdot\varphi_{n,x}+\sigma^{(n)}_{yz,y}=\\&=\rho_0\left(1+\delta_0 f_n(y,h(x))\right)\cdot\ddot{w}_n,\end{aligned}\tag{2.4.6}$$

$$\begin{aligned}&e_0\left(1+\delta_0 f_n(y,h(x))\right)\cdot w_{n,xx}-\varepsilon_0\left(1+\delta_0 f_n(y,h(x))\right)\cdot\varphi_{n,xx}\\&+e_0\delta_0 f_{n,x}(y,h(x))\cdot w_{n,x}-\varepsilon_0\delta_0 f_{n,x}(y,h(x))\cdot\varphi_{n,x}+D^{(n)}_{y,y}=\\&=\rho_0\left(1+\delta_0 f_n(y,h(x))\right)\cdot\ddot{w}_n;\end{aligned}\tag{2.4.7}$$

$$f_n\left(y,h(x)\right)\begin{cases}f_1\left(y,h(x)\right)=\sin\left(\alpha(x)y-\beta(x)\right), & y\in\left[h_0-R;h(x)\right]\\ f_0\left(y,h(x)\right)\equiv 0, & y\in\left[-h_0+R;h_0-R\right]\\ f_2\left(y,h(x)\right)=-\sin\left(\alpha(x)y+\beta(x)\right), & y\in\left[-h(x);-h_0+R\right]\end{cases}\tag{2.4.8}$$

If the nature of the heterogeneity in near-surface zones Ω_1 and Ω_2 (2.4.3) is known, by introducing the hypotheses MELS on the distribution of the shear elastic and electric potential through the thickness of these layers, we respectively obtain

$$\begin{aligned}&w_1\left(x,y,t\right)=\left[1+\delta_0\sin\left(\alpha_m^+(x)y-\beta_m^+(x)\right)\right]\cdot w_0\left(x,h_0-R,t\right),\\&\varphi_1\left(x,y,t\right)=\sin\left(\alpha_m^+(x)y-\beta_m^+(x)\right)\cdot\left[\varphi_{0+}\left(x,h(x),t\right)-\varphi_0\left(x,h_0-R,t\right)\right]+\\&+\varphi_0\left(x,h_0-R,t\right),\end{aligned}\tag{2.4.9}$$

$$\begin{aligned}&w_2\left(x,y,t\right)=\left[1+\delta_0\sin\left(\alpha_m^-(x)y-\beta_m^-(x)\right)\right]\cdot w_0\left(x,-h_0+R,t\right),\\&\varphi_2\left(x,y,t\right)=\sin\left(\alpha_m^-(x)y-\beta_m^-(x)\right)\cdot\left[\varphi_{0-}\left(x,-h(x),t\right)-\varphi_0\left(x,-h_0+R,t\right)\right]+\\&+\varphi_0\left(x,-h_0+R,t\right).\end{aligned}\tag{2.4.10}$$

Here appears the primary electroelastic signal in homogeneous layer Ω_0

$$w_0(x,y,t)=\left[A_{01}\sin(\alpha_0 ky)+A_{02}\cos(\alpha_0 ky)\right]\cdot e^{i(kx-\omega t)},$$

$$\varphi_0(x,y,t)=\left\{\begin{array}{l} B_{01}\sin(ky)+B_{02}\cos(ky)+ \\ +\dfrac{e_0}{\varepsilon_0}\left[A_{01}\sin(\alpha_0 ky)+A_{02}\cos(\alpha_0 ky)\right] \end{array}\right\}\cdot e^{i(kx-\omega t)}, \tag{2.4.11}$$

and electrical oscillations damped from the non-smooth surfaces $y=\pm h(x)$ through the depth of corresponding vacuum half-spaces,

$$\varphi_n^{(e)}(x,y,t)=\varphi_{0\pm}\exp(\mp ky)\cdot e^{i(kx-\omega t)}. \tag{2.4.12}$$

Electromechanical surface dynamic loads. Geometric heterogeneity of the surface (roughness) acts on the propagating wave. On the base surfaces of the layer $y=\pm(h_0-R)$ surface variable electromechanical loads occur during the propagation of horizontally polarized electroelastic monochromatic signal $F(x,y,t)=F_{j0}(y)\cdot\exp i(kx-\omega t)$ in the waveguide:

$$\begin{array}{l} \sigma_{yz}^{(n)}(x,\pm(h_0-R))=\displaystyle\int_{h_0-R}^{h(x)}\left[G_0 w_{n,xx}+e_0\varphi_{n,xx}+\omega^2\rho_0 w_n\right]\cdot dy+\omega^2\rho_0\delta_0\int_{h_0-R}^{h(x)} f_n(y,h(x))w_n\cdot dy \\ +G_0\delta_0\displaystyle\int_{h_0-R}^{h(x)}\left[f_n(y,h(x))\cdot w_{n,x}\right]_{,x}\cdot dy+e_0\delta_0\int_{h_0-R}^{h(x)}\left[f_n(y,h(x))\cdot\varphi_{n,x}\right]_{,x}\cdot dy, \end{array} \tag{2.4.13}$$

$$\begin{array}{l} D_y^{(n)}(x,\pm(h_0-R))=\displaystyle\int_{h_0-R}^{h(x)}\left[e_0 w_{n,xx}-\varepsilon_0\varphi_{n,xx}\right]\cdot dy+ \\ +e_0\delta_0\displaystyle\int_{h_0-R}^{h(x)}\left[f_n(y,h(x))\cdot w_{n,x}\right]_{,x}\cdot dy-\varepsilon_0\delta_0\int_{h_0-R}^{h(x)}\left[f_n(y,h(x))\cdot\varphi_{n,x}\right]_{,x}\cdot dy, \end{array} \tag{2.4.14}$$

where the under-integral expressions with indices $n=1;2$ are determined by the MELS hypotheses (2.4.9) and (2.4.10) and correspond to the layers Ω_1 and Ω_2. Obviously, for perfectly smooth surfaces of the layer, when $R\to 0$, we have $\delta_0\to 0$ and $h(x)\to h_0$, and these loads disappear.

Choosing the non-smoothness of the layer surface in the sinusoidal form (2.4.16), we are able to evaluate the distribution of given mechanical stresses $\sigma_{yz}^{(+)}(x)$ and electric displacements $D_y^{(+)}(x)$ at the base surfaces $y=\pm(h_0-R)$ of the layer.

Dispersion of wave signal and internal resonance. Inputting MELS hypotheses (2.4.9) and (2.4.10), some boundary conditions are satisfied automatically. From the continuity conditions of shear stresses and normal components of the electric displacement

on the virtual slices $y=\pm(h_0-R)$, we get a system of four complex algebraic homogeneous equations with respect to complex amplitude constants. The condition for the existence of non-trivial solutions gives a dispersion equation in the form of

$$\det\left\|g_{ij}\left(\omega/k,\ h(x),\ \delta_0,\ \chi_0^2\right)\right\|_{8\times 8}=0. \qquad (2.4.15)$$

Choosing non-smoothness of the layer surface in the sinusoidal form

$$h(x)=h_0\left[1-\delta_0\left(1-\sin(k_0x)\right)\right],\ \text{where}\ \delta_0=\left(R/2h_0\right)\ll 1, \qquad (2.4.16)$$

We can evaluate the frequency dispersion $\omega=\omega\left(\lambda/\lambda_0,\ \delta_0,\ \chi_0^2\right)$ in each period of the surface irregularities $x\in\left[0;\lambda_0\right]$.

Numerical analysis shows that in the propagation of short waves $R\ll\lambda\ll h_0$, taking into account only near-surface heterogeneity of the material, without taking into account the surface roughness, it leads to the Love model problem: homogeneous half-space, bordered with a transversely weakly inhomogeneous thin layer. During the propagation of short waves $R\ll\lambda\ll h_0$, considering only the surface roughness, excluding the surface inhomogeneity of the material leads to another Love model problem: homogeneous half-space bordering with longitudinally weakly inhomogeneous thin layer. It turns out, that during the propagation of shear wave signal, surface inhomogeneity leads to the appearance of wave with certain length λ/λ_0, where λ_0 is the average step of periodic roughness. Newly appeared wave disappears periodically in some zones $x\in\left[\lambda_{n1}^*;\lambda_{n2}^*\right]\subset\left[(n-1)\lambda_0;n\lambda_0\right]$ on step $n\lambda_0$ of periodic roughness.

From conditions (2.4.4) and (2.4.5) on the non-smooth surfaces $y=\pm h(x)$, we get the condition of possible internal resonance, when the electromechanical surface loads (2.4.13) and (2.4.14) excite a wave with the same frequency of propagating wave signal

a) $$\alpha_0^2=\left[h'(x)\right]^2, \qquad (2.4.17)$$

b) $$\alpha_0=\left[1-\delta_0\left(1-\sin(k_0x)\right)\right]^{-1}\cdot\left(m\pi\right)/\left(kh_0\right). \qquad (2.4.18)$$

It is seen from equation (2.4.17), that the internal resonance in the adhesive layer is possible for "slow" electroelastic wave signals in elastic half-spaces with $\mathrm{v}_\phi\left(k\right)=C_{3t}\cdot\left\{1-\left[h'(x)\right]^2\right\}$. The resonant frequency

$$\omega_R = \left(2\pi C_{3t}/\lambda_0\right)\left(\lambda_0/\lambda_R\right)\cdot\sqrt{1-\left[2\pi\left(\delta_0/\lambda_0\right)\cdot\sin\left(2\pi\left(\lambda_R/\lambda_0\right)\left(x/\lambda_R\right)\right)\right]^2} \qquad (2.4.19)$$

obviously depends on the relative linear dimensions of the wave signal and roughness.

For the internal resonance frequency from equation (2.4.18) in the adhesive layer we obtain the following form:

$$\omega_R^{(m)} = \left(2\pi C_{3t}/\lambda_R\right)\cdot\sqrt{1-\left[1-2\pi\left(\delta_0/\lambda_0\right)\left(1-\sin\left(2\pi\left(\lambda_R/\lambda_0\right)\left(x/\lambda_R\right)\right)\right)\right]^{-2}\cdot m^2/\left(2h_0/\lambda_R\right)^2}\,. \qquad (2.4.20)$$

Graphical representation of the frequency $\omega(x/\lambda_R)$ in interval $x\in\left[0;\lambda_0\right]$ are shown in Fig. 2.4.2.a and 2.4.2.b, respectively, for (2.4.20) and (2.4.19).

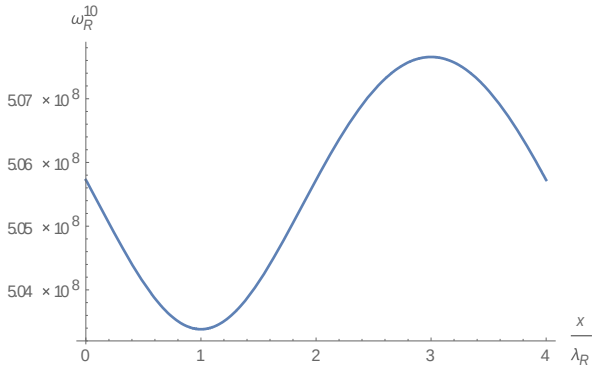

Fig. 2.4.2.a Frequency characteristic of internal resonance, for localized signal mod

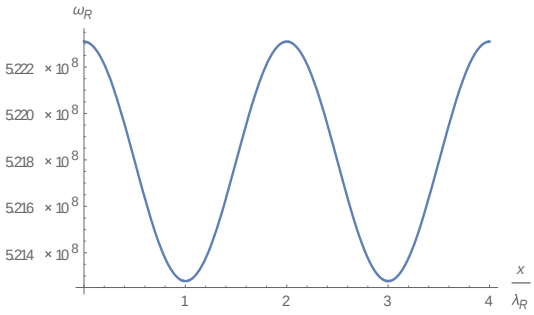

Fig. 2.4.2.b Frequency characteristic of internal resonance, for periodic signal mod

CHAPTER 3

THE INFLUENCE OF SURFACE WEAK INHOMOGENEITIES ON THE PROPAGATION OF HIGH-FREQUENCY ELECTROELASTIC (SH) WAVE SIGNAL IN THE PIEZOELECTRIC WAVEGUIDE

3.1 The propagation of high-frequency electroelastic (SH) wave signal in homogeneous piezoelectric layer waveguide with mechanically free and electrically open (closed) weakly inhomogeneous surfaces

Assume, that a piezoelectric layer occupies in the Cartesian coordinate system $\{x; y; z\}$ the domain $\Omega \equiv \{|x|<\infty;\ h_{-}(x) \le y \le h_{+}(x);\ |z|<\infty\}$ and has non-smooth surfaces $y = h_{\pm}(x)$. Generally, the surface non-smoothness can be efficiently described by functions $y = h_{\pm}(x) \in L^2(\equiv)$. Keeping the generality of considerations, the surface roughness can be described by

$$\begin{aligned} h_{-}(x) &= -h_0\left(1+\varepsilon_{-}\sin\left(k_{-}x\right)+\delta_{-}\cos\left(k_{-}x\right)\right), \\ h_{+}(x) &= h_0\left(1+\varepsilon_{+}\sin\left(k_{+}x\right)+\delta_{+}\cos\left(k_{+}x\right)\right). \end{aligned} \tag{3.1.1}$$

Suppose, that the surface of the waveguide $y = h_{+}(x)$ is coated with a soft dielectric layer $(\varepsilon_e \equiv \varepsilon_{11})$ of negligibly small thickness, forming an electrically open surface. The surface of the waveguide $y = h_{-}(x)$ is coated with a good conductor layer of negligibly small thickness, forming an electrically closed surface.

During technological processing of the basic piezoelectric layer, in addition to the surface roughness, inhomogeneity of the material appears in the near-surface areas. Due to small thickness, these areas are especially important in studies of shortwave signal propagation. To account for these inhomogeneities in the near-surface areas, let us introduce virtual sections $y = h_0(1-\gamma_{+})$ and $y = -h_0(1-\gamma_{-})$, dividing the basic waveguide into three-layer piezoelectric waveguide consisting of basic homogeneous layer of constant thickness $2H_0 = 2h_0(1-\gamma_{+}-\gamma_{-})$:

$$\Omega_0 \equiv \{|x|<\infty;\ -h_0(1-\gamma_{-}) \le y \le h_0(1-\gamma_{+});\ |z|<\infty\}, \tag{3.1.2}$$

and two near-surface thin layers, inhomogeneous over the variable thicknesses $\zeta_+(x) \equiv h_0(1+\gamma_+) - h_+(x)$ and $\zeta_-(x) \equiv \left|h_0(1+\gamma_-) + h_-(x)\right|$, respectively (Fig. 3.1.1):

$$\Omega_- \equiv \left\{|x| < \infty;\ h_-(x) \le y \le -h_0(1-\gamma_-);\ |z| < \infty\right\}, \tag{3.1.3}$$

$$\Omega_+ \equiv \left\{|x| < \infty;\ h_0(1-\gamma_+) \le y \le h_+(x);\ |z| < \infty\right\}. \tag{3.1.4}$$

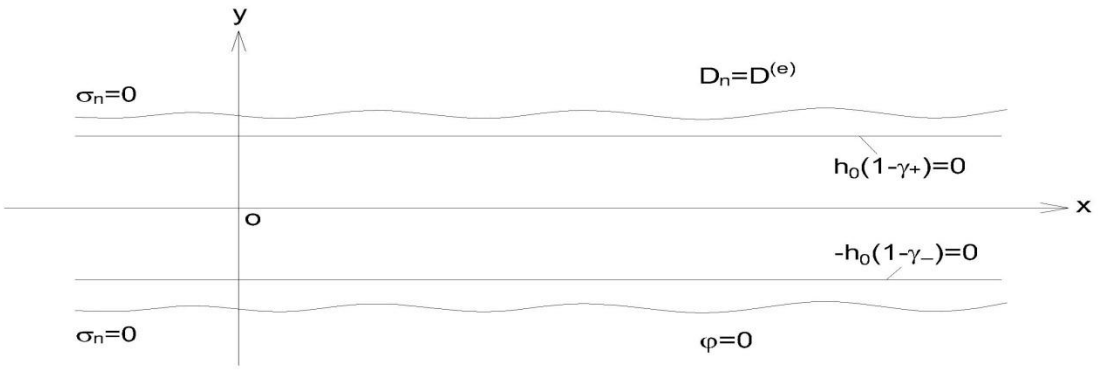

Fig. 3.1.1 Homogeneous piezoelectric waveguide with weakly inhomogeneous, mechanically free and electrically open (closed) surfaces

Let us assume, that high-frequency (short-wave) elastic shear (*SH*) wave signal is propagating in the composite waveguide, where the length of the normal wave is much smaller than the base layer thickness: $\lambda_0 \ll 2H_0 - 2h_0$. Assume also, that the material of the basic piezoelectric layer Ω_0 belongs to the $4mm$ (tetragonal) or $6mm$ (hexagonal) symmetry class, and the ox_3 axis is parallel to the $\bar{p}$ axis of piezo-crystal symmetry of fourth or sixth order, respectively. Then, the electro-active shear deformation $\{0;\ 0;\ w(x,y,t);\ \varphi(x,y,t)\}$ is separated from non-electro-active plane deformations $\{u(x,y,t);\ v(x,y,t);\ 0;\ 0\}$. The quasi-static equations of electroelasticity for these crystals in the basic layer of composite waveguide have the following forms

$$\nabla^2 w_0(x,y,t) = c_{0t}^{-2} \cdot \ddot{w}_0(x,y,t), \tag{3.1.5}$$

$$\nabla^2 \varphi_0(x,y,t) = (e_{15}/\varepsilon_{11}) \cdot \nabla^2 w_0(x,y,t). \tag{3.1.6}$$

Here e_{15} is the piezoelectric modulus and ε_{11} is the dielectric coefficient of the homogeneous piezoelectric.

The equations of electroelasticity of laterally inhomogeneous piezoelectric layer must be solved in $\Omega_\pm^p$, respectively:

$$G_{\pm}(y)\frac{\partial^2 w_{\pm}(x,y,t)}{\partial x^2}+e_{\pm}(y)\frac{\partial^2 \varphi_{\pm}(x,y,t)}{\partial x^2}+\frac{\partial \sigma_{yz}^{\pm}(x,y,t)}{\partial y}=\rho_{\pm}(y)\cdot \ddot{w}_{\pm}(x,y,t), \tag{3.1.7}$$

$$e_{\pm}(y)\frac{\partial^2 \mathrm{w}_{\pm}(x,y,t)}{\partial x^2}-\varepsilon_{\pm}(y)\frac{\partial^2 \varphi_{\pm}(x,y,t)}{\partial x^2}+\frac{\partial D_y^{\pm}(x,y,t)}{\partial y}=0. \tag{3.1.8}$$

For the homogeneous material, the material relations for mechanical stress and induction of electric field are

$$\begin{aligned}\sigma_{yz}^{0}(x,y,t)&=G_0\frac{\partial w_0(x,y,t)}{\partial y}+e_0\frac{\partial \varphi_0(x,y,t)}{\partial y},\\ D_y^{0}(x,y,t)&=e_0\frac{\partial w_0(x,y,t)}{\partial y}-\varepsilon_0\frac{\partial \varphi_0(x,y,t)}{\partial y},\end{aligned} \tag{3.1.9}$$

while in the inhomogeneous case:

$$\begin{aligned}\sigma_{yz}^{\pm}(x,y,t)&=G_{\pm}(y)\frac{\partial w_{\pm}(x,y,t)}{\partial y}+e_{\pm}(y)\frac{\partial \varphi_{\pm}(x,y,t)}{\partial y},\\ D_y^{\pm}(x,y,t)&=e_{\pm}(y)\frac{\partial w_{\pm}(x,y,t)}{\partial y}-\varepsilon_{\pm}(y)\frac{\partial \varphi_{\pm}(x,y,t)}{\partial y}.\end{aligned} \tag{3.1.10}$$

Electromechanical boundary conditions

$$h_{-}'(x)\sigma_{zx}^{-}(x,h_{-}(x),t)+\sigma_{yz}^{-}(x,h_{-}(x),t)=0, \tag{3.1.11}$$

$$\varphi_{-}(x,h_{-}(x),t)=0. \tag{3.1.12}$$

are satisfied on the outer, mechanically free, electrically closed surface $y=h_{-}(x)$ of the inhomogeneous over the variable thickness $\left|-h_0(1-\gamma_{-})-h_{-}(x)\right|$ layer.

Electromechanical boundary conditions

$$h_{+}'(x)\sigma_{zx}^{+}(x,h_{+}(x),t)+\sigma_{yz}^{+}(x,h_{+}(x),t)=0, \tag{3.1.13}$$

$$h_{+}'(x)D_{x}^{+}(x,h_{+}(x),t)+D_{y}^{+}(x,h_{+}(x),t)=0, \tag{3.1.14}$$

are satisfied on the outer, mechanically free, electrically open surface $y=h_{+}(x)$ of inhomogeneous over the variable thickness $\left|h_{+}(x)-h_0(1-\gamma_{+})\right|$ layer.

Full continuity conditions of electromechanical fields for homogeneous and inhomogeneous piezoelectric layers are satisfied on the virtual section $y=-h_0(1-\gamma_{-})$

$$w_0(x,-h_0(1-\gamma_{-}),t)=w_{-}(x,-h_0(1-\gamma_{-}),t); \tag{3.1.15}$$

$$\varphi_0(x,-h_0(1-\gamma_{-}),t)=\varphi_{-}(x,-h_0(1-\gamma_{-}),t); \tag{3.1.16}$$

$$\sigma_{yz}^{0}(x,-h_0(1-\gamma_-),t)=\sigma_{yz}^{-}(x,-h_0(1-\gamma_-),t);\tag{3.1.17}$$

$$D_{y}^{0}(x,-h_0(1-\gamma_-),t)=D_{y}^{-}(x,-h_0(1-\gamma_-),t).\tag{3.1.18}$$

Similarly, the continuity conditions of electromechanical fields are satisfied on virtual sections $y=h_0(1-\gamma_+)$:

$$w_0(x,h_0(1-\gamma_+),t)=w_+(x,h_0(1-\gamma_+),t);\tag{3.1.19}$$

$$\varphi_0(x,h_0(1-\gamma_+),t)=\varphi_+(x,h_0(1-\gamma_+),t);\tag{3.1.20}$$

$$\sigma_{yz}^{0}(x,h_0(1-\gamma_+),t)=\sigma_{yz}^{+}(x,h_0(1-\gamma_+),t);\tag{3.1.21}$$

$$D_{y}^{0}(x,h_0(1-\gamma_+),t)=D_{y}^{+}(x,h_0(1-\gamma_+),t).\tag{3.1.22}$$

In addition to the material relations (3.1.9), (3.1.10), due to the presence of non-smooth surfaces in the multilayer waveguide, tangential components of mechanical strain and electric field induction of corresponding layers are involved in the boundary conditions (3.1.11), (3.1.13) and (3.1.14):

$$\sigma_{zx}^{\pm}(x,y,t)=G_{\pm}(y)\frac{\partial w_{\pm}(x,y,t)}{\partial x}+e_{\pm}(y)\frac{\partial \varphi_{\pm}(x,y,t)}{\partial x}\tag{3.1.23}$$

$$D_{x}^{\pm}(x,y,t)=e_{\pm}(y)\frac{\partial w_{\pm}(x,y,t)}{\partial x}-\varepsilon_{\pm}(y)\frac{\partial \varphi_{\pm}(x,y,t)}{\partial x}\tag{3.1.24}$$

The boundary conditions (3.1.11)-(3.1.14) do not include the electric potential and the normal component of the electric field induction of the external media, since the surface $y=h_-(x)$ is isolated by perfect conductor (cf. (3.1.12)), and the surface $y=h_+(x)$ is isolated by good dielectric (cf. (3.1.14)).

Thus, the homogeneous piezoelectric layer-waveguide with surface inhomogeneities is modelled as a multilayer waveguide of different materials. The wave process (localization of shear elastic wave in the near-surface inhomogeneous thin layers Ω_- and Ω_+, delay of normal waves of certain frequencies, occurrence of dynamic surface loads, etc.) investigation during propagation of electroelastic normal shear wave signal is mathematically formulated as a boundary value problem with quasi-static equations of electroelasticity (3.1.5) to (3.1.8) in corresponding layers with electromechanical boundary conditions (3.1.11)–(3.1.22) on the sections of materials separation.

The obtained boundary-value problem is complicated from a mathematical viewpoint by the fact, that differential equations (3.1.7) and (3.1.8) with variable coefficients need to be solved in Ω_- and Ω_+. Due to non-smoothness of the surfaces $y = h_-(x)$ and $y = h_+(x)$, the boundary conditions (3.1.11), (3.1.13) and (3.1.14) will also include variable coefficients.

To overcome mathematical difficulties, let us consider so-called weak inhomogeneity of the material and surface geometry in the near-surface areas. Then, for the solution of arising mathematical boundary value problem, it is convenient to apply a hypothetical approach. The wave solution of the system (3.1.5) and (3.1.6) in Ω_0 will be written in the form of normal wave

$$w_0(x,y,t) = \left[A_0 e^{\alpha_0 k y} + B_0 e^{-\alpha_0 k y} \right] e^{i(kx-\omega_0 t)}, \tag{3.1.25}$$

$$\varphi_0(x,y,t) = \left\{ C_0 e^{ky} + D_0 e^{-ky} + (e_{15}/\varepsilon_{11}) \cdot \left[A_0 e^{\alpha_0 k y} + B_0 e^{-\alpha_0 k y} \right] \right\} e^{i(kx-\omega_0 t)}. \tag{3.1.26}$$

Here $\alpha_0 = \sqrt{1-\eta_0^2}$ is the formation coefficient of elastic waves over the thickness of Ω_0, and $\eta_0 \square (\omega_0/k) \cdot \left(\rho_0/\tilde{G}_0\right)^{1/2}$ is the phase velocity of the normal wave in Ω_0. Evidently, in general, both of them are functions of the variable wave number $k(x)$.

Considering the thinness of the other two boundary layers and the complexity of the analytical solution of the electroelasticity equations in virtually cut layers Ω_- and Ω_+, heterogeneous over the thickness, hypotheses ***MELS*** [9, 10, 12] are introduced for distributions of elastic shear and potential of electric field.

Then, in Ω_+, elastic shear and potential of electric field read as follows:

$$\begin{aligned} &w_+(x,y,t) = w_0\left(x, h_0(1-\gamma_+), t\right) + \\ &+ f_+\left(y; kh_0; h_+(x)/h_0\right) \cdot \left[w_+(x, h_+(x), t) - w_0\left(x, h_0(1-\gamma_+), t\right) \right], \end{aligned} \tag{3.1.27}$$

$$\begin{aligned} &\varphi_+(x,y,t) = \varphi_0\left(x, h_0(1-\gamma_+), t\right) + \\ &+ f_+\left(y; kh_0; h_+(x)/h_0\right) \cdot \left[\varphi_+(x, h_+(x), t) - \varphi_0\left(x, h_0(1-\gamma_+), t\right) \right]. \end{aligned} \tag{3.1.28}$$

Here $f_+(y; kh_0; h_+(x)/h_0) \square sh\left[\alpha_+ k(y - h_0(1-\gamma_+))\right] / sh\left[\alpha_+ k(h_+(x) - h_0(1-\gamma_+))\right]$ is the distribution (or formation) function of the electromechanical field in inhomogeneous piezoelectric layer, corresponding to the electroelasticity equations (3.1.7), (3.1.8) and corresponding boundary conditions (3.1.19)-(3.1.22). Moreover, the condition (3.1.19) and

(3.1.20) are satisfied automatically with choice of distribution functions (3.1.27), (3.1.28). Furthermore, the functions $w_+(x,h_+(x),t)$ and $\varphi_+(x,h_+(x),t)$ are obtained from the conditions (3.1.13) and (3.1.14), and therefore distributions (3.1.27) and (3.1.28) are expressed in terms of arbitrary constant amplitudes $\{A_0;B_0;C_0;D_0\}$ of electroelastic wave signal:

$$w_+(x,y)=A_0e^{\alpha_0kh_0(1-\gamma_+)}+B_0e^{-\alpha_0kh_0(1-\gamma_+)}$$
$$+\frac{sh\left[\alpha_+k\left(y-h_0(1-\gamma_+)\right)\right]}{\alpha_+}\cdot\left[A_0e^{\alpha_0kh_0(1-\gamma_+)}-B_0e^{-\alpha_0kh_0(1-\gamma_+)}\right], \tag{3.1.29}$$

$$\varphi_+(x,y)=C_0e^{kh_0(1-\gamma_+)}+D_0e^{-kh_0(1-\gamma_+)}+\frac{e_0}{\varepsilon_0}\cdot\left[A_0e^{\alpha_0kh_0(1-\gamma_+)}+B_0e^{-\alpha_0kh_0(1-\gamma_+)}\right]+$$
$$+\frac{e_0}{\varepsilon_0}\cdot sh\left[\alpha_+k\left(y-h_0(1-\gamma_+)\right)\right]\cdot\left\{\begin{array}{l}\left[\frac{1}{k\cdot\alpha_+}\cdot\left(1-\frac{\xi_+(x,k)}{\alpha_+}\right)-\frac{1}{\xi_+(x,k)}\right]\cdot A_0e^{\alpha_0kh_0(1-\gamma_+)}+\\+\left[\frac{1}{k\cdot\alpha_+}\cdot\left(1+\frac{\xi_+(x,k)}{\alpha_+}\right)-\frac{1}{\xi_+(x,k)}\right]\cdot B_0e^{-\alpha_0kh_0(1-\gamma_+)}\end{array}\right\}+$$
$$+sh\left[\alpha_+k\left(y-h_0(1-\gamma_+)\right)\right]\cdot\left\{\begin{array}{l}\left[\frac{1}{k\cdot\alpha_+}\cdot\left(1-\frac{\xi_+(x,k)}{\alpha_+}\right)-\frac{1}{\xi_+(x,k)}\right]\cdot C_0e^{kh_0(1-\gamma_+)}+\\+\left[\frac{1}{k\cdot\alpha_+}\cdot\left(1+\frac{\xi_+(x,k)}{\alpha_+}\right)-\frac{1}{\xi_+(x,k)}\right]\cdot D_0e^{-kh_0(1-\gamma_+)}\end{array}\right\}. \tag{3.1.30}$$

Note, that the formation function $f_+(y;kh_0;h_+(x)/h_0)$ of unknown characteristics of the wave field is represented by the formation coefficient $\alpha_+(k)\square\left[\left(\rho_+\omega_0^2/k^2G_+\right)-1\right]^{1/2}$ and by the variable thickness $\zeta_+(x)$ of the layer. Similarly, the elastic shear and the potential of the electric field in Ω_- by virtue of (3.1.27) and (3.1.28) are represented in the following forms:

$$w_-(x,y,t)=w_0\left(x,-h_0(1-\gamma_-),t\right)+$$
$$+f_-\left(y;kh_0;h_-(x)/h_0\right)\cdot\left[w_-(x,h_-(x),t)-w_0\left(x,-h_0(1-\gamma_-),t\right)\right] \tag{3.1.31}$$

$$\varphi_-(x,y,t)=\left\{1-f_-\left(y;kh_0;h_-(x)/h_0\right)\right\}\varphi_0\left(x,-h_0(1-\gamma_-),t\right) \tag{3.1.32}$$

where the formation function $f_-(y;kh_0;h_-(x)/h_0)\square sh\left[\alpha_-k(y+h_0(1-\gamma_-))\right]/sh\left[\alpha_-k(h_-(x)+h_0(1-\gamma_-))\right]$ in the

inhomogeneous piezoelectric layer is represented by the new formation coefficient $\alpha_{-}(k) \square \left[\left(\rho_{-}\omega_0^2/k^2G_{-}\right)-1\right]^{1/2}$ and variable thickness $\zeta_{-}(x)$.

The conditions (3.1.12), (3.1.15) and (3.116) are satisfied automatically with choice of distribution functions (3.1.29) and (3.1.30), and we obtain $w_{-}(x,h_{-}(x),t)$ from the condition (3.1.11). Therefore, the distributions (3.1.29) and (3.1.30) are expressed in terms of arbitrary constant amplitudes $\{A_0;B_0;C_0;D_0\}$ of electroelastic wave signal

$$w_{-}(x,y)=A_0e^{-\alpha_0kh_0(1-\gamma_{-})}-B_0e^{\alpha_0kh_0(1-\gamma_{-})}$$
$$+sh\left[\alpha_{-}k\left(y+h_0(1-\gamma_{-})\right)\right]\cdot\left\{\begin{array}{l}\left[\frac{\chi_0^2}{\xi_{-}(x,k)}+\frac{\alpha_0}{\alpha_{-}}\cdot\left(1+\chi_0^2\right)\right]\cdot A_0e^{-\alpha_0kh_0(1-\gamma_{-})}-\\-\left[\frac{\chi_0^2}{\xi_{-}(x,k)}-\frac{\alpha_0}{\alpha_{-}}\cdot\left(1+\chi_0^2\right)\right]\cdot B_0e^{\alpha_0kh_0(1-\gamma_{-})}+\\+\frac{e_0}{G_0}\left(\frac{1}{\alpha_{-}}+\frac{1}{\xi_{-}(x,k)}\right)\cdot C_0e^{-kh_0(1-\gamma_{-})}-\\-\frac{e_0}{G_0}\left(\frac{1}{\alpha_{-}}-\frac{1}{\xi_{-}(x,k)}\right)\cdot D_0e^{kh_0(1-\gamma_{-})}\end{array}\right\}, \quad (3.1.33)$$

$$\varphi_{-}(x,y)=\left\{1-\frac{sh\left[\alpha_{-}k\left(y+h_0(1-\gamma_{-})\right)\right]}{\xi_{-}(x,k)}\right\}\cdot\left\{\begin{array}{l}C_0e^{-kh_0(1-\gamma_{-})}+D_0e^{kh_0(1-\gamma_{-})}+\\+\frac{e_0}{\varepsilon_0}\cdot\left[A_0e^{-\alpha_0kh_0(1-\gamma_{-})}+B_0e^{\alpha_0kh_0(1-\gamma_{-})}\right]\end{array}\right\}. \quad (3.1.34)$$

Here $\xi_{\pm}(x,k)=sh\left[\alpha_{\pm}k\left(h_{\pm}(x)\mp h_0(1-\gamma_{\pm})\right)\right]$ characterizes the functions of the near-surface distributions in Ω_{+} and Ω_{-}, respectively.

The distributions (3.1.25), (3.1.26), as well as (3.1.29)-(3.1.32), describe the picture of distribution over the thickness of the composite waveguide.

For evaluation of the wave number $k\left(h_{\pm}(x)/h_0;\gamma_{\pm};\omega_0\right)$, which satisfies dispersion equation, we satisfy the boundary conditions (3.1.17), (3.1.18), (3.1.21) and (3.1.22) and obtain a system of four homogeneous algebraic equations with respect to the amplitude constants $\{A_0;B_0;C_0;D_0\}$. Then, the dispersion equation is obtained from the condition of existence of nontrivial solutions:

$$\det\left\|g_{ij}\left(G_k;\rho_k;e_k;\varepsilon_k;h_{\pm}(x);\omega_0;k\left(x,\omega_0\right)\right)\right\|_{4\times4}=0. \quad (3.1.35)$$

Here $\left\{g_{ij}\left(G_k;\rho_k;e_k;\varepsilon_k;h_{\pm}(x);\omega_0;k\left(x,\omega_0\right)\right)\right\}_{4\times4}$ have bulky forms and therefore are not brought. Due to the presence of expressions $h'_{\pm}(x)\cdot\sigma^{+}_{zx}(x,h_{+}(x),t)$ and $h'_{\pm}(x)\cdot D^{+}_{x}(x,h_{+}(x),t)$ in the boundary conditions (3.1.11), (3.1.13) and (3.1.14), the dispersion equation (3.1.35) is extremely complicated. Nevertheless, for selected formation functions $f_{\pm}(y;kh_0;h_{\pm}(x)/h_0)$, the imaginary part of the dispersion equation is satisfied automatically.

It is easy to see from the expressions of the distributions of the physico-mechanical fields, the distribution of amplitude and frequency of the wave field over the waveguide depend on as physico-mechanical constants of boundary materials, as well as on characteristic linear dimensions of the surface non-smoothness of the composite waveguide.

Frequency characteristics of propagating wave signal. It is shown in [12], that during propagation of long-wave signals, the interaction of propagating normal wave and weak surface non-smoothness practically does not occur.

The dispersion equation (3.1.35) obviously does not admit analytical solution. Nevertheless, it is studied numerically. In the case of propagation of short-wave (high frequency) electroelastic signal, the presence of surface geometrical inhomogeneities leads to the dependence of the wave number on the $x-$coordinate, i.e. the signal has the form $\exp\left[k(x)\cdot x-\omega_0 t\right]$. Even though in this case damping waves of the form $\exp\left[-\alpha_i\left(\omega_0;k(x)\right)\cdot y\right]$, can be neglected and uncoupled problems for two piezoelectric half-spaces with different electromechanical surface conditions can be obtained, but then the influence of the surface non-smoothness in the base layer of the waveguide can not be accurately computed. Therefore, quantitatively small, but qualitatively important components of the wave field can be preserved during computations.

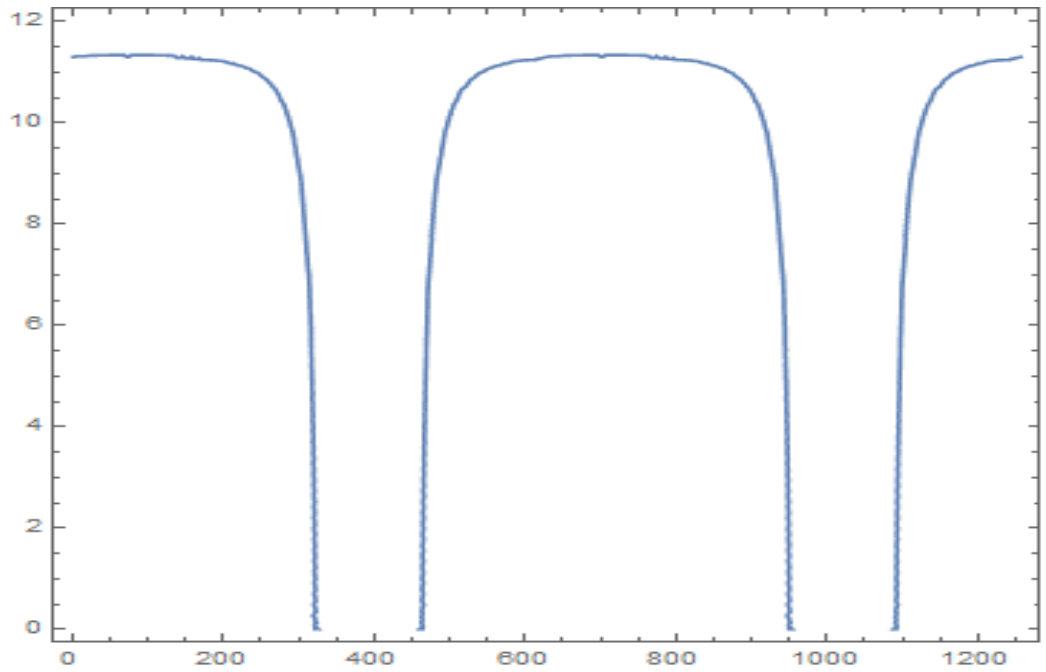

Fig. 3.1.2 Dependence of the wave number $k(x)$ on the x coordinate at fixed source frequency $\omega_0 = 200000\,\text{Hz}$

For the comparative analysis, we first present the characteristic frequency description of the plane electroelastic shear wave signal propagation in piezoelectric homogeneous waveguide with mechanically free, non-smooth surfaces when one of the surfaces of the waveguide-layer is electrically open and the other one is electrically closed.

Fig. 3.1.2 shows the dependence of the wave number for fast normal waves for harmonic mode of oscillations $sh\left[\alpha_0 k(y - h_{\pm}(x))\right]$. It also follows, that for each source frequency $\omega_0 = const$, fast wave signal is converted into a wave process with a given wave number $k_0(x)$, with corresponding period cycle of the wave formation. The period (in the calculations it is set to $T = 200\pi$) is formed by the relationship of linear dimensions of the base layer and surface roughness. Fig. 3.1.2 and Fig. 3.1.3 show, that there are certain periodic zones $\left\{\left[x_0; x_1\right] + 200\pi\right\}$, where the wave number $k(x)$ and frequency $\omega(x)$ are not defined. It is also obvious, that for high frequency (shortwave) signal of order $\lambda \square \pi/25\,\text{m}$, the frequency can increase from $\omega \approx 85 \cdot 10^3\,\text{Hz}$ to $\omega \approx 5 \cdot 10^5\,\text{Hz}$.

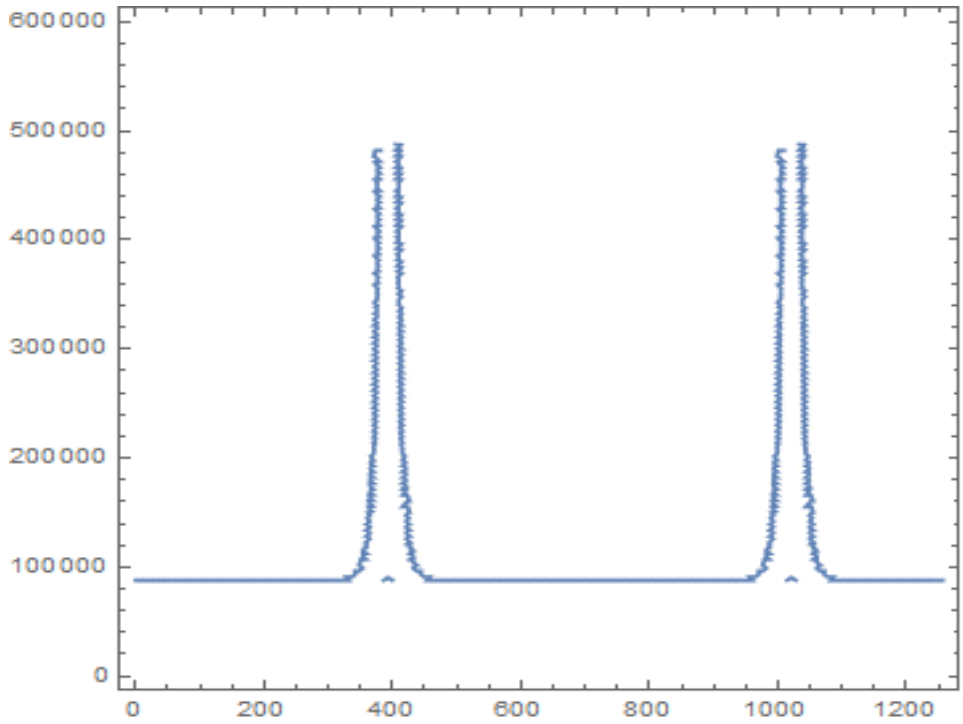

Fig. 3.1.3 Frequency dependence $\omega(x)$ of fast wave signals on the x coordinate when the wave number is prescribed $k_0 = 50\,\text{m}^{-1}$

Note, that even though the wave number decreases in the areas of definition and the frequency increases synchronously, their ratio remains constant, and also ultrashort wave solutions do not exist, for example, when $k_n \geq 250$ m^{-1}.

For slow waves, when the phase speed is smaller than the values of shear body waves in the piezoelectric, the distortion of wave functions and frequencies occurs similarly, but in different directions. Unlike fast waves, in this case the wave number and the frequency are changing in different intervals and by opposite signs of monotonicity (Fig. 3.1.4 and Fig. 3.1.5). Note, that in this case the same periodic zones $\left\{\left[x_0; x_1\right] + 200\pi\right\}$ appear, where the wave number $k(x)$ and frequency $\omega(x)$ are not defined. It is also seen from Fig. 3.1.4 and 3.1.5, that for high-frequency (short-wave) signal of order $\lambda \approx \pi/80$ m, the frequency can decrease from $\omega \approx 285 \cdot 10^3$ Hz to $\omega \approx 0$ Hz.

From the other hand, the wave number increases in the areas of definition and the frequency decreases synchronously, nevertheless their ratio remains constant. The ultrashort wave solutions do not exist, for example, when $k_n \geq 165\,\text{m}^{-1}$.

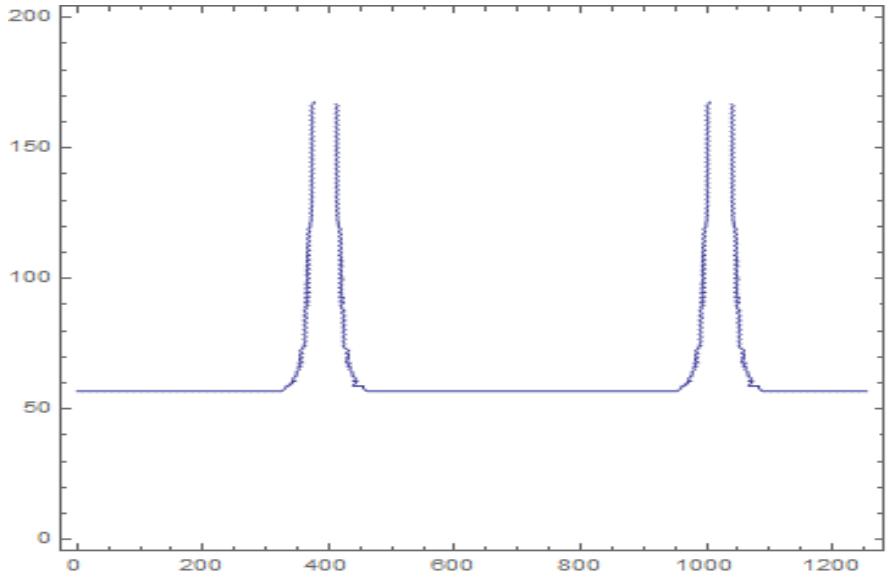

Fig. 3.1.4 Dependence of the wave number $k(x)$ on the x coordinate at fixed source frequency $\omega_0 = 100000$ Hz

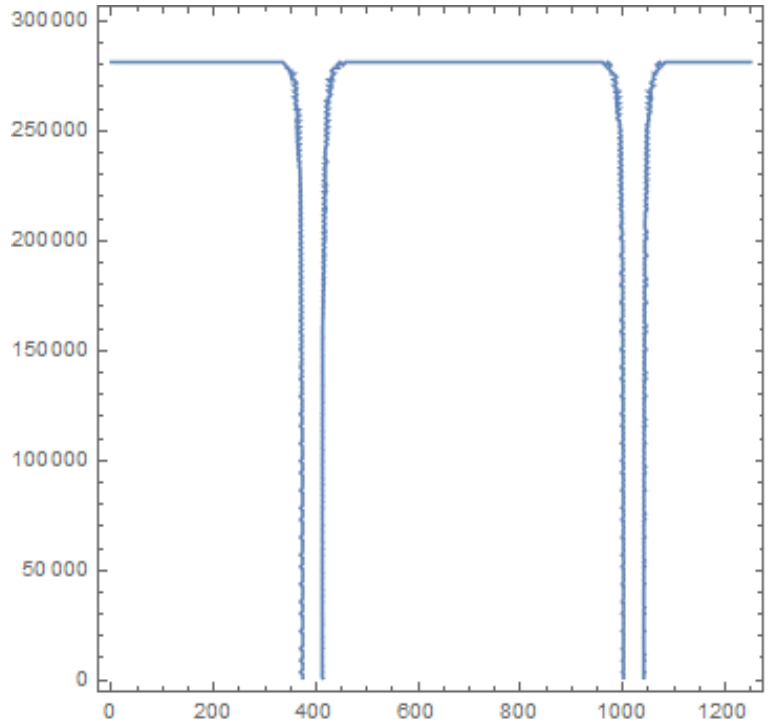

Fig. 3.1.5 Frequency dependence $\omega(x)$ of fast wave signals on also appear the x coordinate when the wave number is fixed to $k_0 = 160$ m^{-1}

Obviously, on the basis of (3.1.25), (3.1.26), (3.1.29), (3.1.30), (3.1.33) and (3.1.34), the distribution of the electroelastic wave over the thickness of the piezoelectric waveguide

taking into account virtually selected geometrically and physically inhomogeneous near-surface layers, is computed (see Fig. 3.1.6 and Fig. 3.1.7).

$$w(x,y)=\begin{cases} w_{+}\left(x,y,h_{+}(x)\right); & in \quad y\in\left[h_0(1-\gamma_{+});\ h_{+}(x)\right] \\ w_0(x,y); & in \quad y\in\left[-h_0(1-\gamma_{-});\ h_0(1-\gamma_{+})\right] \\ w_{-}\left(x,y,h_{-}(x)\right); & in \quad y\in\left[h_{-}(x);-h_0(1-\gamma_{-})\right] \end{cases} \tag{3.1.36}$$

$$\varphi(x,y)=\begin{cases} \varphi_{+}\left(x,y,h_{+}(x)\right); & in \quad y\in\left[h_0(1-\gamma_{+});\ h_{+}(x)\right] \\ \varphi_0(x,y); & in \quad y\in\left[-h_0(1-\gamma_{-});\ h_0(1-\gamma_{+})\right] \\ \varphi_{-}\left(x,y,h_{-}(x)\right). & in \quad y\in\left[h_{-}(x);-h_0(1-\gamma_{-})\right] \end{cases} \tag{3.1.37}$$

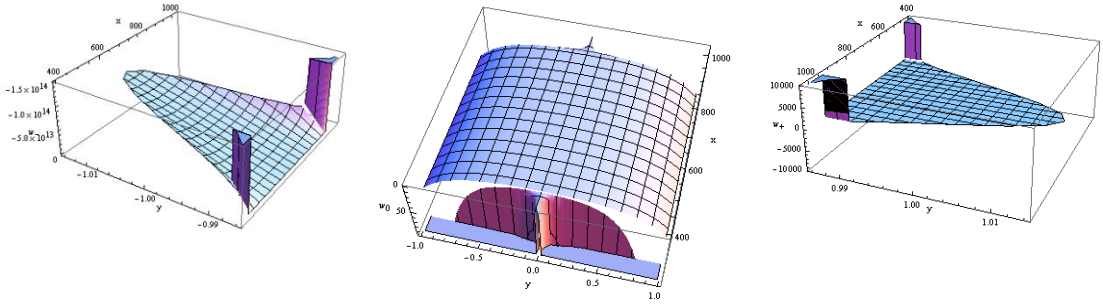

Fig. 3.1.6 Distribution of the elastic shear over the thickness of the waveguide $h_{-}(x)\le y\le h_{+}(x)$

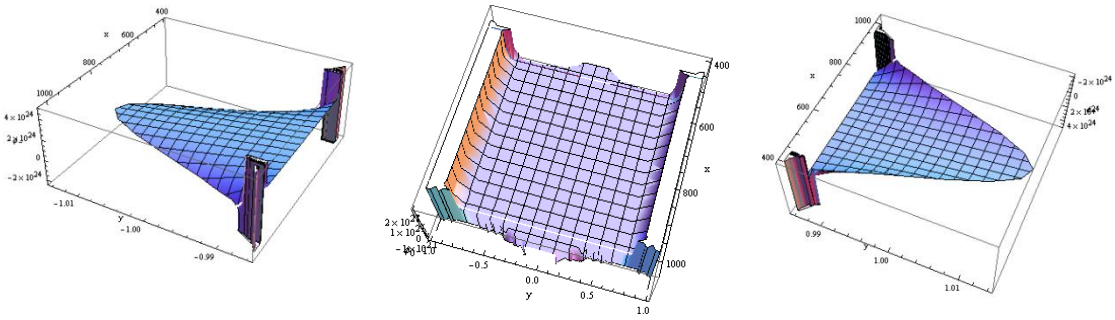

Fig. 3.1.7 Distribution of the electric field potential over the thickness of the waveguide $h_{-}(x)\le y\le h_{+}(x)$

Numerical computations are done for test values of adjacent material parameters of the composite waveguide and linear dimensions of the surface non-smoothness of the waveguide. The algorithm of calculations and obtained formulas allow to construct the

required composite waveguide with desired parameters, as well as predict phenomenological materials for waveguides with better features.

3.2 The propagation of high-frequency electroelastic (SH) wave signal in homogeneous piezoelectric layer waveguide with mechanically rigidly clamped and electrically open (closed) weakly inhomogeneous surfaces

Let us assume, that in Cartesian coordinate system $\{x; y; z\}$ we have a piezoelectric layer $\Omega \square \{|x|<\infty;\ h_{-}(x)\le y\le h_{+}(x);\ |z|<\infty\}$ with non-smooth surfaces $y=h_{\pm}(x)\in \mathrm{L}_2$. Suppose, that the smooth surfaces $y=h_{\pm}(x)$ of the waveguide are mechanically rigidly clamped, forming mechanically closed borders. The non-smooth surface $y=h_{-}(x)$ is clamped with a rigid dielectric layer forming electrically closed surface, and the other non-smooth surface $y=h_{+}(x)$ is clamped with a soft dielectric layer ($\varepsilon_e \square \varepsilon_{11}$) forming an electrically open surface.

During technological processing of the basic piezoelectric layer, in addition to the surface roughness, inhomogeneity of the material appears in the near-surface zones. These near-surface zones are especially important in studies of shortwave signal propagation in composite waveguides. To account for these inhomogeneities in the near-surface zones, we first introduce virtual slices $y=h_0(1-\gamma_{+})$ and $y=-h_0(1-\gamma_{-})$. Then, with the basic waveguide, we will already consider three-layer piezoelectric waveguide, consisting of basic homogeneous layer of constant thickness $2H_0=2h_0(1-\gamma_{+}-\gamma_{-})$:

$$\Omega_0=\{|x|<\infty;\ -h_0(1-\gamma_{-})\le y\le h_0(1-\gamma_{+});\ |z|<\infty\}, \tag{3.2.1}$$

and two inhomogeneous over the thickness near-surface thin layers of variable thicknesses $\zeta_{+}(x)=h_0(1+\gamma_{+})-h_{+}(x)$ and $\zeta_{-}(x)=|h_0(1+\gamma_{-})+h_{-}(x)|$, respectively

(see Fig. 3.2.1)

$$\Omega_{-}=\{|x|<\infty;\ h_{-}(x)\le y\le -h_0(1-\gamma_{-});\ |z|<\infty\}, \tag{3.2.2}$$

$$\Omega_{+}=\{|x|<\infty;\ h_0(1-\gamma_{+})\le y\le h_{+}(x);\ |z|<\infty\}. \tag{3.2.3}$$

Let us assume, that high-frequency (short-wave) elastic shear (SH) wave signal propagates in the composite waveguide, the length of which is much smaller than the base layer thickness $\lambda_0 \square 2H_0-2h_0$. Additionally assume, that the material of the basic piezoelectric layer Ω_0 belongs to the tetragonal class $4mm$ symmetry or hexagonal class $6mm$

symmetry, for which, when the axis ox_3 is parallel to the axis of piezo-crystal symmetry $\overline{p}$, of fourth (or sixth) order, the electro-active shear deformations $\{0;\ 0;\ w(x,y,t);\ \varphi(x,y,t)\}$ are separated from non-electro-active plane deformations $\{u(x,y,t);\ v(x,y,t);\ 0;\ 0\}$.

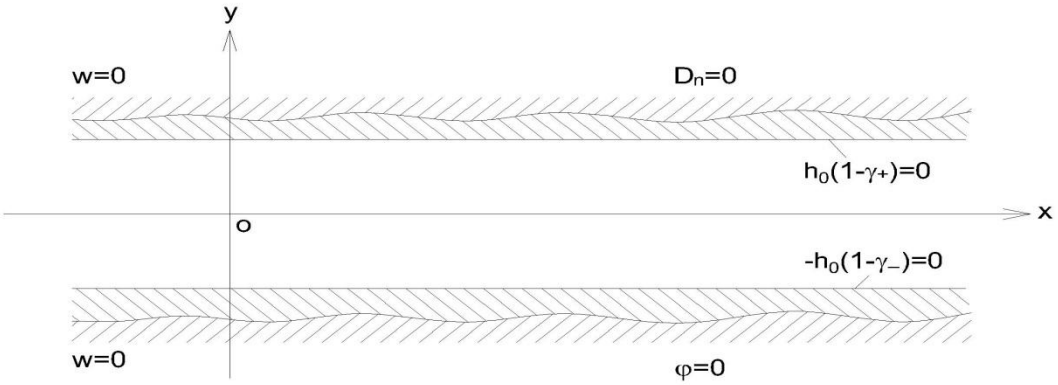

Fig. 3.2.1 Homogeneous piezoelectric waveguide with weakly inhomogeneous, mechanically rigidly clamped and electrically open (closed) surfaces

As in the previous paragraph, the quasi-static equations of electroelasticity for these crystals in the basic layer of composite waveguide will have the following form:

$$\nabla^2 w_0(x,y,t) = c_{0t}^{-2} \cdot \ddot{w}_0(x,y,t), \tag{3.2.4}$$

$$\nabla^2 \varphi_0(x,y,t) = (e_{15}/\varepsilon_{11}) \cdot \nabla^2 w_0(x,y,t). \tag{3.2.5}$$

The equations of electroelasticity of laterally inhomogeneous piezoelectric layer will be solved in virtually selected layers $\Omega_{\pm}^{p}$ as well, (3.1.7) and (3.1.8) of previous paragraph. These equations will be solved taking into account the material relations for the component of mechanical strain and induction of electric field of homogeneous material (3.1.9) or laterally inhomogeneous material (3.1.10).

Electromechanical boundary conditions are satisfied on the outer, mechanically rigidly clamped, electrically closed surface $y = h_{-}(x)$ of inhomogeneous, over the thickness near-surface thin layer with variable thickness $\left|-h_0(1-\gamma_{-}) - h_{-}(x)\right|$

$$w_{-}(x, h_{-}(x), t) = 0; \tag{3.2.6}$$

$$\varphi_{-}(x, h_{-}(x), t) = 0. \tag{3.2.7}$$

Electromechanical boundary conditions are satisfied on outer, mechanically rigidly clamped, electrically open surface $y = h_{+}(x)$ of inhomogeneous over the thickness near-surface thin layer with variable thickness $\left|h_{+}(x) - h_0(1-\gamma_{+})\right|$:

$$w_+(x,h_+(x),t)=0; \tag{3.2.8}$$

$$h'_+(x)D_x^+(x,h_+(x),t)+D_y^+(x,h_+(x),t)=0. \tag{3.2.9}$$

As in the previous problem, full continuity conditions of electromechanical fields for homogeneous and inhomogeneous piezoelectric layers are satisfied on virtually selected slices $y=-h_0(1-\gamma_-)$ and $y=h_0(1-\gamma_+)$:

$$w_0(x,-h_0(1-\gamma_-),t)=w_-(x,-h_0(1-\gamma_-),t), \tag{3.2.10}$$

$$\varphi_0(x,-h_0(1-\gamma_-),t)=\varphi_-(x,-h_0(1-\gamma_-),t), \tag{3.2.11}$$

$$\sigma_{yz}^0(x,-h_0(1-\gamma_-),t)=\sigma_{yz}^-(x,-h_0(1-\gamma_-),t), \tag{3.2.12}$$

$$D_y^0(x,-h_0(1-\gamma_-),t)=D_y^-(x,-h_0(1-\gamma_-),t), \tag{3.2.13}$$

$$w_0(x,h_0(1-\gamma_+),t)=w_+(x,h_0(1-\gamma_+),t), \tag{3.2.14}$$

$$\varphi_0(x,h_0(1-\gamma_+),t)=\varphi_+(x,h_0(1-\gamma_+),t), \tag{3.2.15}$$

$$\sigma_{yz}^0(x,h_0(1-\gamma_+),t)=\sigma_{yz}^+(x,h_0(1-\gamma_+),t), \tag{3.2.16}$$

$$D_y^0(x,h_0(1-\gamma_+),t)=D_y^+(x,h_0(1-\gamma_+),t). \tag{3.2.17}$$

It is seen from the given boundary conditions, that in addition to the commonly used material relations, due to the presence of non-smooth surfaces in the multilayer waveguide, the tangential component of the induction of the electric field of Ω_+ is involved in the boundary condition (3.2.9):

$$D_x^\pm(x,y,t)=e_\pm(y)\frac{\partial w_\pm(x,y,t)}{\partial x}-\varepsilon_\pm(y)\frac{\partial \varphi_\pm(x,y,t)}{\partial x}. \tag{3.2.18}$$

The boundary conditions (3.2.6)-(3.2.9) do not include the values of potential and normal component of the electric field induction of the vacuum half-spaces, because the surface $y=h_-(x)$ is isolated by perfect conductor (c.f. (3.2.7)), and the surface $y=h_+(x)$ is isolated by soft dielectric (c.f. (3.2.9)).

Thus, the homogeneous piezoelectric layer-waveguide with surface inhomogeneities is modelled as a three-layer waveguide of different materials. The problem of wave process investigation (localization of shear elastic wave in forming near-surface inhomogeneous thin layers Ω_- and Ω_+, delay of normal waves of certain frequencies, occurrence of dynamic surface loads, etc.) during the propagation of electroelastic normal shear wave

signal, mathematically is formulated as a boundary value problem with quasi-static equations of electroelasticity in the respective layers, with coupled electromechanical boundary conditions on the slices of materials separation (3.2.6)-(3.2.17).

From mathematical point of view the obtained boundary-value problem is complicated by the fact that in both virtually selected layers Ω_- and Ω_+, the equations of electroelasticity of the laterally inhomogeneous piezoelectric with variable coefficients should be solved. Due to non-smoothness of the surface $y = h_+(x)$, variable coefficients will also be available in the boundary condition (3.2.12).

To avoid mathematical difficulties, for solving the wave propagation problem, taking into account the material weak inhomogeneity and surface geometry in near-surface zones, a hypothetical approach is applied. For propagation of normal wave signal in the composite waveguide, the wave solution of the system of equations (3.2.4) and (3.2.5) in the basic homogeneous piezoelectric layer Ω_0 will be written in the form of normal wave:

$$w_0(x,y,t) = \left[A_0 e^{\alpha_0 k y} + B_0 e^{-\alpha_0 k y} \right] e^{i(kx-\omega_0 t)}, \tag{3.2.19}$$

$$\varphi_0(x,y,t) = \left\{ C_0 e^{ky} + D_0 e^{-ky} + (e_{15}/\varepsilon_{11}) \cdot \left[A_0 e^{\alpha_0 k y} + B_0 e^{-\alpha_0 k y} \right] \right\} e^{i(kx-\omega_0 t)}. \tag{3.2.20}$$

Considering the thinness of the other two boundary layers and the complexity of the analytical solution of the electroelasticity equations in virtually selected heterogeneous layers Ω_- and Ω_+, over the thickness of each layer we introduce hypotheses ***MELS*** for distributions of elastic shear and potential of electric field. The elastic shear and potential of the electric field in the virtually selected heterogeneous piezoelectric layer Ω_+ are introduced as follows:

$$w_+(x,y,t) = \left[1 - f_+\left(y; kh_0; h_+(x)/h_0 \right) \right] \cdot w_0\left(x, h_0(1-\gamma_+), t \right), \tag{3.2.21}$$

$$\begin{aligned} &\varphi_+(x,y,t) = \varphi_0\left(x, h_0(1-\gamma_+), t \right) + \\ &+ f\left(y; kh_0; h_+(x)/h_0 \right) \cdot \left[\varphi_+(x, h_+(x), t) - \varphi_0\left(x, h_0(1-\gamma_+), t \right) \right]. \end{aligned} \tag{3.2.22}$$

Moreover, the condition (3.2.8), (3.2.14) and (3.2.15) are satisfied automatically with the choice of distribution function in (3.2.21) and (3.2.22). The surface value $\varphi_+(x, h_+(x), t)$ is obtained from the condition (3.2.9), and therefore the expressions (3.2.21) and (3.2.22) are represented by arbitrary constant amplitudes $\{A_0; B_0; C_0; D_0\}$ of electroelastic wave signal:

$$w_+(x,y,t)=\left[1-\frac{sh\left[\alpha_+k(y-h_0(1-\gamma_+))\right]}{sh\left[\alpha_+k(h_+(x)-h_0(1-\gamma_+))\right]}\right]\cdot w_0\left(x,h_0(1-\gamma_+),t\right), \tag{3.2.23}$$

$$\varphi_+(x,y)=\frac{sh\left[\alpha_+k(y-h_0(1-\gamma_+))\right]}{\alpha_+}\cdot\left\{C_0e^{kh_0(1-\gamma_+)}-D_0e^{-kh_0(1-\gamma_+)}\right\}$$
$$+\left[1+\frac{sh\left[\alpha_+k(y-h_0(1-\gamma_+))\right]}{sh\left[\alpha_+k(h_+(x)-h_0(1-\gamma_+))\right]}\right]\cdot\left\{\begin{array}{l}C_0e^{kh_0(1-\gamma_+)}+D_0e^{-kh_0(1-\gamma_+)}+\\+\dfrac{e_0}{\varepsilon_0}\cdot\left[A_0e^{\alpha_0kh_0(1-\gamma_+)}+B_0e^{-\alpha_0kh_0(1-\gamma_+)}\right]\end{array}\right\}. \tag{3.2.24}$$

Note, that the formation function $f_+(y;kh_0;h_+(x)/h_0)=sh\left[\alpha_+k(y-h_0(1-\gamma_+))\right]/sh\left[\alpha_+k(h_+(x)-h_0(1-\gamma_+))\right]$ of unknown characteristics of the wave field is represented by the formation coefficient $\alpha_+(k)$ and by the variable thickness $\zeta_+(x)$ of the layer.

Similarly, the elastic shear and the potential of the electric field in virtually selected inhomogeneous piezoelectric layer Ω_- are represented in the following forms using the relations (3.2.21) and (3.2.22)

$$w_-(x,y,t)=\left\{1-f_-\left(y;kh_0;h_-(x)/h_0\right)\right\}w_0\left(x,-h_0(1-\gamma_-),t\right), \tag{3.2.25}$$

$$\varphi_-(x,y,t)=\left\{1-f_-\left(y;kh_0;h_-(x)/h_0\right)\right\}\varphi_0\left(x,-h_0(1-\gamma_-),t\right), \tag{3.2.26}$$

where the formation function $f_-(y;kh_0;h_-(x)/h_0)=sh\left[\alpha_-k(y+h_0(1-\gamma_-))\right]/sh\left[\alpha_-k(h_-(x)+h_0(1-\gamma_-))\right]$ in the inhomogeneous piezoelectric layer is represented by the new formation coefficient $\alpha_-(k)$ and variable thickness $\left|h_0\left(1+\gamma_-\right)+h_-\left(x\right)\right|$, characterizing the layer.

The conditions (3.2.6), (3.2.7), (3.2.10) and (3.2.11) are satisfied automatically with the choice of distribution function in (3.2.25) and (3.2.26). Therefore, the expressions of the distributions (3.2.25) and (3.2.26) are expressed by arbitrary constant amplitudes $\{A_0;B_0;C_0;D_0\}$ of electroelastic wave signal:

$$w_-(x,y)=\left\{1-\frac{sh\left[\alpha_-k\left(y+h_0(1-\gamma_-)\right)\right]}{sh\left[\alpha_-k\left(h_-(x)+h_0(1-\gamma_-)\right)\right]}\right\}\cdot\left\{A_0e^{-\alpha_0kh_0(1-\gamma_-)}+B_0e^{\alpha_0kh_0(1-\gamma_-)}\right\}, \tag{3.2.27}$$

$$\varphi_{-}(x,y)=\left\{1-\frac{sh\left[\alpha_{-}k\left(y+h_0(1-\gamma_{-})\right)\right]}{sh\left[\alpha_{-}k\left(h_{-}(x)+h_0(1-\gamma_{-})\right)\right]}\right\}\cdot\left\{\begin{array}{l}C_0e^{-kh_0(1-\gamma_{-})}+D_0e^{kh_0(1-\gamma_{-})}+\\+\dfrac{e_{15}}{\varepsilon_{11}}\cdot\left[A_0e^{-\alpha_0kh_0(1-\gamma_{-})}+B_0e^{\alpha_0kh_0(1-\gamma_{-})}\right]\end{array}\right\}. \qquad (3.2.28)$$

The introduced distributions of characteristics of the wave field (3.2.19), (3.2.20), as well as (3.2.25)-(3.2.28) describe the picture of distribution over the thickness of the composite waveguide. In order to evaluate the wave number $k\left(h_{\pm}(x)/h_0;\gamma_{\pm};\omega_0\right)$, which is determined from dispersion equation, we obtain a system of four homogeneous algebraic equations with respect to the amplitude constant $\left\{A_0;B_0;C_0;D_0\right\}$, satisfying the boundary conditions (3.2.12), (3.2.13), (3.2.16) and (3.2.17).

The dispersion equation of the formed wave field is obtained from the condition of existence of nontrivial solutions in the following form:

$$\det\left\|g_{ij}\left(G_k;\rho_k;e_k;\varepsilon_k;h_{\pm}(x);\omega_0;k\left(x,\omega_0\right)\right)\right\|_{4\times4}=0, \qquad (3.2.29)$$

where

$$g_{11}=G_0k\alpha_0\left\{\begin{array}{l}\left(1+\dfrac{\alpha_{-}/\alpha_0}{sh\left[\alpha_{-}k(h_{-}(x)+h_0(1-\gamma_{-}))\right]}\right)+\\+\chi_0^2\cdot\left(1-\dfrac{\alpha_{-}/\alpha_0}{sh\left[\alpha_{-}k(h_{-}(x)+h_0(1-\gamma_{-}))\right]}\right)\end{array}\right\}\cdot\exp\left[-\alpha_0kh_0(2-\gamma_{-}-\gamma_{+})\right],$$

$$g_{12}=G_0k\alpha_0\left\{\begin{array}{l}\chi_0^2\cdot\left(1-\dfrac{\alpha_{-}/\alpha_0}{sh\left[\alpha_{-}k(h_{-}(x)+h_0(1-\gamma_{-}))\right]}\right)-\\-\left(1+\dfrac{\alpha_{-}/\alpha_0}{sh\left[\alpha_{-}k(h_{-}(x)+h_0(1-\gamma_{-}))\right]}\right)\end{array}\right\}\cdot\exp\left[\alpha_0kh_0(2-\gamma_{-}-\gamma_{+})\right],$$

$$g_{13}=e_0k\left(1-\frac{\alpha_{-}}{sh\left[\alpha_{-}k(h_{-}(x)+h_0(1-\gamma_{-}))\right]}\right);\quad g_{14}=-e_0k\left(1+\frac{\alpha_{-}}{sh\left[\alpha_{-}k(h_{-}(x)+h_0(1-\gamma_{-}))\right]}\right),$$

$$g_{21}=2e_0\cdot\exp\left[-\alpha_0kh_0(2-\gamma_{-}-\gamma_{+})\right],\quad g_{22}=2e_0\cdot\exp\left[\alpha_0kh_0(2-\gamma_{-}-\gamma_{+})\right],$$

$$g_{23}=g_{24}=\varepsilon_0\left(1-\frac{sh\left[\alpha_{-}k(h_{-}(x)+h_0(1-\gamma_{-}))\right]}{\alpha_{-}}\right),\ g_{24}=\varepsilon_0\left(1-\frac{sh\left[\alpha_{-}k(h_{-}(x)+h_0(1-\gamma_{-}))\right]}{\alpha_{-}}\right),$$

$$g_{31}=\left\{\left(h_{+}'(x)\right)^2-\frac{\varepsilon_{+}}{\varepsilon_0}\cdot\frac{e_0}{e_{+}}h_{+}'(x)+1\right\}e_{+}\alpha_{+}k\cdot cth\left[\alpha_{+}k(h_{+}(x)-h_0(1-\gamma_{+}))\right]-\frac{e_0}{\varepsilon_0},$$

$$g_{32}=\left\{\left(h'_{+}(x)\right)^{2}-\frac{\varepsilon_{+}}{\varepsilon_{0}}\cdot\frac{e_{0}}{e_{+}}\cdot h'_{+}(x)+1\right\}e_{+}\alpha_{+}k\cdot cth\left[\alpha_{+}k(h_{+}(x)-h_{0}(1-\gamma_{+}))\right]-\frac{e_{0}}{\varepsilon_{0}},$$

$$g_{33}=\left\{\begin{array}{l}-\varepsilon_{+}kh'_{+}(x)\cdot\left[1+h'_{+}(\mathrm{x})\right]\cdot ch\left[\alpha_{+}k(h_{+}(\mathrm{x})-h_{0}(1-\gamma_{+}))\right]-\\ -\dfrac{sh\left[\alpha_{+}k(h_{+}(\mathrm{x})-h_{0}(1-\gamma_{+}))\right]}{\alpha_{+}}\end{array}\right\}\cdot\exp\left[kh_{0}(2-\gamma_{-}-\gamma_{+})\right],$$

$$g_{34}=\left\{\begin{array}{l}\varepsilon_{+}kh'_{+}(x)\cdot\left[1+h'_{+}(x)\right]\cdot ch\left[\alpha_{+}k(h_{+}(x)-h_{0}(1-\gamma_{+}))\right]+\\ +\dfrac{sh\left[\alpha_{+}k(h_{+}(x)-h_{0}(1-\gamma_{+}))\right]}{\alpha_{+}}\end{array}\right\}\cdot\exp\left[-kh_{0}(2-\gamma_{-}-\gamma_{+})\right],$$

$$g_{41}=g_{42}=\left(G_{0}/e_{0}\right)\cdot\left(1+\chi_{0}^{2}\right),\quad g_{42}=\left(G_{0}/e_{0}\right)\cdot\left(1+\chi_{0}^{2}\right),\quad g_{44}=0,\qquad g_{43}=0.$$

Formally, the dispersion equation is obtained in complex form. Obviously this is due to the presence of expression $h'_{\pm}(x)\cdot D_{x}^{+}(x,h_{+}(x),t)$ in the boundary condition (3.2.9). However, for $f_{\pm}(y;kh_{0};h_{\pm}(x)/h_{0})$, the imaginary part of the dispersion equation is satisfied automatically.

It is easy to see from the coefficient relations of distributions of physic-mechanical fields (3.2.19), (3.2.20), (3.2.23), (3.2.24), (3.2.25) and (3.2.26), that and amplitude distribution and frequency of the wave field through the waveguide depend on the physico-mechanical constants of boundary materials, as well as characteristic linear dimensions of the surface non-smoothness of composite waveguide.

Frequency characteristics of propagating wave signal. It is shown in [12], that during propagation of long-wave signals, the interaction of propagating normal wave and weak surface non-smoothness practically does not occur. Although in this case wave forms, damped over the depth of the base layer, i.e. $\exp\left[-\alpha_{i}\left(\omega_{0};k(x)\right)\cdot y\right]$, can be neglected, reducing to two uncoupled problems of piezoelectric half-spaces with different electromechanical surface conditions, but in this case we generally lose the ability to accurately calculate the influence of the surface non-smoothness for forming waves in the base layer of the waveguide. Therefore, in the calculations remain quantitatively small, but qualitatively important components.

First, present the characteristic frequency description of the problem of plane electroelastic shear wave signal propagation in piezoelectric homogeneous waveguide with

mechanically rigidly clamped, weakly inhomogeneous surfaces, when one surface of the waveguide-layer is electrically open and the other is electrically closed.

Fig.3.2.2 shows the dependence of the wave number for fast normal waves for harmonic mode of oscillations $sh\left[\alpha_0 k(y-h_{\pm}(x))\right]$.

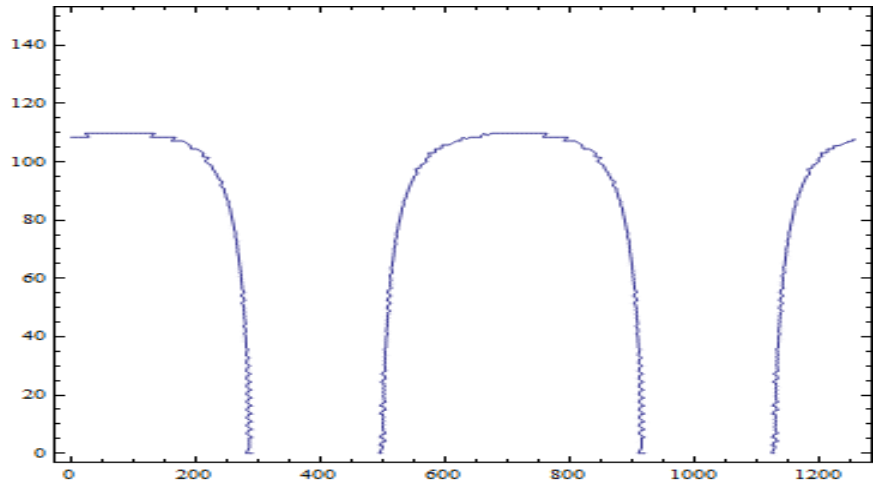

Fig. 3.2.2 Dependence of the wave number $k(x)$ on x coordinate at fixed source frequency $\omega_0 = 200000\,\text{Hz}$

It follows from Fig. 3.2.2, that for each source frequency $\omega_0 = const$, fast wave signals are converted into a wave process with a given wave number $k_0(x)$, with corresponding period cycle of the wave formation.

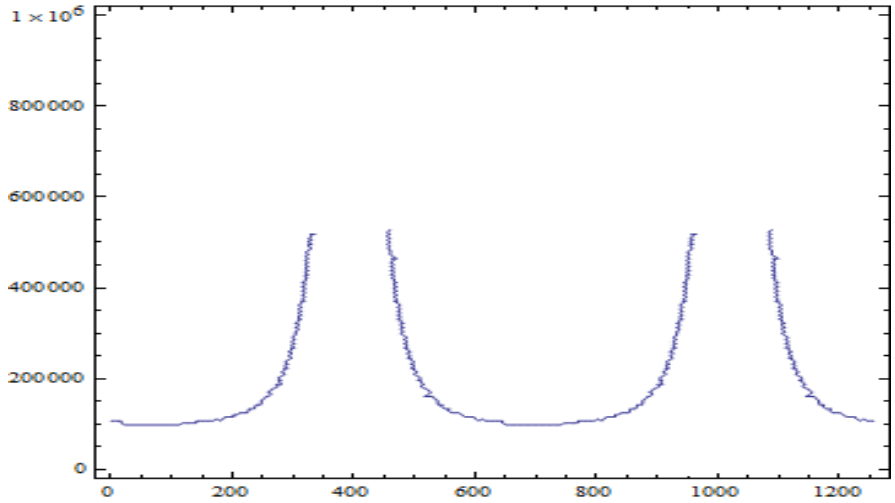

Fig. 3.2.3 Frequency dependence $\omega(x)$ of fast wave signals on x coordinate for fixed wave length $k_0 = 50$ m^{-1}

The period (in the calculations it is $T = 200\pi$) is formed by the relationship of linear dimensions of the base layer and surface roughness. Fig. 3.2.2 and Fig. 3.2.3 show that there are certain periodic zones $\{[x_0; x_1] + 200\pi\}$, where the wave number $k(x)$ and frequency $\omega(x)$ are not defined. It is also seen from the figures that at high frequency (shortwave) signal of order $\lambda \approx \pi/25$ m, the frequency can raise from $\omega \approx 85 \cdot 10^3$ Hz to $\omega \approx 5 \cdot 10^5$ Hz. Note, that the wave number decreases in the areas of definition and the frequency increases synchronously and their ratio remains constant, moreover ultrashort wave solutions do not exist, for example, when $k_n \geq 250$ m^{-1}.

For slow waves when the phase speed is less than the values of shear body waves in the piezoelectric, the distortion of wave functions and frequencies occur similarly, but in different directions. In contrast to the case of fast waves, in this case, the wave number and the frequency are changing in other intervals and by opposite signs of monotony (see Figs. 3.2.4 and 3.2.5).

It is necessary to pay attention to the fact, that in this case the same periodic zones $\{[x_0; x_1] + 200\pi\}$ appear, where the given wave number $k(x)$ and frequency $\omega(x)$ are not defined. It is also seen from Fig. 3.2.4 and 3.2.5, that for high-frequency (short-wave) signal of order $\lambda \approx \pi/80$ m, the frequency can decrease from $\omega \approx 285 \cdot 10^3$ Hz to $\omega \approx 0$ Hz.

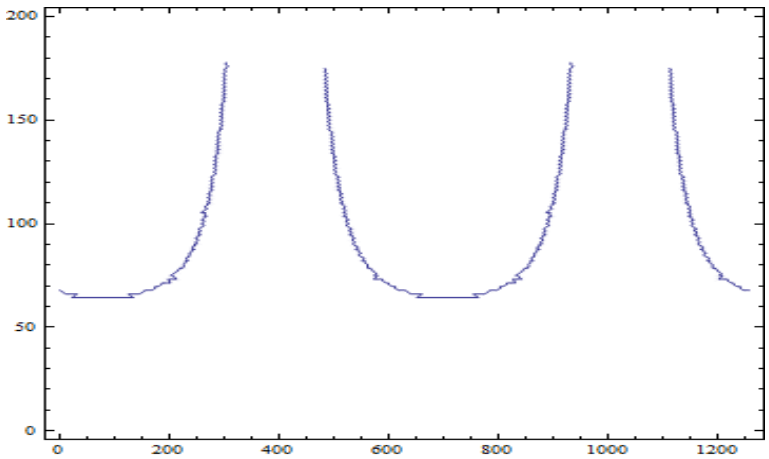

Fig. 3.2.4 Dependence of the wave number $k(x)$ on x coordinate at fixed source frequency $\omega_0 = 100000$ Hz

Note that the wave number increase in the areas of definition and the frequency decreases synchronously and their ratio remains constant, moreover, ultrashort wave solutions do not exist, for example, when $k_n \geq 165$ m^{-1}.

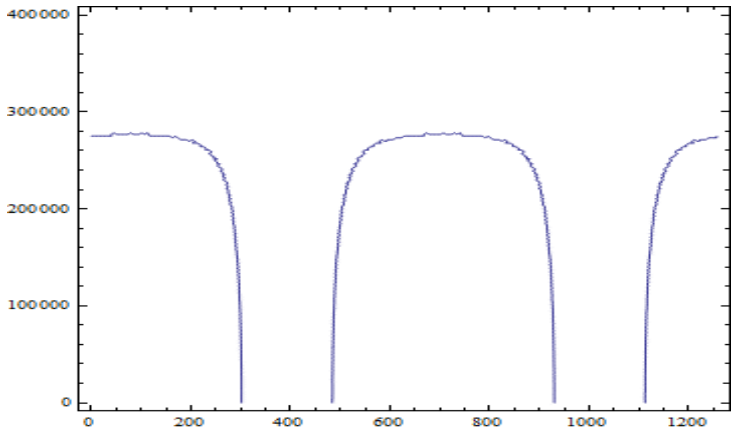

Fig. 3.2.5 Frequency dependence $\omega(x)$ of fast wave signals on x coordiante for fixed wave length $k_0 = 160$ m^{-1}

Figs. 3.2.6 and 3.2.7 show the dispersion dependence of fast and slow waves, respectively.

Obviously with the help of obtained relations, the distribution of electroelastic wave through all thickness of piezoelectric waveguide is built taking into account the virtually selected geometrically and physically inhomogeneous near-surface layers, respectively (Fig. 3.2.8 and Fig. 3.2.9):

$$w(x,y) = \begin{cases} w_+\left(x,y,h_+(x)\right); & in \quad y \in \left[h_0(1-\gamma_+);\ h_+(x)\right] \\ w_0(x,y); & in \quad y \in \left[-h_0(1-\gamma_-);\ h_0(1-\gamma_+)\right] \\ w_-\left(x,y,h_-(x)\right); & in \quad y \in \left[h_-(x);-h_0(1-\gamma_-)\right] \end{cases} \tag{3.2.30}$$

$$\varphi(x,y) = \begin{cases} \varphi_+\left(x,y,h_+(x)\right); & in \quad y \in \left[h_0(1-\gamma_+);\ h_+(x)\right] \\ \varphi_0(x,y); & in \quad y \in \left[-h_0(1-\gamma_-);\ h_0(1-\gamma_+)\right] \\ \varphi_-\left(x,y,h_-(x)\right). & in \quad y \in \left[h_-(x);-h_0(1-\gamma_-)\right] \end{cases} \tag{3.2.31}$$

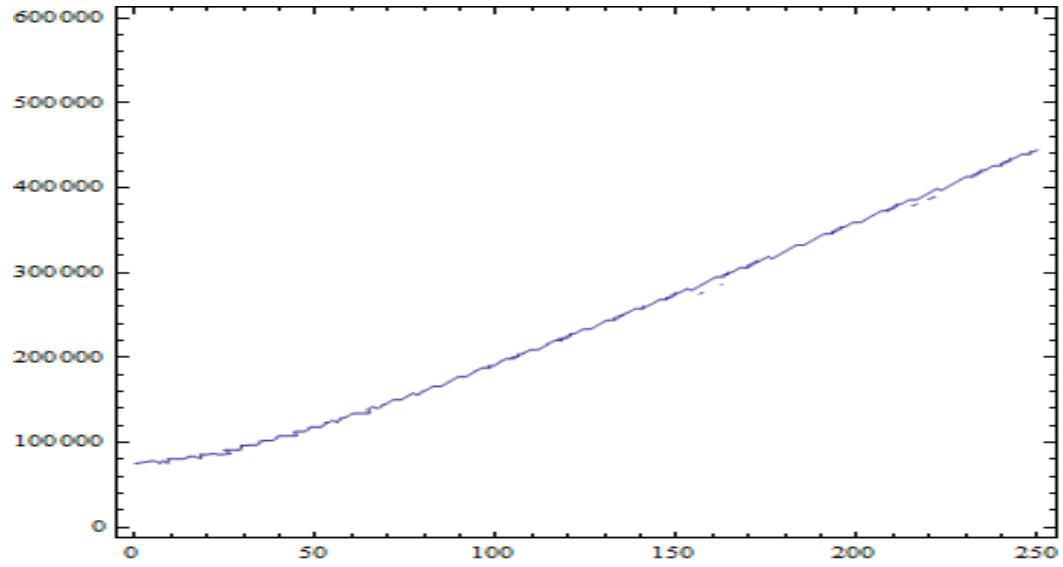

Fig. 3.2.6 Frequency dependence $\omega(k)$ of fast wave signals on the wave number k for fixed x coordinate $x = 200$

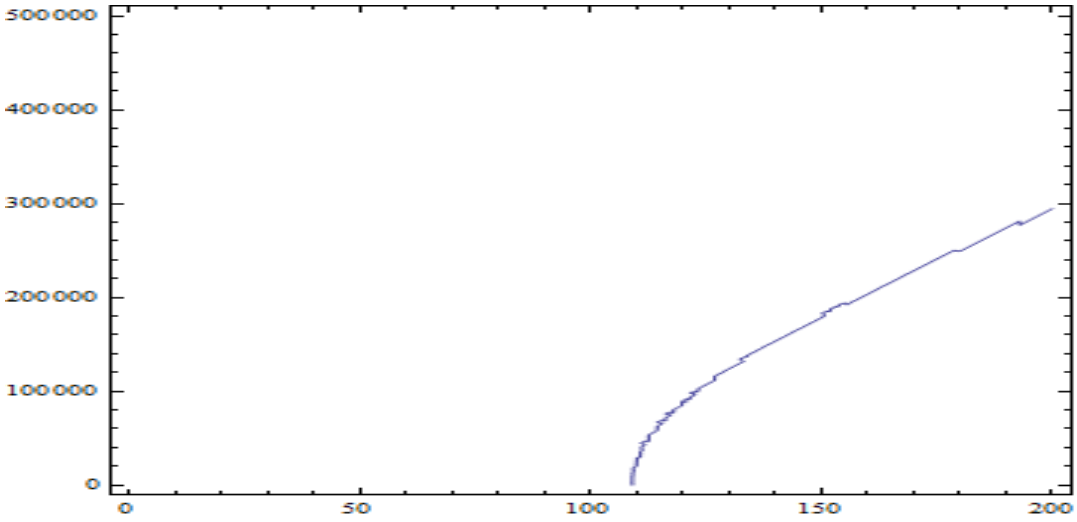

Fig. 3.2.7 Frequency dependence $\omega(k)$ of fast wave signals on the wave number k for fixed x coordinate $x = 200$

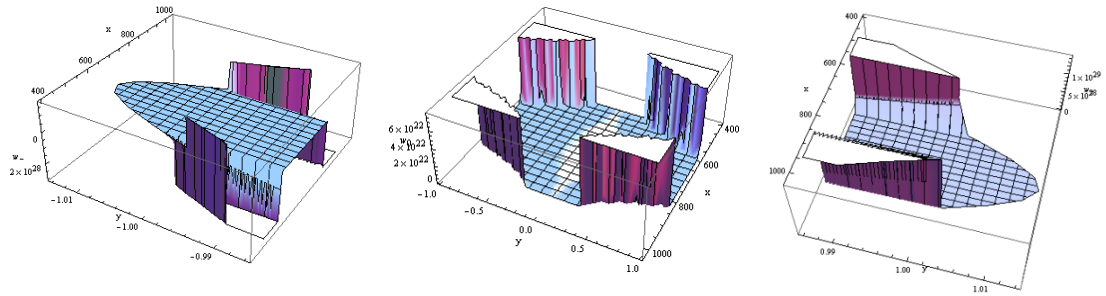

Fig. 3.2.8 Distribution of the elastic shear over the thickness of the waveguide $h_-(x) \le y \le h_+(x)$

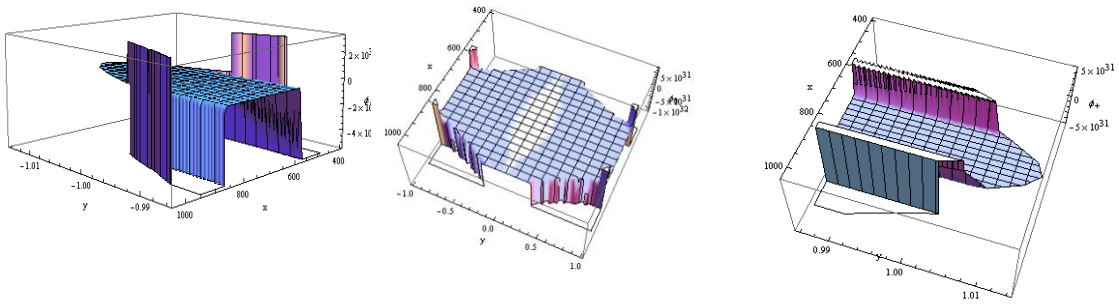

Fig. 3.2.9 Distribution of the electric field potential over the thickness of the waveguide $h_{-}(x) \le y \le h_{+}(x)$

§ 3.3 The propagation of high-frequency electroelastic (SH) wave signal in homogeneous piezoelectric layer waveguide with weakly inhomogeneous surfaces filled with perfect conductor (or dielectric)

Let us assume, that in Cartesian coordinate system $\{x;y;z\}$ we have a piezoelectric layer $\Omega \equiv \{|x|<\infty;\ h_-(x)\le y\le h_+(x);\ |z|<\infty\}$ with rough surfaces $y=h_\pm(x)$ (see [17]). Generally, surface roughness is described by a random function $y=h_\pm(x)\in \mathrm{L}_2$. Based on these, without losing the generality of further considerations, the surface roughness can be described respectively by functions of the weak inhomogeneity of $y=h_\pm(x)$

$$\begin{aligned} h_-(x) &= -h_0\left[1+\varepsilon_-\sin(k_-x)+\delta_-\cos(k_-x)\right],\\ h_+(x) &= h_0\left[1+\varepsilon_+\sin(k_+x)+\delta_+\cos(k_+x)\right]. \end{aligned} \tag{3.3.1}$$

Assume that the surface roughness $y=h_+(x)$ up to the surface $y=h_0(1+\gamma_+)$ is filled with a perfect dielectric material, and the surface roughness $y=h_-(x)$ up to the surface $y=-h_0(1+\gamma_-)$ is filled with a perfect conductor material. Then we obtain a composite waveguide of constant thickness consisting of three layers: the conductor layer $\Omega_-^c \equiv \{|x|<\infty;\ -h_0(1-\gamma_-)\le y\le h_-(x);|z|<\infty\}$, which has thickness $\zeta_c(x)\equiv |h_0(1+\gamma_-)+h_-(x)|$, the base piezoelectric layer $\Omega \equiv \{|x|<\infty;\ h_-(x)\le y\le h_+(x);\ |z|<\infty\}$, which has the thickness $\zeta_p(x)\equiv |h_+(x)-h_-(x)|$, and the dielectric layer $\Omega_+^d \equiv \{|x|<\infty;\ h_+(x)\le y\le h_0(1+\gamma_+);\ |z|<\infty\}$, which has the thickness $\zeta_d(x)\equiv h_0(1+\gamma_+)-h_+(x)$. These three layers are of variable thickness.

In studies on propagation of shortwave signals in composite waveguide is also important to consider near-surface zones of material heterogeneity, arising during technological processing of the base piezoelectric layer. For accounting these heterogeneities in the near-surface zones, we take virtual sections $y=h_0(1-\gamma_+)$ and $y=-h_0(1-\gamma_-)$. Instead of the waveguide base layer of variable thickness, we are going to consider a three-layer piezoelectric waveguide consisting of a base homogeneous layer

$$\Omega_0 \equiv \left\{ |x| < \infty;\ -h_0(1-\gamma_-) \le y \le h_0(1-\gamma_+);\ |z| < \infty \right\}, \tag{3.3.2}$$

and two inhomogeneous, through the thickness, near-surface thin layers of variable thickness (Fig. 3.3.1)

$$\Omega_-^p \equiv \left\{ |x| < \infty;\ h_-(x) \le y \le -h_0(1-\gamma_-);\ |z| < \infty \right\}, \tag{3.3.3}$$

$$\Omega_+^p \equiv \left\{ |x| < \infty;\ h_0(1-\gamma_+) \le y \le h_+(x);\ |z| < \infty \right\}. \tag{3.3.4}$$

Thus, in the near-surface zone at the surface $y = h_-(x)$ there is a composite layer Ω_0 composed of laterally inhomogeneous piezoelectric and homogeneous perfectly conducting materials $\Omega_- = \Omega_-^p \cup \Omega_-^c$.

Also in the near-surface zone at the surface $y = h_+(x)$ we have a composite layer Ω_0 composed of homogeneous dielectric and laterally inhomogeneous piezoelectric materials $\Omega_+ = \Omega_+^p \cup \Omega^d$.

Thus, the homogeneous piezoelectric waveguide, surface roughness of which is filled, is modeled as a multilayered waveguide made of different materials. We will investigate the localization of the shear elastic wave in the formed near-surface inhomogeneous thin layers $\Omega_- = \Omega_-^p \cup \Omega_-^c$ and $\Omega_+ = \Omega_+^p \cup \Omega^d$ (Fig. 3.3.1).

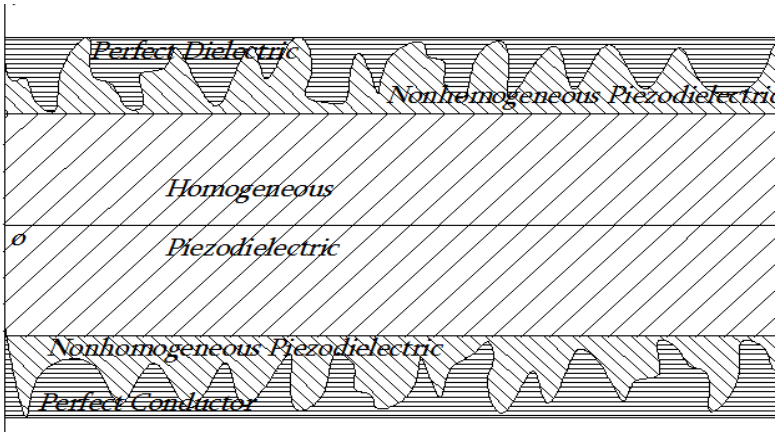

Fig. 3.3.1 Five-layer waveguide with base homogeneous piezoelectric layer with weakly inhomogeneous, mechanically free surfaces

Let us assume, that high-frequency (shortwave) elastic shear (*SH*) wave signal, whose length is much less than the base layer thickness $\lambda_0 \ll 2h_0$, is propagating in the composite waveguide. Moreover, the material of the main piezoelectric layer Ω_0 belongs to the class $4mm$ of tetragonal symmetry, or to the class $6mm$ of hexagonal symmetry, for which,

when the axis ox_3 is parallel to the axis of symmetry of the fourth (or sixth) order piezoelectric crystal $\overline{p}$, electroactive shear deformation $\{0;\ 0;\ w(x,y,\mathrm{t});\ \varphi(x,y,\mathrm{t})\}$ is separated from the non-electroactive plane deformation $\{u(x,y,\mathrm{t});\ v(x,y,\mathrm{t});\ 0;\ 0\}$. Quasi-static equations of electroelasticity for these crystals in the base layer of the composite waveguide have the following forms:

$$\nabla^2 w(x,y,t) = c_{0t}^{-2} \cdot \ddot{w}(x,y,t), \tag{3.3.5}$$

$$\nabla^2 \varphi(x,y,t) = (e_{15}/\varepsilon_{11}) \cdot \nabla^2 w(x,y,t). \tag{3.3.6}$$

The equations of electroelasticity of laterally inhomogeneous piezoelectric layer must be solved in virtually selected layers $\Omega_{\pm}^{p}$ respectively:

$$\begin{aligned} &G_{\pm}(y)\frac{\partial^2 w_{\pm}(x,y,t)}{\partial x^2} + e_{\pm}(y)\frac{\partial^2 \varphi_{\pm}(x,y,t)}{\partial x^2} + \\ &+\frac{\partial \sigma_{yz}^{\pm}(x,y,t)}{\partial y} = \rho_{\pm}(y) \cdot \ddot{w}_{\pm}(x,y,t), \end{aligned} \tag{3.3.7}$$

$$e_{\pm}(y)\frac{\partial^2 w_{\pm}(x,y,t)}{\partial x^2} - \varepsilon_{\pm}(y)\frac{\partial^2 \varphi_{\pm}(x,y,t)}{\partial x^2} + \frac{\partial D_y^{\pm}(x,y,t)}{\partial y} = 0, \tag{3.3.8}$$

where the material relations for the component of mechanical stress and induction of the electric field have the forms:

$$\begin{aligned} \sigma_{yz}^{\pm}(x,y,t) &= G_{\pm}(y)\frac{\partial w_{\pm}(x,y,t)}{\partial y} + e_{\pm}(y)\frac{\partial \varphi_{\pm}(x,y,t)}{\partial y}, \\ D_y^{\pm}(x,y,t) &= e_{\pm}(y)\frac{\partial w_{\pm}(x,y,t)}{\partial y} - \varepsilon_{\pm}(y)\frac{\partial \varphi_{\pm}(x,y,t)}{\partial y}. \end{aligned} \tag{3.3.9}$$

The motion equation for perfectly conducting layer Ω^{c} will have in the following form:

$$G_{-}^{c}\frac{\partial^2 w_{-}^{c}(x,y,t)}{\partial x^2} + \frac{\partial \sigma_{yz}^{c}(x,y,t)}{\partial y} = \rho_{-}^{c} \cdot \ddot{w}_{-}^{c}(x,y,t), \tag{3.3.10}$$

where the relation for mechanical shear stress is the following

$$\sigma_{yz}^{c}(x,y,t) = G_{-}^{c}\frac{\partial w_{-}^{c}(x,y,t)}{\partial y}. \tag{3.3.11}$$

The equations of elastic shear motion and electrostatics in the dielectric layer Ω^{d} will have the following forms:

$$G_+^d \frac{\partial^2 w_+^d(x,y,t)}{\partial x^2} + \frac{\partial \sigma_{yz}^d(x,y,t)}{\partial y} = \rho_+^d \cdot \ddot{w}_+^d(x,y,t), \tag{3.3.12}$$

$$-\varepsilon_+^d \frac{\partial^2 \varphi_+^d(x,y,t)}{\partial x^2} + \frac{\partial D_y^d(x,y,t)}{\partial y} = 0, \tag{3.3.13}$$

where the material relations for the component of mechanical stress and induction of the electric field have the forms

$$\sigma_{yz}^d(x,y,t) = G_+^d \frac{\partial w_+^d(x,y,t)}{\partial y}; \quad D_y^d(x,y,t) = -\varepsilon_+^d \frac{\partial \varphi_+^d(x,y,t)}{\partial y}. \tag{3.3.14}$$

The separation of the near-surface zones to multiple layers leads to increase in the number of boundary conditions on existing and introduced virtual surfaces of the multilayer waveguide.

Only one boundary condition will be posted on the mechanically free surface $y = -h_0 \cdot (1+\gamma_-)$ of the perfectly conducting thin layer

$$\sigma_{yz}^c(x,-h_0-\gamma_-,\mathrm{t}) = G^c \frac{\partial w^c(x,y,t)}{\partial y}\bigg|_{y=-h_0-\gamma_-} = 0. \tag{3.3.15}$$

The continuity conditions of the electromechanical fields in piezoelectric and the continuity conditions of the perfect conductor are satisfied on the rough surface $y = h_-(x)$:

$$w_-(x,h_-(x),t) = w^c(x,h_-(x),t); \qquad \varphi_-(x,h_-(x),t) = 0, \tag{3.3.16}$$

$$h_-'(x)\cdot\sigma_{zx}^-(x,h_-(x),t) + \sigma_{zy}^-(x,h_-(x),t) = h_-'(x)\cdot\sigma_{zx}^c(x,h_-(x),t) + \sigma_{zy}^c(x,h_-(x),t). \tag{3.3.17}$$

The continuity conditions of the electromechanical fields of homogeneous and heterogeneous piezoelectric layers are satisfied on the virtually selected surface $y = -h_0(1-\gamma_-)$

$$\begin{aligned} w_0(x,-h_0(1-\gamma_-),t) &= w_-(x,-h_0(1-\gamma_-),t), \\ \varphi_0(x,-h_0(1-\gamma_-),t) &= \varphi_-(x,-h_0(1-\gamma_-),t), \end{aligned} \tag{3.3.18}$$

$$\sigma_{yz}^0(x,-h_0(1-\gamma_-),t) = \sigma_{yz}^-(x,-h_0(1-\gamma_-),t), \tag{3.3.19}$$

$$D_y^0(x,-h_0(1-\gamma_-),t) = D_y^-(x,-h_0(1-\gamma_-),t). \tag{3.3.20}$$

Similarly, the continuity conditions of the electromechanical fields, taking into account the fact that the electric field is related to the vacuum half-space from outside through the dielectric layer, are satisfied on the mechanically free surface $y = h_0\left(1+\gamma_+\right)$:

$$\varphi_+^d\left(x, h_0\left(1+\gamma_+\right), t\right) = \varphi^{(e)}\left(x, h_0\left(1+\gamma_+\right), t\right), \tag{3.3.21}$$

$$\sigma_{yz}^d\left(x, h_0\left(1+\gamma_+\right), \mathrm{t}\right) = G_+^d \left.\frac{\partial w_+^d\left(x,y,t\right)}{\partial y}\right|_{y=h_0\left(1+\gamma_+\right)} = 0, \tag{3.3.22}$$

$$D_y^d\left(x, h_0\left(1+\gamma_+\right), \mathrm{t}\right) = -\varepsilon^{(e)} \left.\frac{\partial \varphi^{(e)}\left(x,y,t\right)}{\partial y}\right|_{y=h_0\left(1+\gamma_+\right)} = 0. \tag{3.3.23}$$

The continuity conditions of electromechanical fields considering surface roughness are satisfied on the rough surface $y = h_+\left(x\right)$:

$$w_+\left(x, h_+\left(x\right), t\right) = w_+^d\left(x, h_+\left(x\right), t\right), \quad \varphi_+\left(x, h_+\left(x\right), t\right) = \varphi_+^d\left(x, h_+\left(x\right), t\right), \tag{3.3.24}$$

$$\begin{aligned} h_+'\left(x\right)\cdot\sigma_{zx}^+\left(x, h_+\left(x\right), t\right) + \sigma_{zy}^+\left(x, h_+\left(x\right), t\right) &= h_+'\left(x\right)\cdot\sigma_{zx}^d\left(x, h_+\left(x\right), t\right) + \sigma_{zy}^d\left(x, h_+\left(x\right), t\right), \\ h_+'\left(x\right)\cdot D_x^+\left(x, h_+\left(x\right), t\right) + D_y^+\left(x, h_+\left(x\right), t\right) &= h_+'\left(x\right)\cdot D_x^d\left(x, h_+\left(x\right), t\right) + D_y^d\left(x, h_+\left(x\right), t\right), \end{aligned} \tag{3.3.25}$$

and on the virtually selected surface $y = h_0\left(1-\gamma_+\right)$ are satisfied the continuity conditions of electromechanical fields

$$\begin{aligned} w_0\left(x, h_0\left(1-\gamma_+\right), t\right) &= w_+\left(x, h_0\left(1-\gamma_+\right), t\right), \\ \varphi_0\left(x, h_0\left(1-\gamma_+\right), t\right) &= \varphi_+\left(x, h_0\left(1-\gamma_+\right), t\right), \end{aligned} \tag{3.3.26}$$

$$\begin{aligned} \sigma_{yz}^0\left(x, h_0\left(1-\gamma_+\right), t\right) &= \sigma_{yz}^+\left(x, h_0\left(1-\gamma_+\right), t\right), \\ D_y^0\left(x, h_0\left(1-\gamma_+\right), t\right) &= D_y^+\left(x, h_0\left(1-\gamma_+\right), t\right). \end{aligned} \tag{3.3.27}$$

It is shown from the introduced boundary conditions, that tangential components of the mechanical strain and induction of electric fields are participating in conditions (3.3.17) and (3.3.25) due to the rough surfaces $h_\mp\left(x\right)$ respectively. The tangential components of the mechanical strain and induction of electric fields have the following forms:

$$\begin{aligned} \sigma_{zx}^\pm\left(x,y,t\right) &= G_\pm\left(y\right)\frac{\partial w_\pm\left(x,y,t\right)}{\partial x} + e_\pm\left(y\right)\frac{\partial \varphi_\pm\left(x,y,t\right)}{\partial x}, \\ D_{zx}^\pm\left(x,y,t\right) &= e_\pm\left(y\right)\frac{\partial w_\pm\left(x,y,t\right)}{\partial x} - \varepsilon_\pm\left(y\right)\frac{\partial \varphi_\pm\left(x,y,t\right)}{\partial x}, \end{aligned} \tag{3.3.28}$$

$$\sigma_{zx}^{d}\left(x,y,t\right)=G_{+}^{d}\frac{\partial w_{+}^{d}\left(x,y,t\right)}{\partial x},\quad D_{x}^{d}\left(x,y,t\right)=-\varepsilon_{+}^{d}\frac{\partial \varphi_{+}^{d}\left(x,y,t\right)}{\partial x},\tag{3.3.29}$$

$$\sigma_{zx}^{c}\left(x,y,t\right)=G^{c}\frac{\partial w^{c}\left(x,y,t\right)}{\partial x}.\tag{3.3.30}$$

The potential and normal component of induction of the electric field in the vacuum half-space on the surface $y=h_0\left(1+\gamma_{+}\right)$ are involved in the boundary conditions (3.3.20) and (3.3.21) as well. The quasi-static potential of the electric field $\varphi^{(e)}\left(x,y,t\right)$ is determined from the equation

$$\nabla^2\varphi^{(e)}\left(x,y,t\right)=0.\tag{3.3.31}$$

Considering its decay at infinity $y\to\infty$, it will have the following form

$$\varphi^{(e)}\left(x,y,t\right)=E_0e^{-ky}e^{i(kx-\omega_0t)}.\tag{3.3.32}$$

Thus, the problem of wave process (localization of shear elastic waves in formed near-surface heterogeneous thin layers $\Omega_{-}=\Omega_{-}^{p}\cup\Omega_{-}^{c}$ and $\Omega_{+}=\Omega_{+}^{p}\cup\Omega_{d}$, delay of normal waves of certain frequencies, dynamic surface load, etc.) is reduced to the boundary-value problem for system of quasi-static equations (3.3.5)-(3.3.8), (3.3.10), (3.3.12), (3.3.13) and (3.3.31) with related electromechanical boundary conditions (3.3.15)-(3.3.30).

Problem Solution. The normal wave solution of the system of equations (3.3.5) and (3.3.6) in the base homogeneous piezoelectric layer Ω_0 at propagation of normal wave signal in the composite waveguide, is written in the following form

$$w_0\left(x,y,t\right)=\left[A_0e^{\alpha_0ky}+B_0e^{-\alpha_0ky}\right]e^{i(kx-\omega_0t)},\tag{3.3.33}$$

$$\varphi_0\left(x,y,t\right)=\left\{C_0e^{ky}+D_0e^{-ky}+\left(e_{15}/\varepsilon_{11}\right)\cdot\left[A_0e^{\alpha_0ky}+B_0e^{-\alpha_0ky}\right]\right\}e^{i(kx-\omega_0t)}.\tag{3.3.34}$$

Considering the thinness of the other four boundary layers and the complexity of the analytical solution of the electroelasticity equations in virtually cut heterogeneous layers Ω_{-}^{p} and Ω_{+}^{p}, through the thickness of each layer we introduce the hypotheses MELS [9, 10, 12] for distributions of elastic shear and potential of electric field.

The elastic shear and electric field potential in the virtually selected heterogeneous piezoelectric layer Ω_{+}^{p} we introduce in the following forms:

$$w_+(x,y,t)=f_+\left(kh_0;h_+(x)/h_0\right)\cdot\begin{bmatrix}w_+\left(x,h_+(x),t\right)-\\-w_0\left(x,h_0(1-\gamma_+),t\right)\end{bmatrix}+w_0\left(x,h_0(1-\gamma_+),t\right),\qquad(3.3.35)$$

$$\varphi_+(x,y,t)=f_+\left(kh_0;h_+(x)/h_0\right)\cdot\begin{bmatrix}\varphi_+\left(x,h_+(x),t\right)-\\-\varphi_0\left(x,h_0(1-\gamma_+),t\right)\end{bmatrix}+\varphi_0\left(x,h_0(1-\gamma_+),t\right).\qquad(3.3.36)$$

Here $f_+\left(kh_0;h_+(x)/h_0\right)=sh\left[\alpha_+k\left(y-h_0(1-\gamma_+)\right)\right]/sh\left[\alpha_+k\left(h_+(x)-h_0(1-\gamma_+)\right)\right]$ is the distribution function (or formation) of electromechanical field in heterogeneous piezoelectric layer, corresponding to the electroelasticity equations (3.3.7) and (3.3.8). Obviously, here the formation function $f_+\left(kh_0;h_+(x)\right)$ of the indefinite characteristics of the wave field is represented by the formation coefficient $\alpha_+(k)=\left[\left(\rho_+\omega_0^2/k^2G_+\right)-1\right]^{1/2}$ and by the variable thickness of the layer $h_+(x)-h_0(1-\gamma_+)$.

Similarly, the elastic shear and potential of electric field in the homogeneous dielectric layer Ω_+^d have the following form:

$$w_d(x,y,t)=f_d\left(kh_0;h_+(x)/h_0\right)\cdot\begin{bmatrix}w_d\left(x,h_0(1+\gamma_+),t\right)-\\-w_+\left(x,h_+(x),t\right)\end{bmatrix}+w_+\left(x,h_+(x),t\right),\qquad(3.3.37)$$

$$\varphi_d(x,y,t)=f_d\left(kh_0;h_+(x)/h_0\right)\cdot\begin{bmatrix}\varphi_d\left(x,h_0(1+\gamma_+),t\right)-\\-\varphi_+\left(x,h_+(x),t\right)\end{bmatrix}+\varphi_+\left(x,h_+(x),t\right),\qquad(3.3.38)$$

where the formation coefficient

$f_d\left(kh_0;h_+(x)/h_0\right)\square\ sh\left[\alpha_dk\left(y-h_+(x)\right)\right]/sh\left[\alpha_dk\left(h_0(1+\gamma_+)-h_+(x)\right)\right]$

in the homogeneous dielectric layer is presented by the parameters of the homogeneous layer $\alpha_d(k)\square\left[\left(\rho_d\omega_0^2/k^2G_d\right)-1\right]^{1/2}$ and $\zeta_d(x)$. In this case, the representations (3.3.37) and (3.3.38) automatically satisfy to the boundary conditions (3.3.24) and (3.3.26).

Similarly, the elastic shear and potential of electric field in the virtually selected heterogeneous piezoelectric layer Ω_-^p will be introduced in the following form:

$$w_-(x,y,t)=f_-\left(kh_0;h_+(x)/h_0\right)\cdot\begin{bmatrix}w_c\left(x,h_-(x),t\right)-\\-w_0\left(x,-h_0(1-\gamma_-),t\right)\end{bmatrix}+w_0\left(x,-h_0(1-\gamma_-),t\right),\quad(3.3.39)$$

$$\varphi_{-}(x,y,t)=\left\{1-f_{-}\left(kh_0;h_{+}(x)/h_0\right)\right\}\cdot\varphi_0\left(x,-h_0(1+\gamma_{-}),t\right), \tag{3.3.40}$$

where the formation function

$$f_{-}\left(kh_0;h_{+}(x)/h_0\right)=sh\left[\alpha_{-}k\left(y+h_0(1-\gamma_{-})\right)\right]/sh\left[\alpha_{-}k\left(h_{-}(x)+h_0(1-\gamma_{-})\right)\right]$$

in the inhomogeneous piezoelectric layer is represented by the new formation coefficient $\alpha_{-}(k)=\left[\left(\rho_{-}\omega_0^2/k^2G_{-}\right)-1\right]^{1/2}$ and variable thickness $\zeta_{-}(x)$ for the given layer.

The potential of the electric field is absent in the perfectly conducting layer Ω_{-}^{c}, and for elastic shear will have the following representation:

$$w_c(x,y,t)=f_c\left(kh_0;h_{+}(x)/h_0\right)\cdot\begin{bmatrix}w_c\left(x,-h_0(1+\gamma_{-}),t\right)-\\-w_{-}\left(x,h_{-}(x),t\right)\end{bmatrix}+w_{-}\left(x,h_{-}(x),t\right), \tag{3.3.41}$$

where the formation function

$$f_c\left(kh_0;h_{+}(x)/h_0\right)\square\ sh\left[\alpha_c k\left(y-h_{-}(x)\right)\right]/sh\left[\alpha_c k\left(-h_0(1+\gamma_{-})-h_{-}(x)\right)\right]$$

in the homogeneous perfectly conducting layer is represented by formation coefficient $\alpha_c(k)\square\left[\left(\rho_c\omega_0^2/k^2G_c\right)-1\right]^{1/2}$ and variable thickness $\zeta_c(x)$.

It is important to note that the boundary conditions (3.3.16), (3.3.18), (3.3.21), (3.3.24) and (3.3.26) for elastic shear and electric field potential are automatically satisfied by the selection of formation functions $f_d\left(kh_0;h_{+}(x)/h_0\right)$, $f_{+}\left(kh_0;h_{+}(x)/h_0\right)$, $f_{-}\left(kh_0;h_{+}(x)/h_0\right)$, $f_c\left(kh_0;h_{+}(x)/h_0\right)$ and formation coefficients $\alpha_d=\left[\left(\rho_d\omega_0^2/k^2G_d\right)-1\right]^{1/2}$ for the dielectric layer, $\alpha_c=\left[\left(\rho_c\omega_0^2/k^2G_c\right)-1\right]^{1/2}$ for conductor the layer and $\alpha_{\pm}=\left[\left(\rho_{\pm}\omega_0^2/k^2G_{\pm}\right)-1\right]^{1/2}$ for the virtually selected inhomogeneous piezoelectric layers in hypothetical representations (3.3.35)-(3.3.41).

In addition, the characteristic formation coefficients for each layer are involved in the distribution representations, as well as electromechanical field values on surfaces of adjacent layers are involved.

We receive all elastic shear and electric field potential values on the smooth and rough surfaces $y=h_0\pm\gamma_{+}$, $y=-h_0\pm\gamma_{-}$, $y=h_{\pm}(x)$ expressed by arbitrary amplitude constants

$\{A_0, B_0, C_0, D_0, E_0\}$ of piezoelectric waveguide and vacuum half-space, satisfying the boundary conditions (3.3.15), (3.3.19), (3.3.22) and (3.3.27) on smooth surfaces $y = h_0 \pm \gamma_+$ and $y = -h_0 \pm \gamma_-$.

The representations for elastic shear and potential of the electric field, using the obtained surface values of distributions (3.3.35)-(3.3.41) for elastic shear and potential of the electric field can be written in the expanded form:

$$w_c(x,y) = w_-\left(x, h_-(x)\right) = \left[\begin{array}{l} A_0 \exp\left[-\alpha_0 k h_0 (1-\gamma_-)\right] \cdot \left\{\begin{array}{l} 1+\chi_0^2 \alpha_0 k + \\ +(\alpha_0/\alpha_-)\xi_-(x,k)\cdot(1+\chi_0^2)\end{array}\right\} + \\ +B_0 \exp\left[\alpha_0 k h_0 (1-\gamma_-)\right] \cdot \left\{\begin{array}{l} 1-\chi_0^2 \alpha_0 k - \\ -(\alpha_0/\alpha_-)\xi_-(x,k)\cdot(1+\chi_0^2)\end{array}\right\} + \\ + \left\{\begin{array}{l} C_0 \exp\left[-k h_0 (1-\gamma_-)\right] - \\ -D_0 \exp\left[k h_0 (1-\gamma_-)\right]\end{array}\right\} \cdot \chi_0^2 \alpha_-^{-1} \cdot \left(\xi_-(x,k) + k\alpha_-\right) \end{array}\right], \quad (3.3.42)$$

$$w_-(x,y) = \left\{\begin{array}{l} A_0 \exp\left[-\alpha_0 h_0 (1-\gamma_-)\right] + B_0 \exp\left[\alpha_0 h_0 (1-\gamma_-)\right] + sh\left[\alpha_- k \left(y + h_0(1-\gamma_-)\right)\right] \times \\ \times \left\{\begin{array}{l} \left[A_0 \exp\left[-\alpha_0 k h_0 (1-\gamma_-)\right] - B_0 \exp\left[\alpha_0 k h_0 (1-\gamma_-)\right]\right] \times \\ \times (\alpha_0/\alpha_-)\cdot\left[1+\chi_0^2 \xi_-(x,k)\cdot\left(\xi_-(x,k)+k\alpha_-\right)\right] + \\ +\left[C_0 \exp\left[-k h_0 (1-\gamma_-)\right] - D_0 \exp\left[k h_0 (1-\gamma_-)\right]\right]\cdot \chi_0^2 \left(\alpha_-^{-1} + k\xi_-^{-1}(x,k)\right) \end{array}\right\} \end{array}\right\}, \quad (3.3.43)$$

$$\varphi_-(x,y) = \left\{1 - \xi_-^{-1}(x,k)\cdot sh\left[\alpha_- k\left(y + h_0(1-\gamma_-)\right)\right]\right\} \times$$
$$\times \left\{\begin{array}{l} C_0 \exp\left[-k h_0 (1-\gamma_-)\right] + D_0 \exp\left[k h_0 (1-\gamma_-)\right] + \\ +(e_0/\varepsilon_0)\cdot\left[A_0 \exp\left[-\alpha_0 k h_0 (1-\gamma_-)\right] + B_0 \exp\left[\alpha_0 k h_0 (1-\gamma_-)\right]\right] \end{array}\right\}, \quad (3.3.44)$$

$$\varphi_+(x,y)=$$

$$=\left[\begin{array}{l}\left(e_0/\varepsilon_0\right)\left[\begin{array}{l}A_0\exp\left[\alpha_0 kh_0\left(1-\gamma_+\right)\right]+\\B_0\exp\left[-\alpha_0 kh_0\left(1-\gamma_+\right)\right]\end{array}\right]+\left[\begin{array}{l}C_0\exp\left[kh_0\left(1-\gamma_+\right)\right]+\\+D_0\exp\left[-kh_0\left(1-\gamma_+\right)\right]\end{array}\right]+\\+\dfrac{sh\left[\alpha_+ k\left(y-h_0\left(1-\gamma_+\right)\right)\right]}{\alpha_+}\cdot\left[\begin{array}{l}\left(e_0/\varepsilon_0\right)\cdot\alpha_0\times\\\times\left[\begin{array}{l}A_0\exp\left[\alpha_0 kh_0\left(1-\gamma_+\right)\right]-\\-B_0\exp\left[-\alpha_0 kh_0\left(1-\gamma_+\right)\right]\end{array}\right]+\\+\left[\begin{array}{l}C_0\exp\left[kh_0\left(1-\gamma_+\right)\right]-\\-D_0\exp\left[-kh_0\left(1-\gamma_+\right)\right]\end{array}\right]\end{array}\right]\end{array}\right], \tag{3.3.45}$$

$$w_+(x,y)=$$

$$=\left[\begin{array}{l}\left[A_0\exp\left[\alpha_0 kh_0\left(1-\gamma_+\right)\right]+B_0\exp\left[-\alpha_0 kh_0\left(1-\gamma_+\right)\right]\right]+\\+\left(\alpha_0/\alpha_+\right)sh\left[\alpha_+ k\left(y-h_0\left(1-\gamma_+\right)\right)\right]\left[\begin{array}{l}A_0\exp\left[\alpha_0 kh_0\left(1-\gamma_+\right)\right]-\\-B_0\exp\left[-\alpha_0 kh_0\left(1-\gamma_+\right)\right]\end{array}\right]\end{array}\right], \tag{3.3.46}$$

$$w_d(x,y)=w_+(x,h_+(x))=$$

$$=\left[\begin{array}{l}\left[\begin{array}{l}A_0\exp\left[\alpha_0 kh_0\left(1-\gamma_+\right)\right]+\\+B_0\exp\left[-\alpha_0 kh_0\left(1-\gamma_+\right)\right]\end{array}\right]+\\+\left(\alpha_0/\alpha_+\right)\cdot\xi_+(x,k)\left[\begin{array}{l}A_0\exp\left[\alpha_0 kh_0\left(1-\gamma_+\right)\right]-\\-B_0\exp\left[-\alpha_0 kh_0\left(1-\gamma_+\right)\right]\end{array}\right]\end{array}\right], \tag{3.3.47}$$

$$\varphi_d(x,y)=$$

$$=\left\{\begin{array}{l} f_d\left(kh_0,h_+(x/h)\right)\cdot E_0 e^{-kh_0(1+\gamma_+)}+\left[1-f_d\left(kh_0,h_+(x/h)\right)\right]\times \\ \times\left[\begin{array}{l}(e_0/\varepsilon_0)\cdot\left[A_0\exp\left[\alpha_0 kh_0(1-\gamma_+)\right]+B_0\exp\left[-\alpha_0 kh_0(1-\gamma_+)\right]\right]+ \\ +C_0\exp\left[kh_0(1-\gamma_+)\right]+D_0\exp\left[-kh_0(1-\gamma_+)\right]+ \\ +(e_0/\varepsilon_0)\cdot(\alpha_0/\alpha_+)\cdot\xi_+(x,k)\cdot\left\{\begin{array}{l}A_0\exp\left[\alpha_0 kh_0(1-\gamma_+)\right]- \\ -B_0\exp\left[-\alpha_0 kh_0(1-\gamma_+)\right]\end{array}\right\}+ \\ +\alpha_+^{-1}\cdot\xi_+(x,k)\cdot\left[C_0\exp\left[kh_0(1-\gamma_+)\right]-D_0\exp\left[-kh_0(1-\gamma_+)\right]\right]\end{array}\right]\end{array}\right\}. \qquad (3.3.48)$$

Here $\xi_\pm(x,k)=sh\left[\alpha_\pm k\left(h_\pm(x)+h_0(1-\gamma_\pm)\right)\right]$ characterize the near-surface distributions in the formed heterogeneous layers Ω_+^p and Ω_-^p, respectively.

The introduced distributions of wave the field (3.3.42)-(3.3.48) allow to build the picture of distribution over the thickness of the composite waveguide, by substituting the wave number $k\left(h_\pm(x)/h_0;\gamma_\pm;\omega_0\right)$, determined from the dispersion equation.

We obtain a system of five homogeneous algebraic equations related to the amplitude constants $\{A_0,B_0,C_0,D_0,E_0\}$, satisfying the boundary conditions (3.3.17), (3.3.20), (3.3.23) and (3.3.25). The dispersion equation of the formed wave field is obtained from the condition of existence of nontrivial solutions in the following form:

$$g_{35}\left(\alpha_d;\varepsilon^{(e)}/\varepsilon^d;\mathrm{h}_+(x);kh_0\right)\times\det\left\|g_{ij}\left(G_k;\rho_k;e_k;\varepsilon_k;h_\pm(x);\omega_0;k(x,\omega_0)\right)\right\|_{4\times4}=0, \qquad (3.3.49)$$

where the variable coefficients $\left\{g_{ij}\left(G_k;\rho_k;e_k;\varepsilon_k;h_\pm(x);\omega_0;k(x,\omega_0)\right)\right\}_{4\times4}$ (tensor) of dispersion equation is too bulky and for that reason it is not shown here (see [17]). The coefficients of the fifth column of the tensor equal to zero $g_{15}=g_{25}=g_{45}=g_{55}=0$, and g_{35} is positively definite, i.e. $g_{35}\left(\alpha_d;\varepsilon^{(e)}/\varepsilon^d;h_+(x);kh_0\right)\geq0$ and characterizes oscillations of the electric field in vacuum.

Obviously this is due to the presence of expressions $h'_\pm(x)\sigma_{zx}^\pm\left(x,h_+(x),t\right)$ and $h'_\pm(x)D_x^\pm\left(x,h_+(x),t\right)$ in boundary conditions (3.3.17) and (3.3.25). However, for the selected formation functions $f_d\left(kh_0;h_+(x)/h_0\right)$, $f_+\left(kh_0;h_+(x)/h_0\right)$, $f_-\left(kh_0;h_+(x)/h_0\right)$

and $f_c\left(kh_0; h_+(x)/h_0\right)$, the imaginary part of the dispersion equation is satisfied automatically.

It is easy to see from the coefficient relations in Appendix 1, that the amplitude distribution and frequency of the wave field over the waveguide depend on as physico-mechanical constants of boundary materials, as well as characteristic linear dimensions of the surface not-smoothness of the composite waveguide.

The study on the propagation of high-frequency (shortwave $kh_0 \gg 1$) wave signal in waveguides with rough surfaces, in fact, are due to the fact that the linear dimensions of these roughness are small compared to the thickness of the base layer $\gamma_\pm = \sqrt{\varepsilon_\pm^2 + \delta_\pm^2} \gg 1$.

Frequency characteristics of propagating wave. The dispersion equation (3.3.49) certainly does not have an explicit analytical solution. However, in obvious limiting cases there is the short-wave approximation, i.e. $kh_0 \gg 1$, and long-wave approximation, i.e. $kh_0 \ll 1$. As it was mentioned above, as a result of $kh_0 \ll 1$, in the second case, the normal propagating wave signal does not interact with the surface non-smoothness.

In the case of propagation of short-wave (high frequency) electroelastic signal, the presence of surface geometrical inhomogeneity leads to the wave number dependence on the coordinates of distribution, i.e. $k = k(x)$.

In the problem of propagation of plane electroelastic shear wave signal in homogeneous piezoelectric waveguide with non-smooth surfaces, when one non-smooth surface of the waveguide is filled with perfect conductor and the other with dielectric, the investigation of frequency picture gives interesting results.

Calculations show that at low frequency (long-wave) signals, up to some wave length k_{0n}, which is determined by the physico-mechanical material constant of adjacent materials, geometric relations of linear dimensions of Ω_0 and the surface non-smoothness, the dependence of the wave number $k(x)$ for normal waves with harmonic mode oscillations $\sin\left[\alpha_0 k\left(y - h_\pm(x)\right)\right]$ are almost identical to the dependence $k(x)$ of section 3.1.

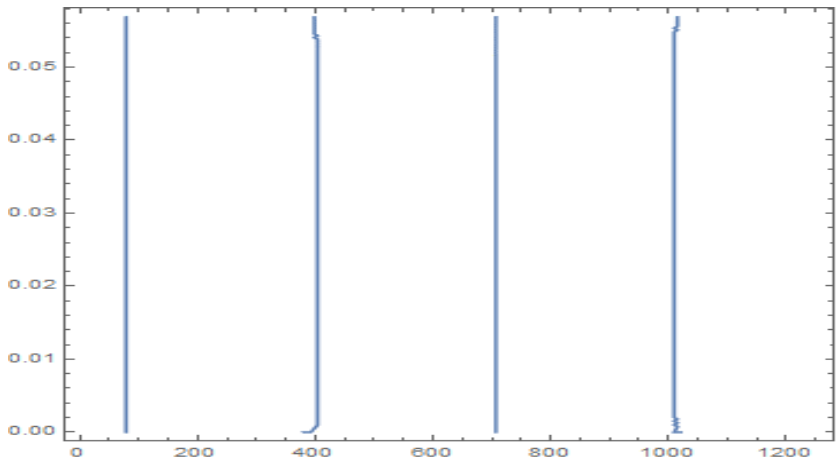

Fig. 3.3.2 Dependence of the wave number $k(x)$ on x coordinate at fixed source frequency $\omega_0 = 100\,\text{Hz}$

This means, that low-frequency electroelastic wave signal does not "feel" the presence of the surface weak non-smoothness and the very thin layers on the surfaces of the waveguide layer. The dispersion surface of normals and the dependence of the wave number for waves with non-harmonic distributions $sh\left[\alpha_0 k\left(y - h_{\pm}(x)\right)\right]$ are shown in Fig. 3.3.3 and Fig. 3.3.4, from where it is obvious that the dispersion surface at high frequency (shortwave) signal varies strongly.

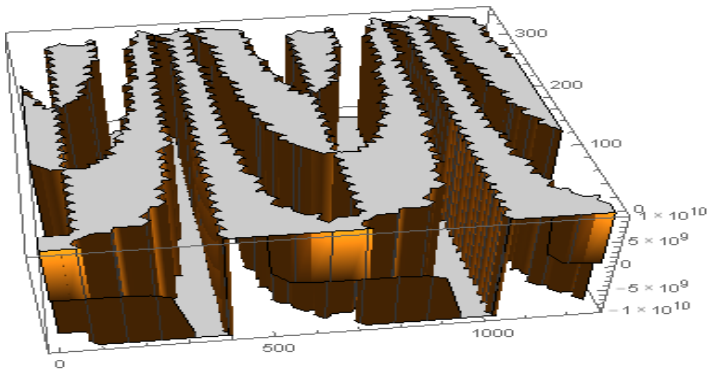

Fig. 3.3.3 Dispersion surface for wave with distribution functions $sh\left[\alpha_0 k\left(y - h_{\pm}(x)\right)\right]$, where the wave number $k = k(x)$

Here, as in the previous case, the high frequencies lead to weak quantitative change of the second wave with wave number k_{02}. This is clearly seen from Figs. 3.3.3 and 3.3.4. Quite interesting transformation occurs with low-frequency form, with the corresponding wave number k_{01}. At already relatively short wave signals $k_{01} \square 25$ (for $\lambda_{01} \square 0.25\text{mm}$), the

wave number $k_{11}(x)$ strongly changes direction, opening space for the emergence of new wave mode (Fig. 3.3.4).

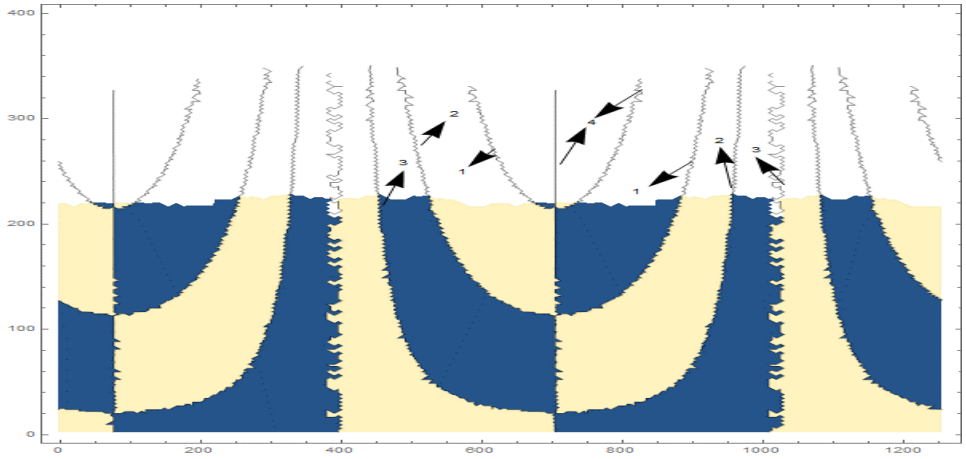

Fig. 3.3.4 Dependence of the wave number $k = k(x)$ on x coordinate at fixed source frequency $\omega_0 = 100$ Hz

The wave number $k_{21}(x)$ of the newly emerged mode first decreases, making leap on vertical line $x_{01} = const$, and then increases to the existence limit of high frequency oscillations.

According to the same scheme, two high-frequency wave modes (Fig. 3.3.4) with variable wave numbers $k_{31}(x)$ and $k_{41}(x)$ occur there. It is interesting, that the existance limit of these ultrashort waves is the same, i.e. $k_{n1} \le 350$.

It follows from Figs. 3.3.4 and 3.3.4, that at higher frequencies of the wave signal occurs branching of first low-frequency harmonic (Fig. 3.3.2) on four waves with different wave lengths $\lambda_{n1}(x) = 2\pi / k_{n1}(x)$ respectively. So, it means that the function $k_{n1}(x)$ has multiple branches which are not intersecting. On some points the branches are becoming very closer to each other which is shown on figs. 3.3.5 and 3.3.6.

Different orientations of the closing curves describing the wave numbers, implies that there is fuss of new mode due to the surface roughness of the waveguide (Fig. 3.1.3 of section 3.1), which is dissected on the newly formed wave modes $k_{21}(x)$, $k_{31}(x)$ and $k_{41}(x)$ under wave interaction of the first main mode (Fig. 3.3.4).

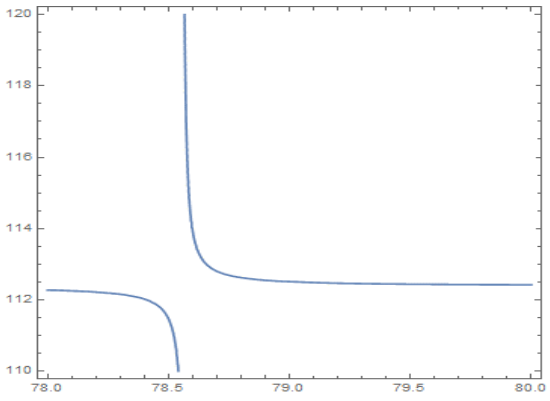

Fig. 3.3.5 Curves for the wave number functions $k_{21}(x)$ and $k_{11}(x)$

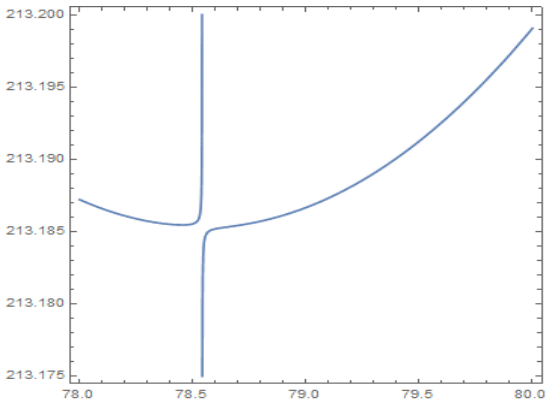

Fig. 3.3.6 Curves for the wave number functions $k_{41}(x)$ and $k_{11}(x)$

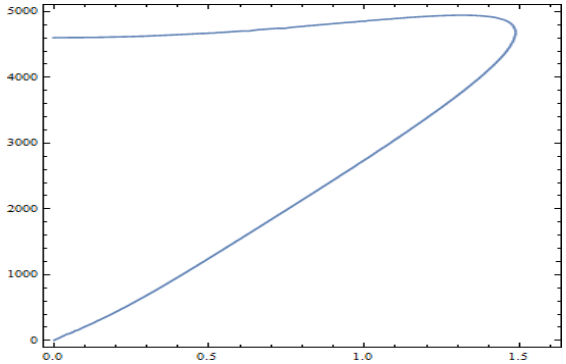

Fig. 3.3.7 Dependence of fast, long wave frequency $\omega(k)$ from wave number, when $k \in [0;1.6]$

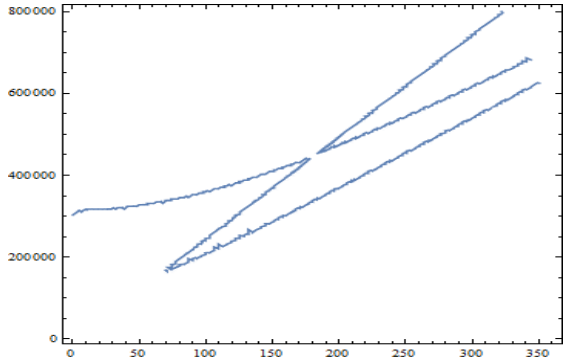

Fig. 3.3.8 Dependence of fast, short wave frequency $\omega(k)$ from wave number, when $k \in [1.6;350]$

Such branching, of course, is a consequence of the wave signal dissipation on the surface roughness and scattering of the wave energy along selected layers of the waveguide. It also follows from Fig. 3.3.4, that the branching of the wave number indicates the branching at different changing wave lengths $\lambda_{n1}(x) = 2\pi / k_{n1}(x)$. This leads to the appearance of new wave modes with different dispersions.

For fast waves when the phase speed is greater than the values of the shear body waves in the adjacent materials, $V_{\phi}(k;\omega) \geq c_{nt}$, the dispersion of long waves when $k \in [0;1.6]$ happens in the interval $\omega(k) \in [0;5000]$ (Fig. 3.3.7) and is close to the value $\omega_{01}(k) \approx 316000$ (Fig. 3.3.4).

Fig. 3.3.8 shows, that the second frequency is induced at a certain value of the wavelength. Also, for the fast short wave the frequency is very large

$\omega(k) \in \left[17 \times 10^4; 8 \times 10^5\right]$. It is necessary to pay attention to the fact, that starting from some value of the wave length, a wave with a specific length can be propagated with three different frequencies.

In the case of slow wave signals, when the phase velocity is less than the values of the shear body waves in the adjacent materials $V_\phi(k;\omega) < c_{nt}$, receive an interesting phase picture (Fig. 3.3.9 and Fig. 3.3.10).

It is seen from Fig. 3.3.9, that in contrast to fast long waves (Fig. 3.3.7), where to each wavelength corresponds two frequency values, in this case to each frequency value correspond two wave modes with different wavelengths. In this case the interval $\lambda \in \left[2\pi/1.6; 2\pi/0.5\right]$ is larger than in the case of faster and longer waves.

For slow and short waves, when $\lambda \in \left(\pi/175; \pi/90\right]$, to each wave length correspond two frequencies, and in the interval $\lambda \in \left(\pi/90; \pi/30\right]$ to each wave length correspond three oscillation frequencies. In the case of slow waves it is noteworthy that there is a frequency zone of silence. For waves of the length $\lambda \in \left[\pi/30; 2\pi/0.5\right]$, frequencies does not exist.

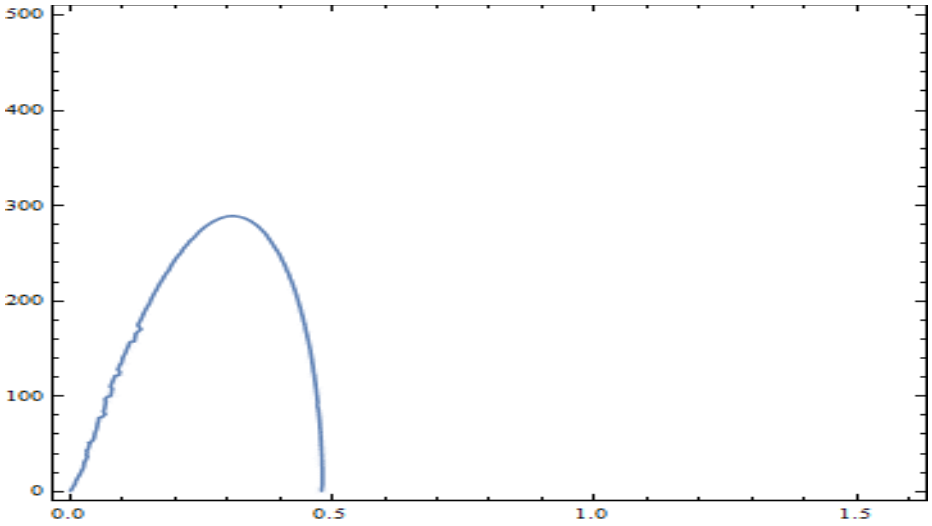

Fig. 3.3.9 Dependence of slow, long wave frequency $\omega(k)$ from wave number, when $k \in [0; 0.5]$

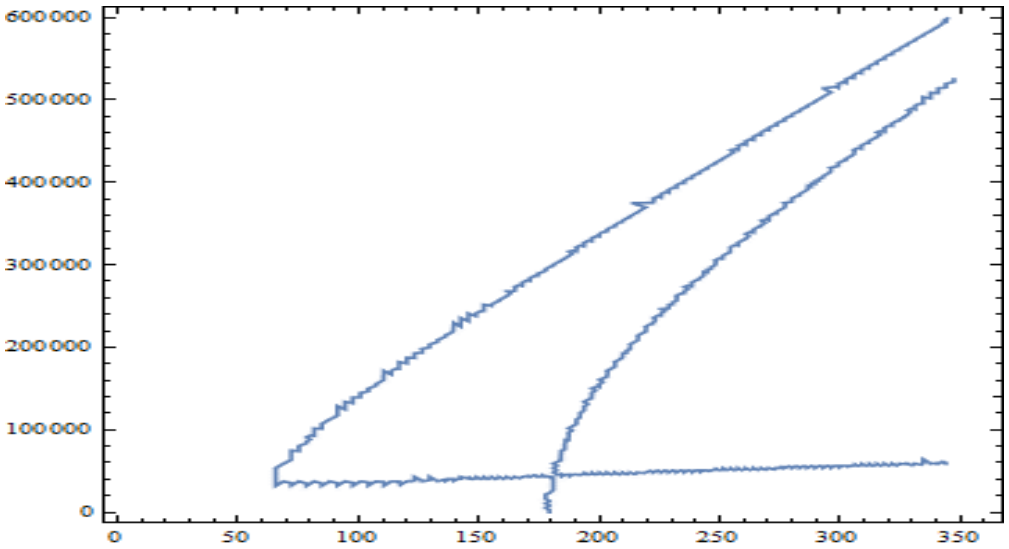

Fig. 3.3.10 Dependence of slow, short wave frequency $\omega(k)$ from wave number, when $k \in [60;350]$

Comparing obtained results by frequencies, it is easy to see that, if long waves are propagating in the range of relatively low frequencies, $\omega_{s,l} \in [0;300]$ and $\omega_{q,l} \in [0;5000]$, then short waves are propagating in the range of very high frequencies $\omega_{s,l} \in [170000;800000]$ and $\omega_{q,l} \in [0;600000]$.

Amplitude distribution at propagation of wave signal. The distribution of wave field characteristics (3.3.42)-(3.3.48) allow to reduce that, in the thin surface layers of conductor and dielectric, elastic shears equal to the surface shears of virtually selected layers from the base layer's $w_c(x,y,t) = w_-(x,h_-(x),t)$ and $w_d(x,y,t) = w_+(x,h_+(x),t)$ respectively.

It is also clear, that in all relations, the main dominant is the wave signal (3.3.33) and (3.3.34), and the components due to the interaction of the wave signal with surface roughness, appear in the form $\xi_n^{-1}(x,k)\cdot sh\left[\alpha_n k\left(y+h_0(1-\gamma_n)\right)\right]$ and $(\alpha_0/\alpha_n)\cdot sh\left[\alpha_n k\left(y-h_0(1-\gamma_n)\right)\right]$. These components at any wavelength can not cause internal resonance, since at values $\alpha_n(x)\cdot k(x)\to 0$ they do not go to infinity.

Relations (3.3.42)-(3.3.48) also show, that due to the summation of the surface values and the effect of the interaction of the wave signal with surface roughness, amplitude distributions of slow and fast, short waves (at high-frequency oscillations $\omega(k) \square 10^5$) have maximal values in the formed near-surface inhomogeneous thin layers $\Omega_- = \Omega_-^p \cup \Omega_-^c$ and

$\Omega_+ = \Omega_+^p \cup \Omega^d$ (Fig. 3.3.1). This corresponds to the case when the length of the propagating wave signal is comparable with the linear characteristics of the surface roughness $\lambda \square \gamma_\pm$.

Then using the relations (3.3.42) and (3.3.43), the elastic shear in the geometrically and physically heterogeneous near-surface layer $\Omega_- = \Omega_-^p \cup \Omega_-^c$ will be represented in the form

$$w_{-c}(x,y) = \begin{cases} w_c(x,y) & in \quad y \in \left[-h_0(1+\gamma_-);\ h_-(x)\right] \\ w_-\left(x, h_-(x)\right) & in \quad y \in \left[h_-(x);\ -h_0(1-\gamma_-)\right] \end{cases} \tag{3.3.50}$$

From the other hand, the elastic shear in the geometrically and physically heterogeneous surface layer $\Omega_+ = \Omega_+^p \cup \Omega^d$ will be presented in the form

$$w_{+d}(x,y) = \begin{cases} w_+(x,y) & in \quad y \in \left[h_0(1-\gamma_+);\ h_+(x)\right], \\ w_d\left(x, h_+(x)\right) & in \quad y \in \left[h_+(x);\ h_0(1+\gamma_+)\right]. \end{cases} \tag{3.3.51}$$

CONCLUSION

The thesis is devoted to investigation of wave processes in waveguides with material and geometric inhomogeneities. Among others, the following important results are obtained:

- The influence of the longitudinal, weak inhomogeneity on propagation of normal shear wave signal in elastic waveguide is studied in the case of mechanically free or clamped boundary conditions.
- It is shown, that in the case of clamped smooth surfaces, asymmetric localization of wave energy occurs in a neighborhood of the middle surface of isotropic elastic layer, while in the case of mechanically free smooth surfaces, the localization is symmetric.
- The weak inhomogeneity of the mechanically free surfaces leads to distortion of propagating normal wave in virtually cut thin layers of variable thickness of the near-surface zones of the waveguide. Frequency zones of transmission and zones of prohibited frequencies of formed wave appear.
- The influence of mechanically free, geometrically weak inhomogeneous surfaces on the propagation of shear normal wave in elastic waveguide is investigated.
- It is shown, that weak surface inhomogeneities lead to instability of propagating normal wave signal in waveguide.
- Partial localization of wave energy occurs in selected near-surface layers of the waveguide, frequency zones of silence (as well as frequency zones of bandwidth) appear for newly formed waves.
- The efficacy of usage of virtual cross sections method and MELS hypotheses is shown on model problem about distribution of wave field in thin surface layers of waveguide when plane wave signal is propagating in it.
- The impact of surface non-smoothness on characteristics of propagation of high-frequency horizontally polarized wave signal in isotropic elastic half-space is studied.
- It is shown, that the weak non-smoothness leads to strong distortion of the wave signal over the waveguide thickness, and along wave signal propagation direction as well.

- Localization of horizontally polarized shear (SH) shortwave (high frequency) signals occurs in the near-surface zone of variable thickness. The presence of surface weak inhomogeneity leads to prohibition of wave of certain lengths depending on the linear characteristics of the inhomogeneity parameters.
- The use of virtual sections and MELS hypotheses, unlike the direct solution, allows to identify near-surface wave effects: effective dynamic load, internal resonance, frequency prohibition, etc.
- Surface heterogeneities of homogeneous elastic waveguide convert plane wave signal into non-attenuated oscillatory motion and distort the plane front of the signal.
- At the wave signal lengths, comparable with the characteristic dimensions of the non-smooth surface of the waveguide, due to the presence of surface heterogeneities, oscillations occur in the near-surface layer, which in the case of certain wave signal lengths can cause internal resonance.
- The propagation of high-frequency electroelastic wave signal in composite waveguide of homogeneous piezoelectric layer with rough surfaces filled with perfect conductor and perfect dielectric materials respectively is studied.
- The influence of surface roughness and surface smoothing by different materials (the effect of different physical-mechanical boundary conditions) on the propagation of high frequency electroelastic wave signal is discussed.
- The behaviors of wave amplitude and frequency characteristics are numerically investigated in the composite waveguide at the propagation of normal wave signal.
- It is shown, that the filling of the surface roughness with different materials, leads to the appearance of up to four wave modes, depending on the length of the wave signal. It turns out, that if the surface roughness of the piezoelectric layer is not filled, only one shortwave mode occurs.

REFERENCES

[1] Achenbach, J.D., Wave Propagation in Elastic Solids, New York, Elsevier, 1984, p. 364

[2] Hambardzumyan S.A., Theory of anisotropic plates, (2nd ed.), Moscow: Nauka, 1987, 360 p. (In Russian)

[3] Hambardzumyan S.A., Baghdasaryan G.E., Belubekyan M.V., Magnetoelasticity of thin plates and shells, Nauka, 1977, 324 p. (In Russian)

[4] Apostol B.F., The Effect of Surface Inhomogeneities on the Propagation of Elastic Waves, Journal of Elasticity, 2014, Vol. 114, issue 1, pp. 85-99

[5] Auld B.A., Acoustic Fields and Waves in Solids, Krieger publishing company malabar, Florida, 1990, Vol. 2, Second Edition, p. 421

[6] Avetisyan A.S., About the problem of the propagation of transversal waves in piezoelectric, Proc. of NAS Armenia, ser. Mechanics, 1985, Vol. 38, issue 1, pp. 12-19 (In Russian)

[7] Avetisyan A.S., Love's electro elastic surface waves in case of inhomogeneous piezoelectric layer, Proc. of NAS Armenia, ser. Mechanics, 1987, Vol. 40, issue 1, pp. 24-29 (In Russian)

[8] Avetisyan A.S., About propogation of electroelastic monochromatic wave in nonhomogeneous piezoelectic, Proc. of NAS Armenia, ser. Mechanics, 1988, Vol. 41, issue 5, pp. 34-40 (In Russian)

[9] Avetisyan A.S., On the formulation of the electro-elasticity theory boundary value problems for electro-magneto-elastic composites with interface roughness. Proc. of NAS Armenia, ser. Mechanics, 2015, Vol. 68, issue 2, pp. 29-42

[10] Avetisyan A.S., The boundary problem modelling of rough surfaces continuous media with coupled physico mechanical fields, Reports of NAS of Armenia, 2015, Vol. 115, issue 2, pp. 119-131

[11] Avetisyan A.S., Belubekyan M.V., Ghazaryan K.B., Magneto-electro- thermo-elastic hypotheses for contact problems of composite waveguides, The

International Conference «Modern problems of thermomechanics», 22-25 September, 2016, Lvov, Ukraine, Collection of scientific papers, pp. 142-144

[12] Avetisyan A.S., Hunanyan A.A., The efficiency of application of virtual cross-sections method and hypotheses MELS in problems of wave signal propagation in elastic waveguides with rough surfaces, Journal of Advances in Physics, (2016), Vol. 11, issue 6, pp. 3564-3574

[13] Avetisyan A.S., Hunanyan A.A., Amplitude-phase distortion of the normal high-frequency shear waves in homogeneous elastic waveguide with weakly rough surfaces, Proc. of NAS Armenia. Mechanics, 2017, Vol. 70, issue 2, pp. 28-42

[14] Avetisyan A.S., Kamalyan A.A., On Propagation of Electroelastic Shear Wave in 6mm Class Piezodielectric Inhomogeneous Layer, Reports of NAS of Armenia, 2014, Vol. 114, issue 2, pp.108-115 (In Russian)

[15] Avetisyan A.S., Kamalyan A.A., The Influence of Cross Inhomogeneity of Piezoelectric Layer and Combinations of Boundary Conditions on the Shear Electroelastic Signal Propagation, Proceedings of State Engineering University of Armenia, ser. Mechanics, Machine Science, Machine-Building, 2014, Vol. 17, issue 1, pp. 9-25 (In Russian)

[16] Avetisyan A.S., Kamalyan A.A., Hunanyan A.A., The propagation of plane wave signal in piezodielectric waveguide with boundary of geometric and physical inhomogeneities, IV International Conference, Topical Problems of Continium Mechanics, 21–26 September, 2015 Tsakhkadzor, Armenia, pp. 5-9 (In Russian)

[17] Avetisyan A.S., Kamalyan A.A., Hunanyan A.A., Features of localization of wave energy at rough surfaces of piezodielectric waveguide, Proc. of NAS Armenia, ser. Mechanics, 2017, Vol. 70, issue 1, pp. 40-63

[18] Avetisyan A.S., Sarkisyan S.V., About electromagnetoelastic vibrations and waves propagation in nonhomogeneous media, Mechanical Modelling of New Electromagnetic Materials, Stockholm, 1990, pp. 387-393

[19] Bakirtas I. et Maugin G.A., 5 Wave Propagation in Inhomogeneous Media, Elsevier, International Geophysics, 1972, Vol. 17, pp. 223-307

[20] Banerjee S., Kundu T., Elastic wave propagation in sinusoidally corrugated waveguides, J. Acoust. Soc. Am, 2006, Vol. 119, issue 4, pp. 2006–2017

[21] Aghalovyan L.A., Asimptotic Theory of Anisotropic Plates and Shells, World Scientific Publishing, Singapore London, 2015, 376p.

[22] Belubekjan M.V., Belubekjan V.M., About shear localized wave propagation along the moving surfaces of piezoelectrics, Proc. of NAS Armenia, ser. Mechanics, 1994, Vol. 47, issues 3-4, pp.78-89 (In Russian)

[23] Belubekian M.V., Mukhsikhachoyan A.R., On the shear "standing" surface wave existence along a corrugated surface, Reports NAS RA, 1992, Vol. 93, issue 2, pp. 63-67 (In Russian)

[24] Belubekyan M.V., Mukhsikhachoyan A.R., Shear surface waves in weakly inhomogeneous elastic media, Acoustic Journal, 1996, Vol. 42, issue 2, pp. 179-182 (In Russian)

[25] Belubekyan M.V., Sahakyan S.L., Hunanyan A.A., Shear waves in longitudinal periodical weak-inhomogeneous layer, Proc. of YSU (Physical and Mathematical Sciences), 2015, issue 1, pp. 36-40

[26] Benhmammouch O., Vaitilingom L., Khenchaf A., and Caouren N., Electromagnetic Waves Propagation above Rough Surface: Application to Natural Surfaces, Piers Online, 2008, Vol. 4, issue 7, pp. 775-780

[27] Biryukov, S.V., Gulyaev, Y.V., Krylov, V., Plessky, V., Surface acoustic waves in inhomogeneous media, Springer Series on Wave Phenomena, 1995, Vol. 20, 388 p.

[28] Bluestein J. L., A New Surface Wave in Piezoelectric materials, Appl. Phys. Lett. 1968, Vol. 13, issue 12, pp. 412-413

[29] Brekhovskikh L.M., Godin O., Acoustics of Layered Media I: Plane and Quasi-Plane Waves, Springer Berlin Heidelberg, 1998, 240 p.

[30] Brekhovskikh L.M., Waves in Layered Media 2e, Applied mathematics and mechanics, Elsevier Science, 2012, Vol. 16, 520 p.

[31] Brevdo L., Wave Packets, Signaling and Resonances in a Homogeneous Waveguide, Journal of Elasticity, 1997, Vol. 49, issue 3, pp. 201–237

[32] Castaings M., SH ultrasonic guided waves for the evaluation of interfacial adhesion, Ultrasonics, 2014, Vol. 54, issue 7, pp. 1760–1775

[33] Carbone G., Scaraggi M., Tartaglino U., Adhesive contact of rough surfaces: comparison between numerical calculations and analytical theories, Eur. Phys. J E Soft Matter., 2009, Vol. 30, issue 1, pp. 65-74

[34] Charnotskii M., Propagation of polarized waves in inhomogeneous media, Journal of the Optical Society of America A, 2016, Vol. 33, issue 7, pp. 1385-1394

[35] Cheng N.C., Sun C.T., Wave propagation in two layered piezoelectric plates. - J. Acoust. Soc. Amer., 1975, Vol. 57, issue 3, pp. 632-639

[36] Chimenti D.E., Lobkis O.I., The effect of rough surfaces on guided waves in plates, Ultrasonics, 1998, Vol. 36, issue 1-5, pp. 155–162

[37] Cocheril Y. and Vauzelle R., A new ray-tracing based wave propagation model including rough surfaces scattering, Progress In Electromagnetics Research, 2007, Vol. 75, pp. 357-381

[38] Curtis R.G., Redwood M., Transvers surface waves on a piezoelectric materials currying a metal layer of finite thickness, J. Appl. Phys., 1973, Vol. 44, issue 5, pp. 2002-2007

[39] Danoyan Z.N., Piliposian G.T., Surface electro-elastic Love waves in a layered structure with a piezoelectric substrate and a dielectric layer, Int. J. Solid and Structures, 2007, Vol. 44, pp. 5829-5847

[40] Didenkulova I., Pelinovsky E., Soomere T., Exact travelling wave solutions in strongly inhomogeneous media, Estonian Journal of Engineering, 2008, Vol. 14, issue 3, pp. 220-231

[41] Dmitrieva I.Yu., Mathematical modeling of electromagnetic wave propagation in inhomogeneous medium, Electronics and Nanotechnology (ELNANO), 2013 IEEE XXXIII International Scientific Conference, pp. 147-150

[42] Eason G., Wave propagation in inhomogeneous elastic media, solution in terms of Bessel functions, Acta Mech., 1969, Vol.7, issue 2, pp. 137–160

[43] Fedorov F.I., Theory of elastic waves in crystals, Moscow: Nauka, 1965,

a. 386 p. (In Russian)

[44] Ferencz C., Electromagnetic wave propagation in inhomogeneous, moving media: A general solution of the problem, Radio Science, 2011, Vol. 46, issue 5, pp. 1-14

[45] Flannery C.M, von Kiedrowski H., Effects of surface roughness on surface acoustic wave propagation in semiconductor materials, Ultrasonics, 2002, Vol. 40, issues 1-8, pp. 83-87

[46] Frank C.K.Jr., Keller J.B., Elastic Wave Propagation in Homogeneous and Inhomogeneous Media, The Journal of the Acoustical Society of America, 2005, Vol. 31, issue 6, 694 p.

[47] Gilinsky I.A., Popov V.V., The excitation of electroacoust waves in piezoelectric materials by external sources, Jour. of tech. physics, 1976, Vol. 46, issue 11, pp. 2232-2242 (In Russian)

[48] Golub M.V., Zhang C., In-plane time-harmonic elastic wave motion and resonance phenomena in a layered phononic crystal with periodic cracks, J. Acoust. Soc. Am., 2015, Vol. 137, issue 1, 238

[49] Greenwood, J.A., Williamson J-B-P., Contact of nominally flat surfaces, Proc. of the Royal Soc. of London, ser. A, Math. and Phys. Sci., 1966, pp. 300-319

[50] Gulyaev Yu.V., Electroacoustic surface waves in solids, JETP Letters, 1969, Vol .9, issue 1, pp. 63-65 (In Russian)

[51] Hasanyan D.J., Piliposian G.T., Kamalyan A.H., Karakhanyan M.I., Some dynamic problems for elastic materials with functional inhomogeneities: anti-plane deformations, Continuum Mech. And Thermodynamics, 2003, Vol. 15, issue 5, pp.519-527.

[52] Hertz H., On the contact of elastic solids, Journal of pure and applied mathematics, 1882, Vol. 1882, issue 92, pp. 156-171 (In German)

[53] Hunanyan A.A., Localization of high-frequency normal shear waves in elastic homogeneous waveguide with weakly inhomogeneous surfaces, Young Scientists School-Conference, 3-7 October, 2016, Tsakhkadzor, Armenia, pp. 140-144 (In Russian)

[54] Hunanyan A.A., The instability of shear normal wave in elastic waveguide of weakly inhomogeneous material, Proc. of NAS Armenia, ser. Mechanics, 2016, Vol. 69, issue 3, pp. 16-27

[55] Huttunen T., Monk P., Collino F., Kaipio J. P., The Ultra-Weak Variational Formulation for Elastic Wave Problems, SIAM Journal on Scientific Computing, 2006, Volume 25, Issue 5, pp. 1717–1742

[56] Huseyin G.A, Wave Propagation in Heterogeneous Media with Local and Nonlocal Material Behavior, Journal of Elasticity, 2016, Vol. 122, issue 1, pp. 1–25

[57] Jackson R.L. and Green I., On the Modeling of Elastic Contact between Rough Surfaces, Tribology Transactions, 2011, Vol. 54, issue 2, pp. 300-314

[58] Johnson K.L., Kendall K., Roberts A.D., Surface energy and the contact of elastic solids, Proc. Of the Royal Soc. of London, ser. A, 1971, vol. 324, pp. 301-313

[59] Kamalyan A.A., Hunanyan A.A., A new type of localization of wave energy near non-smooth surfaces of piezoelectric waveguide, Young Scientists School-Conference, 3-7 October, 2016, Tsakhkadzor, Armenia, pp. 75-79 (In Russian)

[60] Gordon S.K., John S., Acoustic surface waves, Physics-Uspekhi, Advances in Physical Sciences, 1974, Vol. 113, issue 1, pp. 157-179 (In Russian)

[61] Kalinin V.A, Lobov G.D., Shitok V.V., Radiophysics for engineers, ed. Baskakova S.I., M.: Natioanl Research University (MPEI), 1994, 129 p. (In Russian)

[62] Kessenikh G.G., Lyubimov V.N., Filippov V.V., Transverse surface waves in isotropic substrate with a piezoelectric layer, Acoustic Journal, 1985, Vol. 31, issue 4, pp. 492-495 (In Russian)

[63] Kirchhoff, Lectures on math. physics, mechanics, Leipzig, 1883. (3nd ed.) (In German)

[64] Krasnova T., Jansson P.., Bostrcom A., Ultasonic wave propagation in an anisotropic cladding with a wavy interface, Wave Motion, 2005, Vol. 41, issue 2, pp. 163–177

[65] Kudryavcev B.A., Parton V.Z., Magnetoelasticity, The results of science and technology VINITI, ser. Mechanics of Solids, 1981, Vol. 14, pp. 3-59 (In Russian)

[66] Kuznetsova I.E., Zaitsev B.D., The peculiarities of the Bleustein-Gulyaev wave propagation in structures constaining conductive layer, Ultrasonics, 2015, Vol. 59, issue 2, pp. 45-49

[67] Lazarev Yu.F., MatLAB 5.x, Scientific Library of Innovative University of Eurasia, Kiev: BHV, 2000, 384 p. (In Russian)

[68] Lamb H., On Waves in an Elastic Plat. Proc. Roy. Soc. London, 1917, Vol. 93, issue 648, pp. 114–128

[69] Landau L.D., Lifshitz E.M., Electrodynamics of Continuous Media, Moscow: Nauka, 1982, 620 p. (In Russian)

[70] Lobkist O.I., Chimenti D.E., Elastic guided waves in plates with rough surfaces, Appl. Phys. Lett., 1996, Vol. 69, pp. 3486-3502.

[71] Lothe J., Barnett D.M., On the existence of surface wave solution for anisotropic elastic half-spaces with free surface, J. Appl. Phys., 1976, Vol. 47, issue 2, pp. 428-453

[72] Lothe J., Barnett D.M., Integral formalism for surface waves in piezoelectric crystals. Existance considerations, J. Appl. Phys., 1976, Vol. 47, issue 5, pp. 1799-1807

[73] Love A.E.H., «Some problems of geodynamics», first published in 1911 by the Cambridge University Press and published again in 1967 by Dover, New York, USA. (Chapter 11: Theory of the propagation of seismic waves)

[74] Maerfeld C., Tournois P., Pure spear elastic surface wave guided by the interface of two semi-infinite media, Appl. Phys. Lett., 1971, Vol. 19, issue 4, pp. 117-118

[75] Manen D.-J. van, Robertsson J.O.A., Modeling of Wave Propagation in Inhomogeneous Media, Physical Review Letters, 2005, Vol. 94, issue 16, pp. 164-301

[76] Maugin G., Mechanics of Electromagnetic Continuous Media, Moscow: Mir, 1991, 560 p. (In Russian)

[77] Mokhel A.N., Salganik R.L., Fedotov A.A., Contact interaction of rough elasic solids in the presence of two highly different scales of roughness extent, Computational continuum mechanics, 2008, Vol. 1, issue 4, pp. 61-68 (In Russian)

[78] Paul H.S., Anandam S., Transvers waves in piezoelectric 622 crystall class, Pure and Appl. Geophys, 1971, Vol. 88, issue 5, pp. 35-43

[79] Parton V.Z., Kudryavcev B.A., Electromagnetoelasticity of piezoelectric and electroconductive bodies, Moscow: Nauka, 1988, 472 p. (In Russian)

[80] Persson B.N.J., Bucher F., Chiaia B., Elastic contact between randomly rough surfaces: Comparison of theory with numerical results, Physical Review B, 2002, Vol. 65, issue 18, pp. 184-206

[81] Piliposian G. T., Avetisyan A.S., Ghazaryan K.B., Shear wave propagation in periodic phononic/photonic piezoelectric medium, International Journal Wave Motion, Elsevier publisher, January 2012, Vol. 49, issue 1, pp. 125-134

[82] Piliposyan D.G., Ghazaryan K.B., Piliposyan G.T., Internal resonances in a periodic magneto-electro-elastic structure, J. Appl. Phys., 2014, Vol. 116, pp. 94-107

[83] Pinel N., Bourlier C., Saillard J., Degree of Roughness of Rough Layers: Extensions of the Rayleigh Roughness Criterion and Some Applications, Progress In Electromagnetics Research B, 2010, Vol. 19, pp. 41-63

[84] Pobedrya B.E., Mechanics of composite materials, Pub. in Moscow University, 1984, 336 p. (In Russian)

[85] Potel C., Leduc D., Morvan B., Pareige P., Izbicki J.L., Depollier C., Lamb Wave Propagation In Isotropic Media With Rough Interface : Comparison Between Theoretical And Experimental Results, 5th World Congress on Ultrasonics WCU 2003, September 7-10, 2003, Paris, France

[86] Sargsyan S.H., General two-dimensional theory of magnetoelasticity of thin shells, Erevan: pub. in NAS, 1992, 232 p. (In Russian)

[87] Potel C., Bruneua M., N'Djomo L.C.F., Leduc D., Elkettani M.E., Izbicki J.-L.; Shear horizontal acoustic waves propagating along two isotropic solid plates bonded with a non-dissipative adhesive layer: Effects of the rough interfaces, Jour. Of Appl. Physics, 2015, Vol. 118, issue 22 (doi: 10.1063/1.4937150)

[88] Predoi M.V., Castaings M., Hosten B., Bacon C., Wave propagation along transversely periodic structures, J. Acoust. Soc. Am., 2007, Vol. 121, pp. 1935–1952

[89] Qian Zh.-H., Hiros S., Kishimoto K., Modulation of Bleustein-Gulyaev Waves in a Functionally Graded Piezoelectric Substrate by a Finite-Thickness Metal Waveguide Layer, Journal of Solid Mechanics and Materials Engineering, 2009, Vol. 3, issue 11, pp. 1182–1192

[90] Qing-Tian D., Zhi-chun Y., Propagation of guided waves in bonded composite structures with tapered adhesive layer, Appl. Math. Modell., 2011, Vol. 35, issue 11, pp. 5369–5381

[91] Reissner E., On the theory of bending of elastic plates. J. Math. And Phys., 1944, Vol. 23, issue 1-4, pp. 184-191

[92] Reyleigh J.W., On waves propagated along the plane surface of an elastic solid, Proc. Math. Soc. London, 1885/1886, Vol. 1-17, issue 1, pp. 4-11.

[93] Royer, D., Dieulesaint, E., Elastic Waves in Solids I. Free and Guided Propagation. Springer, Berlin, 2000, 374 p.

[94] Shchegrov A.V., Propagation of surface acoustic waves across the randomly rough surface of an anisotropic elastic medium, J. Appl. Phys., 1995, Vol. 78, issue 3, pp. 1565-1574

[95] Santamarina, J.C., Cascante, G., Effect of Surface Roughness on Wave Propagation Parameters, Geotechnique, 1998, Vol. 48, issue 1, pp. 129-137

[96] Sharma J.N., Sharma K.K., Kumar Ash., Modelling of Acousto-Diffusive Surface Waves in Piezoelectric-Semiconductor Composite Structures, J. of Mech. of Mater. and Struct., 2011, Vol. 6, issue 6, pp. 791-812

[97] Sinha B.K., Tiersten H.F., Elastic and piezoelectric surface waves guided by thin films, J. Appl. Phys., 1973, Vol. 44, issue 11, pp.4831-4854

[98] Singh S.S., Love Wave at a Layer Medium Bounded by Irregular Boundary Surfaces, Journal of Vibration and Control, 2010, Vol. 17, issue 5, pp. 641-650

[99] Stoneley R., Elastic Waves at the Surface of Separation of Two Solids, Roy. Soc. Proc. London, ser. A 106, 1924, pp. 416-428

[100] Svetovoy V.B., Palasantzas G., Influence of surface roughness on dispersion forces, Adv. Colloid Interface Sci., 2015, Vol. 216, pp. 1-19

[101] Tarasenko A.A., Jastrabik L., Tarasenko N.A., Effect of roughness on the elastic surface wave propagation, Eur. Phys. J. Appl. Phys., 2003, Vol. 24, issue 1, pp. 3-12

[102] Timoshenko S.P., Theory of Plates and Shells, Moscow: Gostehizdat, 1948, 460 p. (In Russian)

[103] Tikhonravov A.V., Trubetskov M.K., Tikhonravov A.A., Duparre A., Effects of interface roughness on the spectral properties of thin films and multilayers, Applied Optics, 2003, Vol. 42, issue 5, pp. 5140-5148

[104] Thorsos E.I., The validity of the Kirchoff approximation for rough surface scattering using a Gaussian roughness spectrum, Journal of the Acoustical Society of America, 1988, Vol. 83, issue 1, pp. 78–92

[105] Tseng C.C., White R.M., Propagation of piezoelectric and elastic surface waves on the bazal plane of hexagonal piezoelectric crystals, J. Appl. phys., 1967, Vol. 38, issue 11, pp. 4274-4280

[106] Valier-Brasier T., Potel C., Bruneau M., Modes coupling of shear acoustic waves polarized along a one-dimensional corrugation on the surfaces of an isotropic

solid plate, Appl. Phys. Lett., 2008, Vol. 93, issue 16 (doi: http://dx.doi.org/10.1063/1.2999632)

[107] Valier-Brasier T., Potel C., Bruneau M., Shear acoustic waves polarized along the ridged surface of an isotropic solid plate: Mode coupling effects due to the shape profile, J. Appl. Phys., 2010, Vol. 108, issue 7, (doi: http://dx.doi.org/10.1063/1.3486020)

[108] Vashishth, A K, Vishakha G., Wave propagation in transversely isotropic porous piezoelectric materials, Int. J. of Solids and Structures, 2009, Vol. 46, issue 20, pp. 3620-3632

[109] Victorov I.A., Talashev A.A., Propagation of Rayleigh waves on the boundaries of piezoelectric and semiconductor, Acoustic Journal, 1972, Vol .18, issue 2, pp. 197-205 (In Russian)

[110] Viktorov I. A., Sound surface waves in solids., Moscow: Nauka, 1981, p. 287 (in Russian)

[111] Zhang J., Li Youming, Numerical simulation of elastic wave propagation in inhomogeneous media, Wave Motion, 1997, vol. 25, issue 2, pp. 109-125

[112] Zhang Z., Wen Z., Hu J., Calculation of acoustic waves in a multilayered piezoelectric structure, Jour. of Semiconductors, 2013, Vol.34, issue 1, pp. 012002-1-012002-6